

Universidad CEU San Pablo
CEINDO – CEU Escuela Internacional de
Doctorado

PROGRAMA en CIENCIA Y TECNOLOGÍA DE LA SALUD



CEU

*Escuela Internacional
de Doctorado*

Implicación de la vía de señalización de
la pleiotrofina y la midkina en la
neuroinflamación y en los efectos
conductuales del alcohol

TESIS DOCTORAL

Presentada por

Rosalía Fernández Calle

Dirigida por

Gonzalo Herradón Gil-Gallardo

Esther Gramage Caro

MADRID

2019

Universidad CEU San Pablo
CEINDO – CEU Escuela Internacional de
Doctorado

PROGRAMA en CIENCIA Y TECNOLOGÍA DE LA SALUD



CEU

*Escuela Internacional
de Doctorado*

Implicación de la vía de señalización de
la pleiotrofina y la midkina en la
neuroinflamación y en los efectos
conductuales del alcohol

TESIS DOCTORAL

Memoria que presenta

Rosalía Fernández Calle

Para optar al grado de Doctor con Mención Internacional por
la Universidad San Pablo CEU

Dirigida por

Gonzalo Herradón Gil-Gallardo

Esther Gramage Caro

MADRID

2019



La presente tesis, titulada “Implicación de la vía de señalización de la pleiotrofina y la midkina en la neuroinflamación y en los efectos conductuales del alcohol” se presenta como un compendio de trabajos publicados. Cumple las condiciones exigidas por la normativa establecida para este tipo de tesis, aprobada por el comité de dirección de la CEINDO el 30 de noviembre de 2017.

Las publicaciones incluidas en esta tesis son las siguientes:

1. **Título:** Inhibition of RPTP β/ζ blocks ethanol-induced conditioned place preference in pleiotrophin knockout mice.

Autores: Rosalía Fernández-Calle, Esther Gramage, José María Zapico, Beatriz de Pascual-Teresa, Ana Ramos y Gonzalo Herradón.

Publicado en: *Behavioural Brain Research*.

Volumen: 369

Página de inicio: 111933

Factor de impacto: 2,77 (JCR 2018)

Cuartil: Q3 (neurociencia) (JCR).

Fecha de publicación: 2019

DOI: 10.1016/j.bbr.2019.111933

2. **Título:** Inhibition of Receptor Protein Tyrosine Phosphatase β/ζ (PTPRZ1) modulates behavioral responses to ethanol.

Autores: Rosalía Fernández-Calle, Marta Vicente-Rodríguez, Miryam Pastor, Esther Gramage, Bruno Di Geronimo, José María Zapico, Claire Coderch, Carmen Pérez-García, Amy W. Lasek, Beatriz de Pascual-Teresa, Ana Ramos y Gonzalo Herradón.

Publicado en: *Neuropharmacology*.

Volumen: 137

Páginas: 86-95

Factor de impacto: 4,367 (JCR 2018)

Cuartil: Q1 (farmacología y farmacia) (JCR).

Fecha de publicación: 2018

DOI: 10.1016/j.neuropharm.2018.04.027

3. **Título:** Endogenous pleiotrophin and midkine regulate LPS-induced glial responses.
Autores: Rosalía Fernández-Calle, Marta Vicente-Rodríguez, Esther Gramage, Carlos De la Torre-Ortiz, Carmen Pérez-García, María P. Ramos y Gonzalo Herradón.
Publicado en: *Neuroscience Letters*.
Volumen: 662
Páginas: 213-218
Factor de impacto: 2,173 (JCR 2018)
Cuartil: Q3 (neurociencia) (JCR).
Fecha de publicación: 2018
DOI: 10.1016/j.neulet.2017.10.038

4. **Título:** Pleiotrophin regulates microglia-mediated neuroinflammation.
Autores: Rosalía Fernández-Calle, Marta Vicente-Rodríguez, Esther Gramage, Jimena Pita, Carmen Pérez-García, Marcel Ferrer-Alcón, María Uribarri, María P. Ramos y Gonzalo Herradón.
Publicado en: *Journal of Neuroinflammation*.
Volumen: 14
Página de inicio: 46
Factor de impacto: 5,193 (JCR 2017)
Cuartil: Q1 (neurociencia) (JCR).
Fecha de publicación: 2017
DOI: 10.1186/s12974-017-0823-8



CEU

*Universidad
San Pablo*

D. **Gonzalo Herradón Gil-Gallardo** y Dña. **Esther Gramage Caro**, profesores del Departamento de CC Farmacéuticas y de la Salud, de la Facultad de Farmacia de la Universidad CEU San Pablo.

HACEN CONSTAR:

Que Dña. **Rosalía Fernández Calle** ha realizado bajo su dirección el trabajo titulado “**Implicación de la vía de señalización de la pleiotrofina y la midkina en la neuroinflamación y en los efectos conductuales del alcohol**” con objeto de obtener el Grado de Doctor; y que dicho trabajo reúne todos los requisitos necesarios para su juicio y calificación.

Madrid, a 20 de noviembre de 2019

Gonzalo Herradón Gil-Gallardo

Esther Gramage Caro

Este trabajo ha sido financiado por proyectos del ministerio de Economía y Competitividad de España (SAF2014-56671-R), del Plan Nacional Sobre Drogas del Ministerio de Sanidad, Consumo y Bienestar social (PNSD001|2015), y de la Universidad CEU San Pablo con el Banco Santander (USP-BS-APP03/2014) concedidos a Gonzalo Herradón. Rosalía Fernández Calle ha sido beneficiaria de una beca de formación de personal investigador concedida por la Universidad CEU San Pablo. También ha disfrutado de la ayuda a la movilidad CEU-Banco Santander, con la que ha podido realizar una movilidad investigadora en la Universidad de Lund durante el año 2019

A mi familia

AGRADECIMIENTOS

No podría comenzar esta sección sin expresar, en primer lugar, mi agradecimiento a la Universidad San Pablo CEU y su vicerrectorado de investigación, por haberme permitido disfrutar de una beca de formación de personal investigador, y por haber puesto a mi disposición todos los medios materiales y técnicos para la realización de este trabajo.

Gracias a mis directores de tesis, Gonzalo Herradón y Esther Gramage. Gonzalo, te considero mi padre científico, gracias por la confianza que has depositado en mí durante estos años, por acogerme con los brazos abiertos y mostrarme vuestros proyectos de investigación desde que solo era una alumna de tercero de farmacia, por valorarme y apoyarme, tanto en los momentos buenos como en los malos, por pararme los pies cuando me venía arriba y quería hacer a la vez demasiado, y por darme un empujoncillo cuando me faltaban fuerzas. Esther, qué decir de mi mejor maestra, gracias por enseñarme tanto y tan bien, por ser de esas personas que siempre te animan a sacar lo mejor de ti mismo, gracias por enseñarme a cuidar de los detalles (el gen Gramage), a ser exigente conmigo misma sin olvidar que soy humana, que el día tiene 24 horas y que en algún momento tendré que parar para comer. Gracias por tu paciencia con mis presentaciones de *power-point* y por todos tus consejos, tanto científicos como de la vida. Te admiro y aspiro a ser tan buena como tú, eres mi "*female scientific role model*" y me siento orgullosa de haber sido tu primera doctoranda.

Gracias a Carmen Pérez, por estar a mi lado durante toda la tesis, gracias por tu apoyo y cariño constantes, por enseñarme proteómica.

Gracias a Martita, por enseñarme tanto en el laboratorio, por compartir tantas horas conmigo y por animarme a seguir tus pasos.

Gracias a Beatriz Ramos, por hacer que me picara el gusanillo de la investigación cuando me permitió colaborar en el departamento de Fisiología Vegetal durante el verano de primero y segundo de carrera, por concederme la beca del departamento de relaciones internacionales, lo que provocó que, al tener el despacho de Gonzalo Herradón al lado, me armara de valor para entrar a preguntarle... "Oye, ¿Qué investigáis en el departamento de farma?"

Gracias a los demás miembros del departamento de Farmacología y Toxicología: A Carmen Gonzalez, por cuidarnos siempre en el labo, por tus detalles, como traernos a cada doctorando un calendario de adviento, y por tu cariño. A Luis Fernando Alguacil, no olvidaré el congreso de la FENS en el que nos dimos cuenta de que ambos somos fans de Jethro tull (aunque quién no, ¿verdad?), gracias por tus buenos consejos y compartir con nosotros tu experiencia y conocimientos. A Mariano, Mariví, María José, María, Antonio Aguilar y Consuelo, gracias por nuestras conversaciones amenas a la hora de la comida, que te despejaban de cualquier experimento o preocupación existente. A Bea Merino, por no permitir que el laboratorio pareciera Vietnam debido al desorden. A Bea Somoza y Marta Gil, gracias por vuestro apoyo diario. A Nuria, por contagiarnos con tu pasión, alegría y espíritu positivo, porque cuando me diste las prácticas de farmacología general, me dije "me encanta lo que nos está enseñando y cómo lo vive, yo quiero ser como esta mujer".

Agradecimientos

Gracias a Chema, Jesús, Inma, Marta y a todos los que forman parte del personal del animalario, por vuestra inestimable ayuda durante toda la tesis.

Gracias a Antonio Galan, mi tutor durante toda la carrera.

Gracias a MariCarmen, por querernos y cuidarnos como si fuéramos sus hijas.

Gracias a la unidad de cultivos celulares, y en especial a Sergio, por tu paciencia cuando empecé como alumna, por compartir conmigo tus conocimientos, por estar siempre dispuesto a echar una mano, me alegro mucho de que te animaras con la tesis, puedes con todo.

Gracias a Yasmina, por enseñarme a valorar un trabajo bien hecho y por tu ayuda.

Gracias Pilar Ramos y al departamento de bioquímica por toda su colaboración durante esta tesis y por haberme hecho sentir tan a gusto trabajando junto a ellos: Julio, María Gracia, Eva, Begoña, y en especial a Jimena.

Gracias a las doctoras Ana Ramos y Beatriz de Pascual y a los miembros de los equipos de química orgánica y química farmacéutica de esta universidad, José María, Myriam, Claire y Bruno, por su labor encomiable en el proyecto de los inhibidores de RPTP β/ζ .

Al igual que agradezco la inestimable participación de la Dra Amy Lasek (Universidad de Illinois) en este proyecto.

Gracias al doctor Tomas Deierborg (Universidad de Lund), por permitirme realizar una estancia en su laboratorio y aprender tanto, y a los miembros de su laboratorio: Yiyi Yang (me siento muy afortunada de haber podido trabajar contigo codo con codo), a Sara y Antonio, por transmitirme vuestra sabiduría post-doc, Oscar y Agnes. Gracias a todos por haberme hecho sentir como en casa.

Gracias a Krystina, Sarah, Teddy y Fedrick, por haberme hecho sentir parte de vuestra familia durante mi estancia en Suecia.

Gracias a mis erasmus Fahmo, Elisa y Morganna, y a mis estudiantes de trabajo fin de carrera, que me ayudaron a darme cuenta de lo mucho que me gusta enseñar.

Gracias a mis compis del laboratorio, a los que se fueron y los presentes: Adri, Carmen, Ana, Victor, Iñigo, Elena, Belén y Jesús, gracias por tan buenos momentos a vuestro lado. Gracias a Carlos, Mila y Anita "mis pollitos". No puedo estar mas orgullosa de vosotros, gracias por todos los momentos que hemos compartido (tenemos demasiadas anécdotas magnificas como para enumerarlas aquí), no tengo duda de que llegareis lejísimos y me siento súper orgullosa de haber tenido la oportunidad de compartir la poyata con vosotros.

Gracias a Martín, por tus cursillos rápidos sobre cómo diseñar primers, la guía básica sobre cómo sobrevivir a una tesis, la guía sobre qué hacer cuando Word decide dejar de funcionar una semana de depositar la tesis, en fin, creo que nunca cocinaré suficientes croquetas para manifestar lo agradecida que estoy por toda tu ayuda.

Gracias a Javi, por ser tan atento y bueno, siempre dispuesto a ayudar incluso si estas a tope de trabajo, me siento afortunada de que hayamos coincidido en el labo.

Gracias a Miriam, María y Raquel; mis niñas del laboratorio, la de horas que hemos pasado juntas, gracias por las risas, lágrimas, viajes juntas y sesiones de *brain-storming* porque

algo de algún experimento no funcionaba. Miri, gracias por enseñarme tus truquitos del labo, por ser tan divertida y buena amiga. Mery, aunque el laboratorio no fuera lo que más te gustara, te echo de menos cada día, eres brillante y triunfarás en lo que te propongas, gracias por tu ayuda siempre que la he necesitado. Raquel... me siento increíblemente afortunada de haber hecho esta tesis a tu lado, gracias por aguantarme en cualquier estado de animo, por nuestros domingos en el laboratorio, por tu apoyo constante en cualquier situación, porque con solo mirarnos y sabemos si estamos de buen o de mal humor, porque siempre puedo contar contigo y porque no nos permitimos rendirnos ante nada.

Gracias a Rocío, y Julia, mis amigas de la carrera. Ro, gracias por contagiarme tu amor por la farmacología, por animarme a superarme y recordarme que puedo con lo que me proponga, porque sin ti no sé si me habría atrevido a solicitar la beca de doctorado, gracias por estar siempre ahí y ser tan buena amiga. Ju, qué decir, estas siempre ahí a mi lado, gracias por entenderme tan bien, por ser tan atenta y apoyarme en todo, por tu alegría y forma de ser que me hacen desconectar de todo y por cuidarme tanto.

Gracias a Noelia, por infundirme ánimo con el último empujón de la tesis, por pasar tan buenos ratos juntas y hacer de mi experiencia en Lund un recuerdo inolvidable, además de llevarme una gran experiencia, gané una gran amiga.

Gracias Estefi, eres una de las mujeres mas fuertes, proactivas y buenas que he conocido, no importa lo lejos que estemos porque siento tus palabras de aliento como si estuvieras literalmente a mi lado. Gracias por formar parte de mi vida e infundirme parte de esa fortaleza tuya.

Gracias a David, por tu amistad y por poder siempre poder contar contigo, y a Arantxa, por ayudarme a encontrarme cuando me sentí perdida.

Gracias a mi familia, por su comprensión, empatía y apoyo constantes, en especial a mi prima Bea y a mis tíos Alberto y Violeta, por vuestra atención y por estar siempre presentes.

Gracias a Miguel, por tu apoyo incondicional en todos los aspectos de mi vida, por recordarme todo lo que he conseguido cuando parece que se me olvida, por cuidarme y compartirlo todo conmigo.

Gracias a mi padre y a mi madre, por ofrecerme siempre la mejor educación que han podido, por todos los sacrificios que habéis hecho por mi y por los valores que me habéis inculcado. Papá, gracias por hacer que el arte forme parte de mi vida, por anteponer las necesidades familiares a las tuyas, sin ti, no habría sido posible. Mamá, gracias por tu esfuerzo diario, por animarme a llegar más lejos, por transmitirme que con esfuerzo y dedicación puedo llegar donde quiera, os quiero.

A Gigi y Toby, por su amor incondicional y por haberme acompañado durante este recorrido.

En definitiva, gracias a todos los que habéis formado parte de esta etapa de mi vida, llevo un pedacito de cada uno de vosotros en mi corazón.

ÍNDICE DE CONTENIDOS

RESUMEN	3
ABSTRACT	5
INTRODUCCIÓN	9
1. Problemática del consumo y la adicción a las drogas.	9
1.1. Consecuencias del consumo de drogas en el sistema nervioso central. Efectos comportamentales y neuroadaptativos.	11
2.1. Relación del consumo de alcohol y otras drogas de abuso con la neuroinflamación.	17
2.2. Pleiotrofina (PTN) y Midkina (MK).	18
2. Neuroinflamación y neuroprotección.	12
2.2.1. Papel de PTN y MK en los efectos de las drogas de abuso.	20
2.2.2. Mecanismo de acción de PTN y MK.	21
3. Modulación farmacológica de la vía de señalización de PTN/MK/RPTP β/ζ .	28
HIPÓTESIS Y OBJETIVOS	33
MÉTODOS Y RESULTADOS (PUBLICACIONES CONTENIDAS EN LA TESIS)	35
ARTÍCULO 1. Pleiotrophin regulates microglia-mediated neuroinflammation.	37
ARTÍCULO 2. Endogenous pleiotrophin and midkine regulate LPS-induced glial responses.	49
ARTÍCULO 3. Pharmacological inhibition of Receptor Protein Tyrosine Phosphatase β/ζ (PTPRZ1) modulates behavioral responses to ethanol.	57
ARTÍCULO 4. Inhibition of RPTP β/ζ blocks ethanol-induced conditioned place preference in pleiotrophin knockout mice.	69
DISCUSIÓN	81
1. Implicación de la PTN y la MK en la neuroinflamación.	81
2. Modulación farmacológica de RPTP β/ζ como estrategia terapéutica para regular el consumo de alcohol y los efectos conductuales de esta droga.	86
3. Modulación del eje de señalización de PTN//MK/RPTP β/ζ como estrategia terapéutica. Perspectivas futuras.	90
CONCLUSIONES	99
CONCLUSIONS	101
REFERENCIAS	105
ANEXOS (OTRAS PUBLICACIONES DE LA AUTORA RELACIONADAS CON LA TESIS)	127

ANEXO 1. Pleiotrophin overexpression regulates amphetamine-induced reward and striatal dopaminergic denervation without changing the expression of dopamine D1 and D2 receptors: Implications for neuroinflammation. _____ 129

ANEXO 2. Midkine Is a Novel Regulator of Amphetamine-Induced Striatal Gliosis and Cognitive Impairment: Evidence for a Stimulus-Dependent Regulation of Neuroinflammation by Midkine. _____ 143

ANEXO 3. Development of inhibitors of receptor protein tyrosine phosphatase β/ζ (PTPRZ1) as candidates for CNS disorders. _____ 157

INDICE DE FIGURAS Y TABLAS

FIGURA 1. EFECTOS POSITIVOS Y DELETÉREOS DE LA INFLAMACIÓN EN EL SNC. __	13
FIGURA 2. REPRESENTACIÓN DE LOS RECEPTORES DE LA PTN/MK Y SUS VÍAS DE SEÑALIZACIÓN MÁS RELEVANTES. _____	26
FIGURA 4. MECANISMO DE ACCIÓN DE PTN/MK Y DE INHIBIDORES SELECTIVOS DE RPTPB/Z. _____	29
FIGURA 5. ESTRUCTURA DE LOS INHIBIDORES DE RPTPB/Z MY10 Y MY33-3. _____	30
FIGURA 6. ESTRATEGIAS DE MODULACIÓN DE LA VÍA DE SEÑALIZACIÓN DE PTN/MK/RPTPB/Z. _____	92
TABLA 1. ALGUNOS DE LOS INHIBIDORES EXISTENTES DE LOS SUSTRATOS DE RPTPB/Z Y SUS POSIBLES INDICACIONES TERAPÉUTICAS. _____	95

ABREVIATURAS

2BCEC	Del inglés <i>2-bottle choice ethanol consumption test</i>
aa	Aminoácidos
AKT	Proteína quinasa B
ALK	Quinasa de linfoma aplásico, del inglés <i>Anaplastic lymphoma kinase</i>
ATV	Área tegmental ventral
BDNF	Factor neurotrófico cerebral, del inglés <i>brain-derived neurotrophic factor</i>
bFGF	Factor básico de crecimiento de fibroblastos, del inglés <i>basic fibroblast growth factor</i>
BHE	Barrera hematoencefálica
C _{1q}	Factor 1 del complemento
CCL	<i>C-C motif chemokine</i>
CD200	Proteína del grupo de diferenciación 200
COX-2	Ciclooxigenasa 2
CPF	Corteza prefrontal
CPP	Condicionamiento preferencial al sitio, del inglés <i>Conditioned place preference</i>
CX3CR1	Receptor de quimiocinas CX3C 1, del inglés <i>CX3C chemokine receptor 1</i>
CXCL1	C-X-C motif ligand 1
DAMPS	Patrones moleculares asociados a daño, del inglés <i>danger associated molecular patterns</i>
DC45	Cúmulo de diferenciación 45, del inglés <i>cluster of differentiation 45</i>
DID	Del inglés <i>Drinking in the dark</i>
DSM	Del inglés <i>Diagnostic and Statistical Manual of Mental Disorders</i>
EGF	Del inglés <i>epidermic growth factor</i>
ELA	Esclerosis lateral amiotrófica
EP	Enfermedad de Parkinson
ERK1/2	Quinasa regulada por señales extracelulares 1/2
GEMMs	Modelos de ratones modificados genéticamente, del inglés <i>Genetically-engineered mouse models</i>
GFAP	Proteína ácida fibrilar de la glía, del inglés <i>glial fibrillary acidic protein</i>

GIT 1	Del inglés <i>G protein-coupled receptor kinase-interactor 1</i>
GSK3 β	Quinasa glucógeno sintentasa 3 beta
GWAS	Estudio del genoma completo, del inglés, <i>Genome-wide association study</i>
HARP	Péptido regulador afín a la heparina, del inglés <i>heparin affin regulatory peptide</i>
HB-GAM	Del inglés <i>heparin-binding growth-associated molecule</i>
HB-NF	Factor neurotrófico de unión a la heparina, del inglés <i>heparin binding neurotrophic factor</i>
HBGF8	Factor de crecimiento de unión a la heparina del inglés <i>heparin-binding growth factor 8</i>
i.p.	Intraperitoneal
Iba-1	molécula adaptadora de unión al calcio 1, del inglés <i>Ionized calcium binding adaptor molecule 1</i>
IFN- γ	Interferón gamma
IKK	Quinasa inhibidora kappa de células B, del inglés <i>inhibitory kappa B kinases</i>
IL	Interleucina
iNOS	Óxido nítrico sintasa inducible
IRAK	Quinasas asociadas al receptor IL-1, de inglés <i>IL-1 receptor-associated kinase</i>
IRS1	Del inglés <i>insulin receptor substrate 1</i>
kD	Kilodaltons
Lcn2	Del inglés <i>Lipocalin 2</i>
LORR	Del inglés <i>loss of righting reflex</i>
LPS	Lipopolisacárido
LRP	Del inglés <i>Lipoprotein receptor-related protein</i>
LTP	Potenciación a largo plazo, del inglés long-term potentiation
MAGI1	Del inglés <i>membrane-associated guanylate kinase inverted 1</i>
MAPK	Del inglés <i>Mitogen-Activated protein kinases</i>
MCP-1	Del inglés <i>monocyte chemoattractan protein 1</i>
MDMA	3,4-metilendioxi-metanfetamina
Mk	Midkina (gen)
MK	Midkina (proteína)
Mk ^{-/-}	Ratones <i>knock-out</i> de MK

MyD88	Del inglés <i>Myeloid differentiation primary response 88</i>
N-CAM	Molécula de adhesión neuronal cerebral
NEGF2	Factor 2 promotor del crecimiento de neuritas, del inglés <i>neurite growth-promoting factor 2</i>
NF-κB	Factor nuclear potenciador de las cadenas ligeras kappa de las células B activadas
Ng-CAM	Molécula de adhesión neuro-glial
NGF	Factor de crecimiento nervioso, del inglés <i>nerve growth factor</i>
NIAAA	Del inglés <i>National Institute on Alcohol Abuse and Alcoholism</i>
NIK	Quinasa inductora de NF-κB
NLRP13	Del inglés <i>Nod-like receptor protein 13</i>
NMDA2B	N-metil-D-aspartato, receptor, subunidad 2B
NO	Óxido nítrico
NOTCH-2	Del inglés <i>Neurogenic locus notch homolog protein 2</i>
NSCLC	Del inglés <i>non-small-cell lung cancer</i>
p190-RhoGAP	Del inglés <i>GTP-ase-activating protein for Rho GTP-ase</i>
PAMPS	Patrones moleculares asociados a patógenos, del inglés <i>pathogen-associated molecular patterns</i>
PDGF	Factor de crecimiento derivado de las plaquetas, del inglés <i>platelet-derived growth factor</i>
PI3K	Fosfatidilinositol-3-quinasa
PKC	Proteína quinasa C
PLC-γ	Fosfolipasa C-gamma
PSI	Isoforma corta de fosfacán, del inglés <i>phosphacan short isoform</i>
PTKs	Proteínas tirosina quinasas
Ptn	Pleiotrofina (gen)
PTN	Pleiotrofina (proteína)
Ptn ^{-/-}	Ratones <i>knock-out</i> de PTN
PTN-Tg	Ratones transgénicos que sobre expresan PTN
PTP-D1	Dominio D1 de proteína tirosina fosfatasa
PTP-D2	Dominio D2 de proteína tirosina fosfatasa
PTPRZ1	Del inglés <i>protein tyrosine phosphatase receptor Z1</i>

PTPs	Proteínas tirosina fosfatasa, del inglés <i>protein tyrosine phosphatase</i>
RAGE	Del inglés <i>receptor for advanced glycation endproducts</i>
RIP	Del inglés <i>receptor interacting protein</i>
ROS	Especies reactivas de oxígeno, del inglés <i>reactive oxygen species</i>
RPTPs	Receptores proteína fosfatasa de tirosinas
SAL	Salino
SAMHSA	Administración de abuso de sustancias y de salud mental de Estados Unidos, del inglés <i>Substance Abuse and Mental Health Services Administration</i>
SDC	Syndecan
SFKs	Del inglés <i>Src family kinases</i>
SHP	Del inglés <i>Src homology 2 domain-containing tyrosine phosphatases</i>
siRNA	Del inglés <i>small interfering RNA</i>
SN	Sustancia Negra
SNC	Sistema nervioso central
SNP	Polimorfismos de un solo nucleótido, del inglés <i>single nucleotide polymorphism</i>
STAT	Transductor de señal y activador de la transcripción
TAK	Del inglés <i>transforming growth factor-β-activated kinase</i>
TGF- β	Factor de crecimiento transformador beta
TLRs	Del inglés <i>Toll-like-receptors</i>
TNF- α	Factor de necrosis tumoral alfa
TRAF	Factor asociado al receptor de TNF, de inglés <i>TNF receptor-associated factor</i>
TRAM	De inglés <i>TRIF-related adaptor molecule</i>
TREM2	Receptor detonante expresado en células mieloides 2, del inglés <i>triggering receptor expressed on myeloid cells 2</i>
TRIF	Del inglés <i>Toll-interleukin-1 receptor domain-containing adaptor protein</i>
TrkA	Del inglés <i>Tropomyosin receptor kinase A</i>
Tyr	Tirosina
Wnt	De inglés <i>wingless integrated</i>
Wt	Ratones salvajes, de inglés <i>wild-type</i>
Δ -9-THC	Delta-9 tetrahidrocannabinol

RESUMEN/ABSTRACT

RESUMEN

La neuroinflamación persistente en el sistema nervioso central (SNC) se ha postulado como uno de los procesos cerebrales que subyacen en diversas patologías centrales, como las enfermedades neurodegenerativas o la isquemia. Asimismo, el abuso de diversas sustancias, incluido el alcohol, también está asociado con el desequilibrio de la homeostasis del SNC y el desarrollo de neuroinflamación. Actualmente, continúa la búsqueda de tratamientos más efectivos para disminuir el consumo excesivo de alcohol y los efectos nocivos asociados al mismo, incluidos los efectos neurotóxicos de esta droga, relacionados con su capacidad para producir neuroinflamación. Por este motivo, el descubrimiento de nuevos factores capaces de modular la neuroinflamación y que participen en enfermedades centrales que cursan con componente inflamatorio como el alcoholismo, sería relevante para la identificación de nuevas dianas para el tratamiento de diversas patologías del SNC. En este sentido, las citoquinas pleiotrofina (PTN) y midkina (MK) se sobreexpresan en la corteza cerebral de pacientes alcohólicos y en la corteza prefrontal de ratones tratados con alcohol. En estudios previos se demostró que los ratones *knock-out* de PTN (Ptn^{-/-}) y de MK (Mk^{-/-}) son más vulnerables a los efectos reforzadores del alcohol, mientras que estos se encuentran disminuidos o incluso ausentes en el ratón transgénico que sobre expresa PTN en la corteza prefrontal e hipocampo (Ptn-Tg). Por otra parte, se ha demostrado que estas citoquinas se encuentran implicadas en la neuroinflamación desencadenada por distintos estímulos como la administración de amfetamina o por otras patologías como las enfermedades neurodegenerativas. La PTN y la MK son inhibidores endógenos del receptor RPTPβ/ζ (receptor proteína fosfatasa de tirosinas β/ζ, también conocido como PTPRZ1). Ambas citoquinas inactivan la actividad fosfatasa de este receptor y, como resultado, incrementan los niveles de fosforilación de los sustratos de RPTPβ/ζ. Todo esto nos llevó a plantearnos la hipótesis de que la PTN y la MK podrían ser nuevos factores moduladores de la neuroinflamación en distintos contextos patológicos y que la utilización de inhibidores farmacológicos de RPTPβ/ζ debería reproducir las acciones centrales de PTN y MK y, así, limitar los efectos reforzadores del alcohol y su consumo.

Para probar esta hipótesis, esta tesis engloba estudios *in vitro* e *in vivo*, modelos de animales genéticamente modificados (GEMMs) de inactivación de PTN o MK endógenas y de sobreexpresión de PTN, así como el uso de inhibidores de RPTPβ/ζ que mimetizan la actividad de la PTN y la MK sobre este receptor. Por una parte, los datos obtenidos en este trabajo demuestran que la expresión endógena de PTN y MK modula la respuesta astrocítica y la activación microglial inducidas por el lipopolisacárido (LPS) y que la sobreexpresión cerebral de PTN potencia la neuroinflamación en este modelo de endotoxemia. Por otro lado, demostramos por primera vez que MY10 y MY33-3, compuestos inhibidores de RPTPβ/ζ, disminuyen significativamente el consumo de alcohol en ratones en un modelo de consumo por atracción (DID, *drinking in the dark*) y bloquean el condicionamiento preferencial al sitio inducido por el alcohol,

probablemente a través de la capacidad de estos inhibidores de activar ALK (*anaplastic lymphoma kinase*), un sustrato de RPTP β/ζ .

Por lo tanto, los datos aquí recopilados demuestran por primera vez que la PTN es un potente regulador de la neuroinflamación y abren la posibilidad de modular la vía de señalización PTN/MK/RPTP β/ζ como nueva estrategia terapéutica para el tratamiento de trastornos por consumo excesivo de alcohol y de otras patologías que cursen con componente neuroinflamatorio

ABSTRACT

Prolonged neuroinflammation in the central nervous system (CNS) has been proposed as one of the main brain processes underlying several CNS pathologies such as neurodegenerative diseases and stroke. Moreover, drug abuse and heavy alcohol consumption are also linked to an imbalance of the CNS homeostasis and to the development of neuroinflammation. Currently, the urge to find more effective treatments to reduce excessive alcohol consumption and its associated noxious effects, including neurotoxicity and neuroinflammation, is still present. Therefore, the discovery of new modulators of neuroinflammation, involved in CNS diseases characterized by overt-neuroinflammation such as alcoholism, would provide valuable new targets for treatments for multiple CNS pathologies. In this context, the cytokines pleiotrophin (PTN) and midkine (MK) are overexpressed in the cerebral cortex of alcoholic patients and in the prefrontal cortex of alcohol-treated rodents. Previous studies have shown that PTN *knock-out mice* ($Ptn^{-/-}$) and MK *knock-out mice* ($Mk^{-/-}$) are more vulnerable to the rewarding effects of alcohol, whereas this effect is decreased or even blocked in transgenic mice that overexpresses PTN in the prefrontal cortex and the hippocampus (PTN-Tg). On the other hand, it has been confirmed that these cytokines are involved in neuroinflammation triggered by several stimuli such as amphetamine administration or in pathologies such as neurodegenerative diseases. The cytokines PTN and MK are endogenous inhibitors of RPTP β/ζ (receptor protein tyrosine phosphatase β/ζ , also known as PTPRZ1). Both cytokines inactivate this receptor's phosphatase activity and, as a result, induce an increase in the phosphorylation of RPTP β/ζ substrates. This led us to hypothesize that PTN and MK are two novel modulators of neuroinflammation in different pathological contexts and that the use of pharmacological inhibitors of RPTP β/ζ should reproduce the central actions of PTN and MK, and thus, could limit the rewarding effects of alcohol and, potentially, decrease alcohol consumption.

To test this hypothesis, this thesis comprises *in vitro* and *in vivo* studies, using GEMMs (genetically engineered mouse models) involving PTN or MK endogenous inactivation and endogenous PTN overexpression, and the use of RPTP β/ζ inhibitors that mimic PTN and MK actions. The data collected in these studies show that endogenous overexpression of PTN and MK modulate astrocytic and microglial responses induced by LPS (lipopolysaccharide), and that brain PTN overexpression promotes neuroinflammation in this model. In addition, we show that MY10 and MY33-3, inhibitors of RPTP β/ζ , significantly suppress alcohol consumption in mouse models of binge consumption (DID, drinking in the dark) and block alcohol-induced conditioned place preference, possibly through the ability of these inhibitors to activate ALK (*anaplastic lymphoma kinase*), a substrate of RPTP β/ζ .

In conclusion, the data here gathered illustrate for the first time that PTN is a potent regulator of neuroinflammation and suggest that modulation of the PTN/MK/RPTP β/ζ signaling

pathway is a novel therapeutic strategy for the treatment of alcohol use disorders and other central pathologies characterized by overt-neuroinflammation

INTRODUCCIÓN

INTRODUCCIÓN

1. Problemática del consumo y la adicción a las drogas.

El informe europeo sobre drogas estima que alrededor de una cuarta parte de la población entre 15 y 64 años de la Unión Europea ha consumido drogas ilegales en algún momento de su vida. Entre las drogas más consumidas se encuentran el cannabis, la cocaína, la heroína, la anfetamina y otros derivados anfetamínicos como el MDMA (3,4-metilendioxi-metanfetamina) (O.E.D.T., 2019). Según el informe mundial sobre drogas de 2019, el número de fallecimientos relacionados con el consumo de drogas se estima en 585.000 personas durante el año 2017 (UNODC, 2019).

El consumo de alcohol constituye la sexta mayor causa de muerte prematura en países desarrollados (WHO, 2017). En 2016 el consumo de alcohol originó el 5,3% de las muertes mundiales, resultando en el 7,6% de las muertes prematuras de 2016. A nivel mundial, la prevalencia del consumo de alcohol en mujeres tiende a ser menor que en hombres y las regiones europeas son las que presentan los niveles más altos de consumo, 6,4 litros *per cápita* en 2016 (WHO, 2018). Una gran parte del consumo se lleva a cabo en atracones. Los adolescentes europeos de entre 15 y 19 años son los más habituados a este tipo de consumo (43,8%), seguidos por estadounidenses (38,2%) y adolescentes de las regiones del sur del Pacífico (37,9%) (WHO, 2018). Se calcula que solo en 2010, el consumo abusivo de alcohol supuso a Estados Unidos un coste superior a los 200 mil millones de dólares (NIAAA, 2019).

El problema del abuso del alcohol y de sustancias ilegales como la anfetamina trasciende el impacto económico y sociocultural, produciendo severas repercusiones en el ámbito de la salud. Existen múltiples trastornos derivados del alcoholismo o que pueden verse agravados por el abuso de alcohol como enfermedades neuropsiquiátricas, cardiovasculares, gastrointestinales o cáncer (Rehm y col., 2017). En Estados Unidos, el 47,9% de las muertes por cirrosis en el año 2013 estaban relacionadas con el consumo de alcohol (NIAAA, 2019).

Uno de los principales problemas de estas sustancias es su poder adictivo. La asociación americana de psiquiatría define la adicción como una patología cerebral manifestada por el uso compulsivo de sustancias a pesar de las consecuencias dañinas que estas puedan acarrear. Esta asociación elabora un manual diagnóstico y estadístico de los trastornos mentales (*Diagnostic and Statistical Manual of Mental Disorders*, DSM), que actualmente va por la quinta edición, y en el que se clasifican categóricamente los tipos de adicciones. El DSM-5 identifica los trastornos relacionados con el abuso de sustancias como aquellos que resultan del abuso de: alcohol, cafeína, cannabis, alucinógenos, inhaladores, opiáceos, sedantes, hipnóticos, ansiolíticos, estimulantes (incluyendo los derivados de las anfetaminas, cocaína y otros estimulantes), tabaco y otras sustancias desconocidas (Grant y col., 2016).

La adicción ha sido conceptualizada como un desorden que implica impulsividad y compulsividad y da lugar a un ciclo compuesto por tres fases: atracón/intoxicación, abstinencia y preocupación/anticipación también definido como ansia o “*craving*” en inglés (Koob y col.,

2010). La mayoría de las drogas de abuso actúan a nivel del sistema de recompensa cerebral, lo que provoca adaptaciones cerebrales que acaban desembocando en tolerancia (Guerra y col., 2019; Hamilton y col., 2019). El sistema opioide endógeno es clave en el desarrollo de adicciones (Bodnar, 2016) junto con las vías mesocorticolímbicas, que consisten en proyecciones dopaminérgicas desde el área tegmental ventral (ATV) a las zonas límbicas, incluidos el hipocampo y la amígdala (Feltenstein y col., 2008), y el núcleo accumbens, que está relacionado con las experiencias placenteras posteriores a la exposición a drogas y a la motivación consecuente a repetir la exposición (Castro y col., 2015). El hecho de que las estructuras límbicas estén implicadas en la memoria y el aprendizaje también está estrechamente relacionado con las propiedades reforzadoras de las drogas de abuso (Goodman y col., 2016; Harricharan y col., 2017; Kutlu y col., 2016).

En la adicción al alcohol se produce una disminución de la función del sistema de recompensa cerebral, un incremento del estrés y la afectación de funciones cerebrales, lo que contribuye al refuerzo negativo, que se define como el alivio emocional generado por el uso de la droga (Koob, 2014). Existen factores genéticos y ambientales involucrados en el desarrollo de este tipo de adicción (Palmisano y col., 2017). Por ejemplo, el estrés y otros desórdenes psiquiátricos pueden incrementar la susceptibilidad a desarrollar alcoholismo (Becker, 2012; Bolton y col., 2009; Kushner y col., 2000).

Es importante categorizar los niveles de consumo de alcohol para la predicción de posibles problemas de salud asociados. El NIAAA (*National Institute on Alcohol Abuse and Alcoholism*) cuantifica el consumo moderado de alcohol como una bebida al día en mujeres y dos en hombres. Según el NIAAA, sólo el dos por ciento de aquellos que consumen alcohol de forma moderada desarrollan un trastorno por abuso de alcohol y define el consumo por atracón como aquel que eleva los niveles de alcohol en sangre a 0.08 g/dL en un periodo de dos horas (cuatro bebidas en mujeres y cinco en hombres). La administración de abuso de sustancias y de salud mental de Estados Unidos (*Substance Abuse and Mental Health Services Administration*, SAMHSA) estipula como consumo excesivo de alcohol cinco o más episodios de consumo de tipo atracón en un mes.

Como se ha comentado previamente, el desarrollo de un trastorno adictivo combina factores genéticos, ambientales y del propio desarrollo individual. Existen diversas teorías del desarrollo de la adicción como la teoría hedónica (Koob y col., 1997), la sensibilización (Kalivas y col., 1991) y la contra adaptación (Koob y col., 1997) entre otras; sin embargo, ninguna de ellas explica completamente el ciclo de la conducta adictiva (Harricharan y col., 2017). Paralelamente, existen estudios que tratan de identificar los factores genéticos involucrados en los procesos de desarrollo de la adicción, especialmente en el caso del alcohol a través de estudios del genoma completo (GWAS, del inglés *Genome-wide association study*) (Walters y col., 2018). La epigenética también juega un papel fundamental en el estudio del desarrollo de las adicciones a estimulantes, opiáceos, alcohol y nicotina (Mews y col., 2017; Walker y col., 2012).

1.1. Consecuencias del consumo de drogas en el sistema nervioso central. Efectos comportamentales y neuroadaptativos.

La barrera hematoencefálica (BHE) juega un papel fundamental en las funciones cerebrales. Se la considera como un sensor de la homeostasis y cualquier alteración que se produzca en el cerebro puede provocar su disfunción. Los componentes de la BHE son células endoteliales, pericitos y astrocitos embebidos en una malla de matriz extracelular. La BHE junto con el fluido cerebroespinal constituyen la barrera responsable del transporte selectivo de iones y de mediadores encargados de la homeostasis cerebral, transporte de nutrientes y hormonas (Thurgur y col., 2019). La BHE limita la entrada de moléculas en el sistema nervioso central (SNC), aunque en condiciones de desequilibrio, como son los procesos neuroinflamatorios, esta permeabilidad puede verse afectada (Strazielle y col., 2016; Thurgur y col., 2019). Una consecuencia directa de un mal funcionamiento de estas barreras protectoras del SNC es la pérdida de sus propiedades homeostáticas y neuroprotectoras. Se ha demostrado que la inflamación cerebrovascular y la alteración de la BHE son dos factores que contribuyen en gran medida a los desórdenes del SNC (Thurgur y col., 2019).

En este sentido, el abuso crónico de alcohol afecta a la integridad de la BHE, lo que puede provocar el incremento del flujo de mediadores proinflamatorios y leucocitos al interior de las estructuras cerebrales (Obad y col., 2018). Otras drogas como los opiáceos o, especialmente, los derivados de la amfetamina provocan una marcada disrupción de la BHE a nivel de la corteza, el hipocampo, el tálamo, el hipotálamo, el cerebelo y la amígdala (Bowyer y col., 2006; Cadet y col., 2009; Kiyatkin y col., 2007; Sharma y col., 2007).

Algunas de las variables que determinan los efectos deletéreos del consumo excesivo de alcohol sobre el sistema nervioso son la cantidad de alcohol consumido y la frecuencia del consumo, la edad a la que se ha iniciado el consumo, el historial familiar (Keenan y col., 1997), la exposición prenatal y los factores genéticos (Haddad y col., 2008; Hommer, 2003; Lemstra y col., 2008; Obad y col., 2018; Oscar-Berman y col., 2005; Zeigler y col., 2005). Está ampliamente descrito que el consumo abusivo de alcohol provoca un gran número de patologías degenerativas (Obad y col., 2018). Estudios *post-mortem* en cerebros de personas alcohólicas y en modelos animales de alcoholismo han demostrado que el consumo abusivo de alcohol está asociado con un incremento de la incidencia de miopatías y neuropatías (Crews y col., 2004; Fernandez-Sola y col., 2016; Liu y col., 2004; Liu y col., 2006; Obad y col., 2018; Remick, 2013). El abuso de alcohol provoca el desarrollo de neuroinflamación (Obad y col., 2018) y un desequilibrio del sistema inmune innato mediado, en parte, por la liberación de agonistas endógenos de los TLRs (del inglés *Toll-like receptors*) (Coleman y col., 2018b; Crews y col., 2017; Crews y col., 2016). La activación de estos receptores contribuye al incremento de la liberación de citoquinas, a alteraciones en la estructura y función del hipocampo, al daño neuronal y la consiguiente disminución del tamaño cerebral (Obad y col., 2018), y a problemas de memoria y de las

capacidades de aprendizaje (Eckardt y col., 1998; Nolen-Hoeksema y col., 2006; Wilkinson y col., 1980).

El desarrollo de una respuesta neuroinmune exacerbada y los procesos neuroinflamatorios asociados, se observan también tras la administración de otras drogas de abuso, lo que parece contribuir a las complicaciones neuropsiquiátricas que estas generan. Por ejemplo, las drogas de tipo anfetamínico, especialmente las más neurotóxicas como la metanfetamina, provocan una activación microglial y astrocítica muy marcada (Cadet y col., 2009), lo que contribuye a su neurotoxicidad. Del mismo modo, la anfetamina también modula la neuroinflamación, aumentando la reactividad astrocitaria (Vicente-Rodriguez y col., 2016b) y microglial (Shanks y col., 2012). Los efectos neurotóxicos derivados de este tipo de drogas de abuso también pueden contribuir a procesos neurodegenerativos que se han observado en el cerebro de pacientes adictos a este tipo de sustancias (Cadet y col., 2009).

2. Neuroinflamación y neuroprotección.

La inflamación es un componente clave en el proceso de reparación del tejido nervioso. Sin embargo, cuando se prolonga excesivamente, puede tener efectos negativos en el SNC (Fernandez-Calle y col., 2017; Szepesi y col., 2018) (Figura 1). En el proceso neuroinflamatorio están implicados tanto el componente innato como el adaptativo de la respuesta inmune (Amor y col., 2014; Fakhoury, 2015; Kumar, 2019), así como neuronas, macroglía (astrocitos y oligodendrocitos) (Ramírez-Exposito y col., 1998) y microglía (Shabab y col., 2017). La respuesta inmune innata constituye la primera línea de defensa del organismo frente a patógenos, es una reacción inmune antígeno-específica y juega un papel esencial en la subsecuente activación de las respuestas inmunes adaptativas. En la respuesta inmune adaptativa, la respuesta ante ese determinado antígeno será más eficiente debido a la memoria inmunológica (Iwasaki y col., 2015).

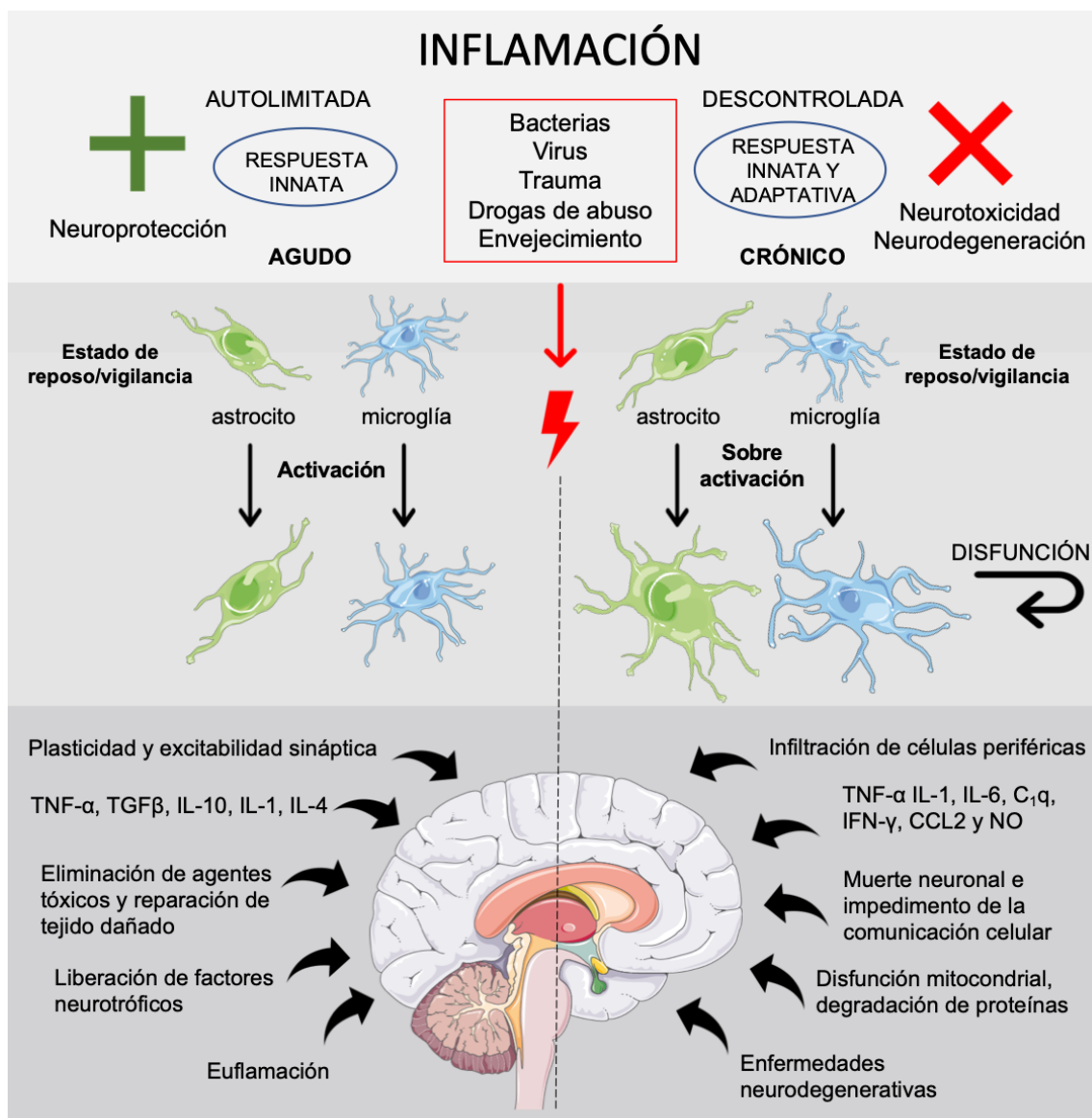


Figura 1. Efectos positivos y deletéreos de la inflamación en el SNC. La inflamación puede desencadenarse en respuesta a la presencia de patógenos externos como bacterias o virus, a un traumatismo, a la exposición a drogas de abuso o debido a factores internos como el envejecimiento, entre otros. El panel de la izquierda representa los efectos positivos de la inflamación, cuando esta tiene lugar de forma autolimitada y favorece la neuroprotección. Las células gliales, astrocitos y microglía pasan de un estado de reposo a uno activado y favorecen procesos como la plasticidad y excitabilidad sináptica, liberación de citoquinas pro y antiinflamatorias y de factores neurotróficos, eliminación de los agentes tóxicos y reparación del daño. Sin embargo, cuando la respuesta inflamatoria tiene lugar de forma descontrolada (panel derecho), la microglía y astrocitos adquieren un estado de hiperactivación disfuncional, en el que se va a impedir la comunicación celular, se incrementa demasiado la producción de citoquinas proinflamatorias, y se generan especies reactivas de oxígeno que van a provocar disfunción mitocondrial, degradación de proteínas y muerte neuronal. Así, la neuroinflamación crónica de alta intensidad es un rasgo característico de enfermedades neurodegenerativas. TNF- α (factor de necrosis tumoral α), TGF- β (factor de crecimiento transformador β) e IL- (interleucina), C₁q (factor 1 del complemento), IFN- γ (interferón- γ), CCL2 (C-C motif chemokine 2), NO (óxido nítrico).

La neuroinflamación se caracteriza por la activación de las células gliales, principalmente astrocitos y microglía, en respuesta a un daño en el SNC, independientemente que su origen sea infeccioso (Kumar, 2019), traumático (Chiu y col., 2016) o por contacto con neurotoxinas como algunas drogas de abuso (Xu y col., 2017b) (Figura 1). La activación de estas células gliales contribuye a la producción de una serie de mediadores proinflamatorios para limitarlo y recuperar la homeostasis. Durante este proceso, la BHE se puede ver comprometida y contribuir a la infiltración de células inmunes periféricas que a su vez pueden potenciar el proceso neuroinflamatorio (DiSabato y col., 2016; Hawkins y col., 2005; Michael y col., 2016; Monahan y col., 2008). Dicho proceso está mediado por varias citoquinas como la interleucina 1 β (IL-1 β), IL-6 y el factor de necrosis tumoral- α (TNF- α), quimiocinas como CCL (del inglés *C-C motif chemokine*) -2 y -5 y CXCL1 (del inglés *C-X-C motif ligand 1*). También se liberan mensajeros secundarios como NO (óxido nítrico), prostaglandinas y especies reactivas de oxígeno (ROS) (DiSabato y col., 2016; Norden y col., 2016).

Existe una estrecha relación entre astrocitos y microglía, y el equilibrio entre estos dos tipos celulares mantiene la homeostasis del SNC (Markiewicz y col., 2006). Durante mucho tiempo se creyó que los astrocitos eran un elemento pasivo de la estructura cerebral y que únicamente procuraban soporte estructural y metabólico a las neuronas. Sin embargo, se ha demostrado que están implicados en importantes procesos como la regulación de la respuesta neuroinmune, la homeostasis iónica y de neurotransmisores, la regulación de la energía metabólica en el cerebro, la transmisión y generación sináptica, la excitabilidad neuronal, procesos de detoxificación y de eliminación de radicales libres, y el mantenimiento de la estructura de la BHE (Markiewicz y col., 2006). Los astrocitos son capaces de producir diversas citoquinas proinflamatorias y antiinflamatorias (Zhang y col., 2019). Además, cuando el SNC sufre un daño, se produce una transformación en los astrocitos denominada astrocitosis reactiva o astrogliosis, proceso que conlleva una hipertrofia y proliferación astrocitaria, un alargamiento de sus terminaciones y un incremento en la expresión de la proteína ácida fibrilar de la glía (del inglés *glial fibrillary acidic protein* o GFAP) (Liberto y col., 2004; Markiewicz y col., 2006; Ridet y col., 1997). La activación de los astrocitos también contribuye a la activación microglial (Xing y col., 2018).

Las células microgliales son los macrófagos residentes del SNC y juegan un papel fundamental en la reparación de tejidos y defensa del organismo. Son las células responsables de la activación de la respuesta inmune innata y adaptativa mediante la liberación de mediadores proinflamatorios (Lehnardt, 2010). La microglía representa el 5-12% de las células totales del SNC sano y derivan de células precursoras mieloides que se dirigen al SNC durante el proceso de embriogénesis (Ginhoux y col., 2015; Kierdorf y col., 2013). Además de mantener la homeostasis cerebral junto con los astrocitos, la microglía está implicada en la maduración neuronal durante el desarrollo y puede desempeñar interacciones bidireccionales con otros tipos celulares del SNC (Ginhoux y col., 2013). Cualquier cambio en el ambiente cerebral puede

desencadenar la activación microglial, que puede resultar nociva si no se regula adecuadamente (Ginhoux y col., 2015).

El término de microglía “en reposo” se utiliza comúnmente para describir las células microgliales en estado basal. Sin embargo, este término no es adecuado, ya que en condiciones fisiológicas estas células se encuentran contrayendo y extendiendo sus prolongaciones, gracias a su citoestructura única que les permite abarcar todo el parénquima. Por tanto, resulta más apropiado referirse a un estado de vigilancia de la microglía. En respuesta a un daño, la microglía evoluciona a una estructura de tipo ameboidea caracterizada por un mayor tamaño del soma y las terminaciones celulares retraídas (Hanisch y col., 2007; Zanier y col., 2015). Tradicionalmente se ha descrito que la microglía puede presentar dos estados fenotípicos (M1 y M2) basados en las moléculas de superficie que presenten y en el tipo de compuestos que secreten (Franco y col., 2015). El estado M1 se corresponde con un estado proinflamatorio en el que la microglía libera ROS, especies reactivas de nitrógeno, TNF- α , IL-1 β o IL-12, mientras que el fenotipo M2 se considera antiinflamatorio y está implicado en la producción y liberación de factores tróficos como el factor de crecimiento transformador β (TGF- β) y el factor neurotrófico cerebral (BDNF) (Bachiller y col., 2018; Tang y col., 2016). Actualmente, este tipo de clasificación fenotípica no se considera del todo correcta puesto que se ha demostrado que la microglía puede presentar ambos fenotipos simultáneamente dependiendo de los estímulos a los que esté sometida (Chen y col., 2016; Morganti y col., 2016).

La transición de la microglía de un estado quiescente a un estado activado está estrechamente relacionada con factores que pueden ser internos como, por ejemplo, factores de transcripción, o factores externos, ya sean factores neuronales como la proteína CD200 (proteína del grupo de diferenciación 200), Fraktalkina o también denominada CX3CR1 (receptor de quimiocinas CX3C 1, del inglés *CX3C chemokine receptor 1*), o receptores como TREM2 (receptor detonante expresado en células mieloides 2, del inglés *triggering receptor expressed on myeloid cells 2*) (Kierdorf y col., 2013). Existen otros factores, como el origen del daño, el trasfondo genético, los factores ambientales, la edad o eventos anteriores que pueden modificar el efecto de la activación microglial y de las vías de señalización neuroinflamatorias (Brad y col., 2003; Carson y col., 2006; Shabab y col., 2017).

Mención aparte merecen los TLRs, receptores de reconocimiento de patógenos presentes tanto en astrocitos como microglía que median la respuesta inmune innata y la adaptativa. A través de ellos, la microglía detecta patrones moleculares asociados a daño o DAMPS (del inglés *danger associated molecular patterns*) y patrones moleculares asociados a patógenos o PAMPs (del inglés *pathogen-associated molecular patterns*) (Lehnardt, 2010). La activación de los TLRs en la microglía está considerada como uno de los enlaces entre la neuroinflamación y el daño neuronal (Lehnardt y col., 2006). Se conocen al menos 13 tipos distintos de TLRs en mamíferos (Kawai y col., 2008; Lehnardt, 2010), de los que Medzhitov y colaboradores (1997) descubrieron que TLR4 inicia la respuesta inmune innata en respuesta a infecciones. TLR4 es el receptor del lipopolisacárido (LPS), componente mayoritario de la

membrana externa de las bacterias Gram negativas. El tratamiento intraperitoneal con LPS constituye uno de los modelos animales más utilizados para estudiar la neuroinflamación (Hamasaki y col., 2018). Es importante destacar que la microglía es uno de los tipos celulares del SNC que presenta mayor expresión de TLR4 (Jack y col., 2005), aunque también se ha detectado su expresión en astrocitos, fibroblastos, células endoteliales, macrófagos y neuronas sensoriales (Lacagnina y col., 2018; Shen y col., 2016).

La activación celular de TLR4 implica una serie de cambios conformacionales que desencadenan una cascada de señalización intracelular que resulta en la activación de NF- κ B (factor nuclear potenciador de las cadenas ligeras kappa de las células B activadas) (Kawai y col., 2007; Lehnardt, 2010; Lu y col., 2008). Estas respuestas pueden tener lugar a través de la activación de dos vías, la vía en la que interviene la proteína adaptadora MyD88 (del inglés *Myeloid differentiation primary response 88*), llamada vía dependiente de MyD88, o por la vía independiente de MyD88. En la vía dependiente de MyD88, MyD88 recluta a las proteínas IRAK-4 e IRAK-1 (del inglés *IL-1 receptor-associated kinase*), a las proteínas TRAF-6 (del inglés *TNF receptor-associated factor*), TAK1 (del inglés *transforming growth factor- β -activated kinase 1*) y por último, al complejo proteico IKK (I- κ B quinasa) y a la vía de las MAPK (del inglés *Mitogen-Activated protein kinases*), que estarán implicadas en la producción de citoquinas inflamatorias. En la vía independiente de MyD88 intervienen las proteínas TRAM (del inglés *TRIF-related adaptor molecule*), TRIF (del inglés *Toll-interleukin-1 receptor domain-containing adaptor protein*), RIP1 (del inglés *receptor interacting protein 1*), TRAF-3, MAPK e IKKs (del inglés *inhibitory kappa B kinases*) entre otras (Lu y col., 2008). La mayoría de las respuestas del sistema inmune innato frente a LPS van a ser operadas por la vía independiente de MyD88 y se dice que esta vía es un activador lento de NF- κ B y de la secreción de TNF- α (Kumar, 2019). Estas vías de señalización van a dar como resultado la sobreexpresión de genes proinflamatorios que codifican citoquinas, quimiocinas, enzimas y otras moléculas para contrarrestar el daño que se esté produciendo en el SNC (Akira y col., 2006; Takeuchi y col., 2001).

La duración y la intensidad del estímulo inflamatorio determinarán si el impacto sobre el SNC será negativo (Figura 1). La inflamación es una respuesta multietapa que cuando se auto limita resulta beneficiosa y neuroprotectora, una vez se ha eliminado el estímulo nocivo. Como se resume en la Figura 1, la activación de la microglía contribuye a la eliminación de agentes tóxicos y neuronas apoptóticas, y libera factores neurotróficos y citoquinas inflamatorias como TNF- α , que participa en el mantenimiento de la excitabilidad y la plasticidad sináptica (Camara y col., 2013). Los astrocitos y la microglía también liberan TGF- β e IL-10, que promueven la supervivencia neuronal y modulan la activación microglial para que esta no se descontrole (Burmeister y col., 2018; Norden y col., 2014). Tal es la importancia del control de la activación microglial y la neuroinflamación que se ha observado que, si se expone al organismo a patógenos que inducen niveles bajos de activación inmune, esto podría conferir mayor resistencia a futuras infecciones y limitar la neuroinflamación deletérea inducida por endotoxinas; este fenómeno se definió como euflamación (Figura 1) (Liu y col., 2016; Tarr y col., 2014). Como hemos comentado,

la sobre activación de astrocitos y microglía provoca daño neuronal directo y citotoxicidad junto con la disrupción de la BHE (Sumi y col., 2010), lo que va a permitir la infiltración de células periféricas en el SNC. La amplificación de la respuesta inflamatoria resultante provoca alteraciones en la interacción entre astrocitos y microglía, eliminando la actividad supresora de los astrocitos sobre la reactividad microglial y una producción descontrolada de citoquinas proinflamatorias, contribuyendo a potenciar aún más la neuroinflamación (Sochocka y col., 2017).

2.1. Relación del consumo de alcohol y otras drogas de abuso con la neuroinflamación.

El alcohol desencadena una respuesta inflamatoria que conlleva un estado de hiperinflamación (Obad y col., 2018). Muchos estudios de diferentes grupos han corroborado que esta respuesta se debe a la activación microglial a través de TLR4 y la cascada de señalización, que finaliza con la translocación nuclear de NF- κ B y la liberación de citoquinas y mediadores inflamatorios como IL-1 β , TNF- α , COX-2 (ciclooxigenasa 2), CCL2 e iNOS (óxido nítrico sintasa inducible) (Blanco y col., 2008; Fernandez-Lizarbe y col., 2009; Lawrimore y col., 2019). La neuroinflamación inducida por el alcohol contribuye al elenco de patologías relacionadas con el consumo excesivo de esta sustancia (Tyler y col., 2019) y se cree que puede tener un papel importante en el desarrollo de la adicción al alcohol (Flores-Bastias y col., 2018).

La neuroinflamación derivada del uso de otras sustancias con potencial adictivo como la morfina también está mediada por TLR4. La morfina induce la liberación de múltiples citoquinas inflamatorias y una marcada activación astrocítica en diversas áreas cerebrales, lo que se cree que puede contribuir al desarrollo de tolerancia y adicción al opiáceo (García-Perez y col., 2017; Qu y col., 2017). En el caso del cannabis, múltiples estudios demuestran que el consumo de delta-9 tetrahidrocannabinol (Δ -9-THC) durante la adolescencia puede predisponer al desarrollo de trastornos neuropsiquiátricos en adultos. En modelos animales se ha demostrado que el THC induce una neuroinflamación persistente en la corteza prefrontal (CPF) caracterizada por una elevada expresión de TNF- α , iNOS y COX-2, y una reducción en la expresión de citoquinas antiinflamatorias como IL-10 (Moretti y col., 2015; Zamberletti y col., 2015).

En cuanto a los psicoestimulantes más consumidos, hay que señalar que la cocaína induce estrés oxidativo y potencia la neuroinflamación a través de la activación de las células gliales y la producción de mediadores inflamatorios tanto por células gliales como no gliales, como los pericitos (Guo y col., 2015; Sil y col., 2019). Estudios recientes sugieren que los efectos adictivos de la cocaína están modulados a través de TLR3 (Zhu y col., 2018). Como se ha comentado previamente, el consumo de anfetamina y sus derivados provoca activación microglial y astrocítica, induciendo neuroinflamación y efectos neurotóxicos (Moratalla y col., 2017). Existen evidencias crecientes que indican que la activación microglial juega un papel fundamental en la neurotoxicidad inducida por anfetamina, ya que precede a la degeneración neuronal y a la activación astrocítica (Xu y col., 2017a). La anfetamina provoca activación microglial y astrogliosis en diversas áreas cerebrales como el cuerpo estriado, hipocampo, CPF y Sustancia Negra (SN) (Cadet y col., 2007; Krasnova y col., 2005; Moratalla y col., 2017). En

cultivos primarios de astrocitos se ha detectado que la anfetamina eleva la expresión de Caspasa-11 y TLR4, potencia la activación de las vías mediadas por este receptor y aumenta la producción de citoquinas proinflamatorias (Bortell y col., 2017; Papageorgiou y col., 2019). Además, la anfetamina induce altos niveles de estrés oxidativo y generación de radicales libres que desencadenarán la toxicidad celular y la disfunción mitocondrial (Cadet y col., 1998; Moratalla y col., 2017). Todo lo anterior contribuye a la conocida neurotoxicidad de este tipo de drogas que puede variar desde denervación dopaminérgica estriatal en el caso de la anfetamina, a pérdida de neuronas dopaminérgicas de la SN en el caso de sus derivados más neurotóxicos como la metanfetamina (Ares-Santos y col., 2014; Moratalla y col., 2017).

Por lo tanto, se puede concluir de forma general, que la exposición prolongada a drogas de abuso potencia la neuroinflamación e incrementa la susceptibilidad al desarrollo de patologías que cursan con neuroinflamación. En este sentido, el desarrollo de estrategias terapéuticas encaminadas a modular la neuroinflamación resultan esenciales para el tratamiento de enfermedades con componente neuroinflamatorio, como son las enfermedades neurodegenerativas y los trastornos derivados del consumo de drogas de abuso.

2.2. Pleiotrofina (PTN) y Midkina (MK).

Las citoquinas pleiotrofina (PTN) y midkina (MK) son los dos únicos miembros de una misma familia de factores de crecimiento de unión a la heparina (Deuel y col., 2002). Ambas citoquinas se encuentran sobreexpresadas en cerebro en distintas patologías centrales que cursan con un importante componente neuroinflamatorio como la enfermedad de Parkinson (EP), la enfermedad de Alzheimer o el infarto cerebral (Herradón & Pérez-García, 2014; Herradón y col., 2019).

La PTN también se conoce como p18, HBGF8 (del inglés *heparin-binding growth factor 8*), HB-GAM (del inglés *heparin-binding growth-associated molecule*), factor 1 osteoblasto-específico, HB-NF (del inglés *heparin binding neurotrophic factor*) o HARP (del inglés *heparin affin regulatory peptide*) (Mikelis y col., 2007; Papadimitriou y col., 2009). Es una proteína de 18 kDa, compuesta por 136 aminoácidos, que se secreta poco después de su síntesis por la maquinaria intracelular. La MK se conoce también como NEGF2 (del inglés *neurite growth-promoting factor 2*) (Tang y col., 2015). Es una proteína de 13 kDa, compuesta por 121 aminoácidos. La PTN y la MK presentan una homología del 50% en su secuencia de aminoácidos, lo que implica que en muchos casos presenten funciones similares (Li y col., 1990; Muramatsu, 2014; Xu y col., 2014).

La PTN está implicada en la supervivencia de las células B, hematopoyesis, haplotaxis de los macrófagos y neutrófilos, en el crecimiento de neuritas y su migración y en el proceso de la angiogénesis (Papadimitriou y col., 2016; Sorrelle y col., 2017). De hecho, la capacidad angiogénica de la PTN juega un papel muy importante en los efectos de esta proteína en distintos tipos de cáncer (Papadimitriou y col., 2009). La PTN también está implicada en la regeneración

de axones tras un daño en el SNC (Mi y col., 2007) y ejerce efectos neurotróficos en los trasplantes neuronales *in vivo* (Hida y col., 2007). La PTN, producida por pericitos, es imprescindible para limitar el daño de tipo isquémico o excitotóxico (Nikolakopoulou y col., 2019). Se ha demostrado que la PTN está implicada en la maduración neuronal que tiene lugar en los nichos neurogénicos cerebrales, lo cual resulta muy importante en los procesos de memoria, aprendizaje y conducta afectiva (Tang y col., 2019).

La MK juega un papel importante en el crecimiento de neuritas y participa en la migración y supervivencia neuronal (Kikuchi y col., 1993; Muramatsu y col., 1991; Owada y col., 1999; Satoh y col., 1993; Zou y col., 2006). Está implicada en la migración de macrófagos y neutrófilos e inhibe la diferenciación de las células T-reguladoras (Horiba y col., 2000; Sato y col., 2001; Takada y col., 1997). La MK también participa en la regeneración de nervios periféricos (Sakakima y col., 2009) y en la protección contra el daño cerebral ocasionado por isquemia (Muramatsu, 2011; Ooboshi, 2011). Al igual que la PTN, y por similitud de funciones, también se la relaciona con el crecimiento tumoral (Hao y col., 2013).

La PTN y la MK presentan niveles altos de expresión en neuronas y glía durante el desarrollo embrionario del SNC (Li y col., 1990; Milner y col., 1989), aunque sus patrones de expresión difieren. El pico de expresión de la MK se produce durante la etapa media de la gestación mientras que el de la PTN ocurre en el momento del nacimiento (Rauvala, 1989; Weckbach y col., 2011). La PTN se expresa durante la fase embrionaria en otros tejidos además del cerebro, como pulmón, riñones, intestino y hueso (Mikelis y col., 2007; Papadimitriou y col., 2016), mientras que la expresión de MK durante la fase embrionaria destaca en el tejido neural, epitelial y mesenquimal (Muramatsu, 2010).

En la etapa adulta los niveles de expresión de la PTN y la MK disminuyen considerablemente y se restringen a ciertos tipos celulares, observándose una mayor expresión de la PTN en el SNC (concretamente en las neuronas y pericitos), la placenta, el tejido seminal y los testículos, el ojo, la vejiga y el estómago (Nikolakopoulou y col., 2019; Papadimitriou y col., 2016). Los niveles de expresión de la MK en el adulto son relativamente bajos; sin embargo, se encuentran niveles detectables de MK en riñones, intestino, epidermis, epitelio bronquial y en otras células como linfocitos y macrófagos. La MK va a participar en los procesos inflamatorios con dos actividades principales, incrementando la expresión de citoquinas y potenciando la migración de neutrófilos y macrófagos (Muramatsu, 2014).

La expresión de ambos genes es constitutiva y ambos se sobreexpresan en situaciones de daño en distintos tipos de tejidos. Existen diversos factores y citoquinas que pueden provocar un aumento de los niveles de expresión de PTN, como TNF- α o el factor de crecimiento epidérmico EGF (del inglés *epidermic growth factor*) (Papadimitriou y col., 2009), el interferón- γ (IFN- γ), el cual incrementa la expresión de PTN en macrófagos a través de STAT-1 (transductor de señal y activador de la transcripción 1) (Li y col., 2010), PDGF (factor de crecimiento derivado de las plaquetas, del inglés *platelet-derived growth factor*) y bFGF (el factor básico de crecimiento de fibroblastos, del inglés *basic fibroblast growth factor*) (Antoine y col., 2005; Li y col., 1992).

Por su parte, el ácido retinoico es el principal inductor de la expresión del gen de la MK (Matsubara y col., 1994).

Como hemos apuntado, los niveles de expresión de PTN y MK pueden aumentar como respuesta a distintos tipos de daño (Herradon y col., 2014; Herradon y col., 2019; Vicente-Rodriguez y col., 2016a). Se incrementan en las áreas tisulares expuestas a un daño y en diversas células como macrófagos inflamatorios, microglía, fibroblastos y células endoteliales (Jin y col., 2009; Martin y col., 2011; Muramatsu, 2011). La expresión de la MK aumenta en múltiples patologías inflamatorias de tipo crónico como en la enfermedad de Alzheimer (Salama y col., 2005), la enfermedad de Crohn (Krzystek-Korpaczka y col., 2010), la nefropatía diabética (Kosugi y col., 2007) o la esclerosis múltiple (Liu y col., 1998; Wang y col., 2008). En algunas de ellas, se ha empezado a dilucidar el papel que esta citoquina juega en la patología. En la enfermedad de Alzheimer, por ejemplo, la MK inhibe la citotoxicidad y polimerización del péptido β -amiloide (Monji y col., 2000; Yu y col., 1998). Asimismo, la deficiencia de MK se ha relacionado con una hipofunción dopaminérgica cerebral (Ohgake y col., 2009).

Por su parte, se han detectado altos niveles de PTN en la SN en pacientes con EP (Marchionini y col., 2007) o en modelos animales de isquemia cerebral (Yeh y col., 1998). Ensayos *in vitro* han demostrado que la PTN ejerce un efecto neurotrófico significativo sobre las neuronas dopaminérgicas (Jung y col., 2004). En modelos animales, la sobreexpresión estriatal de PTN ejerce un efecto neurotrófico y protege frente a agentes parkinsonianos (Gombash y col., 2012; Taravini y col., 2011).

2.2.1. Papel de PTN y MK en los efectos de las drogas de abuso.

Como se ha descrito anteriormente, las drogas de abuso producen efectos neurotóxicos, alteraciones en las vías del sistema de recompensa, desarrollo de neuroinflamación y neurodegeneración (Coelho-Santos y col., 2012; Mohammad Ahmadi Soleimani y col., 2016; Sharma y col., 2018).

Los niveles de expresión de PTN y MK aumentan significativamente en distintas áreas cerebrales como la CPF, hipocampo o el cuerpo estriado, después de la administración de distintas drogas de abuso como la anfetamina, los opiáceos o el cannabis (Herradon y Pérez-García, 2014). Además, se ha visto que una dosis aguda de alcohol (2g/kg) en ratones provoca un aumento significativo de los niveles de Ptn en la CPF (Vicente-Rodriguez y col., 2014a). Por otra parte, se ha demostrado la sobreexpresión de MK en la corteza frontal de pacientes alcohólicos (Flatscher-Bader y col., 2006, 2008). Estas evidencias, junto a las resumidas anteriormente que apuntan a importantes efectos neuroprotectores de PTN y MK en distintos contextos patológicos, sugieren que estas citoquinas podrían modular los efectos neurotóxicos y neuroadaptativos de las drogas de abuso.

En modelos *in vitro* se ha demostrado que la PTN previene la citotoxicidad inducida por cocaína en cultivos de células NG108-15 y PC12 (Gramage y col., 2008). También se han

estudiado las acciones de PTN y/o MK sobre los efectos de las drogas de abuso utilizando distintos modelos de animales modificados genéticamente como el ratón *knock-out* de Ptn ($Ptn^{-/-}$), el ratón *knock-out* de Mk ($Mk^{-/-}$) (Amet y col., 2001; Herradon y col., 2004; Nakamura y col., 1998) o el ratón transgénico de PTN (PTN-Tg), que sobreexpresa esta citoquina en áreas específicas del cerebro, como la CPF y el hipocampo (3 veces mayor expresión que en un animal Wt) y en el cuerpo estriado (20% más de expresión que en animales Wt) (Ferrer-Alcón M y col., 2012; Vicente-Rodriguez y col., 2015; Vicente-Rodriguez y col., 2014a). En estos estudios, se ha comprobado que la amfetamina induce una astrocitosis estriatal más exacerbada en los ratones $Mk^{-/-}$ y $Ptn^{-/-}$ comparado con los ratones salvajes o Wt (del inglés *wild-type*) (Gramage y col., 2011b; Gramage y col., 2010b). Resulta interesante resaltar que en el caso de los animales $Ptn^{-/-}$, la amfetamina induce la pérdida de neuronas dopaminérgicas en la SN, efecto ausente en los ratones Wt (Gramage y col., 2010b), ya que únicamente derivados anfetamínicos más neurotóxicos que la amfetamina son capaces de provocar la pérdida de neuronas dopaminérgicas de la SN (Ares-Santos y col., 2014; Granado y col., 2008). Por tanto, estos resultados apuntan a un posible papel neuroprotector de la PTN y la MK frente a la neurotoxicidad causada por drogas de abuso y a un papel modulador de estas citoquinas en neuroinflamación.

Respecto a los efectos reforzadores de las drogas de abuso, cabe destacar que la PTN y la MK también regulan los efectos comportamentales de distintas drogas (Gramage y col., 2011a). Uno de los ensayos más habituales para estudiar las propiedades reforzadoras de las drogas es el paradigma del condicionamiento preferencial al sitio (del inglés *Conditioned Place Preference*, CPP) (Tzschentke, 2007). En modelos de CPP, se observó que los ratones $Ptn^{-/-}$ presentan más dificultades para extinguir el condicionamiento inducido por amfetamina que los ratones Wt (Gramage y col., 2010a). Por su parte, los ratones $Mk^{-/-}$ presentan más dificultades para extinguir el condicionamiento inducido por cocaína (Gramage y col., 2013). En cuanto al efecto reforzador del alcohol, los animales $Ptn^{-/-}$ y $Mk^{-/-}$ resultan más vulnerables, mientras que los efectos reforzadores del alcohol se encuentran ausentes en los ratones PTN-Tg (Vicente-Rodriguez y col., 2014a; Vicente-Rodriguez y col., 2014b).

Las evidencias aquí resumidas apuntan a las citoquinas PTN, MK y sus vías de señalización como posibles dianas farmacológicas para la modulación de los efectos comportamentales y neurotóxicos de las drogas de abuso.

2.2.2. Mecanismo de acción de PTN y MK.

Se conocen varios receptores para la PTN y la MK (Figura 2) (Xu y col., 2014). La MK es un ligando endógeno del receptor proteína fosfatasa de tirosinas β/ζ (RPTP β/ζ), también conocido como PTPRZ1 (del inglés *protein tyrosine phosphatase receptor Z1*) (Maeda et al., 1999). La MK puede también interactuar con los miembros de la familia de receptores relacionados con la lipoproteína de baja densidad (LRP), que están implicados en la supervivencia de neuronas embrionarias; con integrinas $\beta 1$, como la $\alpha 6\beta 1$ o la $\alpha 4\beta 1$, relacionadas con el crecimiento de neuritas y con la migración de osteoblastos, respectivamente,

(Muramatsu, 2014; Weckbach y col., 2011). Otros receptores también incluyen Nucleolina (Hovanessian, 2006), el receptor NOTCH-2 (del inglés *Neurogenic locus notch homolog protein 2*), miembros de la familia de los receptores Syndecan (SDC) (Muramatsu y col., 2006) y ALK (del inglés *Anaplastic lymphoma kinase*) (Stoica y col., 2002). En este último caso es destacable que la interacción de la MK con ALK resulta fundamental en la proliferación de neuronas adrenérgicas inmaduras (Reiff y col., 2011) y en la activación de las vías de señalización que desembocan en la activación de NF- κ B (Kuo y col., 2007).

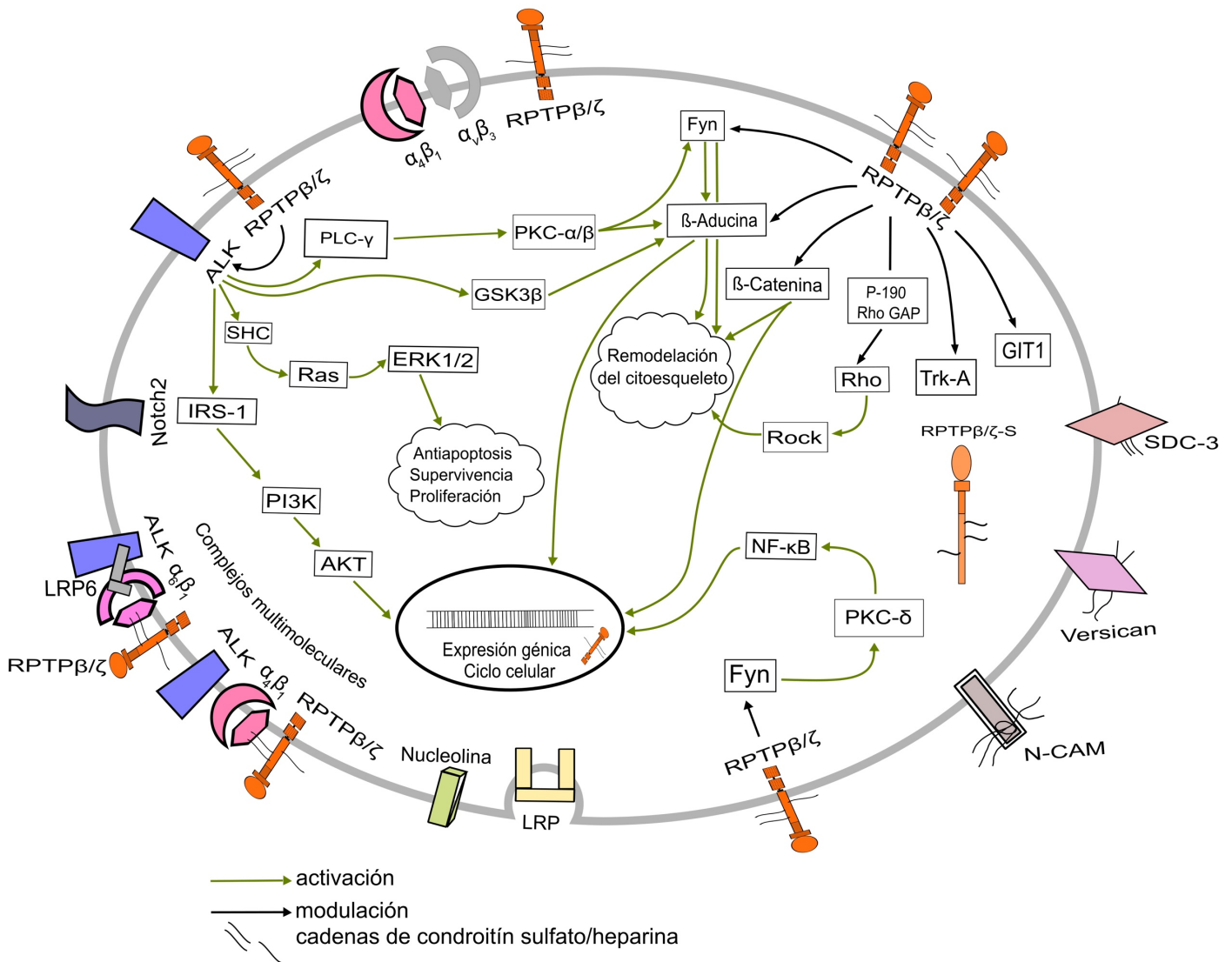


Figura 2. Representación de los receptores de la PTN/MK y sus vías de señalización más relevantes. La PTN y la MK, a través de distintos receptores, modulan diversas vías de señalización. Cuando actúan sobre RPTPβ/ζ (receptor proteína fosfatasa de tirosinas β/ζ, también conocido como PTPRZ1), inactivan su actividad fosfatasa, regulando así los niveles de fosforilación de los sustratos de este receptor como Fyn, β-*aducina*, β-*catenina*, P190 Rho/GAP (*GTP-ase-activating protein for Rho GTP-ase*), TrkA (*Tropomyosin receptor kinase A*) y GIT1 (de inglés *protein-coupled receptor kinase-interactor 1*). ALK (*anaplastic lymphoma kinase*) es otro sustrato de RPTPβ/ζ pero también es un receptor conocido de PTN/MK. A través de la modulación de ALK, PTN/MK regulan distintas vías implicadas en procesos relacionados con la supervivencia y proliferación celular. RPTPβ/ζ puede formar complejos multimoleculares cuando se asocia con integrinas o con miembros de la familia de los receptores para la lipoproteína de baja densidad (LRP) como LRP6 (receptor de lipoproteína 6). La PTN y la MK también pueden interactuar con NOTCH-2 (neurogenic locus notch homolog protein 2), nucleolina, N-CAM (molécula de adhesión neuronal cerebral) Versican y con SDC-3 (syndecan-3). Esquema modificado de Xu y col, 2014.

El primer receptor identificado para la PTN fue SDC-3 (Raulo y col., 1994), el cual está implicado en los efectos de PTN sobre el crecimiento de neuritas y en el papel oncogénico de PTN en cáncer de páncreas y de próstata (Yao y col., 2009). Se ha demostrado que la PTN puede interactuar directamente con las integrinas $\alpha\beta_3$, imprescindibles en la angiogénesis y en la migración celular (Mikelis y col., 2009). La PTN también se puede unir a RPTP β/ζ y ALK, como la MK (Maeda et al., 1996, Meng et al., 2000; (Stoica y col., 2001; Wellstein, 2012). Los mayores niveles de expresión de ALK se encuentran en los bulbos olfatorios, CPF, cuerpo estriado, hipocampo, tálamo y en los núcleos del mesencéfalo (Bilsland y col., 2008; Iwahara y col., 1997; Vernersson y col., 2006). Alteraciones en ALK se han asociado con diversos tipos de cáncer, como neuroblastoma, cáncer de pulmón o cáncer de mama (Chen y col., 2008; George y col., 2008; Lin y col., 2009; Roskoski, 2013; Soda y col., 2007) y con trastornos por abuso de alcohol (Lasek y col., 2011), ya que se encuentra implicado en la regulación de las propiedades reforzadoras del alcohol (Dutton y col., 2017), llegándose a considerar como una potencial diana para el tratamiento de desórdenes relacionados con el abuso de alcohol (Dutton y col., 2017; Wang y col., 2011). Como ya hemos apuntado, se ha propuesto que la activación de ALK por PTN/MK puede ser ligando-independiente, resultado de la interacción de PTN/MK con RPTP β/ζ (Perez-Pinera y col., 2007).

Uno de los receptores de PTN/MK más estudiados por su implicación en los efectos de estas citoquinas es RPTP β/ζ , que está implicado en el desarrollo de oligodendrocitos (Lamprianou y col., 2011) y en procesos neuroinflamatorios en el cerebro adulto (Harroch y col., 2002). Como ya hemos mencionado, PTN y MK inhiben la actividad fosfatasa de RPTP β/ζ provocando un aumento en los niveles de fosforilación de sus sustratos, algunos de los cuales juegan un papel importante en el consumo de alcohol como ha demostrado el grupo de la Dra. Dorit Ron en el caso de la quinasa Fyn (Morisot y col., 2018) y el grupo de la Dra. Amy Lasek en el caso de ALK (Dutton y col., 2017). Es importante señalar que RPTP β/ζ se encuentra principalmente expresado en el SNC en áreas importantes en el circuito de recompensa y el consumo de alcohol, como la CPF o la amígdala (Cressant y col., 2017). También se encuentra expresado en otros órganos como la piel, estómago y testículos, y su expresión no se correlaciona completamente con la expresión de PTN (Papadimitriou y col., 2016).

El receptor RPTP β/ζ forma parte de la familia de las proteínas tirosina fosfatasas (PTPs) (Tanga y col., 2019). La fosforilación reversible en los residuos de tirosina de las proteínas es uno de los mecanismos críticos en el proceso de transducción de la señal y afecta a funciones celulares tales como metabolismo, proliferación, adhesión, diferenciación, migración y desarrollo (Hunter, 1987; Xu y col., 2012). Este proceso se regula por el equilibrio entre las PTKs (proteínas tirosina quinasa) y las PTPs (Tanga y col., 2019). El desequilibrio entre PTKs y PTPs se encuentra implicado en un gran número de patologías humanas como cáncer, diabetes, y enfermedades autoinmunes (Ostman y col., 2006; Tonks, 2006; Xu y col., 2012).

La familia de los receptores proteína fosfatasa de tirosinas de transmembrana (RPTPs) comprende ocho subfamilias (Andersen y col., 2001) en las que la mayoría de los receptores

contienen dos dominios PTP intracelulares consecutivos. En los dominios PTP, la actividad catalítica se encuentra mayoritariamente en el primer dominio proximal de membrana (PTP-D1) y en menor medida en un segundo dominio distal de membrana (PTP-D2). Sin embargo, en la subfamilia número 5, a la que pertenece RPTP β/ζ , el dominio D2 es inactivo y se considera que su función es únicamente reguladora (Barr y col., 2009; Tanga y col., 2019; Tonks, 2006; Xu y col., 2012).

A nivel celular, RPTP β/ζ puede localizarse en la membrana, citoplasma y núcleo (Koutsoumpa y col., 2013) (Figura 2). En la membrana celular, puede interactuar con diferentes moléculas de adhesión celular como N-CAM (molécula de adhesión neuronal cerebral) (Beltran y col., 2003), Ng-CAM (molécula de adhesión neuro-glial) (Milev y col., 1995), nucleolina o contactina (Dubessy y col., 2019), entre otras (Figura 2). Existen tres isoformas mayoritarias de RPTP β/ζ que coexisten en el SNC (Figura 3). RPTP β/ζ -A constituye la isoforma larga del receptor, contiene un dominio N-terminal anhidrasa carbónica, un dominio de tipo fibronectina III localizado en la zona extracelular seguido por una región espaciadora, una región transmembrana y dos dominios PTP consecutivos localizados en el interior del citoplasma. RPTP β/ζ -B es la isoforma corta del receptor y presenta una supresión de la zona próxima a la región espaciadora extracelular de RPTP β/ζ -A. RPTP β/ζ -S es la isoforma secretora que se corresponde con la porción extracelular de RPTP β/ζ -A, también denominada 6B4 proteoglicano/fosfacan (Tanga y col., 2019). Las tres isoformas contienen cadenas de condroitín sulfato en la porción extracelular que resultan esenciales para conseguir una alta afinidad de unión con sus sustratos (Canoll y col., 1996; Chow y col., 2008; Maeda y col., 1999; Maeda y col., 1996; Nandi y col., 2013; Nishiwaki y col., 1998; Tanga y col., 2019). Existe una cuarta isoforma de RPTP β/ζ que también es secretada, pero de menor tamaño que RPTP β/ζ -S, llamada PSI (isoforma corta de fosfacán, del inglés *phosphacan short isoform*) y únicamente se expresa en neuronas (Garwood y col., 2003). Estudios funcionales sugieren que PSI está implicada en el control del crecimiento de los axones durante el desarrollo debido a su interacción con los receptores neuronales L1 y F3/contactina, y que promueve el crecimiento de neuritas de las neuronas corticales (Heck y col., 2005). Por otro lado, la isoforma PSI presenta dos lugares de unión para la PTN (Maeda y col., 1996), al igual que se ha demostrado que RPTP β/ζ también tiene dos zonas de unión para la MK (Maeda y col., 1999).

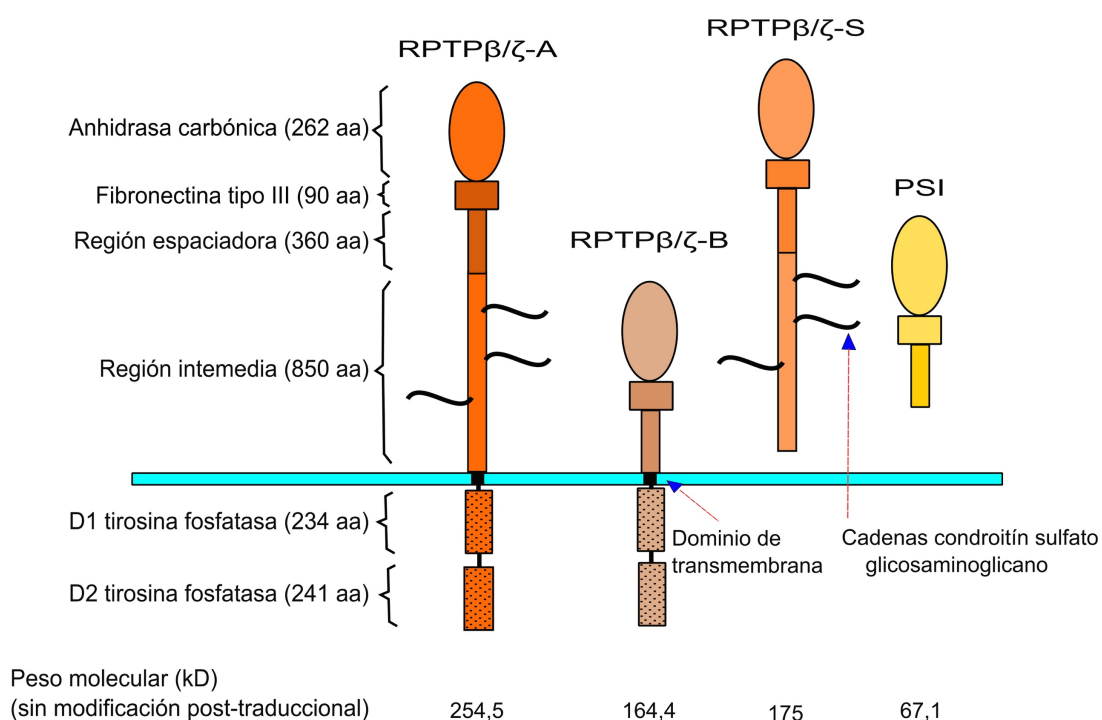


Figura 3. Representación esquemática de las isoformas de RPTPβ/ζ. Los cuatro tipos de isoformas (dos de transmembrana y dos secretadas) en las que se puede encontrar RPTPβ/ζ son la isoforma larga (RPTPβ/ζ-A), corta (RPTPβ/ζ-B), la isoforma secretada (RPTPβ/ζ-S), o también denominada fosfacan, y la isoforma PSI. Las cuatro isoformas tienen en común el dominio de anhidrasa carbónica y el de fibronectina tipo III. RPTPβ/ζ-A, consta también de una secuencia intermedia próxima al dominio transmembrana en la que incluyen cadenas de condroitín sulfato, también presentes en RPTPβ/ζ-S. Tanto RPTPβ/ζ-A como RPTPβ/ζ-B constan de dos dominios tirosina fosfatasa en el interior celular (dominios D1 y D2), siendo el catalíticamente activo el dominio D1. Pesos moleculares en Kilodaltons (kD). Aa (aminoácidos), PSI (*phosphacan short isoform*). Tomada y modificada de Garwood y colaboradores (2003).

El receptor RPTPβ/ζ es estructuralmente muy similar a RPTPγ. Ambas fosfatasa forman parte de la subfamilia número 5 de RPTPs y presentan altos niveles de expresión en el SNC. Sin embargo, RPTPγ se encuentra de manera casi exclusiva en neuronas mientras que RPTPβ/ζ se expresa también en células gliales como astrocitos, oligodendrocitos y sus precursores (Kuboyama y col., 2016; Lamprianou y col., 2006; Senis y col., 2018; Shintani y col., 1998). Otras características que distinguen a estos receptores son que RPTPγ no presenta en su estructura las dos cadenas pesadas de condroitín sulfato y que RPTPγ, además de expresarse en el SNC, se distribuye de forma ubicua en el organismo, mientras que RPTPβ/ζ se expresa en tejidos específicos (Senis y col., 2018; Shintani y col., 1997).

El modo de unión de la PTN con RPTPβ/ζ se ha estudiado en profundidad. La unión de la citoquina con la región extracelular de RPTPβ/ζ provoca la dimerización del receptor, lo que hace que se bloquee el acceso de los sustratos al dominio catalítico D1, anulando la actividad fosfatasa intrínseca de RPTPβ/ζ (Fukada y col., 2006; Maeda y col., 1999; Maeda y col., 1996). Esto hace que aumente el estado de fosforilación de los sustratos del receptor. Por tanto, la inactivación del receptor por PTN se considera ligando-dependiente.

Algunos de los sustratos de RPTP β/ζ más conocidos y estudiados (Figura 2) son β -Catenina (Meng y col., 2000), GIT1 (del inglés *G protein-coupled receptor kinase-interactor 1*) (Kawachi y col., 2001), p190-RhoGAP (del inglés *GTP-ase-activating protein for Rho GTP-ase*) (Tamura y col., 2006), MAGI1 (del inglés *membrane-associated guanylate kinase inverted 1*) (Fukada y col., 2005), la quinasa Fyn (Pariser y col., 2005a), β -aducina (Pariser y col., 2005b; Pariser y col., 2005c), ALK (Perez-Pinera y col., 2007) y TrkA (del inglés *Tropomyosin receptor kinase A*) (Shintani y col., 2008). Uno de estos sustratos, β -Catenina, es el efector clave de la señalización nuclear mediada por Wnt (de inglés *wingless integrated*), que está implicada en la migración, polaridad y transformación celular, así como en la organogénesis durante el desarrollo embrionario (Komiya y col., 2008; Valenta y col., 2012). Por su parte, la β -aducina está asociada con la heterocromatina, los centriolos y con la reorganización del citoesqueleto. Se conoce que PTN regula la distribución celular de la β -aducina a través de PKC- δ (proteína quinasa C δ) (Pariser y col., 2005b). GIT1 es un regulador de la adhesión intracelular (Beltran y col., 2003), y es esencial para mantener la estructura del citoesqueleto y la contractibilidad celular (Stiegler y col., 2017). MAGI1 forma parte de la familia de las proteínas guanilato-quinasa asociadas a la membrana y participa en la asociación de complejos de multiproteínas. Hay estudios que sugieren que MAGI1 también está implicada en la transmisión de señales reguladoras desde la superficie celular hasta el núcleo, en la regulación de la extensión de neuritas y la modulación del dolor (Dobrosotskaya y col., 1997; Ito y col., 2013; Pryce y col., 2019).

La quinasa Fyn presenta múltiples funciones biológicas relacionadas con su habilidad para asociarse y fosforilar a un gran número de moléculas de señalización en sus residuos tirosina. Entre sus funciones destacan la activación de los linfocitos T, la regulación de la función cerebral y la intervención en procesos de señalización mediados por mecanismos de adhesión (Resh, 1998). También participa en la transmisión sináptica excitatoria e inhibitoria, en la plasticidad sináptica y en los procesos de memoria y aprendizaje (Chattopadhyaya y col., 2013; Grant y col., 1992; Ohnishi y col., 2011). Otras funciones conocidas de Fyn tienen que ver con la modulación de la mielinización de los oligodendrocitos (Peckham y col., 2016) inducida por BDNF. Cabe destacar también la participación de Fyn en la regulación de la respuesta neuroinflamatoria a través de la activación microglial (Panicker y col., 2015) y en otros procesos relacionados con la inflamación como la activación del inflammasoma NLRP13 (del inglés *Nod-like receptor protein 13*), a través de la fosforilación de PKC- δ y la consiguiente translocación al núcleo de NF- κ B-p65 (Panicker y col., 2019). Esta proteína también se encuentra implicada en los efectos sedantes del alcohol y en el desarrollo de tolerancia a esta droga a través de su interacción con el receptor NMDA2B (N-metil-D-aspartato, receptor 2B) (Yaka y col., 2003). Como se ha señalado con anterioridad, la activación de la actividad quinasa de Fyn es uno de los eventos moleculares que se encuentran involucrados en la dependencia del alcohol (Pastor y col., 2009; Schumann y col., 2003).

Otros sustratos de RPTP β/ζ que, al igual que Fyn, son conocidos moduladores de la neuroinflamación y/o de los efectos de drogas de abuso, son ALK y TrkA. Como se ha comentado

previamente, además de ser un receptor de PTN y de MK, ALK también es un sustrato de RPTP β/ζ (Perez-Pinera y col., 2007). Además de su participación en procesos de desarrollo cerebral (Rohrbough y col., 2010; Yao y col., 2013), en la respuesta inmune y en la activación del inflammasoma de los macrófagos (Zhang y col., 2018), cabe destacar su implicación en procesos inflamatorios de origen diverso (Zeng y col., 2017) y en la modulación de las respuestas comportamentales tras la exposición a alcohol (He y col., 2015). Por otra parte, RPTP β/ζ disminuye la fosforilación de TrkA (Shintani y col., 2008), reduciendo así la activación de TrkA inducida por su ligando, NGF (factor de crecimiento nervioso, del inglés *nerve growth factor*). Es importante señalar que NGF es un elemento clave de la comunicación entre el sistema inmune y el SNC, se encuentra sobreexpresado en tejidos inflamados y puede modular la actividad de las neuronas periféricas y su supervivencia (Minnone y col., 2017; Mizumura y col., 2015). Las vías de señalización activadas por TrkA incluyen la activación de la proteína Ras, PI3K-AKT (fosfatidilinositol 3-quinasa-Proteína quinasa B), PLC- γ 1 (fosfolipasa C- γ 1) y las vías de señalización controladas por este tipo de proteínas, como la vía de las MAPK (Skaper, 2018).

Las evidencias expuestas hasta este momento, en su conjunto, señalan al eje PTN/MK/RPTP β/ζ como nueva diana farmacológica en patologías centrales que cursen con un evidente componente neuroinflamatorio, así como en el tratamiento de la dependencia de drogas de abuso y en la prevención de sus efectos neurotóxicos en el SNC.

3. Modulación farmacológica de la vía de señalización de PTN/MK/RPTP β/ζ .

La PTN y la MK actúan como inhibidores endógenos de RPTP β/ζ , y a través de la inhibición de la actividad fosfatasa de este receptor, aumentan los niveles de fosforilación y la activación de sus sustratos, (Figura 4A, B). De todo lo resumido hasta este momento, surgiría la hipótesis de que la potenciación de los efectos de PTN y MK podría producir efectos neuroprotectores en patologías neurodegenerativas, proteger frente al daño producido por neurotoxinas y limitar los efectos reforzadores de drogas de abuso. Además, de la potenciación de los efectos de estas citoquinas cabría esperar una modulación de la neuroinflamación característica de los desórdenes mencionados, aunque quizá sea demasiado pronto para anticipar el signo de dicha modulación que, por otra parte, probablemente difiera en condiciones agudas y crónicas.

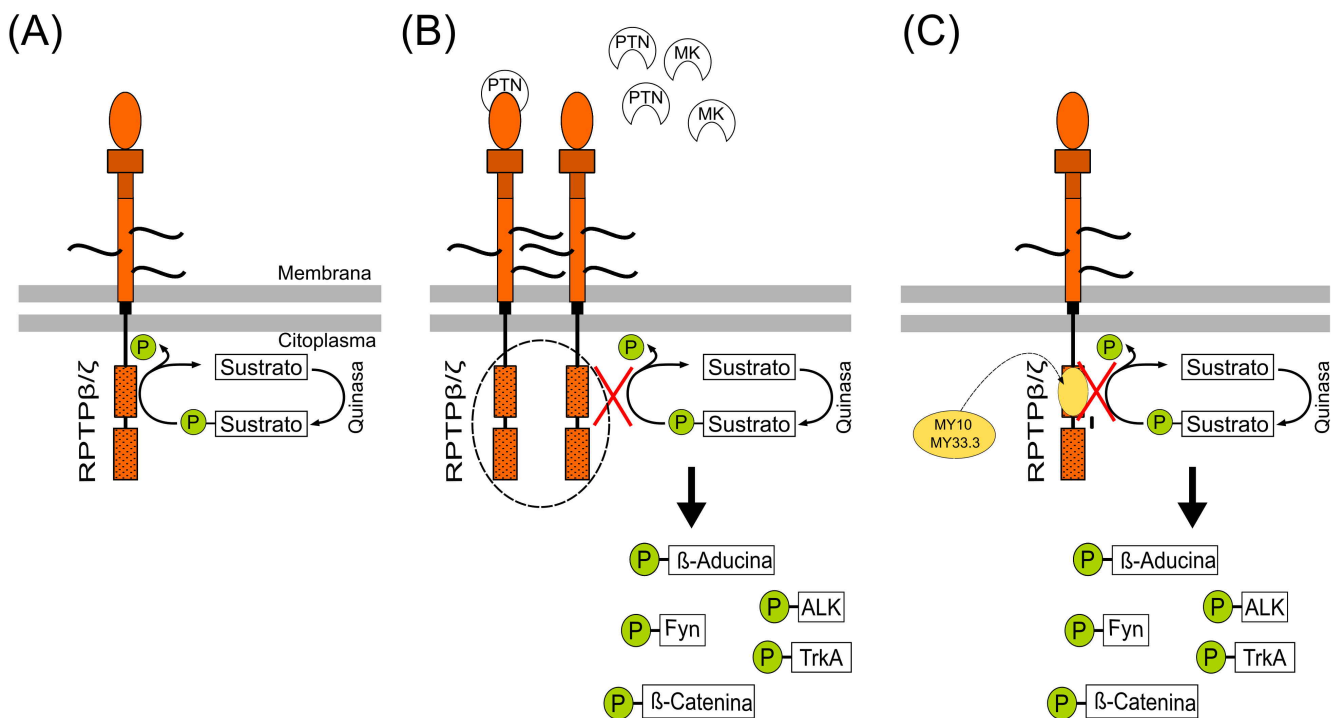


Figura 4. Mecanismo de acción de PTN/MK y de inhibidores selectivos de RPTPβ/ζ. (A) En su forma monomérica en ausencia de ligando, RPTPβ/ζ ejerce su actividad fosfatasa sobre sus sustratos. (B) La PTN y la MK, al interactuar con RPTPβ/ζ provocan la dimerización del receptor, impidiendo el acceso de los sustratos al dominio catalítico D1 y, por tanto, aumentan el estado de fosforilación de sustratos como Fyn, β-ADCINA, β-CATENINA, ALK y TrkA. (C) El empleo de inhibidores selectivos de RPTPβ/ζ, como MY10 o MY33-3, produciría el mismo efecto inhibitorio sobre el receptor que la PTN, pero a través de un mecanismo distinto. Estos compuestos se unen directamente al dominio activo de RPTPβ/ζ e impiden su actividad fosfatasa en los sustratos.

Una posible estrategia para la potenciación de los efectos de estas citoquinas, ya testada en modelos preclínicos, consiste en la inducción de la expresión de la PTN o de la MK, lo que potenciaría las cascadas de señalización derivadas de la inhibición de RPTPβ/ζ y el aumento del estado de fosforilación de los sustratos del receptor (Figura 4B). Se ha descrito que el aumento de la expresión de PTN disminuye el daño dopaminérgico causado por la toxina parkinsoniana 6-hidroxidopamina en la vía nigroestriatal (Gombash y col., 2012; Taravini y col., 2011). La administración intraventricular de MK tiene un efecto citoprotector en patologías isquémicas (Yoshida y col., 2001). En este sentido, existen diversos estudios sobre la administración intracerebral de factores de crecimiento para el tratamiento de enfermedades como EP y la enfermedad de Alzheimer (Allen y col., 2013; Hegarty y col., 2017). Sin embargo, no es posible obviar las limitaciones prácticas que supone la administración intracraneal de fármacos.

Una alternativa a la administración de PTN o MK para potenciar sus vías de señalización a través de RPTPβ/ζ, consistiría en el empleo de inhibidores selectivos de este receptor (Figura 4C). El grupo de Huang y colaboradores desarrolló el primer inhibidor de RPTPβ/ζ, aunque de baja potencia y poca selectividad (Huang y col., 2003). Debido al interés que suponía observar si la inhibición directa de RPTPβ/ζ presentaba las mismas acciones que la sobreexpresión de la

PTN sobre los efectos adictivos de las drogas de abuso, y basándose en la estructura propuesta por Huang y colaboradores (Huang y col., 2003), se desarrollaron pequeños compuestos que actúan como inhibidores más selectivos de RPTP β/ζ , capaces de cruzar la BHE y que mimetizan algunos de los efectos conocidos de la PTN y la MK (Figura 4C) (Pastor y col., 2018). Tras el proceso de evaluación *in vitro*, los dos compuestos más prometedores fueron los compuestos llamados MY10 y MY33-3 (Figura 5).

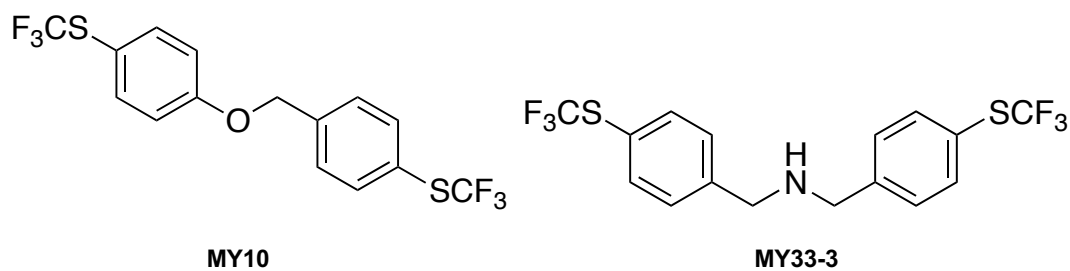


Figura 5. Estructura de los inhibidores de RPTP β/ζ MY10 y MY33-3.

HIPÓTESIS Y OBJETIVOS

HIPÓTESIS Y OBJETIVOS

La pleiotrofina (PTN) y la midkina (MK) son dos factores importantes para la supervivencia y diferenciación de las neuronas catecolaminérgicas. El incremento de sus niveles de expresión está ligado a situaciones inflamatorias y tiene lugar en distintas áreas cerebrales tras la exposición a diferentes drogas de abuso. Debido a que son capaces de modular los efectos neurotóxicos y adictivos de las drogas de abuso, y al interés que supone el desarrollo de herramientas terapéuticas para combatir los trastornos caracterizados por una neuroinflamación excesiva y aquellos derivados del abuso de alcohol, el objetivo general de este trabajo parte de la hipótesis de que la PTN, la MK, y su vía de señalización, constituyen nuevas dianas terapéuticas para modular la neuroinflamación y los trastornos por abuso de alcohol.

Los objetivos específicos planteados en este trabajo fueron:

- 1) **Implicación de la pleiotrofina y la midkina en la neuroinflamación y en la señalización mediada por TLR4 en un modelo agudo de endotoxemia.** Estudio de los efectos de LPS y del antagonista de TLR4 TAK-242 en distintos modelos de Ptn- y Mk-GEMMS (*Genetically engineered mouse models*).
- 2) **Evaluación *in vivo* de los efectos del tratamiento con inhibidores de RPTP β / ζ sobre el consumo de alcohol y los efectos reforzadores de esta droga.** Estudio de los efectos de MY10 y MY33-3 sobre el condicionamiento preferencial al sitio inducido por el alcohol y sobre el consumo de alcohol en ratones salvajes y en ratones Ptn^{-/-}.
- 3) **Evaluación *in vitro* de los efectos del tratamiento con inhibidores de RPTP β / ζ sobre las cascadas de señalización activadas por el alcohol.** Estudio de los efectos de MY10 y MY33-3 sobre el incremento en los niveles de fosforilación de ALK y TrkA inducido por alcohol en células SH-SY5Y.
- 4) **Evaluación de los efectos comportamentales del tratamiento con el inhibidor de RPTP β / ζ MY10 en ratones salvajes y ratones Ptn^{-/-}.** Estudio de los efectos del tratamiento agudo con MY10 en distintos modelos conductuales en ratones salvajes y en ratones Ptn^{-/-}.

MÉTODOS Y RESULTADOS

ARTÍCULO 1. Pleiotrophin regulates microglia-mediated neuroinflammation.

Rosalía Fernández-Calle, Marta Vicente-Rodríguez, Esther Gramage, Jimena Pita, Carmen Pérez-García, Marcel Ferrer-Alcón, María Uribarri, María P. Ramos y Gonzalo Herradón.

Journal of Neuroinflammation, 2017. ISSN: 1742-2094

Volumen: 14

Página de inicio: 46

DOI: 10.1186/s12974-017-0823-8

Resumen

La pleiotrofina (PTN) es una citoquina que se sobreexpresa en el cerebro en diferentes desórdenes caracterizados por una elevada neuroinflamación, como son las enfermedades neurodegenerativas, la adicción a drogas de abuso, traumatismos e isquemia. En el presente trabajo, se ha explorado si la PTN modula la neuroinflamación y si el *Toll-like receptor 4* (TLR4), que resulta crucial en la iniciación de la respuesta inmune, está implicado en dicha función de PTN. Mediante ensayos inmunohistoquímicos, se ha estudiado en la corteza prefrontal (CPF) y en el cuerpo estriado de ratones con sobreexpresión de PTN en el cerebro (PTN-Tg) y de ratones normales (Wt), el efecto de los cambios inducidos por la administración del lipopolisacárido (LPS, 7,5mg/kg i.p.) en el marcador astrocítico de la proteína ácida fibrilar de la glía (GFAP) y en el marcador microglial, molécula adaptadora de unión al calcio 1 (Iba1). Los niveles de expresión de citoquinas en CPF se midieron mediante la técnica X-MAP. La influencia de la señalización mediante TLR4 en los efectos del LPS en ambos genotipos se estudió mediante el pretratamiento con el antagonista de TLR-4 (TAK-242, 3mg/kg i.p.). Las células BV2 (microglía de ratón) se trataron con PTN (0,5 µg/ml) y LPS (1 µg/ml) y se evaluó la liberación de óxido nítrico (NO). La activación microglial inducida por LPS aumentó significativamente en la CPF de los ratones PTN-Tg comparado con los ratones Wt. Los niveles de TNF- α , IL-6 y MCP-1 en respuesta a LPS aumentaron significativamente en la CPF de los ratones PTN-Tg frente a los Wt. El pretratamiento con TAK-242 bloqueó el incremento de la concentración de citoquinas de forma similar en ambos genotipos. La incubación de las células BV2 con PTN y LPS potenció significativamente la liberación de NO comparado con el tratamiento solo con LPS. Estos resultados identifican por primera vez a la PTN como un nuevo y potente modulador de la neuroinflamación. La PTN potencia la activación microglial inducida por LPS. Nuestros resultados sugieren que la regulación de las vías de señalización de la PTN puede conducir a nuevas oportunidades terapéuticas, especialmente en aquellos desórdenes caracterizados por elevados niveles de PTN en el cerebro y neuroinflamación.

Contribución de la doctoranda en este trabajo

Rosalía Fernández Calle llevó a cabo la mayoría de los experimentos incluidos en esta publicación. Contribuyó en el tratamiento de los animales y el procesamiento de las muestras. Realizó el análisis inmunohistoquímico de las figuras 1, 2, 3 y 4, y participó en los ensayos *in vitro* recogidos en la figura 6. Colaboró en el análisis estadístico y ayudó en la escritura del manuscrito.

RESEARCH

Open Access



Pleiotrophin regulates microglia-mediated neuroinflammation

Rosalía Fernández-Calle^{1†}, Marta Vicente-Rodríguez^{1†}, Esther Gramage¹, Jimena Pita², Carmen Pérez-García¹, Marcel Ferrer-Alcón³, María Uribarri³, María P. Ramos² and Gonzalo Herradón^{1*}

Abstract

Background: Pleiotrophin (PTN) is a cytokine found highly upregulated in the brain in different disorders characterized by overt neuroinflammation such as neurodegenerative diseases, drug addiction, traumatic injury, and ischemia. In the present work, we have explored whether PTN modulates neuroinflammation and if Toll-like receptor 4 (TLR4), crucial in the initiation of an immune response, is involved.

Methods: In immunohistochemistry assays, we studied lipopolysaccharide (LPS, 7.5 mg/kg i.p.)-induced changes in glial fibrillary acidic protein (GFAP, astrocyte marker) and ionized calcium-binding adaptor molecule 1 (Iba1, microglia marker) expression in the prefrontal cortex (PFC) and striatum of mice with transgenic PTN overexpression in the brain (PTN-Tg) and in wild-type (WT) mice. Cytokine protein levels were assessed in the PFC by X-MAP technology. The influence of TLR4 signaling in LPS effects in both genotypes was assessed by pretreatment with the TLR4 antagonist (TAK-242, 3.0 mg/kg i.p.). Murine BV2 microglial cells were treated with PTN (0.5 µg/ml) and LPS (1.0 µg/ml) and assessed for the release of nitric oxide (NO).

Results: We found that LPS-induced microglial activation is significantly increased in the PFC of PTN-Tg mice compared to that of WT mice. The levels of TNF-α, IL-6, and MCP-1 in response to LPS were significantly increased in the PFC of PTN-Tg mice compared to that of WT mice. Pretreatment with TAK-242 efficiently blocked increases in cytokine contents in a similar manner in both genotypes. Concomitant incubation of BV2 cells with LPS and PTN significantly potentiated the production of NO compared to cells only treated with LPS.

Conclusions: Our findings identify for the first time that PTN is a novel and potent regulator of neuroinflammation. Pleiotrophin potentiates LPS-stimulated microglia activation. Our results suggest that regulation of the PTN signaling pathways may constitute new therapeutic opportunities particularly in those neurological disorders characterized by increased PTN cerebral levels and neuroinflammation.

Keywords: Microgliosis, Microglia activation, Midkine, Neuroimmune response, Neuroinflammation, Pleiotrophin, TLR4

Background

Inflammation is a key event in the healing process of the damaged tissue, and activation of the innate immune system is fundamental in the response to inflammation. When prolonged, however, inflammation can become deleterious. Within the central nervous system (CNS), the two main players in neuroinflammation are glial cells: microglia, the resident macrophages in the CNS,

and astrocytes [1]. Toll-like receptors (TLRs), which are expressed in the rodent microglia and astrocytes [2], are key molecules in the activation of innate immunity during CNS damage. Activation of TLRs triggers the downstream stimulation of nuclear factor-κB (NFκB) and the induction of genes that encode inflammation-associated molecules and cytokines including TNF-α, IL-1β, IL-6, iNOS, and COX2 [2–4].

Ever-growing evidence points to a key role of inflammatory processes in a broad spectrum of diseases including traumatic brain injury, chronic neurodegenerative diseases, neuropathic pain, ischemia, and neuropsychiatric disorders including drug addiction [5–7].

* Correspondence: herradon@ceu.es

†Equal contributors

¹Pharmacology Lab, Department of Pharmaceutical and Health Sciences, Facultad de Farmacia, Universidad CEU San Pablo, Urb. Montepríncipe, 28668 Boadilla del Monte, Madrid, Spain

Full list of author information is available at the end of the article



Psychostimulants such as amphetamine and its derivatives cause neuroinflammation and limit neurogenesis and induce blood-brain barrier (BBB) damage [8, 9]. All these effects induced by amphetamines are important for the dopaminergic injury induced by these drugs in the nigrostriatal pathway [10], which is the same circuitry affected in Parkinson's disease (PD). Interestingly, recent evidence indicate a 3-fold increased risk of PD in these drug addicts [11], suggesting that common pathogenic mechanisms could underlie both diseases, PD and amphetamines abuse, one of which could be neuroinflammation [9, 12]. In the search for validation of new biomarkers and for the development of new drugs that could modulate the inflammatory processes underlying these and other diseases of the CNS [13], our strategy was to identify proteins with known regulatory functions in inflammation, whose levels of expression are upregulated after amphetamine administrations and in the neurodegenerative areas of the brain of PD patients.

Pleiotrophin (PTN) is a cytokine that is upregulated in different brain areas after administration of different drugs of abuse including amphetamine [14, 15] and in the nigrostriatal pathway of patients with PD [16]. PTN is important for CNS repair and for survival and differentiation of dopaminergic neurons [6]. In addition, evidence points to a modulatory role of PTN on inflammation. In peripheral organs, PTN is known to induce inflammatory mediators [17] and its expression levels are significantly reduced by administration of anti-inflammatory drugs [18]. Little is known about a possible role of PTN on neuroinflammation. Transgenic mice with PTN overexpression in the brain (PTN-Tg) show a ~4-fold increased amphetamine-induced striatal astrogliosis compared to wild-type (WT) mice [19]. However, PTN genetically deficient (PTN^{-/-}) mice show a modest ~20% increase in amphetamine-induced astrogliosis, possibly reflecting proinflammatory compensatory mechanisms [19–21]. We hypothesize that PTN is a novel modulator of neuroinflammation. To test this hypothesis, we have now comparatively studied the astrocytic response, microglial activation, and cytokine release induced by lipopolysaccharide (LPS) in PTN-Tg and in WT mice. Since previous studies suggest a possible contribution of PTN to Toll-like receptor 4 (TLR4)-mediated immune response [22] and TLR4 plays a pivotal role in neuroinflammation, we have also investigated the possible differential contribution of TLR4 to the neuroinflammatory processes induced by LPS in both genotypes.

Methods

Animals

PTN-Tg mice on a C57BL/6J background were generated by pronuclear injection as previously described [23, 24]. The acceptor vector contained the regulatory regions responsible for tissue-specific expression of Thy-1 gene,

which drives neuron-specific expression of transgenes [25, 26]. PTN-specific overexpression in different brain areas, including an ~3–4-fold upregulation in the prefrontal cortex (PFC) and a 20% increase of PTN protein levels in striatum, was established by quantitative real-time polymerase chain reaction (qRT-PCR), in situ hybridization, and by western blot [23, 27, 28].

We used male PTN-Tg and WT animals of 9–10 weeks (20–25 g). Mice were housed under controlled environmental conditions (22 ± 1 °C and a 12-h light/12-h dark cycle) with free access to food and water.

All the animals used in this study were maintained in accordance with the European Union Laboratory Animal Care Rules (86/609/ECC directive), and the protocols were approved by the Animal Research Committee of USP-CEU.

Treatments

To test genotypic differences in LPS-induced neuroinflammation and the involvement of TLR4 in LPS effects in PTN-Tg and WT mice, we assessed the effects of LPS in mice pretreated with the TLR4 antagonist TAK-242 (Merck Millipore, Madrid, Spain). For this purpose, mice were injected (i.p.) with TAK-242 (3 mg/kg) or saline (10 ml/kg; control) 30 minutes before a single i.p. injection of LPS (7.5 mg/kg) or saline (10 ml/kg; control). As a result, we obtained four experimental groups in both genotypes: saline + saline (Sal-Sal), saline + LPS (Sal-LPS), TAK-242 + saline (TAK-Sal), and TAK-242 + LPS (TAK-LPS). For immunohistochemistry analysis, animals were sacrificed 16 h after LPS or last saline administration ($n = 4–5$ /group/genotype) by perfusion with 4% p-formaldehyde. For tisular analysis of cytokine levels, animals were decapitated 16 h after LPS or the last saline administration ($n = 5$ /group/genotype) and the PFC was rapidly removed and frozen in dry ice and stored to –80 °C until the protein extraction procedure.

Immunohistochemistry analysis

Mice were transcardially perfused with 4% p-formaldehyde; the brains were removed and conserved in p-formaldehyde for 24 h and then transferred to a 30% sucrose solution containing 0.02% sodium azide for storage at 4 °C; 30- μ m PFC and striatal free-floating sections were processed as previously described [20, 21, 29]. Immunohistochemistry studies were performed in one slice per 180 μ m (the PFC from the bregma –3.08 mm to –2.46 mm; the striatum from the bregma 1.54 mm to –0.10 mm).

In order to study gliosis, sections were incubated overnight at 4 °C with anti-gial fibrillary acidic protein (GFAP; Millipore, Madrid, Spain; 1:1000) and anti-ionized calcium-binding adaptor molecule 1 (Iba1, Wako, Osaka, Japan; 1:1000) antibodies, following by 30-min incubation with the Alexa-Fluor-555 and Alexa-Fluor-

488 corresponding secondary antibody (Invitrogen, Waltham, MA, USA; 1:500). Sections were mounted on gelatin-coated slides and coverslipped with Fluoromount medium. Photomicrographs were captured with a digital camera coupled to an optical microscope (DM5500B, Leica, Solms, Germany). Analysis was performed using ImageJ (NIH, Bethesda, MD, Version 1.50f), in the three most central slices of each area. Iba1+ cells and GFAP+ astrocytes were counted in whole sections of the PFC and in 1100 $\mu\text{m} \times 1400 \mu\text{m}$ standardized areas in the striatum as previously described [21, 29]. In the case of Iba1-ir, total marked area was calculated as overall image fluorescence, subtracting the mean background fluorescence. Computer-based analysis of the morphology of individual Iba1+ cells was performed using the “Analyze Particle” function in ImageJ software. Images were segmented and smoothed to best fit cell shape. To be sure to select only cells entirely present in the acquired field, cells with an area of $>25 \mu\text{m}^2$ were analyzed. The objects meeting the minimum size to be analyzed were measured for the following parameters: area, perimeter, and circularity. The soma size (cell area) is expressed in square micrometers. The perimeter was calculated based on the outline length of a given object. It measures the length around the periphery of each soma and is expected to be higher in activated and hypertrophic cells. Circularity was calculated by the following formula: $4\pi \times (\text{area}/\text{perimeter}^2)$. This parameter varies from 0 (linear polygon) to 1 (perfect circular object). Mean single-cell values for each parameter were used for statistics.

Cytokine levels

Approximately 5 mg of each sample of the PFC ($n = 5/\text{group}$) was homogenized in 100 μl of homogenization buffer (0.05% Tween 20 and protease inhibitor cocktail (Thermo Fisher Scientific Inc., Waltham, MA, USA) in PBS, pH 7.2). After 3 cycles of 1 min and 50 Hz in the tissue lyzer (Quiagen, Germantown, Maryland, USA), samples were centrifuged at $11000 \times g$ for 30 min at 4 °C. After centrifugation, supernatants were transferred to a new tube and stored at $-80 \text{ }^\circ\text{C}$ until the assay. Total protein content of each sample was measured using the BCA protein assay kit (Thermo Fisher Scientific Inc., Waltham, MA, USA). Levels of tumor necrosis factor- α (TNF- α), interleukin 1 β (IL-1 β), interleukin 6 (IL-6), monocyte chemoattractant protein-1 (MCP-1), interleukin 4 (IL-4), and interleukin 10 (IL-10) were measured by X-Map technology using a Milliplex MADPK-71K adipokine kit according to the manufacturer’s description (Merck Millipore, Spain).

BV2 cell cultures

BV2 murine microglial cells

BV2 murine microglial cells were a generous gift from Professor Antonio Cuadrado (Instituto de Investigaciones

Biomédicas “Alberto Sols” (IIBM), Madrid, Spain). Cells were routinely maintained in RPMI-1640 medium with fetal bovine serum (10%), penicillin (100 U/ml), streptomycin (100 $\mu\text{g}/\text{ml}$), and L-glutamine (4 mM) at 37 °C in 5% CO_2 humidified air following conditions used by others [30, 31]. Prior to each experiment, cells were grown for 24 h on 96-well plates at a concentration of 1×10^4 cells per well.

Measurement of NO production

Nitric oxide (NO) production was quantified by nitrite accumulation in the culture medium using the Griess reagent (2.25% sulfanilamide and 0.22% N-(1-naphthyl)ethylenediamine dihydrochloride), according to protocols previously described [32, 33]. After fasting the cells for 24 h, BV2 cells were stimulated with different concentrations of PTN (0.05 $\mu\text{g}/\text{ml}$ or 0.5 $\mu\text{g}/\text{ml}$), with or without LPS (1.0 $\mu\text{g}/\text{ml}$), for another 24 h. The concentrations of PTN were selected to correlate with the PTN overexpression in the brain of PTN-Tg mice and are within the range of concentrations used before to test the effects of PTN in neuronal injury [34] and in the expansion of human stem cells [35]. The NO production by cells was quantified in a microplate reader (Versa-Max, Molecular Devices, Sunnyvale, CA, USA) at 540 nm and then calculated with reference to the standard curve generated with NaNO_2 .

Statistics

Data are presented as mean \pm standard error of the mean (SEM). Data obtained from image analysis of the striatal and PFC immunostaining and cytokine levels were analyzed using two-way ANOVA considering genotype and treatment as variants. Relevant differences were analyzed by post hoc comparisons with Bonferroni’s post hoc tests. Data obtained from BV2 cells were analyzed using one-way ANOVA followed by post hoc comparisons with Tukey’s post hoc tests. $P < 0.05$ was considered as statistically significant. All statistical analyses were performed using Graph-Pad Prism program (San Diego, CA, USA).

Results

Differential regulation of LPS-induced astrocytic and microglial responses in the PFC of PTN-Tg mice. Effect of TAK-242 on LPS-induced microglial response and changes in cytokine contents in the PFC of PTN-Tg and WT mice
PTN is a cytokine highly upregulated in the brain in different CNS disorders characterized by neuroinflammation [6]. We aimed to study the modulatory role of PTN overexpression (3-fold) in the PFC of PTN-Tg mice [23, 24] on LPS-induced neuroinflammation. To investigate proinflammatory responses in these experiments, we tested the astrocytic and microglial response in PFC sections of WT

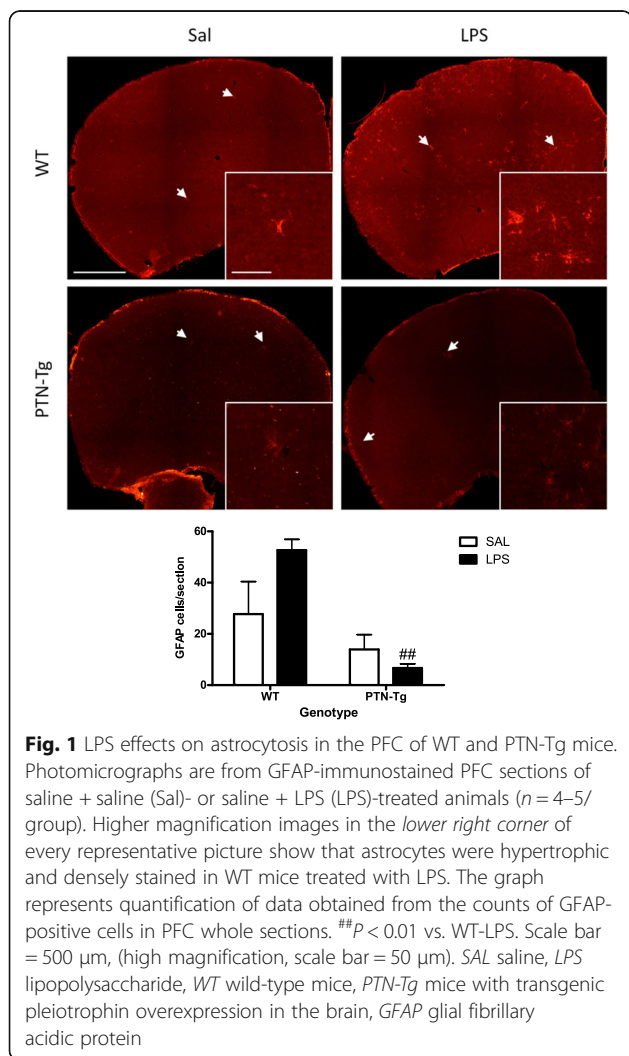
and PTN-Tg mice treated with saline (Sal-Sal) or LPS (Sal-LPS). Astrocyte activation was assessed by morphology and expression of GFAP, an astrocyte-specific intermediate filament protein [36]. LPS treatment tended to increase the number of GFAP+ astrocytes in the PFC of WT mice, being these cells characterized by large densely stained cell bodies as well as long and extensive processes compared to saline-treated animals (Fig. 1). In contrast, these effects on GFAP+ IR induced by LPS were blocked in PTN-Tg mice (Fig. 1).

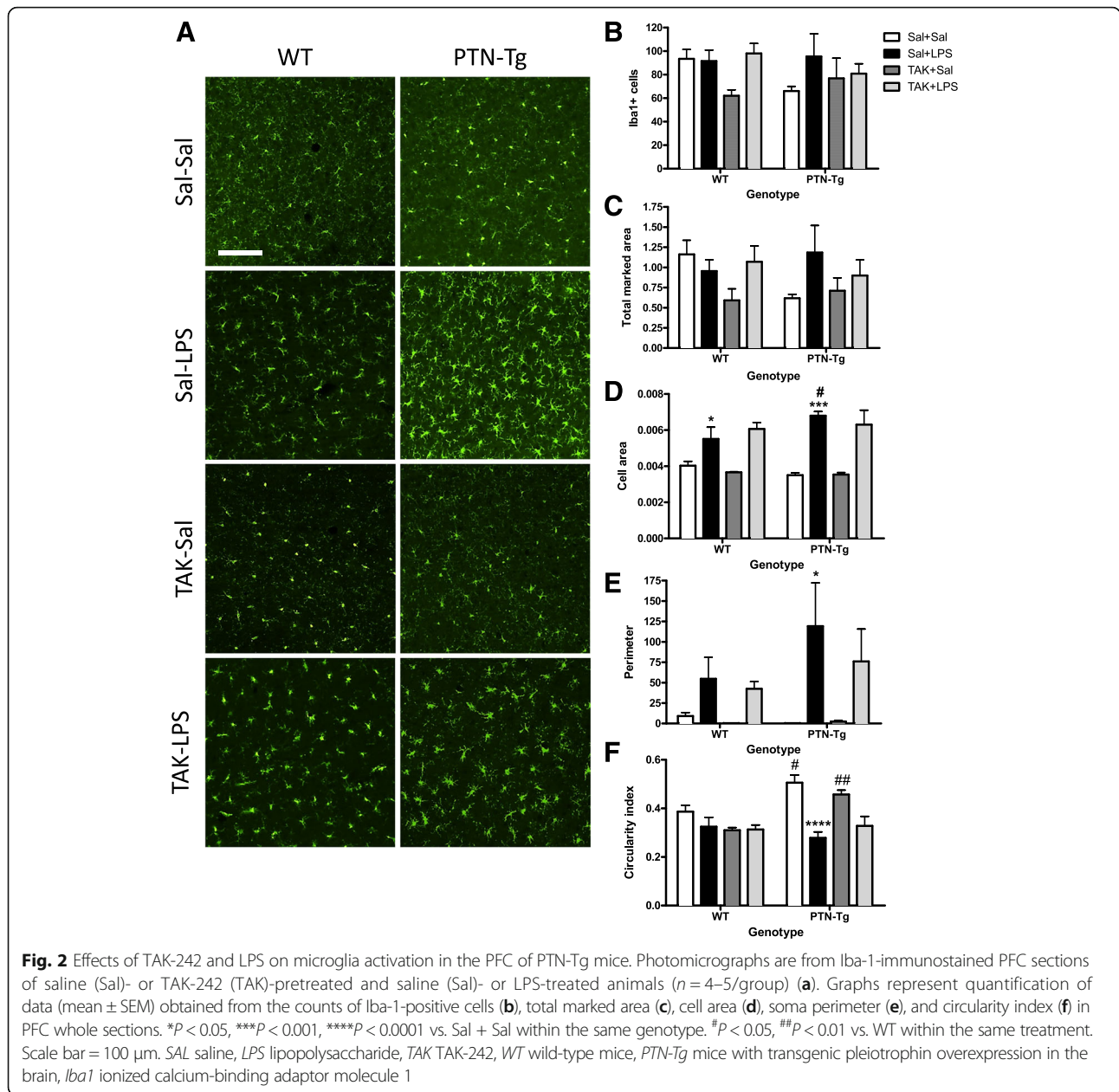
Previous studies have linked LPS-induced activation of microglia and production of proinflammatory factors to brain damage and neurodegeneration [37]. To investigate proinflammatory responses in this experiment, PFC sections were immunostained with anti-Iba1 microglial antibody. In the saline control groups, microglial cells have resting morphology (Fig. 2a, Sal-Sal). Immunohistochemistry for Iba1 did not reflect significant changes in the number of Iba1+ cells in the PFC of WT and PTN-Tg mice after LPS treatment (Fig. 2b). However, we observed a clearly

enhanced hypertrophism characterized by activation, soma enlargement, and sprouting of new ramifications in LPS-treated PTN-Tg mice compared to that in LPS-treated WT mice and saline-treated mice from the same genotype (Fig. 2a, Sal-LPS). Accordingly, the total marked area (Fig. 2c) tended to increase in LPS-treated PTN-Tg mice compared to that in saline-treated mice. As expected, the Iba1+ cell area was increased in LPS-treated mice of both genotypes compared with that in saline-treated mice (Fig. 2d); however, LPS induced an increase in cell area that was significantly enhanced in PTN-Tg mice compared to that in WT mice (Fig. 2d). The increase in the perimeter was also higher in LPS-treated PTN-Tg mice (Fig. 2e). The decrease caused by LPS in the circularity index was more pronounced in PTN-Tg mice (Fig. 2f). Overall, the data demonstrate that LPS-induced microglial response is increased in the PFC of PTN-Tg mice compared to that of WT mice. Interestingly, we observed that the morphological changes induced by LPS in microglial cells of both genotypes were not prevented by the previous administration of the TLR4 antagonist TAK-242 (Fig. 2, TAK-LPS).

We measured the contents of different cytokines in the PFC of mice from both genotypes. Confirming the neuroimmune response to LPS administration, we found that the levels of proinflammatory cytokines such as TNF- α , IL-6, and MCP-1 were many-fold upregulated in the PFC of LPS-treated WT mice compared to those of the saline-treated group (Fig. 3, Sal-LPS vs. Sal-Sal). More importantly, we found a highly significant ~ 7 -fold upregulation of the levels of TNF- α in the PFC of LPS-treated PTN-Tg mice compared to that of WT mice (Fig. 3). Similarly, the levels of IL-6 in the PFC of LPS-treated PTN-Tg mice were increased compared to those of WT mice (Fig. 3). Interestingly, pretreatment with TAK-242 efficiently blocked LPS-induced increases of TNF- α and IL-6 in the PFC of mice from both genotypes (Fig. 3, Sal-LPS vs. TAK-LPS). In addition, we found significantly higher levels of MCP-1 in the PFC of LPS-treated PTN-Tg mice compared to those of WT mice although, in this case, LPS effect on MCP-1 levels was partially blocked by previous administration of TAK-242 in both genotypes (Fig. 3). In contrast, we did not observe relevant genotypic differences in the levels of IL-1 β (Fig. 3). Concerning the anti-inflammatory cytokines IL-10 and IL-4, we did not find genotype- or treatment-related significant differences in their contents in the PFC of LPS-treated PTN-Tg mice compared to those of WT mice (Fig. 3).

Overall, the data demonstrate that LPS-induced microglial activation is enhanced in the PFC of PTN-Tg mice compared to that of WT animals. Interestingly, the data suggest that TLR4 activation is crucial for LPS-induced cytokine release in both genotypes but does not play a significant role in LPS-induced microglial morphological response in either genotype.

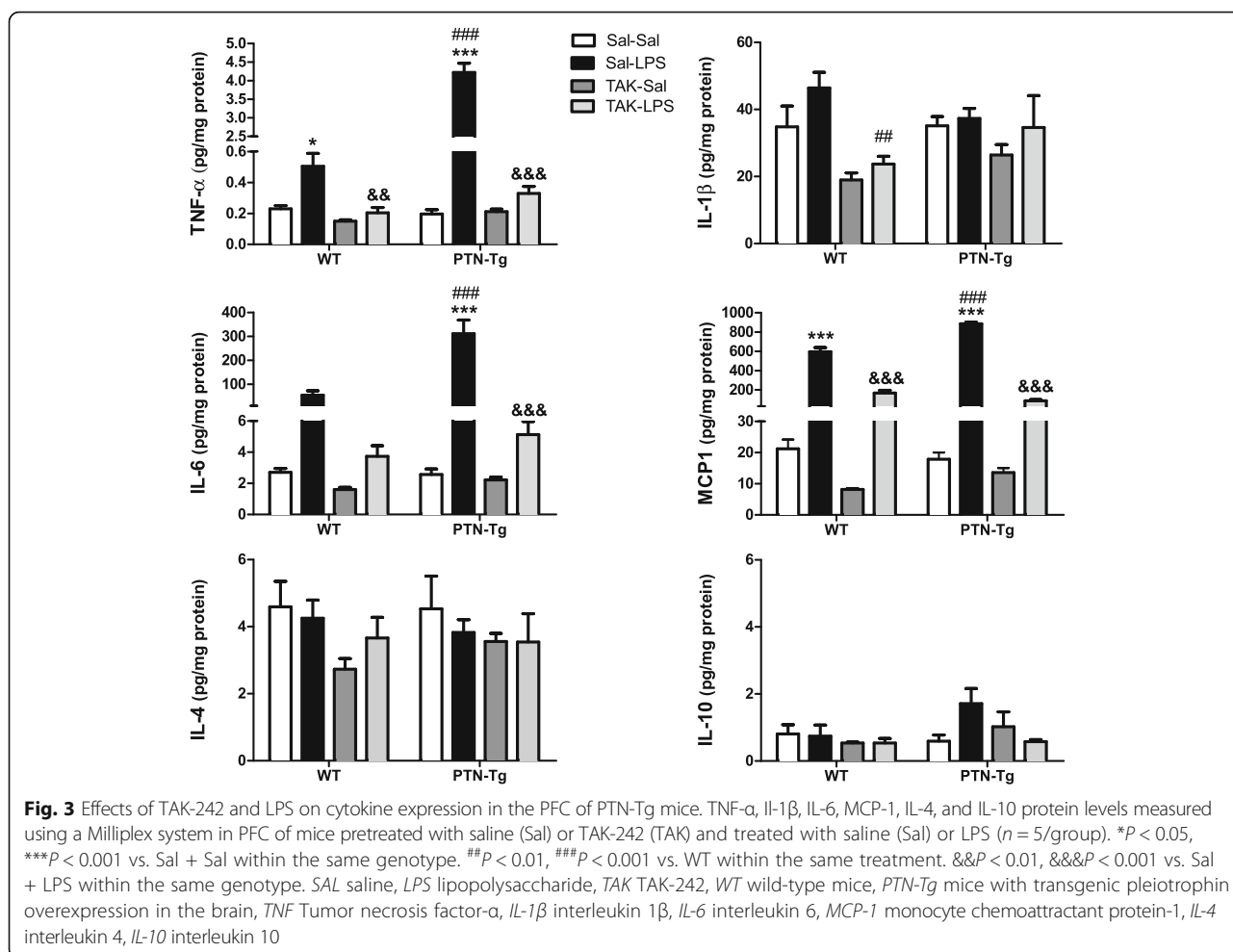




Effects of TAK-242 and LPS in the striatum of WT and PTN-Tg mice

To investigate the effects of a more modest PTN overexpression (~20%, PTN-Tg mouse striatum) [28] on LPS-induced neuroinflammation, we tested the astrocytic and microglial response in striatal sections of WT and PTN-Tg mice treated with saline (Sal-Sal) or LPS (Sal-LPS). We did not find genotypic- or treatment-related significant differences in the number of GFAP+ cells between groups (Fig. 4). Similarly to PFC, LPS treatment tended to increase the number of GFAP+ cells in the striatum of WT mice, whereas this tendency was absent in PTN-Tg mice (Fig. 4). Concerning microglia (Fig. 5),

immunohistochemistry for Iba1 did not reflect significant changes in the number of Iba1+ cells or in the total marked area in the striatum of WT and PTN-Tg mice after LPS treatment (Fig. 5a, b, c). However, signs of hypertrophism, soma enlargement, and sprouting of new ramifications in LPS-treated animals were observed in both genotypes compared to those in saline-treated groups (Fig. 5a). The Iba1+ cell area was significantly increased in both genotypes but especially in LPS-treated PTN-Tg mice compared to that in WT mice (Fig. 5d). On the other hand, the increase in the perimeter was higher in LPS-treated WT mice (Fig. 5e), whereas no differences between groups were found in



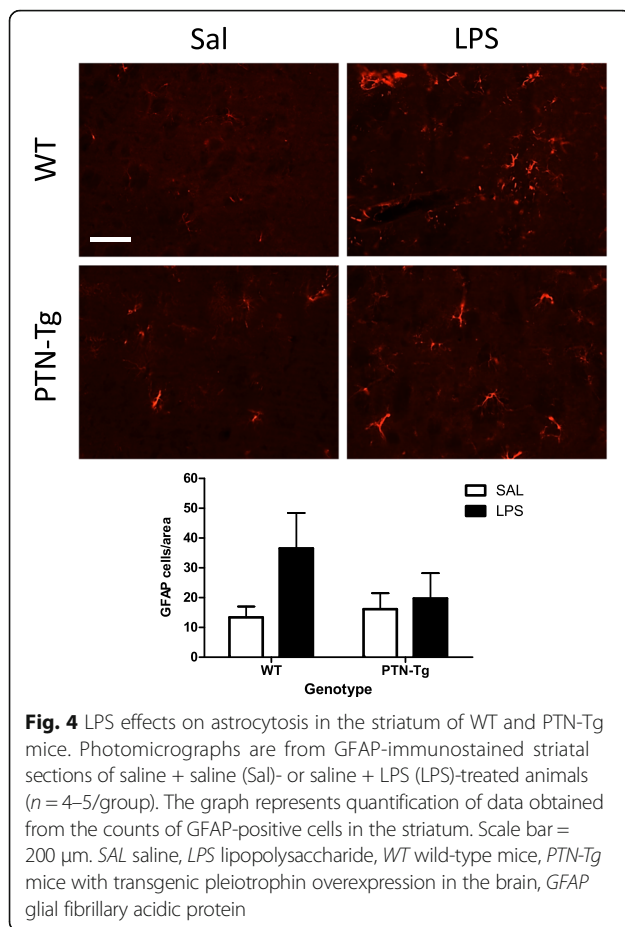
the case of the circularity index (Fig. 5f). We did not observe significant effects of pretreatment with TAK-242 on LPS-induced effects on microglia (Fig. 5). Overall, the data demonstrate that LPS-induced microglial response in the striatum is more modest than that in the PFC and that the moderate PTN overexpression in this brain area of PTN-Tg mice does not play a significant modulatory role on LPS effects.

Pleiotrophin potentiates NO production in LPS-stimulated BV2 cells

To test the possible direct effects of PTN on murine microglia in vitro, we investigated its effects on the production of NO, which is a key inflammatory mediator in LPS-stimulated BV2 microglia. First, we did not detect any effect in BV2 cells incubated with PTN alone (0.05 and 0.5 $\mu\text{g/ml}$, Fig. 6). LPS (1.0 $\mu\text{g/ml}$) induced a significant increase in the production of NO compared with control cells (Fig. 6). Concomitant incubation of BV2 cells with LPS (1.0 $\mu\text{g/ml}$) and PTN (0.5 $\mu\text{g/ml}$) significantly potentiated the production of NO compared to cells only treated with LPS (Fig. 6).

Discussion

Pleiotrophin is a cytokine that is found highly upregulated in diverse pathologies of the CNS characterized by overt neuroinflammation including neurodegenerative diseases, addictive disorders, ischemia, and neuropathic pain [6, 38, 39]. The goal of this study was to investigate whether pleiotrophin regulates the astrocytic response and the activation of microglia in the brain after an inflammatory challenge. We used the systemic LPS treatment acute inflammation murine brain model. In the in vivo study, we found that LPS induced a moderate increase in the number of GFAP+ astrocytes in the PFC and striatum of WT mice. After LPS treatment, astrocytes appear hypertrophic, particularly in the PFC, suggesting a LPS-induced upregulation of GFAP protein concentrations in astrocytes of WT mice. This response was significantly reduced in the PFC of LPS-treated PTN-Tg mice, an area with a more significant PTN overexpression in this genotype [24]. We previously found a small (~20%) increase of striatal GFAP+ astrocytes in amphetamine-treated PTN knockout (PTN-/-) mice which could be attributed to compensatory mechanisms

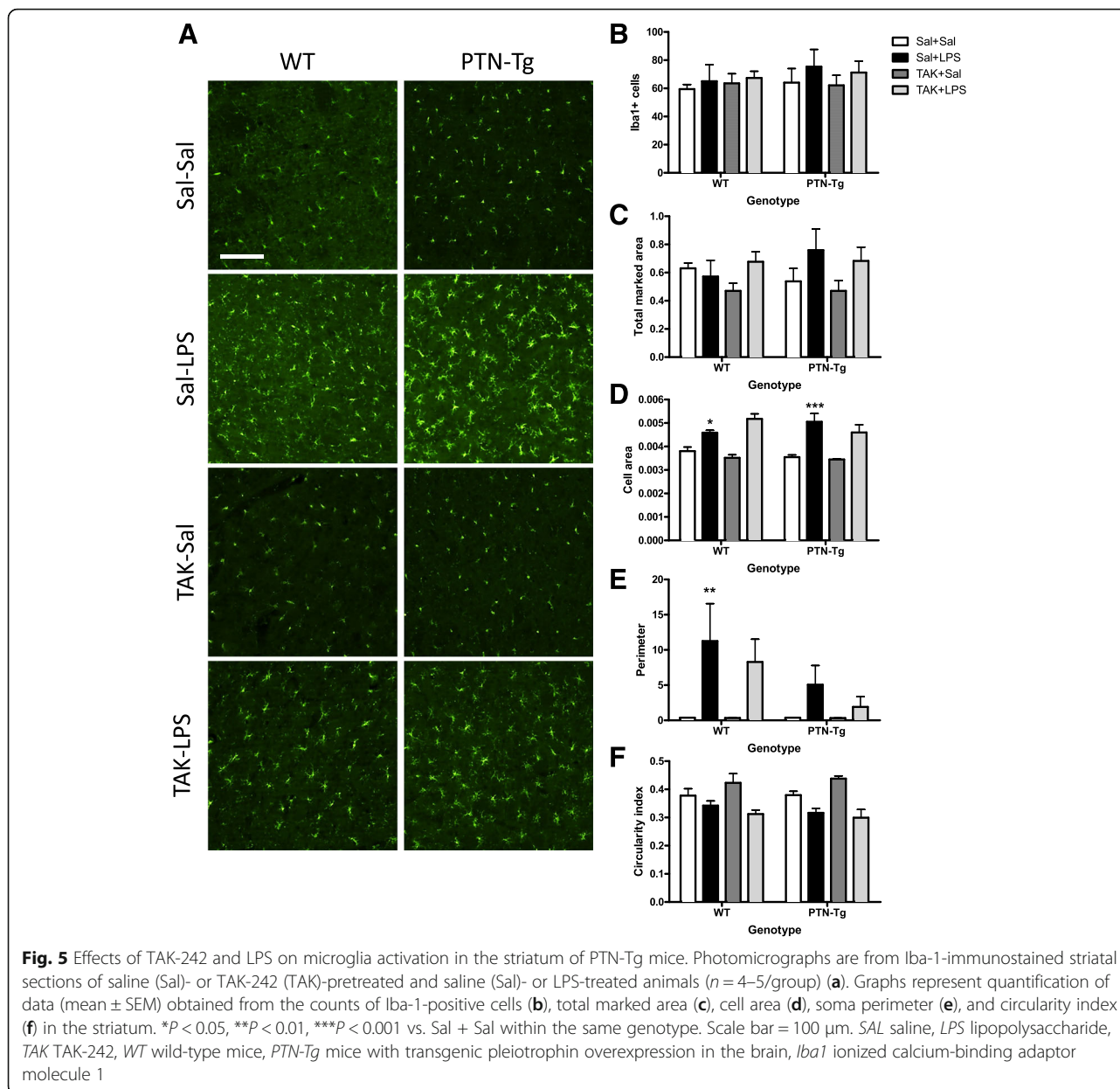


[19, 21]. Interestingly, we recently found a highly significant (13-fold) increase in the number of GFAP+ astrocytes in amphetamine-treated PTN-Tg mice suggesting an enhanced neuroinflammatory response induced by amphetamine in the presence of higher levels of PTN [19]. Taking together, these data suggest that PTN differentially regulates the astrocytic response depending on the inflammatory stimulus.

Although upregulation of GFAP in astrocytes is considered an indicator of reactive astrogliosis and neuroinflammation, the regulation by PTN of two key elements of neuroinflammation, microglia activation, and cytokines release had not been tested before. In WT mice, LPS tended to increase the perimeter of Iba1+ cells and induced a significant increase in these cells area in the PFC, indicating the presence of hypertrophic microglia. In addition, LPS induced significant increases in the levels of TNF- α , IL-6, and MCP-1 in WT mice confirming LPS-induced neuroinflammation in normal mice. Interestingly, we found that PTN overexpression enhances microglial cell morphological changes to an activated-form in the PFC of LPS-treated PTN-Tg mice compared to that of WT mice. This was accompanied by more pronounced LPS-induced increases of TNF- α ,

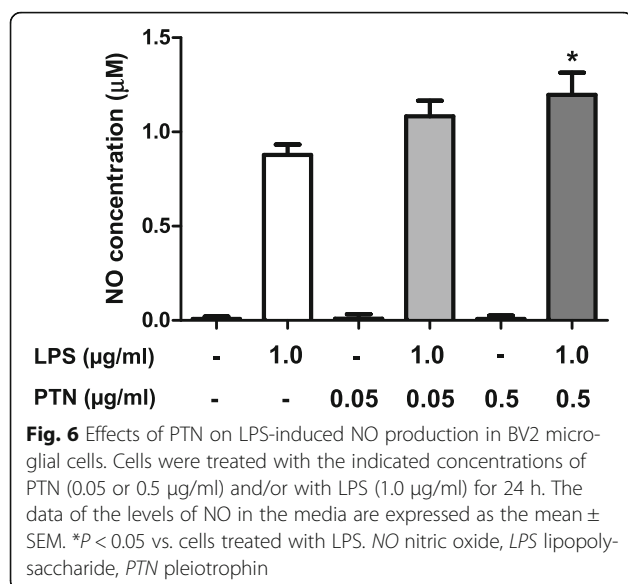
IL-6, and MCP-1 in PTN-Tg mice compared to WT animals, indicating an important role of PTN on microglial activation and neuroinflammation. Interestingly, the TLR4 antagonist TAK-242 did not have any effect on LPS-induced microglia morphological changes in either genotype but efficiently blocked LPS-induced increases of TNF- α , IL-6, and MCP-1 in both genotypes. This is the first study showing that PTN overexpression in vivo significantly potentiates LPS-induced microglial activation and neuroinflammation. It is important to note that we did not find differences between genotypes in saline-treated animals suggesting that PTN is an important cytokine in the promotion of the effects triggered by the inflammatory stimulus but does not trigger proinflammatory cascades itself. Accordingly, our studies in vitro in murine BV2 microglia cells demonstrate that incubation with PTN alone does not cause significant effects on microglia. However, PTN significantly enhanced LPS-induced NO release in BV2 cells. Taking together, these studies may be of relevance since PTN is found highly upregulated in different brain disorders characterized by neuroinflammation such as Parkinson's disease [16], Alzheimer's disease [40], addictive disorders [14, 41, 42], tumors [43], and ischemia [44]. However, we must be cautious because the mechanisms involved in the short-term inflammatory response induced by LPS might differ substantially from those involved in the long-term inflammation associated with the brain disorders mentioned above. In the present work, we have demonstrated for the first time that PTN potentiates microglial activation and neuroinflammation after an acute exposure to the inflammatory stimulus. Additional studies are needed to describe its role in chronic conditions of neuroinflammation.

Inflammation is a host defense mechanism mounted to reduce injury. However, prolonged or uncontrolled inflammation can lead to tissue damage and destruction. On the other hand, recent studies have shown that activated microglia contributes to the maintenance of tissue homeostasis and protection of the CNS under various pathological conditions [45]. Whether microglial activation primed by elevated levels of PTN contributes to the deleterious or homeostatic effects of microglia needs to be clarified. However, it has to be noted that one of the mechanisms that microglia adopts to downregulate inflammation is the production of anti-inflammatory mediators such as IL-4 and IL-10, which suppress the function of proinflammatory cytokines [46]. Here, we demonstrate that the content of IL-10 and IL-4 is not affected by increased PTN levels in the PFC of PTN-Tg mice, whereas the proinflammatory cytokines TNF- α , IL-6, and MCP-1 are highly upregulated compared to WT mice treated with LPS. Thus, our data suggest that high PTN levels lead activated microglia to promotion of neuroinflammation rather than suppression.



The mechanism of action of PTN supports our findings. PTN binds receptor protein tyrosine phosphatase (RPTP) β/ζ (a.k.a. PTPRZ1) [47] and inactivates its phosphatase activity. Inhibition of the phosphatase activity of RPTP β/ζ by PTN binding regulates the tyrosine phosphorylation of substrates of RPTP β/ζ that are known regulators of neuroinflammation such as Fyn kinase [48]. After stimulation with LPS, Fyn is activated in microglia by increased phosphorylation in Y416 [48]. Activated Fyn phosphorylates PKC δ at Y311, contributing to an increase in its kinase activity. The Fyn-PKC δ -signaling axis

further activates the LPS-induced MAP kinase phosphorylation and activation of the NF κ B pathway, implying that Fyn is a major upstream regulator of proinflammatory signaling [48]. These signaling events are observed as well in animal models of PD [48]. Previously, we demonstrated that PTN is a key modulator of tyrosine phosphorylation of Fyn [49], suggesting that PTN could be a major upstream regulator of microglial neuroinflammatory processes in all those neurological disorders in which significantly increased levels of PTN have been detected by triggering inflammogen-induced increase in Fyn kinase activity.



Conclusions

Our findings identify for the first time that PTN is a novel and potent regulator of neuroinflammation. Pleiotrophin potentiates LPS-stimulated microglia activation. Our results indicate that the regulation of PTN signaling pathways may constitute new therapeutic opportunities particularly in those neurological disorders characterized by increased PTN cerebral levels and neuroinflammation.

Abbreviations

ANOVA: Analysis of variance; BBB: Blood-brain barrier; BCA: Bicinchoninic acid; CNS: Central nervous system; COX2: Cyclooxygenase-2 enzyme; GFAP: Glial fibrillary acidic protein; Iba1: Ionized calcium-binding adaptor molecule 1; IL-10: Interleukin 10; IL-1β: Interleukin 1β; IL-4: Interleukin 4; IL-6: Interleukin 6; iNOS: Inducible nitric oxide synthase; LPS: Lipopolysaccharide; MAP kinase: Mitogen-activated protein kinase; MCP-1: Monocyte chemoattractant protein-1; NFκB: Nuclear factor-κB; NO: Nitric oxide; PD: Parkinson's disease; PFC: Prefrontal cortex; PKCδ: Protein kinase C delta type; PTN^{-/-}: PTN genetically deficient mice; PTN: Pleiotrophin; PTN-Tg: Mice with transgenic PTN overexpression in the brain; qRT-PCR: Quantitative real-time polymerase chain reaction; RPMI-1640: Roswell Park Memorial Institute 1640 medium; RPTP β/ζ (PTPRZ1): Receptor protein tyrosine phosphatase β/ζ; SEM: Standard error of the mean; TLR4: Toll-like receptor 4; TLRs: Toll-like receptors; TNF-α: Tumor necrosis factor-α; WT: Wild type

Acknowledgements

This work has been supported by grants SAF2014-56671-R from the Ministerio de Economía y Competitividad of Spain, PNSD001I2015 from the National Plan on Drug Abuse, Ministerio de Sanidad of Spain, and USP-BS-APP03/2014 from the Universidad CEU San Pablo and Banco de Santander to GH. MVR and RFC are supported by fellowships from Fundación Universitaria San Pablo CEU.

Funding

SAF2014-56671-R (Ministerio de Economía y Competitividad of Spain), PNSD001I2015 (National Plan on Drug Abuse, Ministerio de Sanidad of Spain), and USP-BS-APP03/2014 (Universidad CEU San Pablo and Banco de Santander).

Availability of data and materials

The datasets used and/or analyzed during the current study are available from the corresponding author on reasonable request.

Authors' contributions

RFC, MVR, EG, and JP performed the experiments. CPG, MPR, and GH analyzed and interpreted the results. MFA and MU contributed with the development of the transgenic mouse model and data interpretation. GH wrote the manuscript. All authors read and approved the final manuscript.

Competing interests

The authors declare that they have no competing interests.

Consent for publication

Not applicable

Ethics approval and consent to participate

All the animals used in this study were maintained in accordance with the European Union Laboratory Animal Care Rules (86/609/ECC directive) and the protocols were approved by the Animal Research Committee of USP-CEU.

Author details

¹Pharmacology Lab, Department of Pharmaceutical and Health Sciences, Facultad de Farmacia, Universidad CEU San Pablo, Urb. Montepríncipe, 28668 Boadilla del Monte, Madrid, Spain. ²Biochemistry and Molecular Biology lab, Department of Chemistry and Biochemistry, Facultad de Farmacia, Universidad CEU San Pablo, Madrid, Spain. ³BRAINco Biopharma, S.L., Bizkaia Technology Park, Vizcaya, Spain.

Received: 8 December 2016 Accepted: 24 February 2017

Published online: 04 March 2017

References

- Barbierato M, Facci L, Argentini C, Marinelli C, Skaper SD, Giusti P. Astrocyte-microglia cooperation in the expression of a pro-inflammatory phenotype. *CNS Neurol Disord Drug Targets*. 2013;12:608–18.
- Hanke ML, Kielian T. Toll-like receptors in health and disease in the brain: mechanisms and therapeutic potential. *Clin Sci (Lond)*. 2011;121:367–87.
- O'Neill LA. Therapeutic targeting of Toll-like receptors for inflammatory and infectious diseases. *Curr Opin Pharmacol*. 2003;3:396–403.
- Akira S, Takeda K. Functions of toll-like receptors: lessons from KO mice. *C R Biol*. 2004;327:581–9.
- Amor S, Peferoen LA, Vogel DY, Breur M, van der Valk P, Baker D, van Noort JM. Inflammation in neurodegenerative diseases—an update. *Immunology*. 2014;142:151–66.
- Herradon G, Perez-Garcia C. Targeting midkine and pleiotrophin signalling pathways in addiction and neurodegenerative disorders: recent progress and perspectives. *Br J Pharmacol*. 2014;171:837–48.
- Najjar S, Pearlman DM, Alper K, Najjar A, Devinsky O. Neuroinflammation and psychiatric illness. *J Neuroinflammation*. 2013;10:43.
- Silva AP, Martins T, Baptista S, Goncalves J, Agasse F, Malva JO. Brain injury associated with widely abused amphetamines: neuroinflammation, neurogenesis and blood-brain barrier. *Curr Drug Abuse Rev*. 2003;3:239–54.
- Clark KH, Wiley CA, Bradberry CW. Psychostimulant abuse and neuroinflammation: emerging evidence of their interconnection. *Neurotox Res*. 2013;23:174–88.
- Moratalla R, Khairnar A, Simola N, Granado N, Garcia-Montes JR, Porceddu PF, Tizabi Y, Costa G, Morelli M. Amphetamine-related drugs neurotoxicity in humans and in experimental animals: main mechanisms. *Prog Neurobiol*. 2015; doi:10.1016/j.pneurobio.2015.09.011.
- Curtin K, Fleckenstein AE, Robison RJ, Crookston MJ, Smith KR, Hanson GR. Methamphetamine/amphetamine abuse and risk of Parkinson's disease in Utah: a population-based assessment. *Drug Alcohol Depend*. 2015;146:30–8.
- Hwang O. Role of oxidative stress in Parkinson's disease. *Exp Neurobiol*. 2013;22:11–7.
- Nimmo AJ, Vink R. Recent patents in CNS drug discovery: the management of inflammation in the central nervous system. *Recent Pat CNS Drug Discov*. 2009;4:86–95.
- Le Greves P. Pleiotrophin gene transcription in the rat nucleus accumbens is stimulated by an acute dose of amphetamine. *Brain Res Bull*. 2005;65:529–32.
- Alguacil LF, Herradon G. Midkine and pleiotrophin in the treatment of neurodegenerative diseases and drug addiction. *Recent Pat CNS Drug Discov*. 2015;10:28–33.

16. Marchionini DM, Lehrmann E, Chu Y, He B, Sortwell CE, Becker KG, Freed WJ, Kordower JH, Collier TJ. Role of heparin binding growth factors in nigrostriatal dopamine system development and Parkinson's disease. *Brain Res.* 2007;1147:77–88.
17. Achour A, M'Bika JP, Baudouin F, Caruelle D, Courty J. Pleiotrophin induces expression of inflammatory cytokines in peripheral blood mononuclear cells. *Biochimie.* 2008;90:1791–5.
18. Silver K, Desormaux A, Freeman LC, Lillich JD. Expression of pleiotrophin, an important regulator of cell migration, is inhibited in intestinal epithelial cells by treatment with non-steroidal anti-inflammatory drugs. *Growth Factors.* 2012;30:258–66.
19. Vicente-Rodriguez M, Rojo-Gonzalez L, Gramage E, Fernandez-Calle R, Chen Y, Perez-Garcia C, Ferrer-Alcon M, Uribarri M, Bailey A, Herradon G. Pleiotrophin overexpression regulates amphetamine-induced reward and striatal dopaminergic denervation without changing the expression of dopamine D1 and D2 receptors: implications for neuroinflammation. *Eur Neuropsychopharmacol.* 2016;26:1794–805.
20. Gramage E, Rossi L, Granado N, Moratalla R, Herradon G. Genetic inactivation of pleiotrophin triggers amphetamine-induced cell loss in the substantia nigra and enhances amphetamine neurotoxicity in the striatum. *Neuroscience.* 2010;170:308–16.
21. Gramage E, Putelli A, Polanco MJ, Gonzalez-Martin C, Ezquerra L, Alguacil LF, Perez-Pinera P, Deuel TF, Herradon G. The neurotrophic factor pleiotrophin modulates amphetamine-seeking behaviour and amphetamine-induced neurotoxic effects: evidence from pleiotrophin knockout mice. *Addict Biol.* 2010;15:403–12.
22. Asari A, Kanemitsu T, Kurihara H. Oral administration of high molecular weight hyaluronan (900 kDa) controls immune system via Toll-like receptor 4 in the intestinal epithelium. *J Biol Chem.* 2010;285:24751–8.
23. Ferrer-Alcón M, Uribarri M, Díaz A, Del Olmo N, Valdizán EM, Gramage E, Martín M, Castro E, Pérez-García C, Mengod G, Maldonado R, Herradon G, Pazos A, Palacios JM. A new non-classical transgenic animal model of Depression Program No. 776.04/FF9 Neuroscience Meeting Planner. New Orleans: Society for Neuroscience; 2012. Online.
24. Vicente-Rodriguez M, Perez-Garcia C, Ferrer-Alcon M, Uribarri M, Sanchez-Alonso MG, Ramos MP, Herradon G. Pleiotrophin differentially regulates the rewarding and sedative effects of ethanol. *J Neurochem.* 2014;131:688–95.
25. Aigner L, Arber S, Kapfhammer JP, Laux T, Schneider C, Botteri F, Brenner HR, Caroni P. Overexpression of the neural growth-associated protein GAP-43 induces nerve sprouting in the adult nervous system of transgenic mice. *Cell.* 1995;83:269–78.
26. Caroni P. Overexpression of growth-associated proteins in the neurons of adult transgenic mice. *J Neurosci Methods.* 1997;71:3–9.
27. Vicente-Rodriguez M, Perez-Garcia C, Haro M, Ramos MP, Herradon G. Genetic inactivation of midkine modulates behavioural responses to ethanol possibly by enhancing GABA(A) receptor sensitivity to GABA(A) acting drugs. *Behav Brain Res.* 2014;274:258–63.
28. Vicente-Rodriguez M, Herradon G, Ferrer-Alcon M, Uribarri M, Perez-Garcia C. Chronic cocaine use causes changes in the striatal proteome depending on the endogenous expression of pleiotrophin. *Chem Res Toxicol.* 2015;28:1443–54.
29. Gramage E, Martin YB, Ramanah P, Perez-Garcia C, Herradon G. Midkine regulates amphetamine-induced astrocytosis in striatum but has no effects on amphetamine-induced striatal dopaminergic denervation and addictive effects: functional differences between pleiotrophin and midkine. *Neuroscience.* 2011;190:307–17.
30. Luo XL, Liu SY, Wang LJ, Zhang QY, Xu P, Pan LL, Hu JF. A tetramethoxychalcone from *Chloranthus henryi* suppresses lipopolysaccharide-induced inflammatory responses in BV2 microglia. *Eur J Pharmacol.* 2016;774:135–43.
31. Lastres-Becker I, Garcia-Yague AJ, Scannevin RH, Casarejos MJ, Kugler S, Rabano A, Cuadrado A. Repurposing the NRF2 activator dimethyl fumarate as therapy against synucleinopathy in Parkinson's disease. *Antioxid Redox Signal.* 2016;25:61–77.
32. Torika N, Asraf K, Danon A, Apte RN, Fleisher-Berkovich S. Telmisartan modulates glial activation: in vitro and in vivo studies. *PLoS One.* 2016;11:e0155823.
33. Frey D, Jung S, Brackmann F, Richter-Kraus M, Trollmann R. Hypoxia potentiates LPS-mediated cytotoxicity of BV2 microglial cells in vitro by synergistic effects on glial cytokine and nitric oxide system. *Neuropediatrics.* 2015;46:321–8.
34. Hida H, Jung CG, Wu CZ, Kim HJ, Kodama Y, Masuda T, Nishino H. Pleiotrophin exhibits a trophic effect on survival of dopaminergic neurons in vitro. *Eur J Neurosci.* 2003;17:2127–34.
35. Himburg HA, Muramoto GG, Daher P, Meadows SK, Russell JL, Doan P, Chi JT, Salter AB, Lento WE, Reya T, Chao NJ, Chute JP. Pleiotrophin regulates the expansion and regeneration of hematopoietic stem cells. *Nat Med.* 2010;16:475–82.
36. Maragakis NJ, Rothstein JD. Mechanisms of disease: astrocytes in neurodegenerative disease. *Nat Clin Pract Neurol.* 2006;2:679–89.
37. Qin L, Liu Y, Wang T, Wei SJ, Block ML, Wilson B, Liu B, Hong JS. NADPH oxidase mediates lipopolysaccharide-induced neurotoxicity and proinflammatory gene expression in activated microglia. *J Biol Chem.* 2004;279:1415–21.
38. Ezquerra L, Alguacil LF, Nguyen T, Deuel TF, Silos-Santiago I, Herradon G. Different pattern of pleiotrophin and midkine expression in neuropathic pain: correlation between changes in pleiotrophin gene expression and rat strain differences in neuropathic pain. *Growth Factors.* 2008;26:44–8.
39. Gramage E, Herradon G. Connecting Parkinson's disease and drug addiction: common players reveal unexpected disease connections and novel therapeutic approaches. *Curr Pharm Des.* 2011;17:449–61.
40. Wisniewski T, Lalowski M, Baumann M, Rauvala H, Raulo E, Nolo R, Frangione B. HB-GAM is a cytokine present in Alzheimer's and Down's syndrome lesions. *Neuroreport.* 1996;7:667–71.
41. Maillieux P, Preud'homme X, Albala N, Vanderwinden JM, Vanderhaeghen JJ. delta-9-Tetrahydrocannabinol regulates gene expression of the growth factor pleiotrophin in the forebrain. *Neurosci Lett.* 1994;175:25–7.
42. Herradon G, Ezquerra L, Gramage E, Alguacil LF. Targeting the pleiotrophin/receptor protein tyrosine phosphatase beta/zeta signaling pathway to limit neurotoxicity induced by drug abuse. *Mini Rev Med Chem.* 2009;9:440–7.
43. Peria FM, Neder L, Marie SK, Rosemberg S, Oba-Shinjo SM, Colli BO, Gabbai AA, Malheiros SM, Zago MA, Panepucci RA, Moreira-Filho CA, Okamoto OK, Carloti Jr CG. Pleiotrophin expression in astrocytic and oligodendroglial tumors and its correlation with histological diagnosis, microvascular density, cellular proliferation and overall survival. *J Neurooncol.* 2007;84:255–61.
44. Miao J, Ding M, Zhang A, Xiao Z, Qi W, Luo N, Di W, Tao Y, Fang Y. Pleiotrophin promotes microglia proliferation and secretion of neurotrophic factors by activating extracellular signal-regulated kinase 1/2 pathway. *Neurosci Res.* 2012;74:269–76.
45. Chen Z, Trapp BD. Microglia and neuroprotection. *J Neurochem.* 2016;136 Suppl 1:10–7.
46. Colton CA. Heterogeneity of microglial activation in the innate immune response in the brain. *J Neuroimmune Pharmacol.* 2009;4:399–418.
47. Meng K, Rodriguez-Pena A, Dimitrov T, Chen W, Yamin M, Noda M, Deuel TF. Pleiotrophin signals increased tyrosine phosphorylation of beta beta-catenin through inactivation of the intrinsic catalytic activity of the receptor-type protein tyrosine phosphatase beta/zeta. *Proc Natl Acad Sci U S A.* 2000;97:2603–8.
48. Panicker N, Saminathan H, Jin H, Neal M, Harischandra DS, Gordon R, Kanthasamy K, Lawana V, Sarkar S, Luo J, Anantharam V, Kanthasamy AG, Kanthasamy A. Fyn kinase regulates microglial neuroinflammatory responses in cell culture and animal models of Parkinson's disease. *J Neurosci.* 2015;35:10058–77.
49. Pariser H, Ezquerra L, Herradon G, Perez-Pinera P, Deuel TF. Fyn is a downstream target of the pleiotrophin/receptor protein tyrosine phosphatase beta/zeta-signaling pathway: regulation of tyrosine phosphorylation of Fyn by pleiotrophin. *Biochem Biophys Res Commun.* 2005;332:664–9.

ARTÍCULO 2. Endogenous pleiotrophin and midkine regulate LPS-induced glial responses.

Rosalía Fernández-Calle, Marta Vicente-Rodríguez, Esther Gramage, Carlos de la Torre-Ortiz, Carmen Pérez-García, María P. Ramos y Gonzalo Herradón.

Neuroscience Letters, 2018. ISSN: 1872-7972

Volumen: 662

Número de páginas: 213-218

DOI: 10.1016/j.neulet.2017.10.038

Resumen

La pleiotrofina (PTN) y la midkina (MK) son dos factores de crecimiento que modulan la neuroinflamación. La sobreexpresión cerebral de PTN impide la astrocitosis inducida por LPS, pero potencia la activación microglial. La respuesta astrocítica moderada causada por una dosis baja de LPS (0,5 mg/kg) está ausente en el cuerpo estriado de ratones $Mk^{-/-}$, mientras que la respuesta microglial no se ve afectada. En esta ocasión, se han evaluado los efectos de una dosis intermedia de LPS (7,5 mg/kg) en la respuesta glial de ratones $Ptn^{-/-}$ y $Mk^{-/-}$. Se descubrió que la astrocitosis inducida por LPS se impide tanto en la corteza prefrontal como en el estriado de ratones $Ptn^{-/-}$ y $Mk^{-/-}$. Algunos de los cambios morfológicos inducidos por el LPS sobre la microglía tendieron a ser más destacados en los ratones $Ptn^{-/-}$ frente a los animales Wt. Debido a que previamente se ha demostrado que PTN potencia la activación inducida por LPS en células microgliales BV2, se ha evaluado la activación de la quinasa Fyn, sustrato del receptor de PTN, RPTP β/ζ , y la subsiguiente fosforilación de ERK1/2 en células BV2 tratadas con LPS y PTN. La presencia de PTN no tuvo efecto sobre las acciones de LPS en las células BV2, lo que sugiere que PTN no recluta la cascada de señalización Fyn-MAPK en la modulación del efecto de LPS en células BV2. Por lo tanto, las evidencias demuestran que la regulación de la respuesta astrogliar frente a la administración de LPS depende en gran manera de los niveles de expresión de PTN y MK. Se necesitarán más estudios para esclarecer el posible papel de la expresión endógena de PTN y MK en la respuesta microglial inducida por LPS.

Contribución de la doctoranda en este trabajo

Rosalía Fernández Calle contribuyó en el tratamiento de los animales y el procesamiento de muestras. Realizó los experimentos de inmunohistoquímica recogidos en esta publicación y en el análisis de los parámetros morfológicos de la microglía. Realizó y analizó los experimentos de *Western-blot* recogidos en la figura 5. Ayudó en el análisis estadístico y con la escritura del manuscrito.



Contents lists available at ScienceDirect

Neuroscience Letters

journal homepage: www.elsevier.com/locate/neulet

Research article

Endogenous pleiotrophin and midkine regulate LPS-induced glial responses

Rosalia Fernández-Calle^a, Marta Vicente-Rodríguez^a, Esther Gramage^a, Carlos de la Torre-Ortiz^a, Carmen Pérez-García^a, María P. Ramos^b, Gonzalo Herradón^{a,*}^a Departamento de Ciencias Farmacéuticas y de la Salud, Facultad de Farmacia, Universidad San Pablo-CEU, CEU Universities, Urbanización Montepríncipe, 28925, Alcorcón, Madrid, Spain^b Departamento de Química y Bioquímica, Facultad de Farmacia, Universidad San Pablo-CEU, CEU Universities, Urbanización Montepríncipe, 28925, Alcorcón, Madrid, Spain

ARTICLE INFO

Keywords:

Neuroinflammation
Microglia
Astroglia
FYN kinase
Pleiotrophin
Midkine

ABSTRACT

Pleiotrophin (PTN) and Midkine (MK) are two growth factors that modulate neuroinflammation. PTN overexpression in the brain prevents LPS-induced astrogliosis in mice but potentiates microglial activation. The modest astrogliosis response caused by a low dose of LPS (0.5 mg/kg) is blocked in the striatum of MK^{-/-} mice whereas microglial response is unaffected. We have now tested the effects of an intermediate dose of LPS (7.5 mg/kg) in glial response in PTN^{-/-} and MK^{-/-} mice. We found that LPS-induced astrogliosis is prevented in prefrontal cortex and striatum of both PTN^{-/-} and MK^{-/-} mice. Some of the morphological changes of microglia induced by LPS tended to increase in both genotypes, particularly in PTN^{-/-} mice. Since we previously showed that PTN potentiates LPS-induced activation of BV2 microglial cells, we tested the activation of FYN kinase, a substrate of the PTN receptor RPTPβ/ζ, and the subsequent ERK1/2 phosphorylation on LPS and PTN-treated BV2 cells. LPS effects on BV2 cells were not affected by the addition of PTN, suggesting that PTN does not recruit the FYN-MAP kinase signaling pathway in order to modulate LPS effects on microglial cells. Taking together, evidences demonstrate that regulation of astroglial responses to LPS administration are highly dependent on the levels of expression of PTN and MK. Further studies are needed to clarify the possible roles of endogenous expression of PTN and MK in LPS-induced microglial responses.

1. Introduction

Activation of the innate immunity in the Central Nervous System (CNS) is an important step in the healing process of the damaged brain tissue. When prolonged, however, neuroinflammation can become deleterious [1]. Activation of microglia and astroglia are key events in neuroinflammatory processes and contribute to the neuronal alterations characteristic of pathologies with overt neuroinflammation including neurodegenerative diseases [2], multiple sclerosis [3,4] and drug addiction [5].

The contribution of Toll-like receptors (TLRs) to neuroinflammatory processes has been shown [6]. However, the genetic background that modulates neuroinflammation is largely elusive. Recently, we identified

pleiotrophin (PTN) and Midkine (MK) as two novel growth factors that modulate neuroinflammation in different contexts [7–9]. Pleiotrophin and MK are the only cytokines that constitute the PTN/MK developmental gene family [10,11] and overlap many functions including survival and differentiation of neurons [12]. Both PTN and MK bind to receptor protein tyrosine phosphatase (RPTP) β/ζ (a.k.a. PTPRZ1, (R) PTPβ or PTPζ) and inhibit its phosphatase activity [13,14], leading to increased phosphorylation of substrates of RPTPβ/ζ such as FYN kinase [15]. Pleiotrophin and MK are upregulated in different pathologies of the CNS characterized by neuroinflammation including neurodegenerative diseases, addictive disorders, ischemia and neuropathic pain [5], which led us to hypothesize a modulatory role of these cytokines in neuroinflammatory processes. Previously, we observed that highly

Abbreviations: ANOVA, analysis of variance; CNS, central nervous system; GFAP, glial fibrillary acidic protein; Iba1, ionized calcium-binding adaptor molecule 1; IL-1β, interleukin 1β; IL-6, interleukin 6; iNOS, inducible nitric oxide synthase; LPS, lipopolysaccharide; MAP kinase, mitogen-activated protein kinase; MK^{-/-}, MK genetically deficient mice; MK, Midkine; NFκB, nuclear factor-κB; PFC, prefrontal cortex; PTN^{-/-}, PTN genetically deficient mice; PTN, Pleiotrophin; PTN-Tg, mice with transgenic PTN overexpression in the brain; RPMI-1640, Roswell Park Memorial Institute 1640 medium; RPTP β/ζ (PTPRZ1), receptor protein tyrosine phosphatase β/ζ; S.E.M., standard error of the mean; TLRs, Toll-like receptors; TNF-α, tumor necrosis factor-α; WT, wild type

* Corresponding author at: Departamento de Ciencias Farmacéuticas y de la Salud, Facultad de Farmacia, Universidad San Pablo-CEU, CEU Universities, Urbanización Montepríncipe, 28925, Alcorcón, Madrid, Spain

E-mail addresses: rosalia.fernandezcalle@beca.ceu.es (R. Fernández-Calle), martavro@gmail.com (M. Vicente-Rodríguez), esther.gramagecaro@ceu.es (E. Gramage), c.torre3@usp.ceu.es (C. de la Torre-Ortiz), capegar@ceu.es (C. Pérez-García), pramos@ceu.es (M.P. Ramos), herradon@ceu.es (G. Herradón).

<http://dx.doi.org/10.1016/j.neulet.2017.10.038>

Received 6 August 2017; Received in revised form 4 October 2017; Accepted 19 October 2017

Available online 20 October 2017

0304-3940/ © 2017 Elsevier B.V. All rights reserved.

upregulated PTN brain levels enhance amphetamine-induced astrocytosis [7] but prevents LPS-induced astrocytic response [9]. Importantly, a 4-fold upregulation of PTN levels in PFC potentiates LPS-induced microglial activation and release of inflammatory cytokines [9]. On the other hand, the modest astrocytic response elicited by a very low dose of LPS (0.5 mg/kg) seems to be blocked in the striatum of MK^{-/-} mice whereas no significant changes were observed in microglial response [8]. The data suggest a complex regulatory role of PTN and MK in important processes of neuroinflammation such as microglial and astrocytic responses, depending on their own levels of expression and the nature and intensity of the inflammatory stimulus. In order to assess the importance of normal endogenous expression of these cytokines in response to inflammatory stimuli, we aimed to test the effects of an intermediate dose of LPS (7.5 mg/kg) in glial response in different brain areas of PTN^{-/-} and MK^{-/-} mice. In addition, since FYN kinase has been recently shown as an upstream regulator of proinflammatory signaling [16] and is a substrate of RPTPβ/ζ [15], we have explored the possibility that PTN regulates LPS effects in vitro through its ability to modulate FYN kinase signaling.

2. Material and methods

2.1. Animals

PTN^{-/-} and MK^{-/-} mice were kindly provided by Dr. Thomas F. Deuel (The Scripps Research Institute, La Jolla, CA). MK^{-/-} and PTN^{-/-} mice on a C57BL/6J background were generated by methods previously described [17,18]. We used male MK^{-/-}, PTN^{-/-} and WT animals of 9–10 weeks (20–25 g). Mice were housed under controlled environmental conditions (22 ± 1 °C and a 12-h light/12-h dark cycle) with free access to food and water. Mice were maintained in accordance with both the ARRIVE guidelines and the European Union Laboratory Animal Care Rules (Directive 2010/63/EU for animal experiments) and the protocols were approved by the Animal Research Committee of USP-CEU.

2.2. Immunohistochemistry

Mice from all experimental groups (n = 4–5/group) received a single i.p. injection of LPS (Sigma, Madrid, Spain) (7.5 mg/kg) or saline (control, 10 ml/kg) and were sacrificed 16 h after LPS administration. This protocol was previously used by our group in mice with transgenic overexpression of PTN in the brain [9].

Animals were sacrificed by transcardial perfusion with 4% paraformaldehyde. Brains were removed and 30 μm PFC and striatal free-floating sections were processed as previously described [7–9]. Immunohistochemistry studies were performed in one slice per 180 μm (PFC from bregma –3.08 mm to –2.46 mm; Striatum from bregma 1.54 mm to –0.10 mm). Sections were incubated overnight at 4 °C with anti-glial fibrillary acidic protein (GFAP; Millipore, Madrid, Spain; 1:1000) and anti-ionized calcium-binding adaptor molecule 1 (Iba1, Wako, Osaka, Japan; 1:1000) antibodies, following by 30 min incubation with the Alexa-Fluor-555 and Alexa-Fluor-488 corresponding secondary antibody (Invitrogen, Waltham, MA USA; 1:500). Photomicrographs were captured with a digital camera coupled to an optical microscope (DM5500B, Leica, Solms, Germany). Analysis was performed using ImageJ (NIH), in the three most central slices of each area. Iba1+ cells and GFAP+ astrocytes were counted in whole sections of PFC and in 1100 μm x 1400 μm standardized areas in the striatum [9]. Analysis of changes in microglia morphology was performed as recently described [9]. Briefly, total marked area was calculated as overall image fluorescence, subtracting the mean background fluorescence. The soma size (cell area) is expressed in square micrometers. The perimeter was calculated based on the outline length of a given object, is expressed in microns and is expected to be higher in activated cells. Circularity was calculated by the following formula:

$4\pi \times (\text{area/perimeter}^2)$. This parameter varies from 0 (linear polygon) to 1 (perfect circular object). Mean single cell values for each parameter were used for statistics.

2.3. BV2 murine microglial cell cultures

BV2 murine microglial cells were a generous gift from Professor Antonio Cuadrado (Instituto de Investigaciones Biomédicas “Alberto Sols” (IIBM), Madrid, Spain). Cells were routinely maintained in RPMI-1640 medium with fetal bovine serum (10%), penicillin (100 U/ml), streptomycin (100 μg/ml) and L-glutamine (4 mM) at 37 °C in 5% CO₂ humidified air following conditions used by others [19,20].

To test the effects of PTN (Sigma, Spain) on LPS-stimulated BV2 cell cultures, cells were incubated for 30 min with LPS (1.0 μg/ml) and/or PTN (0.5 μg/ml). Total protein from non-stimulated, PTN-, and LPS-stimulated BV2 cell lysates (Six 60-mm plates/each) was quantified by the BCA protein assay (Pierce, Rockford, IL). Equilibrated protein samples were mixed with loading buffer (60 mM Tris pH 6.8, 10% glycerol, 5% SDS, 0.65% β-mercaptoethanol, and 0.01% bromophenol blue), boiled for 5 min, and loaded onto 10% polyacrylamide gels (Invitrogen, Carlsbad, CA) with SDS (SDS-PAGE). The gels were transferred to nitrocellulose membranes, blocked with 50 mM Tris, 150 mM NaCl, 0.1% Tween-20 (TBS-T), and 5% non-fat milk for 1 h. We determined the phosphorylation status of the Y416 residue in FYN kinase activation loop domain by using the phospho Y416 Src family kinase (p-Y416SFK) antibody (Cell signaling, Danvers, MA), which has been used extensively to demonstrate FYN kinase activation [16,21,22]. In addition, membranes were probed with anti-phospho-ERK1/2 (1:1000) (Cell signaling, Danvers, MA) antibodies and re-probed with anti-FYN and anti-ERK1/2 (1:1000) (Cell signaling, Danvers, MA) antibodies to confirm the identity of the protein. Membranes were incubated for one hour with appropriate secondary antibodies (Santa Cruz biotechnology, Santa Cruz, CA) conjugated with horseradish peroxidase diluted 1:5000 in TBS-T with 5% non-fat milk for 30 min. The immunoreactive proteins were visualized using the ECL Enhanced method according to the manufacturer's instructions (Amersham, San Francisco, CA).

2.4. Statistics

Data are presented as mean ± standard error of the mean (S.E.M.). Data obtained from immunohistochemistry studies were analyzed using two-way ANOVA considering genotype and treatment as variants. Relevant differences were analyzed by post-hoc comparisons with Bonferroni's post-hoc tests. Data obtained from BV2 cells were analyzed using one-way ANOVA followed by post-hoc comparisons with Tukey's post-hoc tests. P < 0.05 was considered as statistically significant. All statistical analyses were performed using Graph-Pad Prism program (San Diego, CA, USA).

3. Results

3.1. Differential regulation of LPS-induced astrocytic and microglial responses in the PFC and striatum of PTN^{-/-} and MK^{-/-} mice

First, we found that LPS (7.5 mg/kg) increased the number of GFAP+ astrocytes in the PFC (Fig. 1) and striatum (Fig. 2) of WT mice. The upregulation of GFAP levels in astrocytes was apparent since most of these cells were heavily stained, suggesting astroglial activation. In contrast, these effects on GFAP+ immunoreactivity induced by LPS were blocked in PTN^{-/-} and MK^{-/-} mice independently of the brain area considered (Figs. 1 and 2). The data clearly show that normal levels of endogenous PTN and MK are required for LPS-induced astrocytic response.

PFC and striatal sections were then immunostained with anti-Iba1 microglial antibody. We observed resting morphology of microglia in the PFC of saline-treated animals independently of the genotype

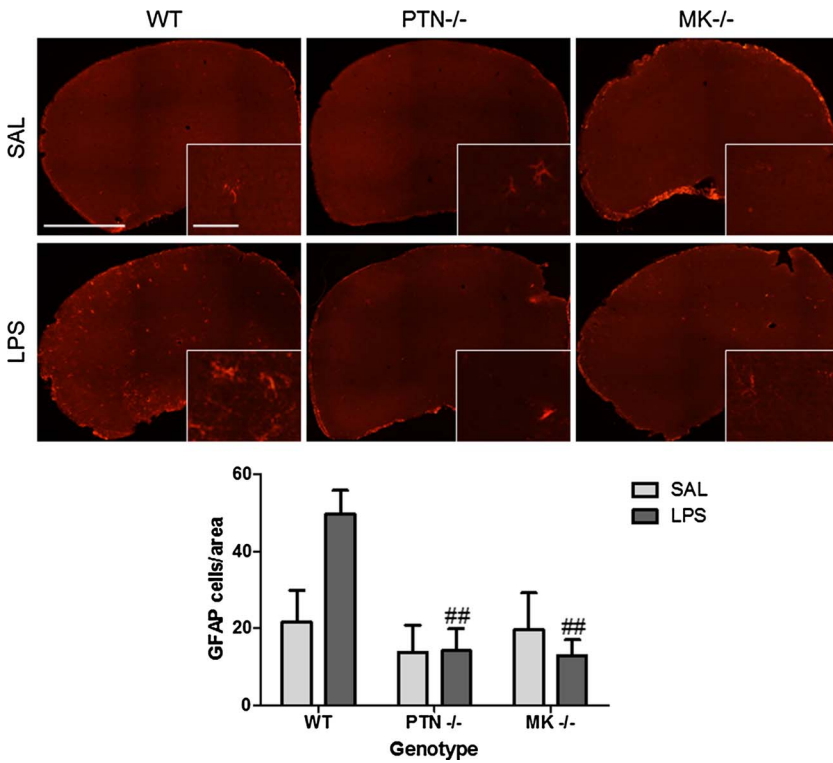


Fig. 1. LPS effects on astrocytosis in the PFC of WT, MK^{-/-} and PTN^{-/-} mice. Photomicrographs are from GFAP-immunostained PFC sections of saline (Sal)- or LPS-treated animals (n = 4–5/group). The graph represents quantification of data obtained from the counts of GFAP-positive cells in PFC whole sections. ## P < 0.01 vs. WT with the same treatment. Scale bar = 500 μm (high magnification: scale bar = 50 μm).

(Fig. 3). Immunohistochemistry for Iba1 did not reflect significant changes in the number of Iba1+ cells in the PFC after LPS treatment (Fig. 3B). However, we observed signs of enhanced hypertrophism in LPS-treated mice, particularly in the case of mice lacking endogenous PTN (Fig. 3). We did not detect significant changes in the total marked area (Fig. 3C), probably because the number of Iba1+ cells tended to be lower in PTN^{-/-} mice. The Iba1+ cell area, a parameter expected to be higher in activated and hypertrophic cells, was significantly

increased by LPS in all genotypes (Fig. 3D). The magnitude of the increase in the perimeter caused by LPS was similar in PFC of all genotypes although only reached significance in the case of WT mice (Fig. 3E). The reduction caused by LPS in the circularity index, a parameter expected to decrease in activated cells, was significantly more pronounced in PTN^{-/-} and MK^{-/-} mice (Fig. 3F). Interestingly, these differences between genotypes in the PFC were nearly lost in the striatum (Fig. 4), a brain area where we only detected that LPS-induced

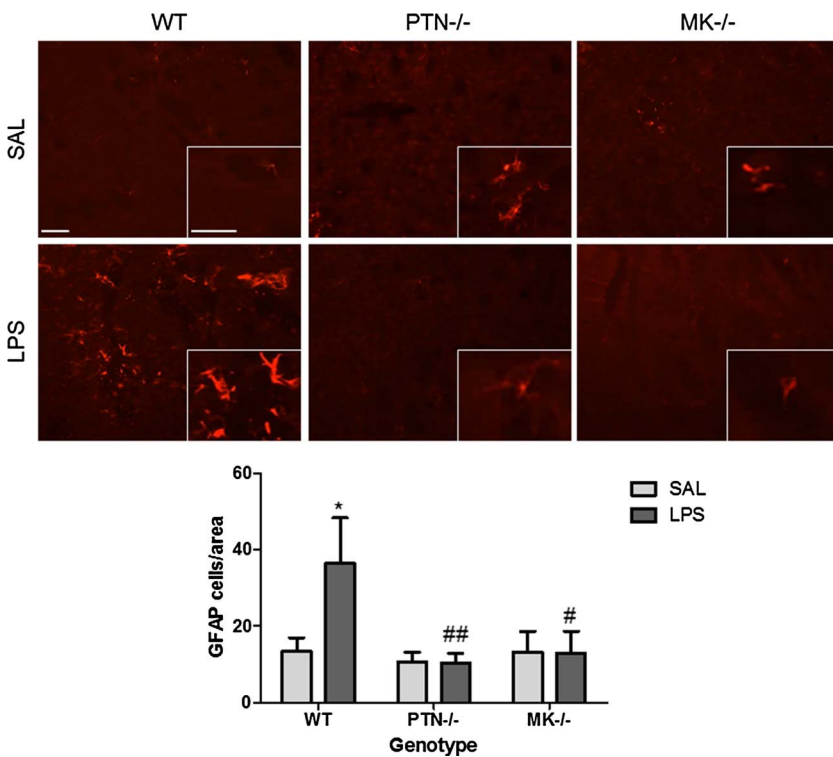


Fig. 2. LPS effects on astrocytosis in the striatum of WT, MK^{-/-} and PTN^{-/-} mice. Photomicrographs are from GFAP-immunostained striatal sections of saline (Sal)- or LPS-treated animals (n = 4–5/group). The graph represents quantification of data obtained from the counts of GFAP-positive cells in standardized striatal sections. * P < 0.05 vs. Sal within the same genotype. # P < 0.05 vs. WT. ## P < 0.01 vs. WT with the same treatment. Scale bar = 200 μm (high magnification: scale bar = 50 μm).

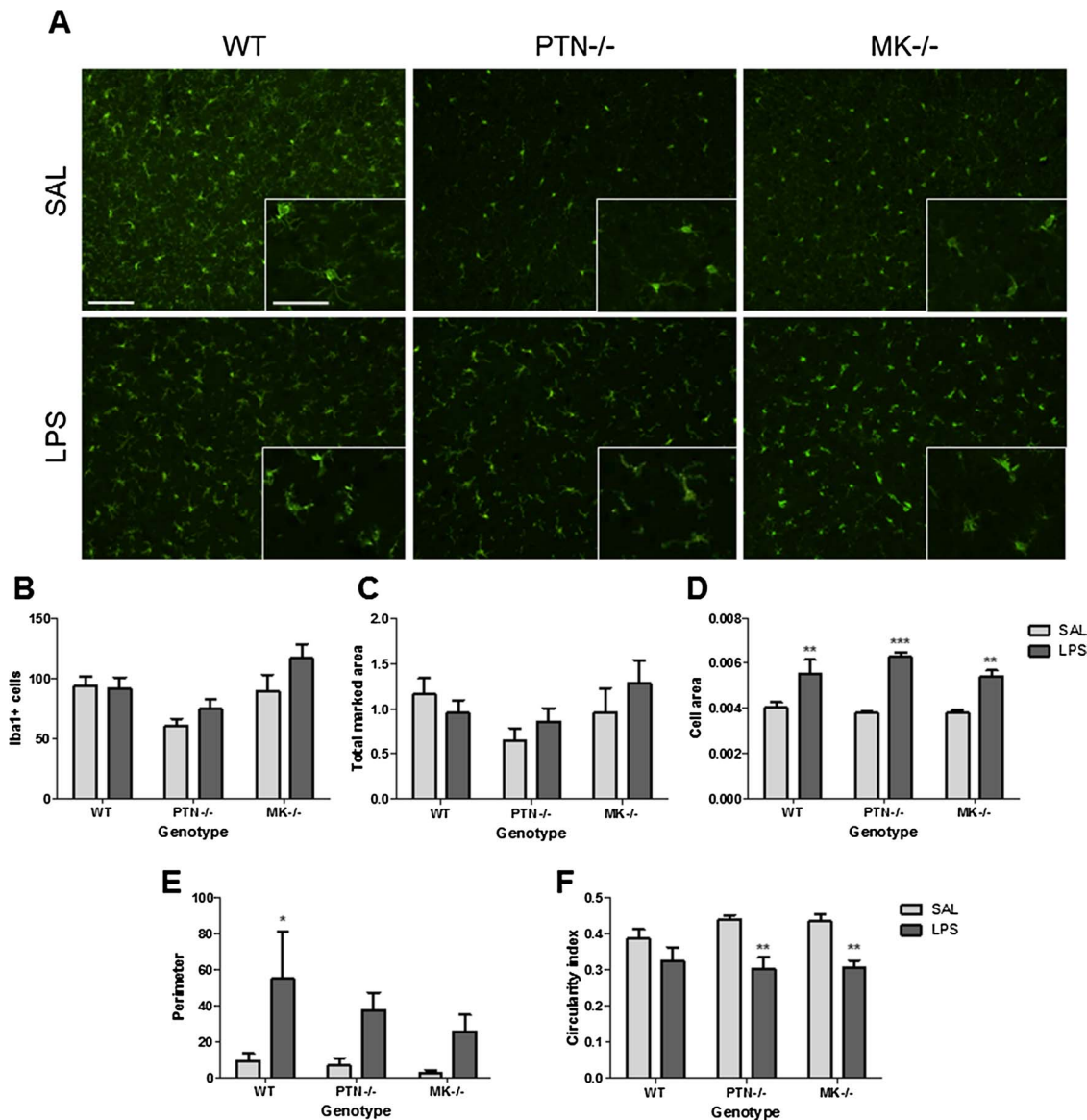


Fig. 3. Effects of LPS on microglia activation in the PFC of WT, MK^{-/-} and PTN^{-/-} mice. Photomicrographs are from Iba-1-immunostained PFC sections of saline (Sal)- or LPS-treated animals (n = 4-5/group) (A). Graphs represent quantification of data (mean ± S.E.M) obtained from the counts of Iba-1-positive cells (B), total marked area (C), cell area (D), soma perimeter (E) and circularity index (F) in PFC whole sections. * P < 0.05, ** P < 0.01, *** P < 0.001 vs. Sal within the same genotype. Scale bar = 100 μm (high magnification: scale bar = 50 μm).

increase of Iba1 + cell area was significantly enhanced in PTN^{-/-} mice (Fig. 4D). Overall, the data show that some of the LPS-induced microglial morphological changes are differentially regulated in PTN^{-/-} and MK^{-/-} mice.

3.2. FYN signaling is not involved in the regulation of LPS effects by PTN in BV2 microglial cells

We recently showed that LPS (1.0 μg/ml)-induced increase of nitric oxide production in murine BV2 microglial cells is significantly enhanced by PTN (0.5 μg/ml), suggesting that PTN potentiates microglial activation *in vitro* [9]. In the present study, we determined the phosphorylation status of the Y416 residue in FYN kinase activation loop domain, which was found very low independently of the treatment (Fig. 5A). PTN alone tended to increase p-Y416 FYN levels; however, PTN did not exert significant effects in LPS-stimulated BV2 cells (Fig. 5A). In addition, we studied LPS-induced MAP kinase activation [16] by assessing the phosphorylation levels of ERK1/2. As expected, we found that LPS induced robust increases of the phosphorylation

levels of ERK1/2 (Fig. 5B). However, these LPS effects were not affected by the addition of PTN to LPS-treated BV2 cells. Overall, the data suggest that PTN does not recruit the FYN-ERK1/2 signaling pathway in order to regulate LPS effects in BV2 cells [9].

4. Discussion

We previously showed that astrocytosis induced by a very low dose of LPS (0.5 mg/kg) is prevented in MK^{-/-} mice [8]. In the present study, astrocytosis induced by a single administration of an intermediate dose of LPS (7.5 mg/kg) is blocked in the brain of PTN^{-/-} and MK^{-/-} mice. The data demonstrate that normal endogenous levels of PTN and MK are required for LPS-induced astrocytic response independently of the intensity of the inflammatory stimulus. However, we previously found that transgenic PTN overexpression in the PFC of PTN-Tg mice attenuates LPS-induced astrocytic response [9]. It has to be noted that, in contrast to the wide distribution of PTN in the CNS during early development, this cytokine is only expressed at low levels in a few cell types in the adult cortex, hippocampus, cerebellum, olfactory bulb and

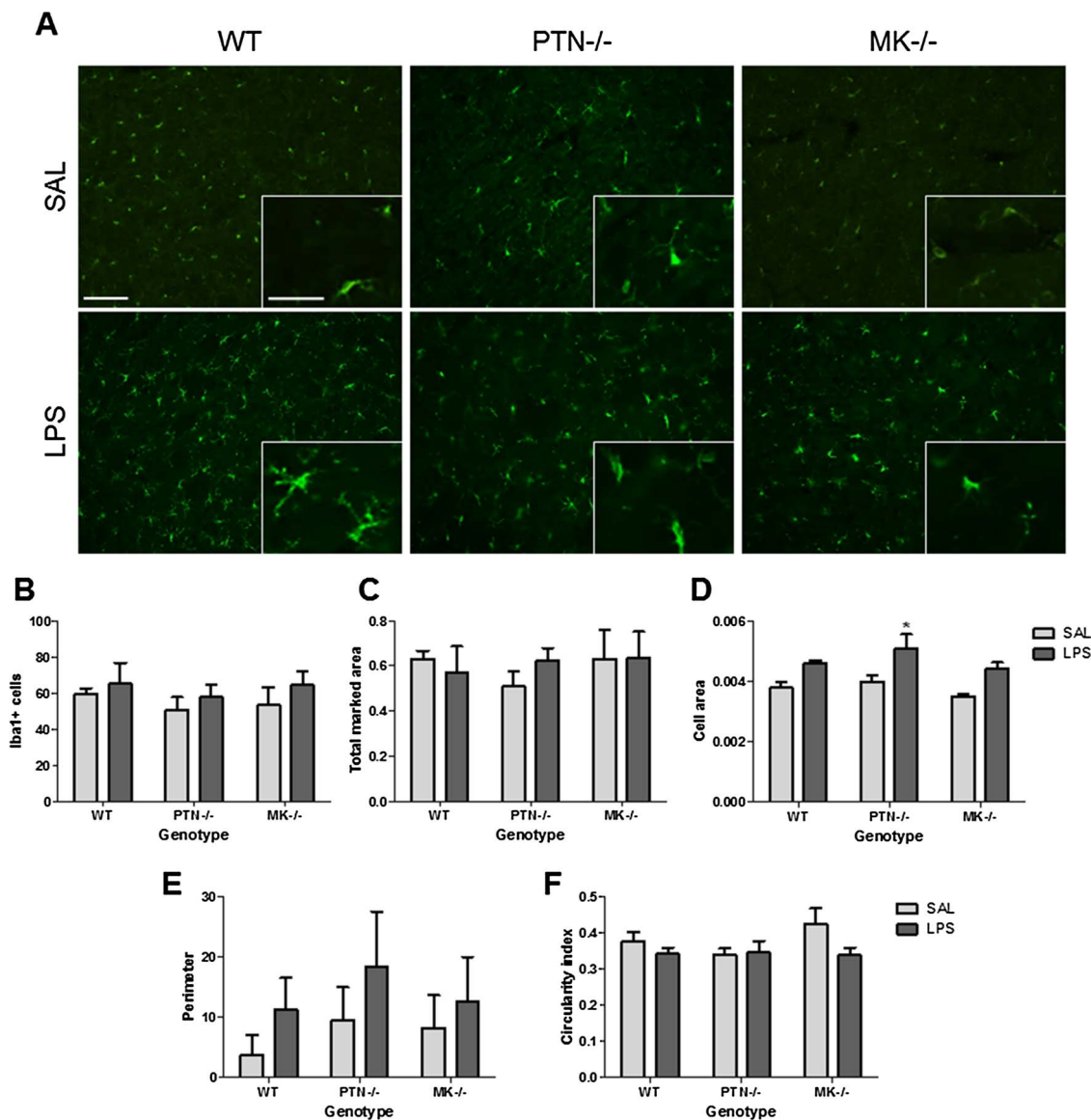


Fig. 4. Effects of LPS on microglia activation in the striatum of WT, MK^{-/-} and PTN^{-/-} mice. Photomicrographs are from Iba-1-immunostained striatal sections of saline (Sal)- or LPS-treated animals (n = 4-5/group) (A). Graphs represent quantification of data (mean ± S.E.M) obtained from the counts of Iba-1-positive cells (B), total marked area (C), cell area (D), soma perimeter (E) and circularity index (F) in standardized striatal sections. * P < 0.05 vs. Sal within the same genotype. Scale bar = 100 μm (high magnification: scale bar = 50 μm).

striatum [5,23]. In contrast, PTN is found highly upregulated in a wide variety of CNS disorders characterized by neuroinflammation including neuropathic pain [24,25], Alzheimer’s disease [26], Parkinson’s disease [27] and brain tumors [28]. Thus, we believe that the data presented here in PTN^{-/-} mice compared to normal wild type mice, add to the knowledge of the physiological functions of normal endogenous PTN levels and their contribution to the response to acute neuroinflammatory stimuli. In contrast, studies in transgenic mice with highly significant overexpression of PTN in the brain may be more relevant to dissect the contribution of high levels of PTN in neuroinflammatory pathological conditions [7,9].

Lack of endogenous expression of these cytokines, particularly PTN, tend to modulate microglia morphological changes in the PFC of LPS-treated knockout mice compared to WT mice. In the PFC of WT mice, LPS increased the perimeter and area of Iba1 + cells, suggesting the presence of hypertrophic microglia. On the other hand, LPS induced a significant decrease in the circularity index in PTN^{-/-} and MK^{-/-} mice compared to WT mice. In the striatum, LPS tended to increase the area and perimeter of microglial cells in all genotypes although this effect was only found to be significant in the area of microglial cells in PTN^{-/-}.

Little was known about the role of endogenous PTN and MK in the microglial response to inflammatory insults. This is the first study showing that normal endogenous expression of PTN and MK *in vivo* modulates LPS-induced microglial morphological changes. It is important to note that we did not find differences between genotypes in saline-treated animals, suggesting that PTN and MK do not regulate innate immunity in naïve animals. Taking into account that PTN and MK are expressed at low levels in the healthy adult brain [5], the present study suggests that lack of endogenous expression of these cytokines impact the microglial changes in response to the endotoxin. Taking together all the microglial morphological parameters analyzed, it is tempting to speculate that absence of these cytokines, particularly PTN, tends to predispose to an enhanced microglial activation. However, it is clear that further studies are needed to clarify the roles of these endogenous cytokines in LPS-induced microglial activation (e.g. cell-specific knockdown).

We previously showed that exogenous PTN potentiates LPS-induced activation of BV2 microglial cells [9]. Previous evidence showed that FYN kinase contributes to MAP kinase phosphorylation during microglial activation [16]. Since FYN is a substrate of the PTN receptor

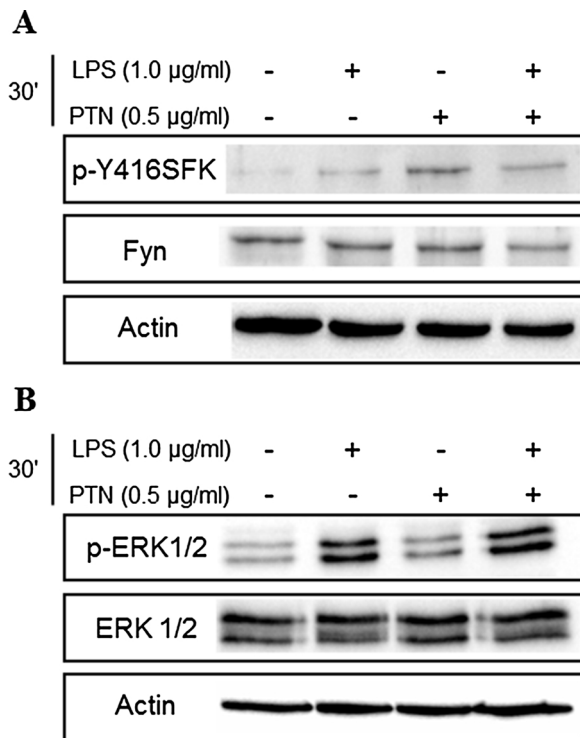


Fig. 5. Effects of LPS and PTN on FYN and MAP kinase phosphorylation in BV2 microglial cells. (A), immunoblots showing p-Y416SFK (FYN) levels in BV2 cell lysates. Total FYN western blots are shown below the phosphorylated protein blot for comparison. (B), immunoblots showing the p44/42 (ERK) phosphorylation. Total ERK1/2 western blots are shown below the phosphorylated protein blot for comparison.

RPTPβ/ζ [15], we tested the effects of PTN and LPS on FYN signaling in BV2 microglial cells. Our results clearly show that treatment of BV2 cells with PTN and/or LPS does not cause relevant changes in the phosphorylation of Y416 in FYN. On the other hand, LPS-induced increases of phosphorylation of ERK1/2 were not modulated by the addition of PTN to LPS-stimulated BV2 cells. Taking together, our data suggest that PTN actions in primed microglia are independent of the FYN-MAP kinase signaling pathway.

5. Conclusion

Our findings show for the first time that endogenous PTN and MK modulate the astrocytic response induced by LPS. The data suggest that PTN and/or MK may be involved in the modulation of LPS-induced microglial activation but further studies are needed to delineate their importance.

Funding

This work has been supported by grants SAF2014-56671-R from Ministerio de Economía y Competitividad of Spain, PNSD001I2015 from National Plan on Drug abuse, Ministerio de Sanidad, Servicios Sociales e Igualdad of Spain. M V-R and R F-C were supported by fellowships from Fundación Universitaria San Pablo CEU.

References

[1] A.I. Faden, J. Wu, B.A. Stoica, D.J. Loane, Progressive inflammation-mediated neurodegeneration after traumatic brain or spinal cord injury, *Br. J. Pharmacol.* 173 (2016) 681–691.
 [2] R.M. McManus, M.T. Heneka, Role of neuroinflammation in neurodegeneration: new insights, *Alzheimers Res. Ther.* 9 (2017) 14.
 [3] F. Mori, R. Nistico, G. Mandolesi, S. Piccinini, D. Mango, et al., Interleukin-1beta promotes long-term potentiation in patients with multiple sclerosis, *Neuromol.*

Med. 16 (2014) 38–51.
 [4] G. Mandolesi, F. De Vito, A. Musella, A. Gentile, S. Bullitta, et al., miR-142-3p is a key regulator of IL-1beta-dependent synaptopathy in neuroinflammation, *J. Neurosci.* 37 (2017) 546–561.
 [5] G. Herradon, C. Perez-Garcia, Targeting midkine and pleiotrophin signalling pathways in addiction and neurodegenerative disorders: recent progress and perspectives, *Br. J. Pharmacol.* 171 (2014) 837–848.
 [6] S. Akira, K. Takeda, Functions of toll-like receptors: lessons from KO mice, *C. R. Biol.* 327 (2004) 581–589.
 [7] M. Vicente-Rodriguez, L. Rojo Gonzalez, E. Gramage, R. Fernandez-Calle, Y. Chen, et al., Pleiotrophin overexpression regulates amphetamine-induced reward and striatal dopaminergic denervation without changing the expression of dopamine D1 and D2 receptors: implications for neuroinflammation, *Eur. Neuropsychopharmacol.* 26 (2016) 1794–1805.
 [8] M. Vicente-Rodriguez, R. Fernandez-Calle, E. Gramage, C. Perez-Garcia, M.P. Ramos, et al., Midkine is a novel regulator of amphetamine-induced striatal gliosis and cognitive impairment: evidence for a stimulus-dependent regulation of neuroinflammation by midkine, *Mediators Inflamm.* 2016 (2016) 9894504.
 [9] R. Fernandez-Calle, M. Vicente-Rodriguez, E. Gramage, J. Pita, C. Perez-Garcia, et al., Pleiotrophin regulates microglia-mediated neuroinflammation, *J. Neuroinflamm.* 14 (2017) 46.
 [10] K. Kadomatsu, M. Tomomura, T. Muramatsu, cDNA cloning and sequencing of a new gene intensely expressed in early differentiation stages of embryonal carcinoma cells and in mid-gestation period of mouse embryogenesis, *Biochem. Biophys. Res. Commun.* 151 (1988) 1312–1318.
 [11] P.G. Milner, Y.S. Li, R.M. Hoffman, C.M. Kodner, N.R. Siegel, et al., A novel 17 kd heparin-binding growth factor (HBGF-8) in bovine uterus: purification and N-terminal amino acid sequence, *Biochem. Biophys. Res. Commun.* 165 (1989) 1096–1103.
 [12] E. Gramage, G. Herradon, Connecting Parkinson's disease and drug addiction: common players reveal unexpected disease connections and novel therapeutic approaches, *Curr. Pharm. Des.* 17 (2011) 449–461.
 [13] N. Maeda, K. Ichihara-Tanaka, T. Kimura, K. Kadomatsu, T. Muramatsu, et al., A receptor-like protein-tyrosine phosphatase PTPzeta/RTPbeta binds a heparin-binding growth factor midkine. Involvement of arginine 78 of midkine in the high affinity binding to PTPzeta, *J. Biol. Chem.* 274 (1999) 12474–12479.
 [14] K. Meng, A. Rodriguez-Pena, T. Dimitrov, W. Chen, M. Yamin, et al., Pleiotrophin signals increased tyrosine phosphorylation of beta-catenin through inactivation of the intrinsic catalytic activity of the receptor-type protein tyrosine phosphatase beta/zeta, *Proc. Natl. Acad. Sci. U. S. A.* 97 (2000) 2603–2608.
 [15] H. Pariser, L. Ezquerra, G. Herradon, P. Perez-Pinera, T.F. Deuel, FYN is a downstream target of the pleiotrophin/receptor protein tyrosine phosphatase beta/zeta-signaling pathway: regulation of tyrosine phosphorylation of FYN by pleiotrophin, *Biochem. Biophys. Res. Commun.* 332 (2005) 664–669.
 [16] N. Panicker, H. Saminathan, H. Jin, M. Neal, D.S. Harischandra, et al., FYN kinase regulates microglial neuroinflammatory responses in cell culture and animal models of parkinson's disease, *J. Neurosci.* 35 (2015) 10058–10077.
 [17] L.E. Amet, S.E. Lauri, A. Hienola, S.D. Croll, Y. Lu, et al., Enhanced hippocampal long-term potentiation in mice lacking heparin-binding growth-associated molecule, *Mol. Cell. Neurosci.* 17 (2001) 1014–1024.
 [18] E. Nakamura, K. Kadomatsu, S. Yuasa, H. Muramatsu, T. Mamiya, et al., Disruption of the midkine gene (Mdk) resulted in altered expression of a calcium binding protein in the hippocampus of infant mice and their abnormal behaviour, *Genes Cells* 3 (1998) 811–822.
 [19] I. Lastres-Becker, A.J. Garcia-Yague, R.H. Scannevin, M.J. Casarejos, S. Kugler, et al., Repurposing the NRF2 activator dimethyl fumarate as therapy against synucleinopathy in parkinson's disease, *Antioxid. Redox Signal.* 25 (2016) 61–77.
 [20] X.L. Luo, S.Y. Liu, L.J. Wang, Q.Y. Zhang, P. Xu, et al., A tetramethoxychalcone from *Chloranthus henryi* suppresses lipopolysaccharide-induced inflammatory responses in BV2 microglia, *Eur. J. Pharmacol.* 774 (2016) 135–143.
 [21] H. Wake, P.R. Lee, R.D. Fields, Control of local protein synthesis and initial events in myelination by action potentials, *Science* 333 (2011) 1647–1651.
 [22] M. Larson, M.A. Sherman, F. Amar, M. Nuvolone, J.A. Schneider, et al., The complex PrP(c)-FYN couples human oligomeric Abeta with pathological tau changes in Alzheimer's disease, *J. Neurosci.* 32 (2012) 16857a–16871a.
 [23] C. González-Castillo, D. Ortuño-Sahagún, C. Guzmán-Brambila, M. Pallás, A.E. Rojas-Mayorquín, Pleiotrophin as a central nervous system neuromodulator, evidences from the hippocampus, *Front. Cell. Neurosci.* 8 (2015) 443.
 [24] L. Ezquerra, L.F. Alguacil, T. Nguyen, T.F. Deuel, I. Silos-Santiago, G. Herradon, Different pattern of pleiotrophin and midkine expression in neuropathic pain: correlation between changes in pleiotrophin gene expression and rat strain differences in neuropathic pain, *Growth Factors* 26 (1) (2008) 44–48.
 [25] Y.B. Martin, G. Herradon, L. Ezquerra, Uncovering new pharmacological targets to treat neuropathic pain by understanding how the organism reacts to nerve injury, *Curr. Pharm. Des.* 17 (2011) 434–448.
 [26] T. Wisniewski, M. Lalowski, M. Baumann, H. Rauvala, E. Raulo, R. Nolo, et al., HB-GAM is a cytokine present in Alzheimer's and Down's syndrome lesions, *Neuroreport* 7 (1996) 667–671.
 [27] D.M. Marchionini, E. Lehrmann, Y. Chu, B. He, C.E. Sortwell, K.G. Becker, et al., Role of heparin binding growth factors in nigrostriatal dopamine system development and Parkinson's disease, *Brain Res.* 1147 (2007) 77–88.
 [28] J. Ma, B. Lang, X. Wang, L. Wang, Y. Dong, H. Hu, Co-expression of midkine and pleiotrophin predicts poor survival in human glioma, *J. Clin. Neurosci.* 21 (11) (2014) 1885–1890.

ARTÍCULO 3. Pharmacological inhibition of Receptor Protein Tyrosine Phosphatase β/ζ (PTPRZ1) modulates behavioral responses to ethanol.

Rosalía Fernández-Calle, Marta Vicente-Rodríguez, Miryam Pastor, Esther Gramage, Bruno Di Geronimo, José María Zapico, Claire Coderch, Carmen Pérez-García, Amy W. Lasek, Beatriz de Pascual-Teresa, Ana Ramos y Gonzalo Herradón.

Neuropharmacology, 2018. ISSN: 1873-7064

Volumen: 137

Número de páginas: 86-95

DOI: 10.1016/j.neuropharm.2018.04.027

Resumen

La pleiotrofina (PTN) y la midkina (MK) son factores neurotróficos que se sobreexpresan en la corteza prefrontal tras la administración de alcohol y que han demostrado reducir el consumo de alcohol y sus efectos reforzadores. La PTN y la MK son inhibidores endógenos del receptor proteína fosfatasa de tirosinas (RPTP) β/ζ , también conocido como PTPRZ1, RPTP β , PTP ζ , lo que sugiere un potencial papel de esta fosfatasa en la regulación de los efectos del alcohol. Para determinar si RPTP β/ζ regula el consumo de alcohol, se trataron ratones con compuestos inhibidores de RPTP β/ζ , diseñados recientemente (MY10, MY33-3), antes de someterles a un protocolo de consumo de alcohol por atracción denominado “*drinking in the dark*”. Los ratones tratados con los inhibidores de RPTP β/ζ , especialmente aquellos tratados con MY10, bebieron menos alcohol que sus respectivos controles. El tratamiento con MY10 bloqueó el condicionamiento preferencial al sitio inducido por el alcohol, presentó un efecto reducido en la ataxia inducida por alcohol y potenció los efectos sedantes del alcohol. También se testó si RPTP β/ζ está implicado en las vías de señalización del alcohol. Se descubrió que el tratamiento con alcohol en células de neuroblastoma produce un incremento de la fosforilación de ALK (quinasa de linfoma aplásico) y TrkA (*tropomyosin receptor kinase A*), sustratos conocidos de RPTP β/ζ . El tratamiento de células de neuroblastoma con MY10 y MY33-3 también produjo un incremento en la fosforilación de ALK y TrkA; sin embargo, el tratamiento concomitante de las células de neuroblastoma con alcohol y MY10 ó MY33-3 bloqueó el aumento de p-ALK y p-TrkA. Estos resultados demuestran por primera vez que TrkA está implicado en la vía de señalización del alcohol y que RPTP β/ζ modula las vías de señalización activadas por el alcohol y las respuestas comportamentales a esta sustancia. Los datos obtenidos apoyan la hipótesis de utilizar RPTP β/ζ como diana farmacoterapéutica para reducir el consumo excesivo de alcohol.

Contribución de la doctoranda en este trabajo

Rosalía Fernández Calle llevó a cabo los experimentos de comportamiento incluidos en las figuras 2, 3, 4 y 5. Colaboró con el análisis estadístico y la interpretación de los datos y ayudó con la escritura del artículo.



Contents lists available at ScienceDirect

Neuropharmacology

journal homepage: www.elsevier.com/locate/neuropharmPharmacological inhibition of Receptor Protein Tyrosine Phosphatase β/ζ (PTPRZ1) modulates behavioral responses to ethanol

Rosalía Fernández-Calle ^{b,1}, Marta Vicente-Rodríguez ^{b,d,1}, Miryam Pastor ^{a,1}, Esther Gramage ^b, Bruno Di Geronimo ^a, José María Zapico ^a, Claire Coderch ^a, Carmen Pérez-García ^b, Amy W. Lasek ^c, Beatriz de Pascual-Teresa ^a, Ana Ramos ^a, Gonzalo Herradón ^{b,*}

^a Departamento de Química y Bioquímica, Facultad de Farmacia, Universidad San Pablo-CEU, CEU Universities, Urbanización Montepríncipe, 28925, Alcorcón, Madrid, Spain

^b Departamento de Ciencias Farmacéuticas y de la Salud, Facultad de Farmacia, Universidad San Pablo-CEU, CEU Universities, Urbanización Montepríncipe, 28925, Alcorcón, Madrid, Spain

^c Department of Psychiatry, University of Illinois at Chicago, 1601 West Taylor Street, Chicago, IL 60612, USA

^d Department of Neuroimaging, Institute of Psychiatry, Psychology & Neuroscience, King's College London, London, UK

ARTICLE INFO

Article history:

Received 2 November 2017

Received in revised form

18 April 2018

Accepted 24 April 2018

Available online 9 May 2018

Keywords:

ALK

TrkA

Alcohol use disorder

Binge-drinking

Pleiotrophin

Midkine

ABSTRACT

Pleiotrophin (PTN) and Midkine (MK) are neurotrophic factors that are upregulated in the prefrontal cortex after alcohol administration and have been shown to reduce ethanol drinking and reward. PTN and MK are the endogenous inhibitors of Receptor Protein Tyrosine Phosphatase (RPTP) β/ζ (a.k.a. PTPRZ1, RPTP β , PTP ζ), suggesting a potential role for this phosphatase in the regulation of alcohol effects. To determine if RPTP β/ζ regulates ethanol consumption, we treated mice with recently developed small-molecule inhibitors of RPTP β/ζ (MY10, MY33-3) before testing them for binge-like drinking using the drinking in the dark protocol. Mice treated with RPTP β/ζ inhibitors, particularly with MY10, drank less ethanol than controls. MY10 treatment blocked ethanol conditioned place preference, showed limited effects on ethanol-induced ataxia, and potentiated the sedative effects of ethanol. We also tested whether RPTP β/ζ is involved in ethanol signaling pathways. We found that ethanol treatment of neuroblastoma cells increased phosphorylation of anaplastic lymphoma kinase (ALK) and TrkA, known substrates of RPTP β/ζ . Treatment of neuroblastoma cells with MY10 or MY33-3 also increased levels of phosphorylated ALK and TrkA. However, concomitant treatment of neuroblastoma cells with ethanol and MY10 or MY33-3 prevented the increase in pTrkA and pALK. These results demonstrate for the first time that ethanol engages TrkA signaling and that RPTP β/ζ modulates signaling pathways activated by alcohol and behavioral responses to this drug. The data support the hypothesis that RPTP β/ζ might be a novel target of pharmacotherapy for reducing excessive alcohol consumption.

© 2018 Elsevier Ltd. All rights reserved.

1. Introduction

Alcohol use disorder (AUD) constitutes a public health crisis. Hazardous use of alcohol is the sixth leading cause of ill health and premature death in high-income countries (Forouzanfar et al., 2016). Approximately 70% of the adults in the WHO European

Region drink alcohol and most alcohol is consumed in heavy drinking occasions (60 g of pure alcohol or more on one occasion) which worsen all risks. Binge drinking accounts for over half of the approximately 88,000 deaths yearly that are attributed to alcohol use in the United States, but binge drinkers also put themselves at increased risk for multiple comorbidities (O'Keefe et al., 2007; Petit et al., 2014; Zakhari and Li, 2007). In the United States, recent studies have shown that the prevalence of 12-month alcohol use, high-risk drinking, and DSM-IV AUD has increased significantly (Grant et al., 2017). Thus, new therapeutic approaches to treat AUD are greatly needed.

In an effort to develop new pharmacotherapies to limit alcohol

* Corresponding author. Laboratory of Pharmacology, Faculty of Pharmacy, Universidad San Pablo-CEU, Urb. Montepríncipe, 28925, Alcorcón, Madrid, Spain.

E-mail address: herradon@ceu.es (G. Herradón).

¹ R. F-C, M. V-R and M. P contributed equally.

consumption and prevent alcoholism, the identification of novel genes and pathways that may predispose individuals to AUD is key. Two genetic factors that have been recently identified as important regulators of alcohol behavioral effects are Pleiotrophin (PTN) and Midkine (MK). PTN and MK are cytokines important in central nervous system (CNS) functions and repair (Herradon and Perez-Garcia, 2014). Both PTN and MK are also upregulated in different brain areas after administration of different drugs of abuse (Herradon and Perez-Garcia, 2014), suggesting PTN and MK signaling may be important in the regulation of drug-induced addictive behaviors. Accordingly, PTN is found upregulated in the nucleus accumbens after a single administration of amphetamine (Le Greves, 2005) and has been shown to contribute to the extinction of amphetamine-seeking behaviors (Gramage et al., 2010a). Importantly, MK expression is higher in the prefrontal cortex (PFC) of human alcoholics and mice selectively bred for high alcohol consumption (Flatscher-Bader and Wilce, 2008; Mulligan et al., 2006) and PTN is upregulated in the PFC of mice injected with a rewarding dose of ethanol (Vicente-Rodriguez et al., 2014a). Both cytokines have been shown to be potent regulators of behavioral effects induced by ethanol (Chen et al., 2017; Vicente-Rodriguez et al., 2014a, 2014b). It has been demonstrated that PTN knockout (PTN^{-/-}) and MK knockout (MK^{-/-}) mice are more sensitive to the rewarding effects of alcohol in the conditioned place preference test (Vicente-Rodriguez et al., 2014a, 2014b). In contrast, PTN transgenic overexpression in the mouse brain blocks the rewarding effects of alcohol (Vicente-Rodriguez et al., 2014a). Overall, the data suggest that PTN and MK could be used for the treatment of drug addiction disorders including AUD (Alguacil and Herradon, 2015).

Both PTN and MK bind to the Receptor Protein Tyrosine Phosphatase (RPTP) β/ζ (a.k.a. PTPRZ1, RPTP β , PTP ζ), and inactivate its phosphatase activity (Herradon and Ezquerro, 2009). This leads to an increase in tyrosine phosphorylation of substrates critical for the effects of these cytokines such as Fyn kinase (Pariser et al., 2005) and Anaplastic Lymphoma Kinase (ALK) (Perez-Pinera et al., 2007). We hypothesize that PTN and MK actions on substance use disorders can be reproduced with rationally designed small molecule inhibitors of RPTP β/ζ (Herradon et al., 2009; Herradon and Perez-Garcia, 2014).

Recently, a new series of blood-brain barrier (BBB) permeable molecules designed to mimic the activity of PTN/MK in the CNS were synthesized (Pastor et al., 2018). These compounds exert their actions by interacting with the intracellular domain of RPTP β/ζ and inhibiting its tyrosine phosphatase activity. The most potent compounds MY10 and MY33-3 (IC₅₀ ~ 0.1 μ M) significantly increased the phosphorylation of key tyrosine residues of RPTP β/ζ substrates involved in neuronal survival and differentiation such as ALK. More interestingly, PTN and MK were previously shown to prevent amphetamine neurotoxicity in vivo and in vitro (Gramage et al., 2010b, 2011) and these RPTP β/ζ inhibitors have shown similar protective effects against amphetamine-induced toxicity (Pastor et al., 2018).

The purpose of this study was to test inhibitors of RPTP β/ζ in binge-like drinking, ethanol conditioned place preference, and other behavioral responses to ethanol, and to study the possible interactions of these molecules with ethanol-induced activation of signaling pathways.

2. Materials and methods

2.1. Subjects

Male C57BL/6J mice (8–10 weeks of age) were tested for behavior. Mice were housed under controlled environmental

conditions (22 ± 1 °C and a 12-h light/12-h dark cycle) with free access to food and water. All the animals used in this study were maintained in accordance with both the ARRIVE guidelines and the European Union Laboratory Animal Care Rules (86/609/ECC directive) or the National Institutes of Health *Guide for the Care and Use of Laboratory Animals*. All protocols were approved by the Animal Research Committee of USP-CEU or the Animal Care Committee of the University of Illinois at Chicago and procedures were used to minimize pain and suffering.

2.2. RPTP β/ζ inhibitors

MY10 and MY33-3 (Fig. 1) were synthesized as previously described (Pastor et al., 2018). MY10 and MY33-3 were administered at a dose of 60 mg/kg in 10% dehydrated ethanol, 20% polysorbate 80, 70% PEG-300 vehicle. Ethanol in the vehicle results in a dose of less than 0.3 g/kg. Pharmacokinetic studies in mice have shown that 1 h after oral administration the brain to plasma ratio is 3:1 (Pastor et al., 2018). Mice were administered compounds or vehicle by oral gavage in a volume of approximately 0.1 ml.

2.3. Drinking in the dark (DID)

Binge-like drinking was measured using the two-bottle DID procedure as previously described using 20% ethanol (Dutton et al., 2017). Mice were individually housed for 2 weeks in the reverse-dark cycle room prior to testing ethanol consumption. Three days before testing ethanol consumption, mice drank water from two tubes made from 10 ml polycarbonate pipettes connected to stainless steel sipper tubes containing ball-bearings to prevent leakage (Rhodes et al., 2005) for one day, in order to acclimate them to the tubes. Three days later mice were given a choice between 20% ethanol and water in the sipper tubes. Fluid consumption was measured every day for 4 days by measuring the volume of fluid in the tubes. The position of the bottles (left or right) was changed every day to control for side preference. On the first 3 days of testing, mice were given access to the ethanol and water tubes 3 h into the dark cycle for a period of 2 h. On the fourth day, mice were given access to ethanol and water tubes for 4 h and the volume consumed was measured at 4 h. All mice were given vehicle (0.1 ml) by oral gavage on days 1 & 2. On the third and fourth days, mice were administered 60 mg/kg MY10, MY33-3 or vehicle (0.1 ml) by oral gavage 1 h before the drinking session in the DID test (n = 12/group). Preference score was calculated as the ratio of the volume of ethanol consumed over the volume of total fluid consumed (Chen et al., 2017; Dutton et al., 2017). For the sucrose consumption test, a separate group of mice were tested exactly as in the ethanol consumption test, except that mice were provided with two tubes containing 2% sucrose in water and water instead of 20% ethanol and water.

Blood samples (20 μ l) were collected immediately after the 4-h drinking session on day 4 to measure blood ethanol concentrations (BECs). Blood was collected in heparinized capillary tubes via tail vein puncture. BECs were determined using a nicotinamide adenine dinucleotide-alcohol dehydrogenase enzymatic assay (Zapata et al., 2006).

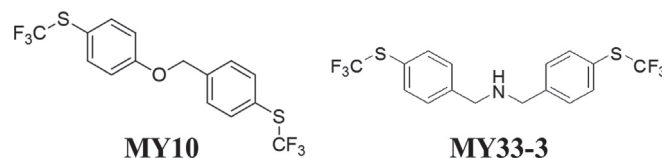


Fig. 1. Structure of the RPTP β/ζ inhibitors MY10 and MY33-3.

2.4. Conditioned place preference (CPP)

We used a 2-compartment apparatus; one compartment had a black floor and walls, and the other had a black floor and white walls. The phases included preconditioning (Pre-C, day 1), conditioning (days 2–4) and testing (CPP, day 5). During preconditioning, mice were free to explore the two compartments for a 15-min period; their behavior was monitored by a videotracking system (SD Instruments, San Diego, California, USA) to calculate the time spent in each compartment. The conditioning phase consisted of two conditioning sessions per day (Gramage et al., 2011). The first session took place in the morning starting at 8 a.m., in which all mice received a single injection of saline i.p. (10 ml/kg) and were confined to one compartment for 5 min. In the afternoon session, starting at 3 p.m., the mice were injected (i.p.) with 2.0 g/kg ethanol, and confined to the other compartment for 5 min. The assignment of the compartments to the ethanol or saline condition was made at random. The procedure used on days 3 and 4 was the same but the order of the treatments (morning/evening) was changed to avoid the influence of circadian variability. Mice were administered the RPTPβ/ζ inhibitor MY10 (60 mg/kg) or vehicle by oral gavage in a volume of approximately 0.1 ml, 1 h before each of the saline and ethanol conditioning sessions (n = 9–10/group). In the testing phase on day 5, mice received a drug-free, 15-min preference test. In this phase the animals freely moved throughout the apparatus, as in the preconditioning phase. The time spent in each compartment was also registered. The difference between the time spent in the ethanol-paired compartment in this phase and the time spent in the same compartment in the preconditioning was considered as indicative of the degree of conditioning induced by ethanol.

For the control CPP experiment in which we conditioned with MY10 in the absence of ethanol, compound or vehicle were administered on days 2, 3 and 4 1 h before injecting mice i.p. with saline (10 ml/kg) and confining them to one side of the apparatus for 5 min (n = 13/group). In the testing phase on day 5, mice received a compound-free, 15-min preference test and the amount of time the mice spent in the MY10-paired compartment was measured.

2.5. Rotarod test

Mice were trained in 2 sessions on 2 consecutive days by placing them on the rotarod (Panlab, Barcelona, Spain) rotating drum (rod), and allowing them to run/climb under continuous acceleration (2–18 r.p.m) for at least 30 s. The next day, animals were re-trained, administered 60 mg/kg MY10 or vehicle by oral gavage (0.1 ml) 1 h before the 2.0 g/kg ethanol administration (n = 8–9/group) and then placed on the rotarod. In a control experiment, animals were administered 60 mg/kg MY10 or vehicle by oral gavage (0.1 ml) 1 h before saline administration (10 ml/kg, i.p.) (n = 4–5/group). The time to fall was recorded and mice were placed back on the rotarod every 10 min until 100 min after ethanol (or saline) administration.

2.6. Loss of the righting reflex (LORR)

Mice were administered 60 mg/kg MY10 or vehicle 1 h before the 3.6 g/kg ethanol administration (n = 8/group), placed on their backs and tested for the ability to right themselves. Mice were considered to have lost the righting reflex if they could not right themselves 3 times within 30 s and regained the righting reflex if they could fully right themselves 3 times within 30 s (Lasek et al., 2011a,b). The duration of LORR was determined as the difference between the time when the reflex was lost and when it was regained.

2.7. Measurement of blood ethanol concentration for ethanol clearance study

Blood ethanol concentration (BEC) was measured in mice used in the LORR experiment one week after the LORR test. Mice were administered 60 mg/kg MY10 or vehicle 1 h before the 2.0 g/kg ethanol administration (n = 5/group) and 20 μl of blood was obtained via tail vein puncture at 30, 60 and 120 min post-injection. BECs were determined using the alcohol dehydrogenase enzymatic assay (Zapata et al., 2006).

2.8. Cell culture

The human neuroblastoma cell line SH-SY5Y was purchased from American Type Culture Collection (ATCC, Manassas, VA, USA) and was incubated at 37 °C in 5% CO₂. SH-SY5Y cells were cultured in a 1:1 mixture of Eagle's minimum essential medium (EMEM) and F12 medium containing 10% fetal bovine serum (FBS). For treatment with ethanol, cells were cultured to 90% confluence and, 3 h before ethanol treatment, medium was changed to a 1:1 mixture of EMEM and F12 medium without serum in order to serum-starve the cells. For concentration-response assays with ethanol, cells were treated with 10–100 mM ethanol for 15 min. For time-response assays with ethanol, cells were treated with 50 mM ethanol for 5, 15 and 30 min. For treatment with ethanol and RPTPβ/ζ inhibitors, cells were treated with 1 μM RPTPβ/ζ inhibitor (MY10 or MY33-3) for 5 min prior to 50 mM ethanol for 15 min. All determinations were carried out in 3–6 independent experiments.

2.9. Western blots

SH-SY5Y cells were lysed in 20 mM Tris-HCl, pH 7.5, 150 mM NaCl, 1 mM EDTA, 1 mM EGTA, 1% Triton X-100, 2.5 mM sodium pyrophosphate, 1 mM β-glycerophosphate, 1 mM Na₃VO₄, 1 μg/ml leupeptin, 1 μg/ml aprotinin, and EDTA-free Complete Protease Inhibitor Cocktail tablets (Roche Diagnostics, Indianapolis, IN, USA). Lysate protein concentration was determined using the BCA Protein Assay Kit (Pierce, Rockford, IL, USA) and equal amounts of protein were subjected to sodium dodecyl sulfate-polyacrylamide gel electrophoresis and transferred to polyvinylidene difluoride membranes. Separate blots were probed with antibodies to either phosphorylated ALK (pALK, Tyr 1278) or phosphorylated TrkA (pTrkA, Tyr 490) (Cell Signaling Technology, Danvers, MA, USA). Antibodies were diluted in 5% bovine serum albumin in Tris-buffered saline with Tween 20 (25 mM Tris-HCl, pH 7.4, 137 mM NaCl, and 0.1% Tween 20). Blots were stripped and re-probed with corresponding anti-TrkA (Upstate, Charlottesville, VA) and anti-ALK (Life Technologies, Carlsbad, CA) antibodies to measure total protein levels. To quantify total protein levels of ALK and TrkA, membranes were re-probed with anti-actin antibodies and normalized against the actin signal (Chemicon, Temecula, CA). Secondary antibodies were horseradish peroxidase-conjugated goat anti-mouse or anti-rabbit IgG (Santa Cruz, Santa Cruz, CA). The membranes were developed with enhanced chemiluminescence detection reagents (Pierce). Films were scanned and densitometry performed using ImageJ software.

2.10. Statistical analysis

All data were expressed as the mean ± SEM and analyzed using Prism software (GraphPad, La Jolla, CA, USA). Rotarod data was analyzed by two-way repeated measures (RM) ANOVA for treatment and time. The DID data was analyzed by Student's t-test for effects of vehicle vs. compound on day 3 (2 h drinking session) and on day 4 (4 h drinking session) and for effects of day (day 2 vs. day

3) within each compound treatment. The preference score data was analyzed by Student's *t*-test for effects of vehicle vs. compound within each compound treatment day (days 3 & 4) and for effects of day (day 2 vs. day 3 and day 2 vs. day 4) within each compound treatment. The BEC and LORR data were analyzed by Student's *t*-test. The CPP data were analyzed by two-way repeated measures (RM) ANOVA for treatment and phase followed by Bonferroni's post-hoc tests. Protein expression analysis in concentration-response and time-response assays with ethanol was performed by 1-way ANOVA followed by Tukey's post-hoc tests. Protein expression analysis in cells treated with compounds and ethanol was performed by 2-way ANOVA followed by Tukey's post-hoc tests, considering compound treatment and ethanol treatment as factors. A *p* value less than 0.05 was considered a statistically significant difference.

3. Results

3.1. RPTPβ/ζ inhibition attenuates binge-like ethanol consumption

To determine if RPTPβ/ζ inhibition affects binge-like ethanol consumption, we treated mice with the inhibitor MY10 before the drinking sessions on days 3 (2 h session) and 4 (4 h session). Fig. 2a shows that MY10-treated mice consumed less ethanol than vehicle-treated mice on day 3 ($t(22) = 2.02$, $P = 0.056$) and day 4 ($t(21) = 2.32$, $P = 0.03$). In addition, MY10-treated mice consumed significantly less ethanol on day 3 when compared with day 2 (before MY10 treatment, $t(22) = 2.57$, $P = 0.018$). Consistent with the decrease in ethanol consumed, mice treated with MY10 showed a reduced preference for the ethanol solution in the 2 h drinking session on day 3 (Fig. 2b; $t(22) = 2.32$, $P = 0.03$) and in the 4 h drinking session on day 4 when compared with vehicle-treated mice ($t(21) = 2.68$, $P = 0.014$) and on days 3 and 4 when compared with day 2 ($t(22) = 2.81$, $P = 0.01$ and $t(21) = 3.84$, $P = 0.001$, respectively). Consistent with the reduced ethanol

consumption, BECs were lower in the MY10-treated group compared with vehicle-treated mice (Fig. 2c; $t(20) = 2.123$, $P = 0.046$) at the end of the 4 h drinking session (day 4). Sucrose drinking was not affected by MY10 treatment (Fig. 2d). Treatment with a second RPTPβ/ζ inhibitor, MY33-3, did not significantly affect ethanol consumption when compared with the vehicle-treated group, but did reduce ethanol consumption when comparing day 2 (before treatment with MY33-3) with day 3 (after treatment with MY33-3, Fig. 2e, $t(22) = 2.31$, $P = 0.03$). In addition, mice treated with MY33-3 on day 3 showed a reduced preference for the ethanol solution when compared to the vehicle-treated mice (Fig. 2f; $t(22) = 2.16$, $P = 0.04$) and a reduced preference when comparing days 2 & 3 ($t(22) = 2.45$, $P = 0.02$). However, on day 4, no significant differences between MY33-3 and vehicle-treated mice were observed (Fig. 2f). As expected, BECs at the end of the 4 h drinking session (day 4) were not affected in mice treated with MY33-3 (Fig. 2g). It is important to note that total fluid consumption (water and ethanol combined) was not affected by any of the treatments (Fig. 2h). Collectively, these data indicate that RPTPβ/ζ inhibition reduced ethanol consumption without affecting sucrose drinking and suggest that MY10 appears to be the most effective RPTPβ/ζ inhibitor with potential use in AUD.

3.2. RPTPβ/ζ inhibition attenuates ethanol reward

The reduced ethanol consumption in mice treated with MY10 suggests that RPTPβ/ζ might be involved in the rewarding properties of ethanol. To test this, we performed the ethanol CPP test in mice treated with MY10 or vehicle daily prior to ethanol and saline conditioning sessions (Fig. 3a). ANOVA revealed a significant treatment × phase interaction ($F(1, 17) = 6.69$; $p = 0.02$). Post-hoc comparisons demonstrated that mice treated with vehicle showed a significant CPP (Fig. 3b; $t(17) = 4.89$; $P < 0.001$). In contrast, mice treated with MY10 did not exhibit CPP (Fig. 3b; $t(17) = 1.39$). To test if MY10 is rewarding or aversive on its own

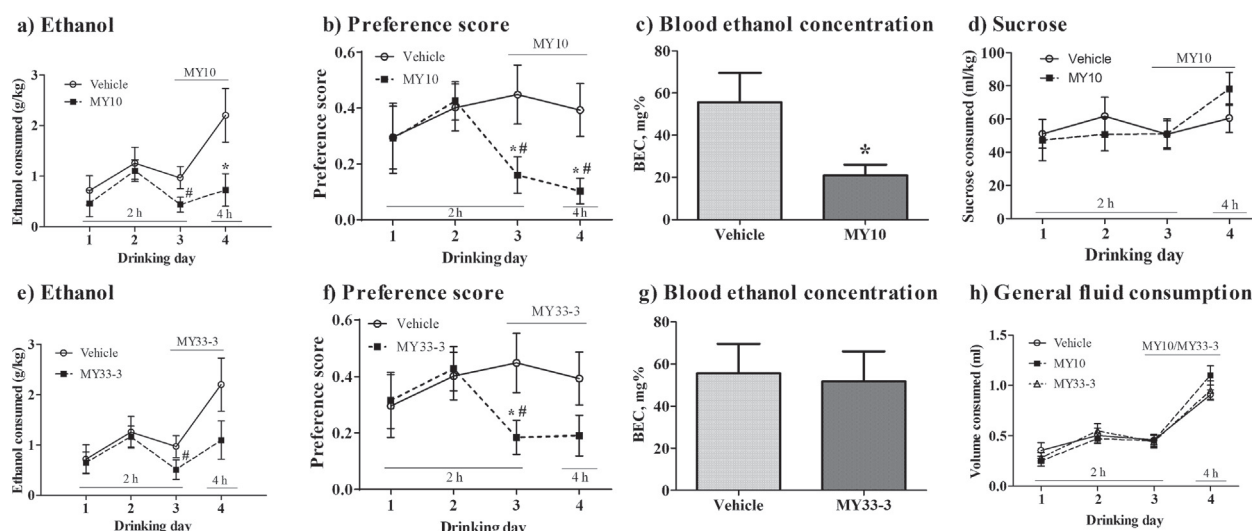


Fig. 2. RPTPβ/ζ inhibition attenuates binge-like ethanol consumption. (a) Ethanol consumed (g/kg) during 2 h of drinking on days 1–3 and during 4 h of drinking on day 4. On days 3 and 4, mice were administered 60 mg/kg MY10 or vehicle ($n = 12$ /group) 1 h before each drinking session in the DID test. (b) Ethanol preference in vehicle- and MY10-treated mice, calculated as the ratio of the volume of ethanol consumed over the volume of total fluid consumed. Ethanol preference on days 1–3 was calculated for 2 h-drinking sessions and on day 4 for a 4 h-drinking session. (c) Blood ethanol concentration (BEC, mg%) in vehicle- and MY10-treated mice after the final 4 h-drinking session on day 4. (d) Volume of 2% sucrose solution (ml/kg) consumed during 2 h of drinking on days 1–3 and 4 h on day 4 in mice treated with vehicle ($n = 5$) or MY10 ($n = 5$). (e) Ethanol consumed (g/kg) during 2 h of drinking on days 1–3 and during 4 h of drinking on day 4. On days 3 and 4, mice were administered 60 mg/kg MY33-3 or vehicle ($n = 12$ /group) 1 h before each drinking session in the DID test. (f) Ethanol preference score in vehicle- and MY33-3-treated mice, calculated as the ratio of the volume of ethanol consumed over the volume of total fluid consumed. Ethanol preference on days 1–3 was calculated for 2 h-drinking sessions and on day 4 for a 4 h-drinking session. (g) Blood ethanol concentration (BEC, mg%) in vehicle- and MY33-3-treated mice after the final 4 h-drinking in the dark session on day 4. (h) Total fluid consumed (water + ethanol, ml) during 2 h-drinking sessions on days 1–3 and the 4 h-drinking session on day 4. On days 3 and 4, mice were administered 60 mg/kg MY10, MY33-3 or vehicle ($n = 12$ /group) 1 h before each drinking session in the DID test. * $p < 0.05$ vs. Vehicle. # $p < 0.05$ vs. Day 2.

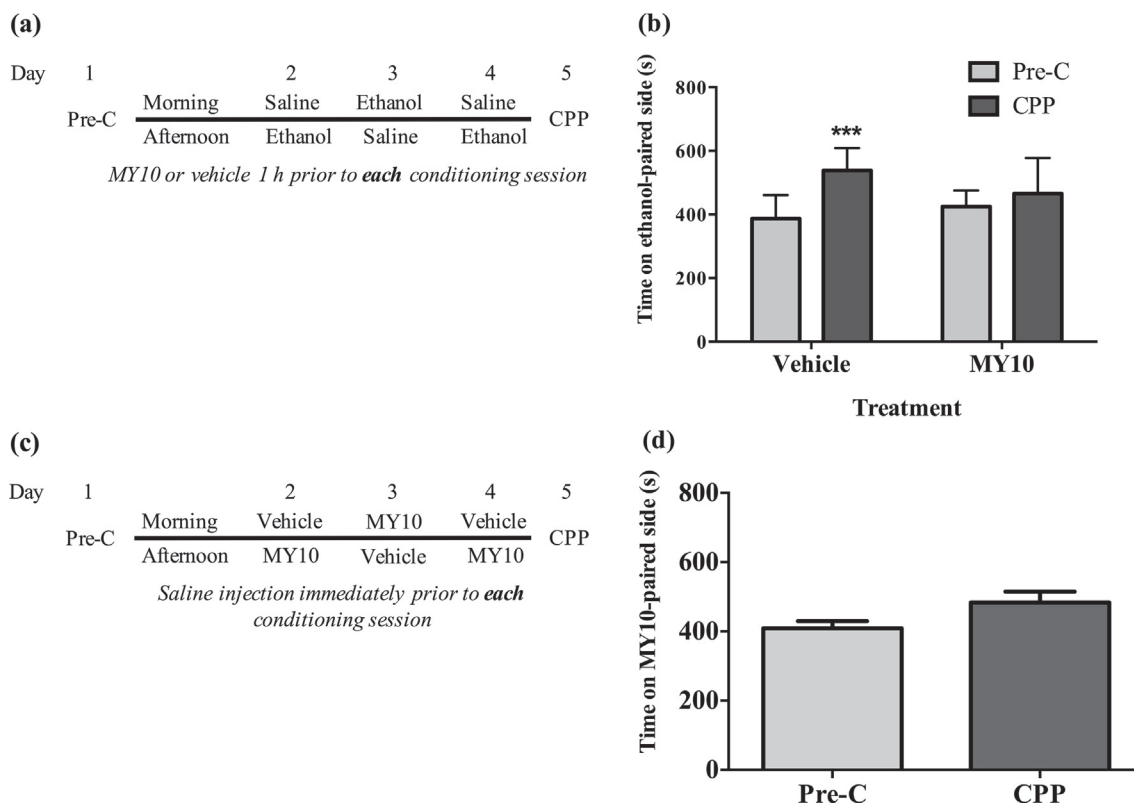


Fig. 3. Ethanol (2.0 g/kg)-induced place preference. (a) Scheme showing treatment conditions for the ethanol CPP test (b) Time (seconds) spent on the ethanol-paired side before conditioning (Pre-C) and after conditioning (CPP) in mice treated with vehicle or 60 mg/kg MY10. The data show that MY10 prevents ethanol CPP. (c) Scheme showing the treatment conditions for the MY10 CPP test (in the absence of ethanol). (d) Time (seconds) spent on the MY10-paired side before conditioning (Pre-C) and after conditioning (CPP) in mice conditioned with 60 mg/kg MY10 (n = 13) instead of ethanol. Time spent on the MY10-paired side did not change after conditioning. ***P < 0.001 vs. Pre-C.

(i.e., in the absence of ethanol), we performed a control experiment in which mice were place conditioned with MY10 (Fig. 3c). Conditioning with MY10 did not alter the time spent in the MY10-paired compartment, indicating that RPTPβ/ζ inhibition in the absence of ethanol does not induce preference or aversion (Fig. 3d). These data suggest that RPTPβ/ζ inhibition attenuates the rewarding properties of ethanol.

3.3. RPTPβ/ζ inhibition has a mild effect on ethanol-induced ataxia and potentiates ethanol sedation

To test the possibility that RPTPβ/ζ could modulate other acute behavioral responses to ethanol we performed experiments to assay the ataxic and sedative effects of ethanol in MY10-treated mice. The motor-incoordinating effects of ethanol were measured using the rotarod test. We tested the recovery from the ataxic effects induced by a rewarding dose of ethanol (2.0 g/kg) known to produce moderate ataxic effects in mice (den Hartog et al., 2013). Acute administration of 2.0 g/kg ethanol produced ataxia in MY10- and vehicle-treated mice illustrated by a reduction in time spent on the rotarod. There were significant effects of time (F(10,150) = 31.22, P < 0.0001; Fig. 4a) and treatment (F(1,15) = 5.19, P = 0.04), but no significant time × treatment interaction (F(1,150) = 0.47, P = 0.91). In agreement with studies reported by others (den Hartog et al., 2013), performance improved over time although this improvement seemed to be transiently delayed in MY10-treated mice (Fig. 4a). However, 100 min after ethanol injection a similar recovery from ataxia was observed in mice treated with MY10 or vehicle (Fig. 4a). Treatment with MY10 or vehicle 1 h before saline injection did not change the amount of

time that mice stayed on the rotarod when compared with basal values (Treatment: F(1,7) = 0.04, P = 0.84; time: F(10,70) = 1.53, P = 0.15; Fig. 4b). These data indicate that RPTPβ/ζ has a limited effect on the motor incoordinating effects induced by a rewarding dose of ethanol in mice. We examined BECs at different time points in mice treated with 60 mg/kg or vehicle 1 h before an injection of 2.0 g/kg ethanol. We did not observe a difference in the BECs between treatments (Fig. 4c), suggesting that MY10 does not affect clearance of a rewarding and ataxic dose of ethanol in mice.

We also examined MY10- and vehicle-treated mice in a LORR test using a sedating dose of ethanol (3.6 g/kg). The time to lose the righting reflex was similar in all mice (data not shown). However, the data show that the amount of time needed for MY10-treated mice to recover the righting reflex after ethanol injection was significantly higher than that in vehicle-treated mice (Fig. 5; t(14) = 2.980, P = 0.01). These data suggest that RPTPβ/ζ counteracts the sedative effects of ethanol.

3.4. RPTPβ/ζ inhibitors modulate ethanol-induced activation of ALK and TrkA

In order to study the molecular mechanisms underlying the actions of RPTPβ/ζ inhibitors in the effects of ethanol, we aimed to test the hypothesis that pharmacological inhibition of RPTPβ/ζ regulates ethanol signaling pathways. Previously, it was shown that ALK is a substrate of RPTPβ/ζ (Perez-Pinera et al., 2007) and that ethanol rapidly activates ALK signaling through phosphorylation of Tyr 1278 in neuroblastoma cells (He et al., 2015). Also, inhibition of RPTPβ/ζ activates TrkA through increased phosphorylation of Tyr 490 (Shintani and Noda, 2008). To determine if ethanol activates

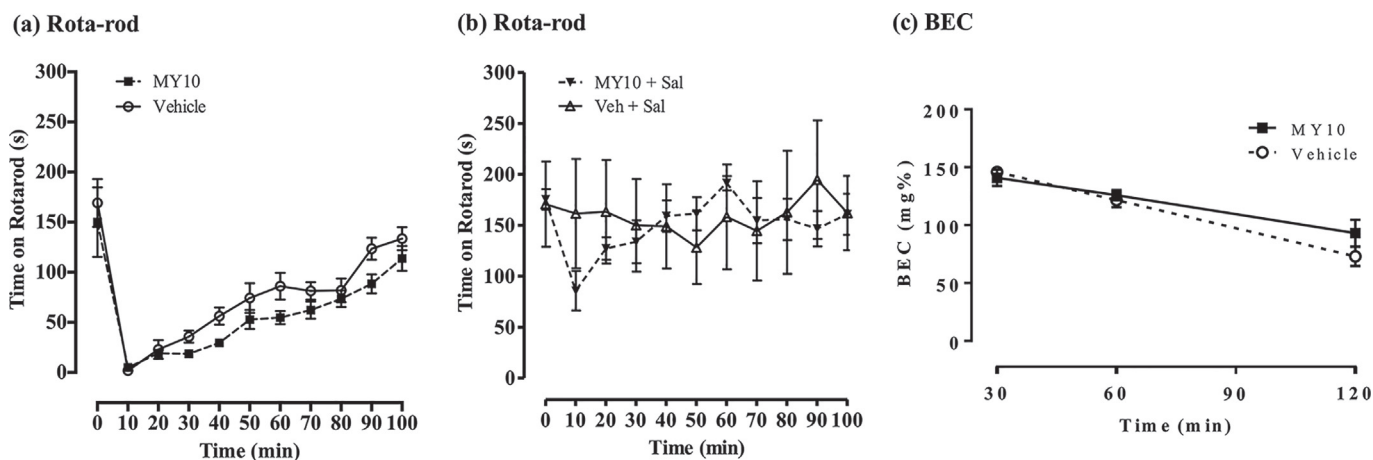


Fig. 4. Ethanol (2.0 g/kg)-induced ataxia. (a) Time spent on a rotarod by mice treated with the RPTP β/ζ inhibitor MY10 (60 mg/kg) or vehicle 1 h before injection of 2.0 g/kg ethanol (Eth). (b) Time spent on a rotarod by mice treated with the RPTP β/ζ inhibitor MY10 (60 mg/kg) or vehicle (Veh) 1 h before injection of saline (Sal, i.p.). (c) Blood ethanol concentration (BEC) in mice pretreated with 60 mg/kg MY10 or vehicle and treated with 2.0 g/kg ethanol. Results are presented in mg% over time.

TrkA signaling and to confirm the effects of ethanol on ALK signaling, we treated SH-SY5Y neuroblastoma cells with different concentrations of ethanol (10–100 mM) for 15 min (Fig. 6a–e) and with 50 mM ethanol for 5–30 min (Fig. 6f–j). The doses of ethanol used in these studies represent blood alcohol concentrations ranging from intoxicating to sedating. Interestingly, we observed an effect of ethanol treatment on TrkA phosphorylation after incubation of SH-SY5Y cells with 10–100 mM ethanol (Fig. 6b; $F(5,21) = 3.04$; $P = 0.04$) and after 5, 15 and 30 min of 50 mM ethanol exposure (Fig. 6g; $F(3,14) = 5.02$; $P = 0.02$). We did not detect significant effects of ethanol treatment on total TrkA protein levels (Fig. 6c,h). Post-hoc comparisons showed that ethanol significantly increased phosphorylation of Tyr 490 in TrkA after 15 min of 50 mM exposure (Fig. 6g). In confirmation of previous studies (He et al., 2015), we observed a significant effect of treatment with ethanol on ALK phosphorylation [specifically the 140 kDa isoform of ALK] in SH-SY5Y cells (Fig. 6d; $F(5,21) = 2.87$; $P = 0.048$). Post-hoc comparisons showed significantly increased ALK phosphorylation after incubation with 50 mM ethanol (Fig. 6d, $P < 0.05$). In the time-course assays, we observed a trend of ethanol to increase ALK phosphorylation after 5, 15 and 30 min of 50 mM ethanol exposure (Fig. 6i; $F(3,15) = 3.00$; $P = 0.07$). We did not detect significant effects of ethanol treatment on total ALK protein levels (Fig. 6e,j).

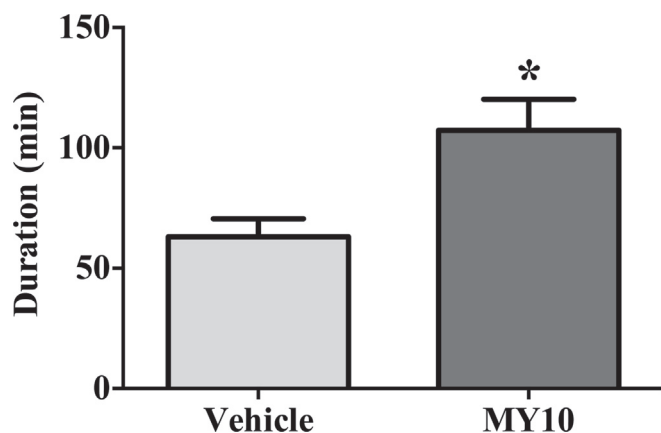


Fig. 5. Ethanol (3.6 g/kg)-induced loss of righting reflex (LORR). Increased duration of LORR induced in mice treated with the RPTP β/ζ inhibitor MY10 (60 mg/kg) or vehicle 1 h before ethanol injection (3.6 g/kg, i.p.) ($n = 8$). * $P < 0.05$ vs. Vehicle.

We next tested the possibility that treatment of SH-SY5Y cells with the RPTP β/ζ inhibitor MY10 (1 μ M) modulates these signaling pathways (Fig. 7a–e). Analysis of TrkA phosphorylation by 2-way ANOVA indicated that there was not a significant main effect of the compound (Fig. 7b; $F(1,10) = 0.01$, $P = 0.93$), but there was a significant main effect of ethanol (Fig. 7b; $F(1,10) = 5.40$, $P = 0.04$) and a significant MY10 \times ethanol interaction (Fig. 7b; $F(1,10) = 8.18$, $P = 0.02$). Post-hoc analyses indicated that ethanol significantly increased phosphorylated TrkA when compared with vehicle (Fig. 7b, $P = 0.03$), whereas the combination of MY10 and ethanol did not increase phosphorylated TrkA when compared with vehicle (Fig. 7b, $P = 0.43$). For phosphorylated ALK, there were no significant main effects of ethanol (Fig. 7d; $F(1,9) = 0.30$, $P = 0.59$) or MY10 (Fig. 7d; $F(1,9) = 0.42$, $P = 0.53$); however, there was a significant MY10 \times ethanol interaction (Fig. 7d; $F(1,9) = 19.8$, $P = 0.001$). Post-hoc analyses demonstrated that ethanol alone (Fig. 7d, $P = 0.03$) and MY10 alone (Fig. 7d, $P = 0.02$) significantly increased phosphorylated ALK when compared with vehicle treatment, whereas treatment with the combination of MY10 and ethanol did not increase phosphorylated ALK when compared with vehicle treatment (Fig. 7d, $P = 0.84$). None of the treatments significantly altered total TrkA (Fig. 7c) or total ALK protein levels (Fig. 7e).

We also tested if treatment of SH-SY5Y cells with the RPTP β/ζ inhibitor MY33-3 (1 μ M) modulates these signaling pathways (Fig. 7f–j). For phosphorylated TrkA, there were no significant effects of ethanol (Fig. 7g; $F(1,18) = 0.07$, $P = 0.79$) or compound (Fig. 7g; $F(1,18) = 3.72$, $P = 0.07$); however there was a significant MY33-3 \times ethanol interaction (Fig. 7g; $F(1,18) = 13.38$, $P = 0.002$). Post-hoc multiple comparisons indicated that ethanol alone (Fig. 7g, $P = 0.04$) and MY33-3 alone (Fig. 7g, $P = 0.001$) significantly increased phosphorylated TrkA when compared with vehicle treatment. However, treatment with the combination of MY33-3 and ethanol did not increase phosphorylated TrkA when compared with vehicle treatment (Fig. 7g, $P = 0.40$). For phosphorylated ALK, we did not observe significant main effects of ethanol (Fig. 7i; $F(1,12) = 1.00$, $P = 0.33$) or MY33-3 (Fig. 7i; $F(1,12) = 3.11$, $P = 0.10$) but there was a significant MY33-3 \times ethanol interaction (Fig. 7i; $F(1,12) = 5.45$, $P = 0.04$). Post-hoc multiple comparisons tests indicated that ethanol alone (Fig. 7i, $P = 0.03$) significantly increased phosphorylated ALK compared with vehicle treatment and that the combination of MY33-3 and ethanol did not significantly increase phosphorylated ALK levels

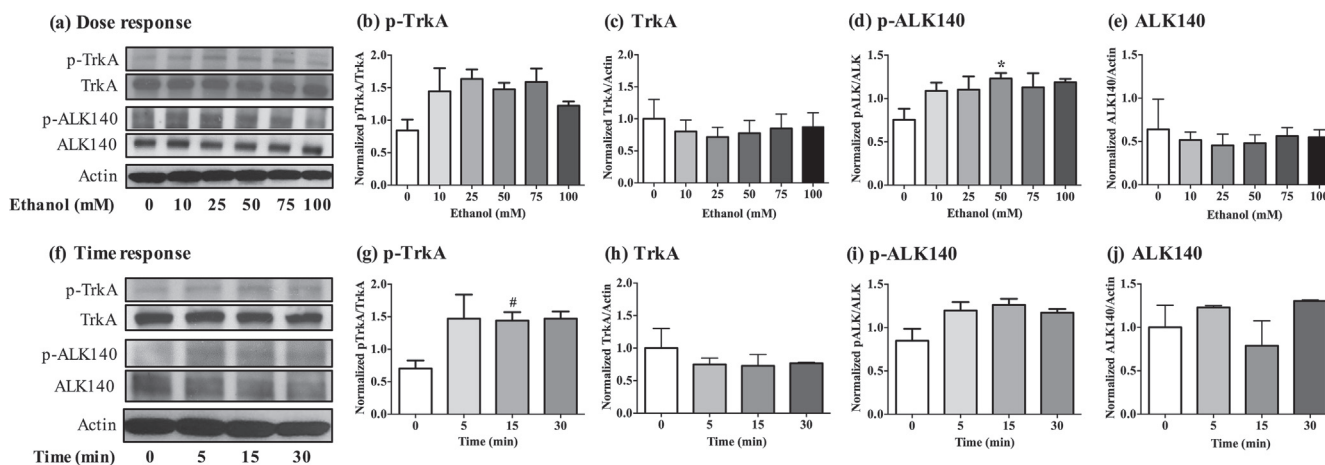


Fig. 6. Ethanol increases phosphorylation of anaplastic lymphoma kinase (ALK) and TrkA in SH-SY5Y cells. (a) Representative western blots showing phosphorylated ALK (pALK, Tyr 1278) 140 and phosphorylated TrkA (p-TrkA, Tyr 490) within 15 min of 0–100 mM ethanol treatment. Total ALK and TrkA western blots are shown below each phosphorylated protein blot for comparison. Both proteins were detected at ~140 kDa. (b) Graph shows the ratio p-TrkA/TrkA of optical density measurements corresponding to the p-TrkA and total TrkA protein levels respectively. (c) Graph shows the ratio TrkA/Actin of optical density measurements corresponding to the total TrkA and actin protein levels respectively. (d) Graph shows the ratio p-ALK140/ALK140 of optical density measurements corresponding to the p-ALK140 and total ALK140 protein levels respectively. (e) Graph shows the ratio ALK140/Actin of optical density measurements corresponding to the total ALK140 and actin protein levels respectively. (f) Representative western blots showing phosphorylated ALK (p-ALK) 140 and phosphorylated TrkA (p-TrkA) within 0–30 min of 50 mM ethanol treatment. Total ALK and TrkA western blots are shown below each phosphorylated protein blot for comparison. Both proteins were detected at ~140 kDa. (g) Graph shows the ratio p-TrkA/TrkA of optical density measurements corresponding to the p-TrkA and total TrkA protein levels respectively. (h) Graph shows the ratio TrkA/Actin of optical density measurements corresponding to the total TrkA and actin protein levels respectively. (i) Graph shows the ratio p-ALK140/ALK140 of optical density measurements corresponding to the p-ALK140 and total ALK140 protein levels respectively. (j) Graph shows the ratio ALK140/Actin of optical density measurements corresponding to the total ALK140 and actin protein levels respectively. Data are presented as the mean ± SEM. *p < 0.05 vs. 0 mM ethanol. #p < 0.05 vs. 0 min.

when compared with vehicle treatment (Fig. 7i, P = 0.19). None of the treatments significantly changed total TrkA (Fig. 7h) or total ALK protein levels (Fig. 7j).

4. Discussion

We previously showed that MK^{-/-} and PTN^{-/-} mice are more sensitive to the rewarding effects of ethanol and that these effects

are blocked in mice with transgenic PTN overexpression in the brain (Vicente-Rodriguez et al., 2014a). Also, it has been recently shown that MK^{-/-} mice drink more alcohol in the DID and 2-bottle choice ethanol consumption tests than WT mice (Chen et al., 2017). Since PTN and MK are endogenous inhibitors of RPTPβ/ζ, and this phosphatase is preferentially expressed in the CNS (Herradon and Perez-Garcia, 2014), we hypothesized that small-molecule inhibitors of RPTPβ/ζ would mimic MK and PTN

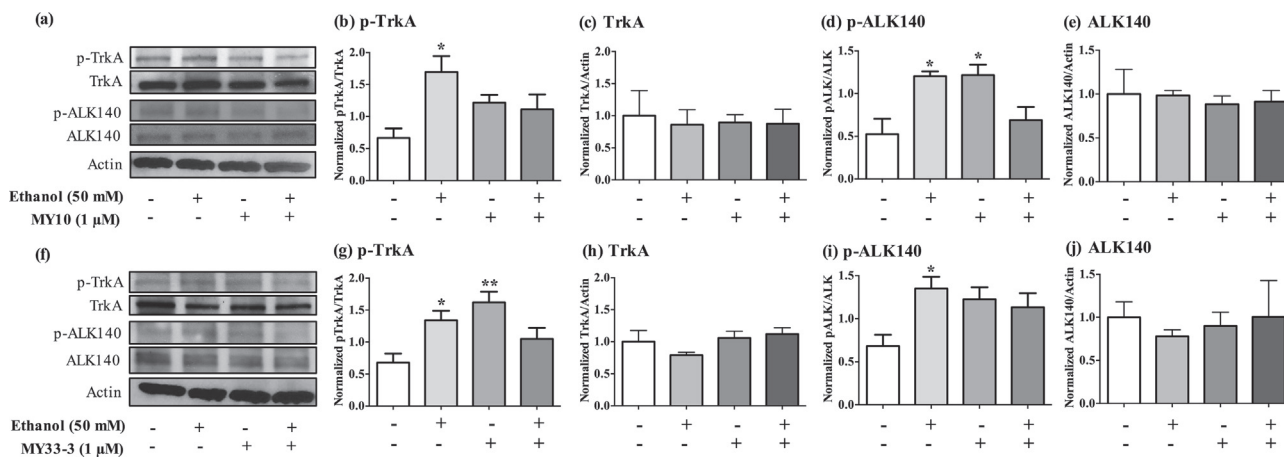


Fig. 7. RPTPβ/ζ inhibitors (MY10 and MY33-3) block ethanol-induced activation of TrkA and ALK in SH-SY5Y cells. (a) Representative western blots showing phosphorylated ALK (p-ALK, Tyr 1278) 140 and phosphorylated TrkA (p-TrkA, Tyr 490) in cells incubated for 5 min with 1 μM MY10 or DMSO (control) and then for 15 min with 50 mM ethanol. Total ALK and TrkA western blots are shown below each phosphorylated protein blot for comparison. Both proteins were detected at ~140 kDa. (b) Graph shows the ratio p-TrkA/TrkA of optical density measurements corresponding to the p-TrkA and total TrkA protein levels respectively. (c) Graph shows the ratio TrkA/Actin of optical density measurements corresponding to the total TrkA and actin protein levels respectively. (d) Graph shows the ratio p-ALK140/ALK140 of optical density measurements corresponding to the p-ALK140 and total ALK140 protein levels respectively. (e) Graph shows the ratio ALK140/Actin of optical density measurements corresponding to the total ALK140 and actin protein levels respectively. (f) Representative western blots showing phosphorylated ALK (p-ALK) 140 and phosphorylated TrkA (p-TrkA) in cells incubated for 5 min with 1 μM MY33-3 or DMSO (control) and then for 15 min with 50 mM ethanol. Total ALK and TrkA western blots are shown below each phosphorylated protein blot for comparison. Both proteins were detected at ~140 kDa. (g) Graph shows the ratio p-TrkA/TrkA of optical density measurements corresponding to the p-TrkA and total TrkA protein levels respectively. (h) Graph shows the ratio TrkA/Actin of optical density measurements corresponding to the total TrkA and actin protein levels respectively. (i) Graph shows the ratio p-ALK140/ALK140 of optical density measurements corresponding to the p-ALK140 and total ALK140 protein levels respectively. (j) Graph shows the ratio ALK140/Actin of optical density measurements corresponding to the total ALK140 and actin protein levels respectively. Data are presented as the mean ± SEM. *p < 0.05, **p < 0.01 vs. unstimulated cells (controls, lane 1).

actions in the nervous system. Here, we tested the effects of RPTP β/ζ inhibitors in a battery of behavioral tests in mice treated with ethanol. We found that the RPTP β/ζ inhibitor, MY10, decreased binge-like drinking in the DID test. MY10 appears to be more effective in reducing ethanol consumption than the other RPTP β/ζ inhibitor, MY33-3, when given at the same dose. It is possible that a higher dose of MY33-3 might be more effective in reducing ethanol consumption. It is interesting to note that both inhibitors were equally potent in *in vitro* phosphatase assays, but MY33-3 was less selective since it also inhibited PTP-1B with significant potency (IC₅₀ ~ 0.7 μ M) (Pastor et al., 2018). Thus, we cannot rule out the possibility that the inhibition of other phosphatases may trigger signaling events that interfere with this compound's effects.

MY10-treated mice drank less ethanol and exhibited decreased ethanol preference in the DID test, and BECs were correspondingly reduced after the 4-h drinking session on the last day of the test. The effect of MY10 on drinking appears to be specific to ethanol because treatment with MY10 did not affect sucrose consumption. These results suggest that MY10 does not cause general anhedonia. We should point out that mice drank less in our DID test compared to previous studies (Dutton et al., 2017). This may be related to several factors. One is that we performed a 2-bottle choice with water, so mice may have consumed less ethanol when given a choice between water and ethanol compared with access to a single bottle of ethanol. The second may be due to the acute stress of the gavage procedure, or the combination of stress and the availability of water during the drinking test. Nonetheless, MY10 was still effective in reducing ethanol consumption, suggesting that RPTP β/ζ is potentially a viable therapeutic target to reduce excessive drinking.

To test the possibility that the RPTP β/ζ inhibitor MY10 decreases ethanol drinking through its ability to block the rewarding effects of ethanol, we tested the effects of MY10 in ethanol place conditioning. The data presented here demonstrate that MY10 reduces ethanol-induced CPP. Importantly, it has been shown that ethanol-induced place preference is blocked in mice with transgenic over-expression in the brain of PTN, an endogenous inhibitor of RPTP β/ζ (Vicente-Rodríguez et al., 2014a). Treatment of mice with MY10 in the absence of ethanol did not affect place conditioning, indicating that MY10 alone does not affect reward or aversion. This is consistent with our sucrose consumption data, indicating that MY10 may not have a general psychotropic effect, but instead may specifically affect ethanol-related behaviors. Taken together, these data provide evidence that RPTP β/ζ inhibition limits alcohol

reward. However, these results must be interpreted with caution because performance in the CPP test is dependent on learning of the ethanol-context association. MY10 may have merely blocked this learning process instead of the rewarding properties of ethanol. Future studies are needed to determine the effect of MY10 on learning and memory to distinguish between its effect on ethanol reward vs. learning.

The exact mechanisms by which inhibiting RPTP β/ζ decreases ethanol consumption and reward are not known and need to be delineated with additional experiments. This receptor is widely expressed in the nervous system (Levy et al., 1993) including relevant areas for ethanol reward such as prefrontal cortex, the nigrostriatal pathway and the ventral tegmental area (Ohyama et al., 1998; Hayashi et al., 2005; Ferrario et al., 2008). ALK, which is a substrate for RPTP β/ζ , is also expressed in those regions (Bilsland et al., 2008; Iwahara et al., 1997; Vernersson et al., 2006). Notably, knockdown of ALK in the mouse ventral tegmental area leads to decreased binge-like ethanol consumption (Dutton et al., 2017), and treatment of mice with ALK inhibitors reduces drinking and ethanol CPP (Dutton et al., 2017). It is possible that the effects of RPTP β/ζ on ethanol consumption and reward are through its ability to regulate ALK phosphorylation and activity in the ventral tegmental area.

Here, we found that inhibition of RPTP β/ζ by MY10 and MY33-3 in neuroblastoma cells increases the phosphorylation of Tyr 1278 in ALK140. We also demonstrated that ethanol treatment increases the phosphorylation of ALK140, in accordance with previously published findings (He et al., 2015). Phosphorylation of Tyr 1278 is an important initial event in the activation of ALK (Guan et al., 2017; Hallberg and Palmer, 2016). Surprisingly, we found that pre-treatment of cells with RPTP β/ζ inhibitors (particularly MY10) prior to ethanol reduced ethanol-induced phosphorylation of Tyr 1278 in ALK140. It was initially puzzling as to why both ethanol and RPTP β/ζ inhibitors activate ALK when given separately, yet the combination of the two treatments blocks ALK activation. This might be explained by ALK trafficking. ALK activation causes endocytosis of the receptor and effectively desensitizes it (Mazot et al., 2012). We hypothesize that pre-treatment of neuroblastoma cells with RPTP β/ζ inhibitors leads to increased autophosphorylation, activation, and endocytosis of ALK, effectively desensitizing ALK prior to ethanol treatment. ALK is then unavailable for ethanol-induced activation through its putative ligand MK (He et al., 2015). A schematic of this is demonstrated in Fig. 8. Because ALK inhibition reduces ethanol consumption, it is tempting to speculate that RPTP β/ζ inhibitors decrease drinking and reward by promoting ALK endocytosis and interfering with ethanol-induced activation of ALK.

In addition to affecting ethanol drinking and CPP, treatment with MY10 delayed recovery from ethanol-induced ataxia, suggesting that the effects of the inhibitor may potentiate the motor effects of ethanol early after acute administration of the drug. It has to be noted that RPTP β/ζ is expressed in the cortex and cerebellum (Levy et al., 1993; Tanaka et al., 2003), critical areas for ethanol-induced ataxia (Van Skike et al., 2010). Interestingly, increased activity of PKC γ has been suggested to be responsible for enhanced sensitivity to the motor-impairing effects of ethanol (Van Skike et al., 2010). Inhibition of RPTP β/ζ by PTN is known to activate different PKC isoforms (Pariser et al., 2005; Herradon and Ezquerro, 2009), suggesting the possibility that inhibition of RPTP β/ζ by MY10 may potentiate ethanol-induced ataxia in the short term through its ability to modulate the activity of PKC γ .

Here, we also demonstrate that ethanol induces a rapid phosphorylation of Tyr 490 in TrkA in cultured neuroblastoma cells. Phosphorylation of this residue is involved in the activation of the Ras/mitogen-activated protein kinase (MAPK or ERK) and the

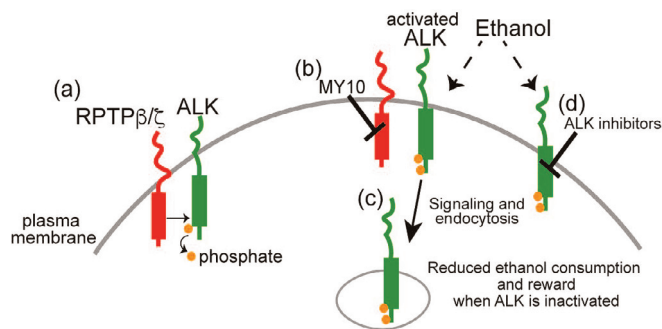


Fig. 8. Schematic showing RPTP β/ζ and ALK interaction and possible involvement in ethanol consumption and reward. (a) Under normal conditions, RPTP β/ζ dephosphorylates ALK and maintains ALK in an inactive state. (b) Inhibition of RPTP β/ζ by inhibitors such as MY10 leads to constitutive ALK phosphorylation and activation. (c) Activated ALK would undergo endocytosis to desensitize the receptor and render it unavailable for ethanol-induced activation. (d) ALK inhibitors also block ethanol-induced activation of ALK. Inactivation of ALK reduces ethanol consumption and reward.

phosphatidylinositol 3-kinase (PI3K)/AKT pathways triggered by TrkA (Obermeier et al., 1994). Previously, it was shown that neonatal ethanol exposure downregulates the expression of TrkA in different regions of the rat brain (Moore et al., 2004). In contrast, short-term exposure to ethanol resulted in elevated levels of nerve growth factor (NGF) and TrkA mRNA and protein expression in the mouse cerebellum (Wang et al., 2010). However, to the best of our knowledge, the functional consequences of the effects of ethanol on TrkA have not been studied. Here we provide the first evidence that ethanol activates TrkA. The mechanisms by which ethanol engages TrkA signaling are currently unknown and remain an important area for investigation. Note that PTN is upregulated in the mouse PFC after ethanol administration (Vicente-Rodriguez et al., 2014a) and that MK expression is increased in the PFC of alcoholics (Flatscher-Bader and Wilce, 2008) and in neuroblastoma cells incubated with ethanol (He et al., 2015). Both PTN and MK bind to RPTPβ/ζ (Maeda et al., 1999; Meng et al., 2000). RPTPβ/ζ negatively regulates TrkA and ALK signaling pathways by dephosphorylating them (Perez-Pinera et al., 2007; Shintani and Noda, 2008). PTN/MK inactivates RPTPβ/ζ phosphatase activity, thereby activating TrkA and ALK signaling. Thus, it is possible that the ability of ethanol to activate ALK and TrkA is indirect, through MK/PTN binding to and inactivating RPTPβ/ζ.

We also found that MY10 potentiates the sedative effects of ethanol, which may be related to either TrkA or ALK activity. ALK knockout mice exhibit increased ethanol-induced sedation compared with wild-type mice (Lasek et al., 2011a), so it is possible that the effect of MY10 on LORR occurs through ALK signaling. TrkA is widely expressed in the CNS including areas such as cortex, thalamus and striatum (Holtzman et al., 1995). In the midbrain, it is known to be expressed in subpopulations of neurons of the interpeduncular nucleus (IPN) (Holtzman et al., 1995) which is part of the limbic system outflow into the brainstem. Interestingly, IPN plays an important role in sleep (Haun et al., 1992), potentially implicating the modulation of the TrkA activity by inhibition of RPTPβ/ζ in the potentiation of ethanol sedative effects caused by MY10. Clearly, additional mechanistic studies are needed to determine how and where in the brain RPTPβ/ζ functions to regulate diverse behavioral responses to ethanol.

5. Conclusion

The data support the concept that RPTPβ/ζ may be a novel target of pharmacotherapy for excessive alcohol consumption. Because of its overall effects in the behavioral assays and its ability to interfere with ethanol signaling pathways, we suggest that MY10 is a potential new compound that may be useful for the treatment of alcohol use disorder.

Acknowledgements

We would like to thank Donghong He for advice and assistance in performing the western blots. This work was supported by National Plan on Drug abuse, Ministerio de Sanidad of Spain (MSSSI, grant PNSD001I2015 to G.H.) and by National Institutes of Health (NIAAA, INIA grant U01 AA020912 to A.W.L.). M V-R and R F-C were supported by fellowships from Fundación Universitaria San Pablo CEU.

References

Alguacil, L.F., Herradon, G., 2015. Midkine and pleiotrophin in the treatment of neurodegenerative diseases and drug addiction. *Recent Pat. CNS Drug Discov.* 10, 28–33.

Bjililand, J.G., Wheeldon, A., Mead, A., Znamenskiy, P., Almond, S., Waters, K.A., Thakur, M., Beaumont, V., Bonnert, T.P., Heavens, R., Whiting, P., McAllister, G.,

Munoz-Sanjuan, I., 2008. Behavioral and neurochemical alterations in mice deficient in anaplastic lymphoma kinase suggest therapeutic potential for psychiatric indications. *Neuropsychopharmacology* 33 (3), 685–700.

Chen, H., He, D., Lasek, A.W., 2017. Midkine in the mouse ventral tegmental area limits ethanol intake and Ccl2 gene expression. *Gene Brain Behav.* 16 (7), 699–708.

den Hartog, C.R., Beckley, J.T., Smothers, T.C., Lench, D.H., Hulseberg, Z.L., Fedarovich, H., Gilstrap, M.J., Homanics, G.E., Woodward, J.J., 2013. Alterations in ethanol-induced behaviors and consumption in knock-in mice expressing ethanol-resistant NMDA receptors. *PLoS One* 8, e80541.

Dutton 3rd, J.W., Chen, H., You, C., Brodie, M.S., Lasek, A.W., 2017. Anaplastic lymphoma kinase regulates binge-like drinking and dopamine receptor sensitivity in the ventral tegmental area. *Addiction Biol.* 22, 665–678.

Ferrario, J.E., Rojas-Mayorquín, A.E., Saldaña-Ortega, M., Salum, C., Gomes, M.Z., Hunot, S., Raisman-Vozari, R., 2008. Pleiotrophin receptor RPTP-zeta/beta expression is up-regulated by L-DOPA in striatal medium spiny neurons of parkinsonian rats. *J. Neurochem.* 107 (2), 443–452.

Flatscher-Bader, T., Wilce, P.A., 2008. Impact of alcohol abuse on protein expression of midkine and excitatory amino acid transporter 1 in the human prefrontal cortex. *Alcohol Clin. Exp. Res.* 32, 1849–1858.

Forouzanfar, M.H., Afshin, A., Alexander, L.T., Anderson, H.R., GBD-2015-Risk-Factors-Collaborators, 2016. Global, regional, and national comparative risk assessment of 79 behavioural, environmental and occupational, and metabolic risks or clusters of risks, 1990–2015: a systematic analysis for the Global Burden of Disease Study 2015. *Lancet* 388, 1659–1724.

Gramage, E., Martin, Y.B., Ramanah, P., Perez-Garcia, C., Herradon, G., 2011. Midkine regulates amphetamine-induced astrogliosis in striatum but has no effects on amphetamine-induced striatal dopaminergic denervation and addictive effects: functional differences between pleiotrophin and midkine. *Neuroscience* 190, 307–317.

Gramage, E., Putelli, A., Polanco, M.J., Gonzalez-Martin, C., Ezquerro, L., Alguacil, L.F., Perez-Pinera, P., Deuel, T.F., Herradon, G., 2010a. The neurotrophic factor pleiotrophin modulates amphetamine-seeking behaviour and amphetamine-induced neurotoxic effects: evidence from pleiotrophin knockout mice. *Addiction Biol.* 15, 403–412.

Gramage, E., Rossi, L., Granado, N., Moratalla, R., Herradon, G., 2010b. Genetic inactivation of pleiotrophin triggers amphetamine-induced cell loss in the substantia nigra and enhances amphetamine neurotoxicity in the striatum. *Neuroscience* 170, 308–316.

Grant, B.F., Chou, S.P., Saha, T.D., Pickering, R.P., Kerridge, B.T., Ruan, W.J., Huang, B., Jung, J., Zhang, H., Fan, A., Hasin, D.S., 2017. Prevalence of 12-month alcohol use, high-risk drinking, and DSM-IV alcohol use disorder in the United States, 2001–2002 to 2012–2013: results from the national epidemiologic survey on alcohol and related conditions. *JAMA Psychiat.* 74, 911–923.

Guan, J., Yamazaki, Y., Chand, D., van Dijk, J.R., Rueth, K., Palmer, R.H., Hallberg, B., 2017. Novel mechanisms of ALK activation revealed by analysis of the Y1278S neuroblastoma mutation. *Cancers* 9 (11), 149.

Hallberg, B., Palmer, R.H., 2016. The role of the ALK receptor in cancer biology. *Ann. Oncol.* 27 (3), 4–15.

Haun, F., Eckenrode, T.C., Murray, M., 1992. Habenula and thalamus cell transplants restore normal sleep behaviors disrupted by denervation of the interpeduncular nucleus. *J. Neurosci.* 12 (8), 3282–3290.

Hayashi, N., Miyata, S., Yamada, M., Kamei, K., Oohira, A., 2005. Neuronal expression of the chondroitin sulfate proteoglycans receptor-type protein-tyrosine phosphatase beta and phosphacan. *Neuroscience* 131 (2), 331–348.

He, D., Chen, H., Muramatsu, H., Lasek, A.W., 2015. Ethanol activates midkine and anaplastic lymphoma kinase signaling in neuroblastoma cells and in the brain. *J. Neurochem.* 135, 508–521.

Herradon, G., Ezquerro, L., 2009. Blocking receptor protein tyrosine phosphatase beta/zeta: a potential therapeutic strategy for Parkinson's disease. *Curr. Med. Chem.* 16, 3322–3329.

Herradon, G., Ezquerro, L., Gramage, E., Alguacil, L.F., 2009. Targeting the pleiotrophin/receptor protein tyrosine phosphatase beta/zeta signaling pathway to limit neurotoxicity induced by drug abuse. *Mini Rev. Med. Chem.* 9, 440–447.

Herradon, G., Perez-Garcia, C., 2014. Targeting midkine and pleiotrophin signalling pathways in addiction and neurodegenerative disorders: recent progress and perspectives. *Br. J. Pharmacol.* 171, 837–848.

Holtzman, D.M., Kilbridge, J., Li, Y., Cunningham Jr., E.T., Lenn, N.J., Clary, D.O., Reichardt, L.F., Mobley, W.C., 1995. TrkA expression in the CNS: evidence for the existence of several novel NGF-responsive CNS neurons. *J. Neurosci.* 15 (2), 1567–1576.

Iwahara, T., Fujimoto, J., Wen, D., Cupples, R., Bucay, N., Arakawa, T., Mori, S., Ratzkin, B., Yamamoto, T., 1997. Molecular characterization of ALK, a receptor tyrosine kinase expressed specifically in the nervous system. *Oncogene* 14 (4), 439–449.

Lasek, A.W., Lim, J., Kliethermes, C.L., Berger, K.H., Joslyn, G., Brush, G., Xue, L., Robertson, M., Moore, M.S., Vranizan, K., Morris, S.W., Schuckit, M.A., White, R.L., Heberlein, U., 2011a. An evolutionary conserved role for anaplastic lymphoma kinase in behavioral responses to ethanol. *PLoS One* 6 (7), e22636.

Lasek, A.W., Giorgetti, F., Berger, K.H., Taylor, S., Heberlein, U., 2011b. Lmo genes regulate behavioral responses to ethanol in *Drosophila melanogaster* and the mouse. *Alcohol Clin. Exp. Res.* 35, 1600–1606.

Le Greves, P., 2005. Pleiotrophin gene transcription in the rat nucleus accumbens is stimulated by an acute dose of amphetamine. *Brain Res. Bull.* 65, 529–532.

Levy, J.B., Canoll, P.D., Silvennoinen, O., Barnea, G., Morse, B., Honegger, A.M.,

- Huang, J.T., Cannizzaro, L.A., Park, S.H., Druck, T., Huebner, K., Sap, J., Ehrlich, M., 1993. The cloning of a receptor-type protein tyrosine phosphatase expressed in the central nervous system. *J. Biol. Chem.* 268 (14), 10573–10581.
- Maeda, N., Ichihara-Tanaka, K., Kimura, T., Kadomatsu, K., Muramatsu, T., Noda, M., 1999. A receptor-like protein-tyrosine phosphatase PTPzeta/RPTPbeta binds a heparin-binding growth factor midkine. Involvement of arginine 78 of midkine in the high affinity binding to PTPzeta. *J. Biol. Chem.* 274, 12474–12479.
- Mazot, P., Cazes, A., Dingli, F., Degoutin, J., Irinopoulou, T., Boutterin, M.C., Lombard, B., Loew, D., Hallberg, B., Palmer, R.H., Delattre, O., Janoueix-Lerosey, I., Vigny, M., 2012. Internalization and down-regulation of the ALK receptor in neuroblastoma cell lines upon monoclonal antibodies treatment. *PLoS One* 7 (3), e33581.
- Meng, K., Rodriguez-Pena, A., Dimitrov, T., Chen, W., Yamin, M., Noda, M., Deuel, T.F., 2000. Pleiotrophin signals increased tyrosine phosphorylation of beta catenin through inactivation of the intrinsic catalytic activity of the receptor-type protein tyrosine phosphatase beta/zeta. *Proc. Natl. Acad. Sci. U. S. A.* 97, 2603–2608.
- Moore, D.B., Madorsky, I., Paiva, M., Barrow Heaton, M., 2004. Ethanol exposure alters neurotrophin receptor expression in the rat central nervous system: effects of prenatal exposure. *J. Neurobiol.* 60, 101–113.
- Mulligan, M.K., Ponomarev, I., Hitzemann, R.J., Belknap, J.K., Tabakoff, B., Harris, R.A., Crabbe, J.C., Blednov, Y.A., Grahame, N.J., Phillips, T.J., Finn, D.A., Hoffman, P.L., Iyer, V.R., Koob, G.F., Bergeson, S.E., 2006. Toward understanding the genetics of alcohol drinking through transcriptome meta-analysis. *Proc. Natl. Acad. Sci. U. S. A.* 103, 6368–6373.
- Obermeier, A., Bradshaw, R.A., Seedorf, K., Choidas, A., Schlessinger, J., Ullrich, A., 1994. Neuronal differentiation signals are controlled by nerve growth factor receptor/Trk binding sites for SHC and PLC gamma. *EMBO J.* 13, 1585–1590.
- Ohyama, K., Kawano, H., Asou, H., Fukuda, T., Oohira, A., Uyemura, K., Kawamura, K., 1998. Coordinate expression of L1 and 6B4 proteoglycan/phosphacan is correlated with the migration of mesencephalic dopaminergic neurons in mice. *Brain. Res. Dev. Brain. Res.* 107 (2), 219–226.
- O'Keefe, J.H., Bybee, K.A., Lavie, C.J., 2007. Alcohol and cardiovascular health: the razor-sharp double-edged sword. *J. Am. Coll. Cardiol.* 50, 1009–1014.
- Pariser, H., Ezquerro, L., Herradon, G., Perez-Pinera, P., Deuel, T.F., 2005. Fyn is a downstream target of the pleiotrophin/receptor protein tyrosine phosphatase beta/zeta-signaling pathway: regulation of tyrosine phosphorylation of Fyn by pleiotrophin. *Biochem. Biophys. Res. Commun.* 332, 664–669.
- Pastor, M., Fernández-Calle, R., Di Geronimo, B., Vicente-Rodríguez, M., Zapico, J.M., Gramage, E., Coderch, C., Pérez-García, C., Lasek, A.W., Puchades-Carrasco, L., Pineda-Lucena, A., de Pascual-Teresa, B., Herradón, G., Ramos, A., 2018. Development of inhibitors of receptor protein tyrosine phosphatase β/ζ (PTPRZ1) as candidates for CNS disorders. *Eur. J. Med. Chem.* 144, 318–329.
- Perez-Pinera, P., Zhang, W., Chang, Y., Vega, J.A., Deuel, T.F., 2007. Anaplastic lymphoma kinase is activated through the pleiotrophin/receptor protein-tyrosine phosphatase beta/zeta signaling pathway: an alternative mechanism of receptor tyrosine kinase activation. *J. Biol. Chem.* 282, 28683–28690.
- Petit, J.M., Hamza, S., Rollot, F., Sigonney, V., Crevisy, E., Duvillard, L., Raab, J.J., Bronowicki, J.P., Bernard-Chabert, B., Di Martino, V., Doffoel, M., Barraud, H., Richou, C., Jouve, J.L., Hillon, P., 2014. Impact of liver disease severity and etiology on the occurrence of diabetes mellitus in patients with liver cirrhosis. *Acta Diabetol.* 51, 455–460.
- Rhodes, J.S., Best, K., Belknap, J.K., Finn, D.A., Crabbe, J.C., 2005. Evaluation of a simple model of ethanol drinking to intoxication in C57BL/6J mice. *Physiol. Behav.* 84, 53–63.
- Shintani, T., Noda, M., 2008. Protein tyrosine phosphatase receptor type Z dephosphorylates TrkA receptors and attenuates NGF-dependent neurite outgrowth of PC12 cells. *J. Biochem.* 144, 259–266.
- Tanaka, M., Maeda, N., Noda, M., Marunouchi, T., 2003. A chondroitin sulfate proteoglycan PTPzeta/RPTPbeta regulates the morphogenesis of Purkinje cell dendrites in the developing cerebellum. *J. Neurosci.* 23 (7), 2804–2814.
- Van Skike, C.E., Botta, P., Chin, V.S., Tokunaga, S., McDaniel, J.M., Venard, J., Diaz-Granados, J.L., Valenzuela, C.F., Matthews, D.B., 2010. Behavioral effects of ethanol in cerebellum are age dependent: potential system and molecular mechanisms. *Alcohol Clin. Exp. Res.* 34 (12), 2070–2080.
- Vernersson, E., Khoo, N.K., Henriksson, M.L., Roos, G., Palmer, R.H., Hallberg, B., 2006. Characterization of the expression of the ALK receptor tyrosine kinase in mice. *Gene Expr. Patterns* 6 (5), 448–461.
- Vicente-Rodríguez, M., Perez-García, C., Ferrer-Alcon, M., Uribarri, M., Sanchez-Alonso, M.G., Ramos, M.P., Herradon, G., 2014a. Pleiotrophin differentially regulates the rewarding and sedative effects of ethanol. *J. Neurochem.* 131, 688–695.
- Vicente-Rodríguez, M., Perez-García, C., Haro, M., Ramos, M.P., Herradon, G., 2014b. Genetic inactivation of midkine modulates behavioural responses to ethanol possibly by enhancing GABA(A) receptor sensitivity to GABA(A) acting drugs. *Behav. Brain Res.* 274, 258–263.
- Wang, Z.Y., Miki, T., Lee, K.Y., Yokoyama, T., Kusaka, T., Sumitani, K., Warita, K., Matsumoto, Y., Yakura, T., Hosomi, N., Ameno, K., Bedi, K.S., Takeuchi, Y., 2010. Short-term exposure to ethanol causes a differential response between nerve growth factor and brain-derived neurotrophic factor ligand/receptor systems in the mouse cerebellum. *Neuroscience* 165, 485–491.
- Zakhari, S., Li, T.K., 2007. Determinants of alcohol use and abuse: impact of quantity and frequency patterns on liver disease. *Hepatology* 46, 2032–2039.
- Zapata, A., Gonzales, R.A., Shippenberg, T.S., 2006. Repeated ethanol intoxication induces behavioral sensitization in the absence of a sensitized accumbens dopamine response in C57BL/6J and DBA/2J mice. *Neuropsychopharmacology* 31, 396–405.

ARTÍCULO 4. Inhibition of RPTP β/ζ blocks ethanol-induced conditioned place preference in pleiotrophin knockout mice.

Rosalía Fernández-Calle, Esther Gramage, José María Zapico, Beatriz de Pascual-Teresa, Ana Ramos y Gonzalo Herradón.

Behavioural Brain Research, 2019. ISSN: 1872-7549

Volumen: 369

Página de inicio: 111933

DOI: 10.1016/j.bbr.2019.111933

Resumen

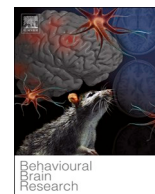
La pleiotrofina (PTN) y la midkina (MK) son factores neurotróficos que se sobreexpresan en la corteza prefrontal tras la administración de alcohol y se ha observado que reducen la ingesta de alcohol y sus efectos reforzadores. La PTN y la MK son inhibidores endógenos del receptor proteína tirosina de fosfatasa (RPTP) β/ζ . Cabe destacar que, la inhibición farmacológica de RPTP β/ζ reduce el consumo de alcohol y bloquea el condicionamiento preferencial al sitio (CPP) inducido por el alcohol en ratones normales (Wt). Debido a que los ratones *knock-out* de PTN (Ptn^{-/-}) son más vulnerables a los efectos reforzadores del alcohol, se ha querido evaluar los efectos de MY10, un compuesto inhibidor de RPTP β/ζ , sobre el CPP inducido por alcohol en ratones Ptn^{-/-}. Los datos que aquí se presentan demuestran por primera vez que a una dosis de MY10 capaz de bloquear el consumo y los efectos reforzadores del alcohol en ratones Wt, también bloquea este efecto en individuos más vulnerables que carecen de PTN, los ratones Ptn^{-/-}. Asimismo, como se ha demostrado que MY10 puede atravesar la barrera hematoencefálica, se probaron sus efectos en una serie de ensayos comportamentales en ratones Wt y Ptn^{-/-}. Los datos obtenidos indican que MY10 no produce efectos comportamentales llamativos en animales Wt. Sin embargo, MY10 tiende a producir un efecto ansiolítico en ratones Ptn^{-/-} en el paradigma del laberinto elevado en cruz. En general, los datos indican que MY10 rescata a los ratones Ptn^{-/-} de su mayor susceptibilidad a los efectos reforzadores del alcohol y que puede inducir cierto efecto ansiolítico en individuos con niveles funcionales de PTN reducidos o nulos. Se requieren estudios adicionales para confirmar el potencial de la inhibición de RPTP β/ζ como nueva estrategia terapéutica en el tratamiento de los desórdenes relacionados con la ansiedad.

Contribución de la doctoranda en este trabajo

Rosalía Fernández Calle llevó a cabo los experimentos comportamentales incluidos en este trabajo. Participó muy activamente en el análisis e interpretación de los datos, y tuvo una gran implicación en la escritura del artículo.

Contents lists available at [ScienceDirect](https://www.sciencedirect.com)

Behavioural Brain Research

journal homepage: www.elsevier.com/locate/bbr

Inhibition of RPTP β/ζ blocks ethanol-induced conditioned place preference in pleiotrophin knockout mice

Rosalía Fernández-Calle^a, Esther Gramage^a, José María Zapico^b, Beatriz de Pascual-Teresa^b, Ana Ramos^b, Gonzalo Herradón^{a,*}

^a Departamento de Ciencias Farmacéuticas y de la Salud, Facultad de Farmacia, Universidad San Pablo-CEU, CEU Universities, Urbanización Montepríncipe, 28925, Alcorcón, Madrid, Spain

^b Departamento de Química y Bioquímica, Facultad de Farmacia, Universidad San Pablo-CEU, CEU Universities, Urbanización Montepríncipe, 28925, Alcorcón, Madrid, Spain

ARTICLE INFO

Keywords:

Conditioned place preference
Pleiotrophin
Fyn
Addiction
ALK
Alcohol
Midkine

ABSTRACT

Pleiotrophin (PTN) and Midkine (MK) are neurotrophic factors that are upregulated in the prefrontal cortex after alcohol administration and have been shown to reduce ethanol drinking and reward. PTN and MK are endogenous inhibitors of Receptor Protein Tyrosine Phosphatase (RPTP) β/ζ . Interestingly, pharmacological inhibition of RPTP β/ζ reduces ethanol consumption and blocks ethanol-induced conditioned place preference (CPP) in wild type mice. Since PTN-knockout (Ptn^{-/-}) mice are more sensitive to the conditioning effects of alcohol, we aimed to test the effects of MY10, a small-molecule inhibitor of RPTP β/ζ , on ethanol-induced CPP in Ptn^{-/-} mice. The data presented here demonstrate for the first time that a regular dose of MY10, known to block ethanol consumption and reward in wild type mice, also blocks the rewarding effects of ethanol in the more vulnerable individuals lacking PTN, the endogenous inhibitor of RPTP β/ζ . In addition, since MY10 readily penetrates the blood brain barrier (BBB), we tested its effects in a series of behavioural tests in Ptn^{+/+} and Ptn^{-/-} mice. The data indicate that MY10 does not cause gross behavioural effects in wild type mice. However, MY10 tended to induce anxiolytic effects in Ptn^{-/-} mice in the elevated plus maze paradigm. Overall, the data indicate that MY10 rescues Ptn^{-/-} mice from their increased susceptibility to the conditioning effects of ethanol and may induce anxiolytic effects in individuals with reduced or absent PTN functions. Further studies are needed to confirm the potential of pharmacological inhibition of RPTP β/ζ as a new therapeutic strategy in the treatment of anxiety-related disorders.

1. Introduction

Alcohol addiction is a serious condition with unyielding health and social consequences. According to the Global Status Report on Alcohol and Health from the World Health Organization (WHO), harmful use of alcohol in 2016 caused more than 5% of the global disease burden and more than 3 million deaths [1].

There are different strategies for the treatment of alcoholism that usually combine cognitive behavioural therapy and pharmacotherapy. However, there is an urgent need to develop more efficient therapies for the treatment of alcohol use disorder (AUD). A number of genome-wide associated studies (GWAS) have been carried out in an effort to unveil

the strong genetic component of alcohol dependence, which have rendered common genetic factors playing roles in other psychiatric disorders including other substance use disorders [2,3]. The identification of novel genetic factors underlying alcohol dependence is expected to hand over new pharmacological targets and/or biomarkers useful in the treatment of AUD.

Pleiotrophin (PTN) and Midkine (MK) are two of those genetic factors with potential roles in AUD. Midkine expression is found highly up-regulated in the prefrontal cortex (PFC) of human alcoholics and in mice selectively bred for high alcohol consumption [4,5]. PTN expression is up-regulated in the mouse PFC after a single administration of a rewarding dose of ethanol (2.0 g/kg) [6]. Interestingly, both

Abbreviations: ALK, anaplastic lymphoma kinase; ANOVA, analysis of variance; AUD, alcohol use disorder; BBB, blood brain barrier; CNS, central nervous system; CPP, conditioned place preference; EPM, elevated plus maze; GWAS, genome-wide associated studies; MK, midkine; PFC, prefrontal cortex; PTN, pleiotrophin; RPTP, receptor protein tyrosine phosphatase; S.E.M., standard error of the mean; SNP, single nucleotide polymorphism; WT, wild type

* Corresponding author at: Lab. Pharmacology, Facultad de Farmacia, Universidad San Pablo-CEU, Urbanización Montepríncipe, 28925, Alcorcón, Madrid, Spain.

E-mail address: herradon@ceu.es (G. Herradón).

<https://doi.org/10.1016/j.bbr.2019.111933>

Received 15 February 2019; Received in revised form 30 April 2019; Accepted 30 April 2019

Available online 01 May 2019

0166-4328/ © 2019 Elsevier B.V. All rights reserved.

cytokines are also up-regulated in different brain areas after the administration of different drugs of abuse including psychostimulants, opioids and cannabis [7]. Both PTN and MK are important in the central nervous system (CNS), in which they play a role in repairing the damaged brain tissue in different pathological contexts [7]. Accordingly, these cytokines cause protective effects against amphetamine-induced neurotoxicity [8,9]. However, the up-regulation of PTN and MK after treatment with different drugs of abuse also suggests the possibility that these cytokines can modulate the behavioural responses induced by these drugs. Accordingly, MK has been shown to modulate the rewarding effects of cocaine [10] and PTN plays a role in the modulation of the behavioural effects of amphetamine [8] and opioids [11]. In the case of alcohol, both cytokines have been shown to regulate the behavioural responses induced by this drug [6,12,13]. Importantly, PTN-knockout ($Ptn^{-/-}$) and MK-knockout mice ($Mk^{-/-}$) are more sensitive to the conditioning effects of alcohol [6,13], whereas Ptn transgenic over expression in the mouse brain blocks the rewarding effects of alcohol [6]. The data suggest that pharmacological potentiating of PTN/MK signaling pathways could be a new therapeutic strategy for the treatment of AUD [14].

PTN and MK are endogenous inhibitors of Receptor Protein Tyrosine Phosphatase (RPTP) β/ζ (a.k.a. PTPRZ, RPTP β , PTP ζ) [15]. They have been shown to enforce the dimerization of RPTP β/ζ , thus denying the access of substrates to the catalytic site of this receptor [15]. This leads to an increase in tyrosine phosphorylation of RPTP β/ζ substrates, among which Fyn kinase [16] and Anaplastic Lymphoma Kinase (ALK) [17] have formerly been shown to be involved in the modulation of alcohol signaling pathways and alcohol-induced behavioural responses [18–20].

Previously, we hypothesized that pharmacological inhibition of RPTP β/ζ could replicate the limiting actions of PTN and MK in alcohol consumption and reward [6,12,13]. To test this hypothesis, new blood-brain barrier (BBB) permeable molecules designed to mimic the activity of PTN/MK in the CNS were synthesized and evaluated [21]. These compounds exert their actions by interacting with the intracellular domain of RPTP β/ζ and inhibiting its tyrosine phosphatase activity. Recently, MY10, the most potent compound, was shown to reduce significantly alcohol consumption and reward in wild type mice by regulating alcohol-induced signaling pathways including ALK activation [22].

Additional studies are needed to confirm that MY10 is a promising compound for the treatment of AUD and structure-based approaches are underway to design new analogues with improved potency, selectivity and/or pharmacokinetic properties. It becomes necessary to test whether an exogenous inhibitor of RPTP β/ζ could "rescue" $Ptn^{-/-}$ mice from the enhanced conditioning effects induced by ethanol in this genetic model [6]. To fill this gap, we aimed to test the effects of MY10 on alcohol conditioning effects in $Ptn^{-/-}$ mice. Another question that remains to be elucidated is whether the treatment with MY10 induces by itself any behavioural effects, since its efficient penetration in the brain has been proven [21]. For this purpose, we also aim to test whether MY10 could induce other behavioural effects that may be relevant for its potential indications in CNS pathologies.

2. Materials and methods

2.1. Pleiotrophin genetically deficient ($Ptn^{-/-}$) mice

The animals used in this study were male $Ptn^{-/-}$, and wild type ($Ptn^{+/+}$) mice of 9–10 weeks age (20–25 g). $Ptn^{-/-}$ male mice on a C57BL/6J background, generated by methods previously described [23,24], were kindly donated by Dr. Thomas F. Deuel (The Scripps Research Institute, La Jolla, CA). Animals were housed under controlled environmental conditions ($22 \pm 1^\circ\text{C}$ and a 12-h light/12-h dark cycle) with free access to food and water. All the animals used in this study were maintained in accordance with the ARRIVE guidelines and the European Union Laboratory Animal Care Rules (86/609/ECC directive) and the protocols were approved by the Animal Research Committee of USP-CEU.

2.2. RPTP β/ζ inhibitor: MY10

MY10 was synthesized as previously described [21]. MY10 was administered at a dose of 60 mg/kg in a vehicle constituted by 10% dehydrated ethanol, 20% polysorbate 80, 70% PEG-300. Ethanol in the vehicle results in a dose of less than 0.3 g/kg. Pharmacokinetic studies in mice have shown good BBB penetration 1 h after oral administration [21]. Mice were administered with MY10 or vehicle by oral gavage in a volume of approximately 0.1 ml.

2.3. Ethanol conditioned place preference (CPP)

2.3.1. Apparatus

The apparatus used consisted of two Plexiglas square compartments of the same size (20 cm long \times 14 cm high \times 27 cm wide). One compartment had black Plexiglas floor and walls and the other had black Plexiglas floor and white walls.

2.3.2. Procedure and induction of the CPP

For these experiments, we used naive $Ptn^{-/-}$ mice. The biased procedure selected for this study was similar to that used in previous ethanol-induced CPP procedures in $Ptn^{-/-}$ mice [6].

To test the effects of MY10 in ethanol-induced CPP in $Ptn^{-/-}$ mice, we used a 5-day protocol divided in three phases. These phases included preconditioning (Pre-C, day 1), conditioning (days 2–4) and testing (CPP, day 5). During preconditioning, mice were free to explore the two compartments for a 15-min period and the time spent in each compartment was registered using a videotracking system (San Diego instruments, San Diego, California, USA). The conditioning phase consisted of two conditioning sessions per day. In one session, the mice received a single injection of saline i.p. (10 ml/kg) and were confined to the initially preferred compartment for 5 min. In the other session, mice were injected (i.p.) with 2.0 g/kg ethanol (20% v/v in isotonic saline) and confined to the other compartment for 5 min [6]. Mice were administered the RPTP β/ζ inhibitor MY10 (60 mg/kg) or vehicle by oral gavage 1 h before each of the saline and ethanol conditioning sessions ($n = 8$ –12/group) [22]. In the testing phase on day 5, mice received a drug-free, 15-min preference test in which the animals freely moved throughout the apparatus. The time spent in each compartment was registered.

For the control CPP experiment in which we conditioned with MY10 in the absence of ethanol, compound or vehicle were administered on days 2, 3 and 4, 1 h before injecting mice i.p. with saline (10 ml/kg) and confining them to one side of the apparatus for 5 min ($n = 6$ /group). In the testing phase on day 5, mice received a compound-free, 15-min preference test and the amount of time the mice spent in the MY10-paired compartment was measured.

2.4. MY10 behavioural effects

To identify possible behavioural responses induced by MY10 in wild type mice and in Ptn genetically deficient mice, a series of behavioural assays was performed in animals from both genotypes after a single administration of MY10 according to the schematic timeline represented in Fig. 1. The set of $Ptn^{-/-}$ mice used in these experiments was different from the one used in ethanol-induced CPP experiments. In all cases, mice were administered MY10 (60 mg/kg) or vehicle, by oral gavage, 1 h before each assay. Based on successful protocols developed before [25,26], appropriate "washing" periods of time between different behavioural tests (Irwin test, Y-maze, open field, elevated plus maze and forced swimming) were allowed to avoid any influence of every behavioural test in subsequent tests (Fig. 1).

2.4.1. Irwin test

A primary behavioural observation was performed following the protocol by Irwin [27]. Mice ($n = 8$ –9/group) were placed in a

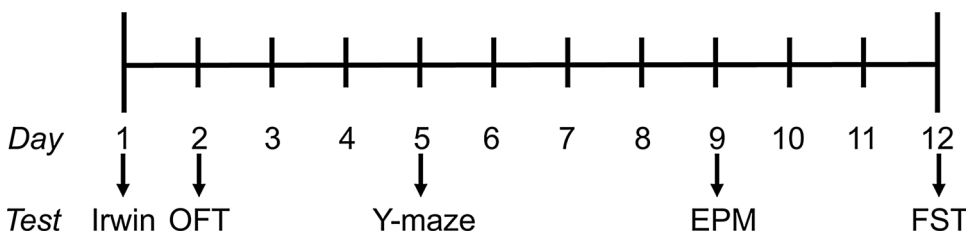


Fig. 1. Schedule of MY10 treatment and testing. Schedule of behavioural testing in MY10 (60 mg/kg)-treated Ptn^{+/+} and Ptn^{-/-} mice. OFT: Open field test. EPM: Elevated Plus Maze. FST: Forced Swim Test.

transparent plastic cylinder (20 cm diameter × 30 cm high) and behavioural alterations were checked according to a standardized observation grid adapted from Irwin [28]. The grid contained the following items: loss of balance, ptosis, loss of traction, abnormal gait, piloerection, low reactivity to touch, altered respiration, aggression, loss of righting reflex, loss of corneal reflex, salivation, lacrimation and number of upright standings. Each animal was observed for 15 min. Several symptoms were evaluated by their presence or absence (loss of balance, ptosis or loss of traction); other symptoms were rated on a 2-

point scale (abnormal gait, piloerection, low reactivity to touch). The final score was expressed by the sum of all symptoms observed in each animal. Upright-standings were also counted for each animal.

2.4.2. Y-maze test

A two-trial memory task, based on a free-choice exploration paradigm in a Y-maze was used as previously described [29] to test recognition processes in response to novelty and working memory in MY10 or vehicle-pretreated mice of both genotypes (n = 7–8/group). Memory was measured with a 60-min inter-trial interval (ITI) between acquisition and retrieval. During the first trial (acquisition phase), the animal was placed in the center of the maze and allowed to visit for 5 min the two arms ('start' and 'other') of a Y-maze constructed of black plastic with three arms each, 34 cm long, 8 cm wide and 14.5 cm high, the third being blocked with a door. During the second trial (retrieval, 5 min), the door was opened, and the animal had free access to all three arms ('start', 'other' and 'new' arms). Discrimination of novelty versus familiarity could then be studied by comparing exploration of the three arms. Preference for the 'new' arm was calculated as a discrimination ratio [new/ (new + other)] for number of arm entries. Scores greater than 0.5 were considered to show preference for the 'novel' arm and indicated the establishment of spatial memory.

2.4.3. Open field test (OFT)

To test general effects of MY10 on locomotion, we performed an open field assay using a maze that consisted in a 49 cm length × 49 cm width × 42 cm height box with a floor divided into a grid of 16 squares. Animals (n = 8/group) were individually placed inside the open field maze and monitored for 10 min. The number of line crossings was registered for each animal.

2.4.4. Elevated plus maze (EPM)

The apparatus used is made of a black Plexiglas with four arms (16 cm long × 5 cm wide) set in cross from a neutral central square (5 cm × 5 cm). Two opposite arms are delimited by vertical walls (closed arms), while the two other opposite arms have unprotected edges (open arms). The maze is elevated 60 cm above the ground and placed in indirect light (100 lx). At the beginning of the 5-min observation session, each mouse (n = 7–8/group) was placed in the central neutral zone, facing one of the open arms. The total numbers of visits and the time spent in the closed and open arms were recorded.

2.4.5. Forced swimming test (FST)

Mice (n = 7–8/group) were gently placed in a beaker (18 cm in diameter) filled to a depth of approximately 10 cm with water at room temperature. Each mouse was tested for 6 min; the first 2 min serving as habituation period. The time they spent immobile was recorded during the last 4 min of the observation period.

2.5. Statistical analysis

All data are expressed as the mean ± SEM and analyzed using Prism software (GraphPad, La Jolla, CA, USA). P values lower than 0.05 were considered a statistically significant difference. CPP data were

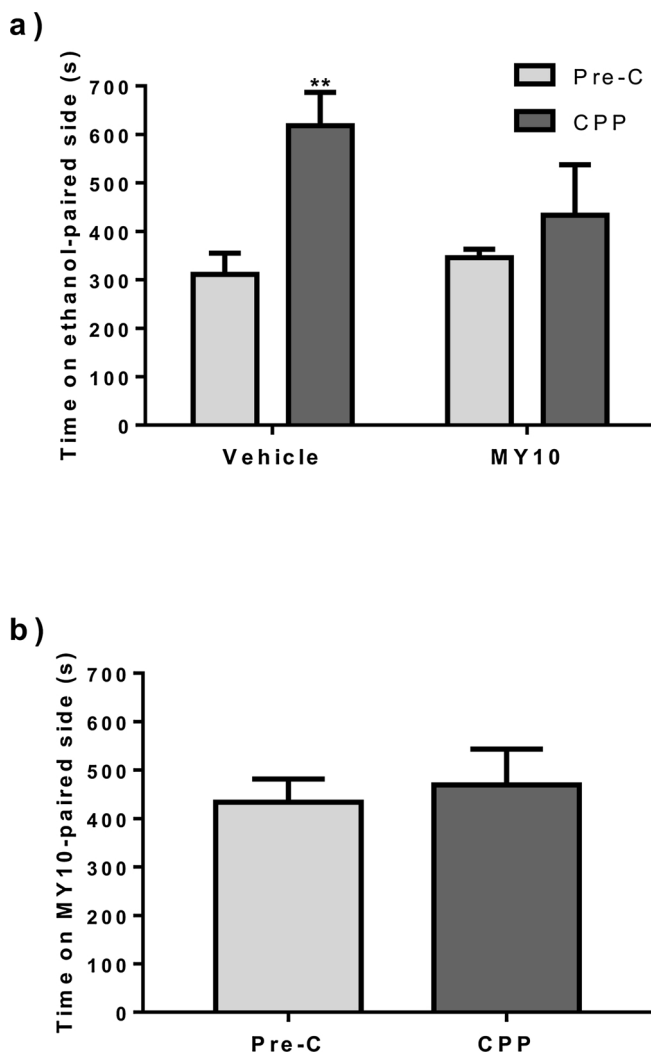


Fig. 2. Ethanol (2.0 g/kg)-induced place preference in Ptn^{-/-} mice. (a) Time (seconds) spent on the ethanol-paired side before conditioning (Pre-C) and after conditioning (CPP) in Ptn^{-/-} mice treated with vehicle or MY10 (n = 8–12/group). (b) Time (seconds) spent on the MY10-paired side before conditioning (Pre-C) and after conditioning (CPP) in Ptn^{-/-} mice conditioned with MY10 (n = 6) instead of ethanol. ** P < 0.01 vs. Pre-C.

3.2. MY10 behavioural effects

To test the possibility that MY10 causes behavioural effects, we administered this compound (60 mg/kg, i.g.) one hour before assessing behavior in $Ptn^{+/+}$ mice undergoing a series of behavioural tests (Fig. 1). In addition, to test the possibility that MY10 may cause different effects in absence of the endogenous inhibitor of RPTP β/ζ , PTN, we tested the effects of MY10 treatment in $Ptn^{-/-}$ mice.

3.2.1. Irwin test

To study preliminary MY10 effects on $Ptn^{+/+}$ and $Ptn^{-/-}$ mice behaviour, we used the Irwin test. MY10 did not cause gross behavioural effects in mice independently of the genotype (Fig. 3a). One of the 8 $Ptn^{+/+}$ mice treated with MY10 experienced loss of balance. Low reactivity to touch was rated on a 2-point scale. We observed low reactivity in 50% of $Ptn^{+/+}$ mice treated with vehicle (one animal scored 1 point and 3 scored 2 points), 62.5% $Ptn^{+/+}$ mice treated with MY10 (4 animals scored 2 points and 1 scored 1 point), 100% of $Ptn^{-/-}$ mice treated with vehicle (7 animals scored 2 points and 1 scored 1 point) and 100% of $Ptn^{-/-}$ mice treated with MY10 (8 animals scored 2 points and 1 animal scored 1 point) (Fig. 3a). Observations point to a general decreased reactivity to touch in $Ptn^{-/-}$ mice independently of the treatment and decreased upright standings in this genotype compared to $Ptn^{+/+}$ mice, the latter tending to disappear after MY10 administration (Fig. 3a).

3.2.2. Open field test (OFT)

Open field test was performed to evaluate locomotor activity after treatment with MY10. 2-way ANOVA showed a significant effect of the genotype ($F(1, 28) = 12.32$; $P = 0.001$) and of the treatment ($F(1, 28) = 5.184$; $P = 0.030$). Concerning the interaction genotype x

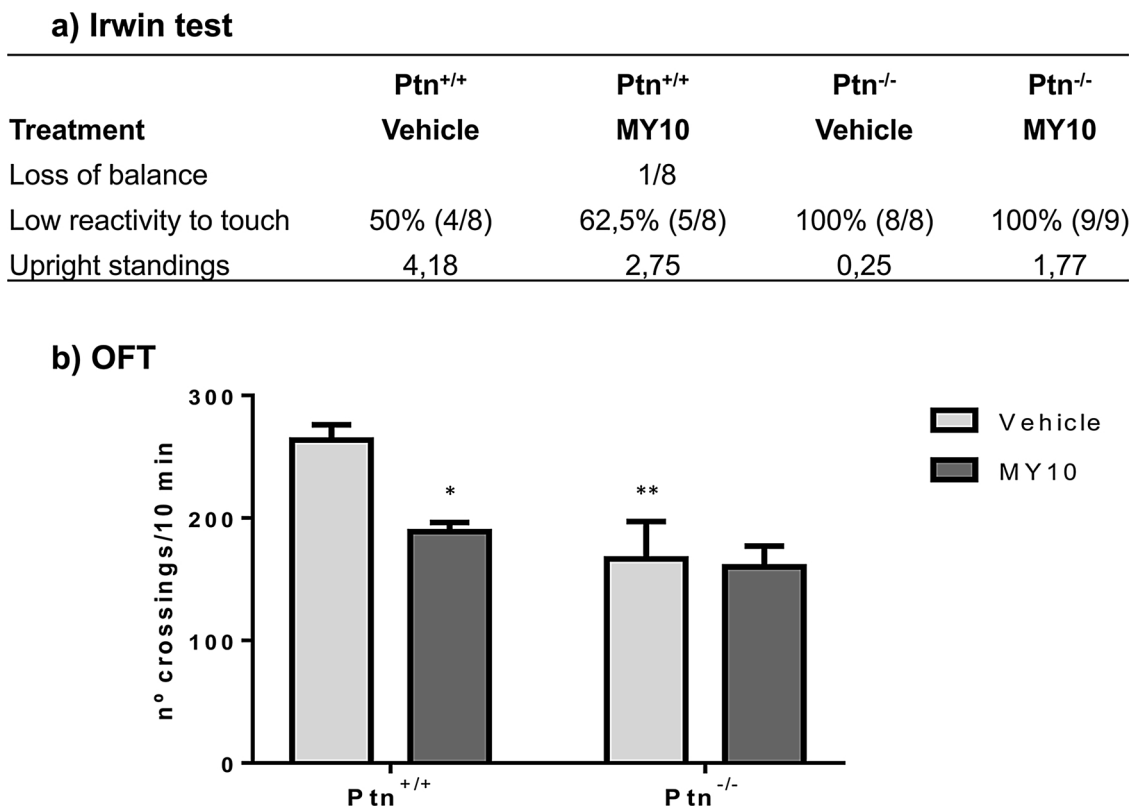


Fig. 3. Behavioural performance of $Ptn^{+/+}$ and $Ptn^{-/-}$ mice in the Irwin test and the open-field test (OFT). (a) The table summarizes the major behavioural effects observed in the Irwin test ($n = 8-9$ /group). Low reactivity to touch was rated on a 2-point scale, the table shows the percentage of animals that experienced this symptom. Number of upright standings are represented as mean of all the values obtained for each of the experimental groups. (b) Figure shows mean \pm SEM of number of crossings by $Ptn^{+/+}$ and $Ptn^{-/-}$ mice pretreated with either vehicle or MY10 in the OFT ($n = 8$ /group). * $P < 0.05$, ** $P < 0.01$ vs vehicle-treated $Ptn^{+/+}$ mice.

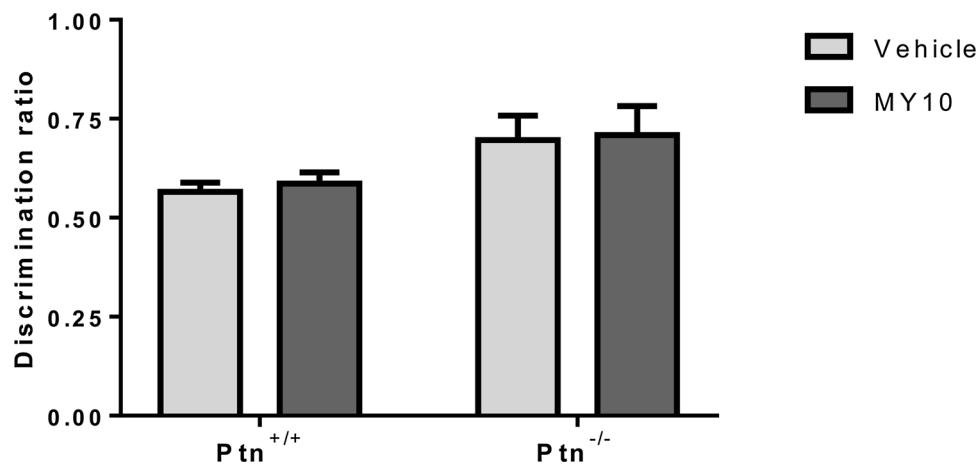


Fig. 4. Behavioural performance of Ptn^{+/+} and Ptn^{-/-} mice in the Y-maze test. Figure shows mean ± SEM of discrimination ratio for Ptn^{+/+} and Ptn^{-/-} mice pretreated with either vehicle or MY10 (n = 7–8/group).

treatment, a trend was observed but did not reach significance ($F(1,28) = 3.662$; $P = 0.065$). Post-hoc analysis revealed that treatment with MY10 reduced the number of crossings in wild type mice but did not affect Ptn^{-/-} mice (Fig. 3b); however, it has to be noted that the number of crossings by vehicle-treated Ptn^{-/-} mice was lower than that of vehicle-treated wild type mice.

3.2.3. Y-maze behaviour

MY10 did not cause readable effects on this spatial memory task. Discrimination of novelty was performed efficiently by mice from both genotypes and was not affected by the treatment (Fig. 4).

3.2.4. Elevated plus maze (EPM)

Two-way ANOVA did not reveal significant effects of the treatment, genotype or the interaction between both variables on the number of entries in closed and open arms (Fig. 5a, b). However, a trend is observed when the interaction genotype × treatment is analyzed in the case of time in open arms ($F(1,26) = 3.748$, $P = 0.063$). Accordingly, Fig. 5 clearly shows that treatment with MY10 did not cause significant changes either in the entries (Fig. 5a, b) or in the time (Fig. 5c, b) spent in open and closed arms by Ptn^{+/+} mice. In the case of Ptn^{-/-} mice, MY10 treatment showed a non-significant trend to increase the number of entries and time spent in open arms (Fig. 5a, c).

3.2.5. Forced swimming test (FST)

MY10 did not cause significant effects in the time of immobility of mice in the forced swimming test independently of the genotype (Fig. 5e).

4. Discussion

In a previous work we described the design and synthesis of MY10, a BBB permeable inhibitor of RPTPβ/ζ [21]. MY10 interacts with the intracellular domain PD1 of RPTPβ/ζ and inhibits its tyrosine phosphatase activity. Interestingly, systemic administration of MY10 (60 mg/kg) reduces alcohol consumption and blocks the rewarding effects of alcohol in mice [22], replicating the effects previously obtained with transgenic mice that overexpress PTN, the endogenous inhibitor of RPTPβ/ζ [6]. On the other hand, we previously described that Ptn^{-/-} mice are more sensitive to the conditioning effects of ethanol [6]. In the present work, we hypothesized that exogenous systemic administration of the RPTPβ/ζ inhibitor MY10 could “rescue” Ptn^{-/-} mice from its phenotype, that is from its increased vulnerability to ethanol conditioning effects. Accordingly, the data presented here show that MY10 blocks ethanol-induced CPP in Ptn^{-/-} mice, in a similar manner as in wild type mice, which are less sensitive to ethanol conditioning effects [6,22]. It has to be noted that we have performed the same biased CPP

protocol previously used with Ptn^{-/-} mice [6]. Numerous CPP protocol variations can be found in the literature, and both biased and unbiased designs are accepted and extensively used depending on the type of study and drug tested [30]. In general, a biased design is appropriate when the drug evaluated exerts unquestionably strong conditioning effects [30]. This is the case of the experiments presented here in which animals conditioned with alcohol spent around 75% of the time in the ethanol-paired compartment.

The cytokines PTN and MK are known to be upregulated in different brain areas after alcohol administration to different species [4,6]. Alcoholism is a disease characterized by a strong genetic component and significant efforts, through GWAS, are being carried out to unveil the genetics of this disease. Although several SNPs in the Ptn gene have been shown to affect bone density [31], other SNPs and mutations have not been linked to PTN expression or function. Overall, data from rodent models and humans suggest that Ptn may be a genetic determinant of AUD and mutations leading to decreased PTN functions can confer increased individual vulnerability to AUD and/or increased probability of relapse in alcoholics with this genotype. The results presented here are relevant, since they demonstrate that MY10 does not only prevent alcohol consumption and reward in normal wild type mice [22], but also blocks the conditioning effects of ethanol in individuals lacking endogenous PTN.

Taken together, evidence suggests that MY10 could be a promising new therapeutic for AUD and/or the lead compound to design and synthesize improved BBB-permeable RPTPβ/ζ inhibitors for this indication. However, little was known about other potential behavioural effects that could result from pharmacological inhibition of RPTPβ/ζ. To fill this gap, we have now performed a behavioural characterization of MY10 effects in wild type and Ptn^{-/-} mice. Although RPTPβ/ζ knockout mice exhibit impaired hippocampal-dependent learning [32,33], the results indicate that inhibition of RPTPβ/ζ by MY10 does not alter recognition processes in response to novelty and working memory independently of the expression of PTN. On the other hand, systemic administration of a single dose of MY10 reduced the locomotor activity in the open field test only in wild type mice. However, it is important to note that Ptn^{-/-} mice showed reduced basal number of crossings in the open field test compared to wild type mice, probably reflecting a reduced exploratory response of Ptn^{-/-} mice to the novelty effect of the environment. More interestingly, the results obtained in the EPM test, although not significant, suggest potential anxiolytic effects of MY10 only in Ptn^{-/-} mice, supporting the need to conduct additional studies to test the possible indication of MY10 in anxiety disorders in individuals with decreased PTN functionality. However, MY10 does not seem to modulate depressive-like behavior in mice. Based on the high prevalence of comorbidity of AUD and conditions

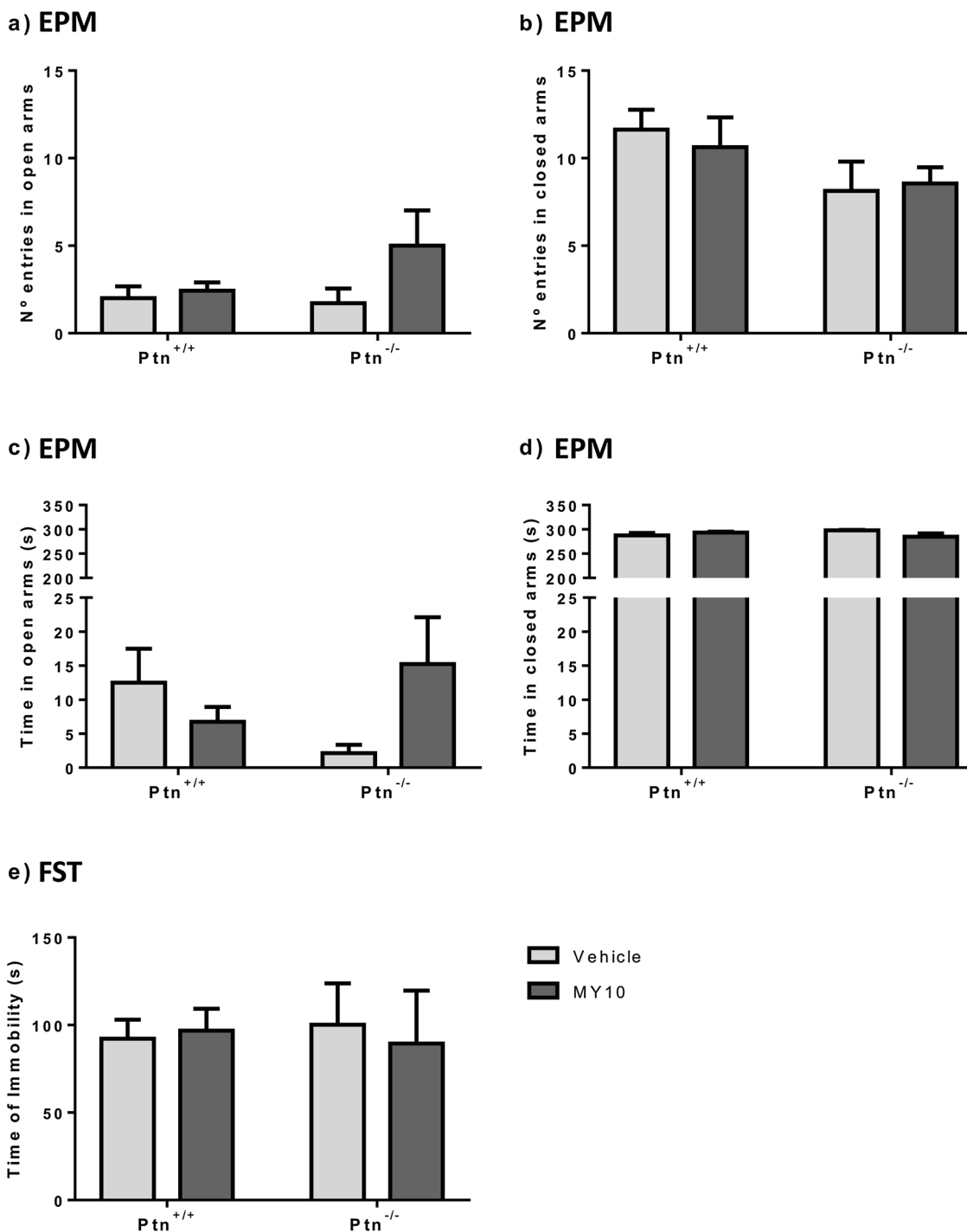


Fig. 5. Behavioural performance of Ptn^{+/+} and Ptn^{-/-} mice in the Elevated Plus Maze (EPM) and in the forced swimming test (FST). (a) Figure shows mean ± SEM of number of entries in the open arms of the EPM by Ptn^{+/+} and Ptn^{-/-} mice (n = 7–8/group) pretreated with either vehicle or MY10. (b) Figure shows mean ± SEM of number of entries in the closed arms of the EPM by Ptn^{+/+} and Ptn^{-/-} mice pretreated with either vehicle or MY10. (c) Figure shows mean ± SEM of time spent in the open arms of the EPM by Ptn^{+/+} and Ptn^{-/-} mice pretreated with either vehicle or MY10. (d) Figure shows mean ± SEM of time spent in the closed arms of the EPM by Ptn^{+/+} and Ptn^{-/-} mice pretreated with either vehicle or MY10. (e) Figure shows mean ± SEM of time of immobility in the FST by Ptn^{+/+} and Ptn^{-/-} mice (n = 7–8/group) pretreated with either vehicle or MY10.

such as depression and anxiety [34], it would be interesting to see if the behavioural responses of MY10 described here are replicated in presence of ethanol given the potential use of MY10 in AUD.

Interestingly, genetic ablation of Ptn has been previously associated with affective processes [35] and with ethanol reward [6]. The amygdala is a brain area involved in the control of both processes. One of the proteins that has been consistently shown to regulate behavioral responses to ethanol in the amygdala is ALK [36]. ALK is a substrate of RPTPβ/ζ that is

modulated by the endogenous inhibitor of this phosphatase, PTN, and by administration of the exogenous inhibitor, MY10 [22], raising the possibility that the effects of MY10 on ethanol reward and emotional regulation may involve the modulation of ALK in amygdala.

In summary, the data presented here demonstrate for the first time that a regular dose of MY10, known to block ethanol consumption and reward in wild type mice [22], also blocks the rewarding effects of ethanol in the more vulnerable individuals lacking PTN, the

endogenous inhibitor of RPTP β / ζ . In addition, the data allow to speculate that MY10 may induce anxiolytic effects in individuals with reduced or absent PTN functions. However, further studies are needed to confirm the potential of pharmacological inhibition of RPTP β / ζ as a new therapeutic strategy in the treatment of anxiety-related disorders.

Acknowledgements

This work has been supported by grants SAF2014-56671-R from Ministerio de Economía y Competitividad of Spain, PNSD001I2015 from National Plan on Drug abuse, Ministerio de Sanidad of Spain. R F-C was supported by fellowship from Fundación Universitaria San Pablo CEU.

References

- [1] WHO, Global Status Report on Alcohol and Health 2018, World Health Organization, Geneva, 2018.
- [2] E.C. Johnson, et al., Exploring the relationship between polygenic risk for cannabis use, peer cannabis use and the longitudinal course of cannabis involvement, *Addiction* 114 (4) (2019) 687–697.
- [3] R.K. Walters, et al., Transancestral GWAS of alcohol dependence reveals common genetic underpinnings with psychiatric disorders, *Nat. Neurosci.* 21 (12) (2018) 1656–1669.
- [4] T. Flatscher-Bader, P.A. Wilce, Impact of alcohol abuse on protein expression of midkine and excitatory amino acid transporter 1 in the human prefrontal cortex, *Alcohol. Clin. Exp. Res.* 32 (10) (2008) 1849–1858.
- [5] M.K. Mulligan, et al., Toward understanding the genetics of alcohol drinking through transcriptome meta-analysis, *Proc. Natl. Acad. Sci. U. S. A.* 103 (16) (2006) 6368–6373.
- [6] M. Vicente-Rodríguez, et al., Pleiotrophin differentially regulates the rewarding and sedative effects of ethanol, *J. Neurochem.* 131 (5) (2014) 688–695.
- [7] G. Herradon, C. Perez-García, Targeting midkine and pleiotrophin signalling pathways in addiction and neurodegenerative disorders: recent progress and perspectives, *Br. J. Pharmacol.* 171 (4) (2014) 837–848.
- [8] E. Gramage, et al., The neurotrophic factor pleiotrophin modulates amphetamine-seeking behaviour and amphetamine-induced neurotoxic effects: evidence from pleiotrophin knockout mice, *Addict. Biol.* 15 (4) (2010) 403–412.
- [9] E. Gramage, et al., Midkine regulates amphetamine-induced astrocytosis in striatum but has no effects on amphetamine-induced striatal dopaminergic denervation and addictive effects: functional differences between pleiotrophin and midkine, *Neuroscience* 190 (2011) 307–317.
- [10] E. Gramage, et al., Regulation of extinction of cocaine-induced place preference by midkine is related to a differential phosphorylation of peroxiredoxin 6 in dorsal striatum, *Behav. Brain Res.* 253 (2013) 223–231.
- [11] E. Gramage, M. Vicente-Rodríguez, G. Herradon, Pleiotrophin modulates morphine withdrawal but has no effects on morphine-conditioned place preference, *Neurosci. Lett.* 604 (2015) 75–79.
- [12] H. Chen, D. He, A.W. Lasek, Midkine in the mouse ventral tegmental area limits ethanol intake and Ccl2 gene expression, *Genes Brain Behav.* 16 (7) (2017) 699–708.
- [13] M. Vicente-Rodríguez, et al., Genetic inactivation of midkine modulates behavioural responses to ethanol possibly by enhancing GABA(A) receptor sensitivity to GABA(A) acting drugs, *Behav. Brain Res.* 274 (2014) 258–263.
- [14] L.F. Alguacil, G. Herradon, Midkine and pleiotrophin in the treatment of neurodegenerative diseases and drug addiction, *Recent Pat. CNS Drug Discov.* 10 (1) (2015) 28–33.
- [15] G. Herradon, L. Ezquerro, Blocking receptor protein tyrosine phosphatase beta/zeta: a potential therapeutic strategy for Parkinson's disease, *Curr. Med. Chem.* 16 (25) (2009) 3322–3329.
- [16] H. Pariser, et al., Fyn is a downstream target of the pleiotrophin/receptor protein tyrosine phosphatase beta/zeta-signaling pathway: regulation of tyrosine phosphorylation of Fyn by pleiotrophin, *Biochem. Biophys. Res. Commun.* 332 (3) (2005) 664–669.
- [17] P. Perez-Pinera, et al., Anaplastic lymphoma kinase is activated through the pleiotrophin/receptor protein-tyrosine phosphatase beta/zeta signaling pathway: an alternative mechanism of receptor tyrosine kinase activation, *J. Biol. Chem.* 282 (39) (2007) 28683–28690.
- [18] R. Yaka, et al., Fyn kinase and NR2B-containing NMDA receptors regulate acute ethanol sensitivity but not ethanol intake or conditioned reward, *Alcohol. Clin. Exp. Res.* 27 (11) (2003) 1736–1742.
- [19] A.W. Lasek, et al., An evolutionary conserved role for anaplastic lymphoma kinase in behavioral responses to ethanol, *PLoS One* 6 (7) (2011) e22636.
- [20] J.W. Dutton 3rd et al., Anaplastic lymphoma kinase regulates binge-like drinking and dopamine receptor sensitivity in the ventral tegmental area, *Addict. Biol.* 22 (3) (2017) 665–678.
- [21] M. Pastor, et al., Development of inhibitors of receptor protein tyrosine phosphatase beta/zeta (PTPRZ1) as candidates for CNS disorders, *Eur. J. Med. Chem.* 144 (2018) 318–329.
- [22] R. Fernández-Calle, et al., Pharmacological inhibition of Receptor Protein Tyrosine Phosphatase beta/zeta (PTPRZ1) modulates behavioral responses to ethanol, *Neuropharmacology* 137 (2018) 86–95.
- [23] L.E. Amet, et al., Enhanced hippocampal long-term potentiation in mice lacking heparin-binding growth-associated molecule, *Mol. Cell. Neurosci.* 17 (6) (2001) 1014–1024.
- [24] E. Nakamura, et al., Disruption of the midkine gene (Mdk) resulted in altered expression of a calcium binding protein in the hippocampus of infant mice and their abnormal behaviour, *Genes Cells* 3 (12) (1998) 811–822.
- [25] O. Valverde, et al., GPR3 receptor, a novel actor in the emotional-like responses, *PLoS One* 4 (3) (2009) e4704.
- [26] E. Gramage, et al., Periadolescent amphetamine treatment causes transient cognitive disruptions and long-term changes in hippocampal LTP depending on the endogenous expression of pleiotrophin, *Addict. Biol.* 18 (1) (2013) 19–29.
- [27] S. Irwin, Comprehensive observational assessment: Ia. A systematic, quantitative procedure for assessing the behavioral and physiologic state of the mouse, *Psychopharmacologia* 13 (3) (1968) 222–257.
- [28] S.A. Booker, et al., Carbamazepine and oxcarbazepine, but not eslicarbazepine, enhance excitatory synaptic transmission onto hippocampal CA1 pyramidal cells through an antagonist action at adenosine A1 receptors, *Neuropharmacology* 93 (2015) 103–115.
- [29] N. del Olmo, et al., Pleiotrophin inhibits hippocampal long-term potentiation: a role of pleiotrophin in learning and memory, *Growth Factors* 27 (3) (2009) 189–194.
- [30] T.M. Tzschenkte, Measuring reward with the conditioned place preference (CPP) paradigm: update of the last decade, *Addict. Biol.* 12 (3–4) (2007) 227–462.
- [31] S. Mencej-Bedrac, et al., -1227C > T polymorphism in the pleiotrophin gene promoter influences bone mineral density in postmenopausal women, *Mol. Genet. Metab.* 103 (1) (2011) 76–80.
- [32] K. Niisato, et al., Age-dependent enhancement of hippocampal long-term potentiation and impairment of spatial learning through the Rho-associated kinase pathway in protein tyrosine phosphatase receptor type Z-deficient mice, *J. Neurosci.* 25 (5) (2005) 1081–1088.
- [33] H. Tamura, et al., Protein tyrosine phosphatase receptor type Z is involved in hippocampus-dependent memory formation through dephosphorylation at Y1105 on p190 RhoGAP, *Neurosci. Lett.* 399 (1–2) (2006) 33–38.
- [34] B.F. Grant, et al., Epidemiology of DSM-5 alcohol use disorder: results from the national epidemiologic survey on alcohol and related conditions III, *JAMA Psychiatry* 72 (8) (2015) 757–766.
- [35] J.W. Krellman, et al., Behavioral and neuroanatomical abnormalities in pleiotrophin knockout mice, *PLoS One* 9 (7) (2014) e100597.
- [36] D. He, et al., Ethanol activates midkine and anaplastic lymphoma kinase signaling in neuroblastoma cells and in the brain, *J. Neurochem.* 135 (3) (2015) 508–521.

DISCUSIÓN

DISCUSIÓN

1. Implicación de la PTN y la MK en la neuroinflamación.

En respuesta a una agresión en el SNC, los astrocitos y la microglía sufren una serie de cambios morfológicos y funcionales que alteran sus mecanismos de regulación de la homeostasis cerebral y contribuyen a la neuroinflamación. Uno de los modelos más ampliamente utilizados para estudiar neuroinflamación es el modelo de endotoxemia. Se conoce que la administración de LPS produce un incremento en la expresión de diversos genes en los astrocitos como *Lcn2* (del inglés *Lipocalin 2*), citoquina mayoritariamente secretada por los astrocitos para promover la neuroinflamación en respuesta a la inflamación sistémica (Kang y col., 2018; Suk, 2016; Zamanian y col., 2012), y una elevada expresión del marcador GFAP y de citoquinas proinflamatorias como IL-1 α , TNF- α o C1q (Liddelow y col., 2017; O'Callaghan y col., 2014).

Estudios previos de nuestro grupo han demostrado que la sobreexpresión de PTN provoca una astrocitosis estriatal muy marcada (~ 300%) en respuesta a la exposición a anfetamina (Vicente-Rodriguez y col., 2016b). Curiosamente, esta astrocitosis inducida por anfetamina también se encuentra incrementada en ratones *Ptn*^{-/-} y *Mk*^{-/-}, aunque de forma muy moderada (~ 20-30%) (Gramage y col., 2010a; Vicente-Rodriguez y col., 2016a). Este fenómeno en los animales carentes de PTN o de MK quizás pueda deberse a la activación de mecanismos compensatorios (Gramage y col., 2010a), ya que, por ejemplo, se ha demostrado que la MK regula la expresión de *Ptn* en diferentes órganos del ratón (Herradon y col., 2005). Estos resultados indican que la PTN y la MK regulan la respuesta astrocítica estriatal frente a la anfetamina y que altos niveles cerebrales de PTN potencian la respuesta neuroinflamatoria ante esta droga de abuso. En esta tesis, quisimos avanzar en el conocimiento de la regulación de la astrocitosis por PTN en un modelo diferente de neuroinflamación, inducida por endotoxemia (LPS). Para ello, se optó por el empleo del marcador GFAP para la detección de los astrocitos reactivos debido a su efectividad como marcador inmunohistoquímico astrocitario, ya que es el componente mayoritario de los filamentos del citoesqueleto de los astrocitos (Eng, 1985). Algunos autores remarcan las limitaciones del uso de GFAP como marcador astrocítico (Matias y col., 2019). Por ejemplo, existen ocho posibles isoformas de GFAP y el número de células GFAP positivas y su expresión basal puede fluctuar entre diferentes regiones cerebrales (Kimmelberg, 2004; Rodriguez y col., 2014). Otras limitaciones del uso de GFAP se encuentran resumidas en la revisión de Matias y colaboradores (2019). A pesar de ello, el uso de GFAP como marcador continúa siendo uno de los más utilizados y fiables para la observación de la respuesta astrocítica en situaciones de daño del SNC (Zhang y col., 2017).

Como cabía esperar, el análisis inmunohistoquímico de GFAP mostró que LPS induce la activación astrocítica tanto en la CPF como en el cuerpo estriado de animales *Wt*. Sin embargo, los datos recogidos demuestran que la sobreexpresión de PTN en la CPF bloquea la respuesta astrocítica inducida por LPS. Este resultado denota la importancia de la naturaleza del estímulo inflamatorio para la caracterización de la respuesta neuroinflamatoria. Al estudiar el cuerpo

estriado, se observó una tendencia similar, pero menos intensa. La respuesta astrocítica más moderada en el cuerpo estriado podría deberse a que, en los animales PTN-Tg, la sobreexpresión de PTN en esta área cerebral es sólo un 20% superior a los niveles basales, mientras que en la CPF es 3 veces superior a la expresión basal (Vicente-Rodriguez y col., 2015). Curiosamente, al igual que ocurre en el ratón PTN-Tg, la astrocitosis inducida por LPS en la CPF y el cuerpo estriado es inexistente en ratones *Ptn^{-/-}* y *Mk^{-/-}*. De nuevo, tenemos que hacer notar que al ser estos últimos ratones *knock-out* constitutivos, es posible que se hayan producido mecanismos adaptativos durante el desarrollo que puedan enmascarar o modificar los efectos de la ausencia de estas citoquinas en este modelo de endotoxemia. Sin embargo, el ratón PTN-Tg, al aportar especificidad de tejido en el que se sobreexpresa PTN, puede modelizar mejor las situaciones patológicas que conllevan neuroinflamación. Por ejemplo, la PTN se encuentra sobreexpresada en el circuito nigroestriatal de pacientes con enfermedad de Parkinson (Marchionini y col., 2007). En conjunto, los datos demuestran que las citoquinas PTN y MK regulan la respuesta astrocitaria de forma diferente dependiendo del estímulo nocivo para el SNC y sugieren que la sobreexpresión de PTN característica de patologías centrales que cursan con neuroinflamación contribuye regulando la respuesta astrocitaria.

Por otro lado, el análisis morfológico y cuantitativo de la microglía que hemos realizado, ha sido ampliamente utilizado con anterioridad para definir el estado de activación de la microglía y si los cambios morfológicos que presentan las células microgliales pueden relacionarse con el desarrollo de neurodegeneración (Davis y col., 2017; Streit y col., 2014; Zanier y col., 2015). Usando como marcador de la microglía Iba-1 (molécula adaptadora de unión al calcio 1, del inglés *Ionized calcium binding adaptor molecule 1*), observamos en ratones PTN-Tg que la sobreexpresión de PTN da lugar a una potenciación de las alteraciones morfológicas de la microglía en la CPF tras el tratamiento con LPS. Destaca un fenotipo microglial hipertrófico, caracterizado por un aumento del tamaño del soma, del área y del perímetro celular, terminaciones celulares retraídas y un incremento de la circularidad celular característicos de la activación de la microglía. La sobreexpresión de PTN en el cuerpo estriado también predispone a un fenotipo activado de la microglía, siendo este efecto más modesto que en la CPF (Fernandez-Calle y col., 2017), lo cual podría estar relacionado con la limitada sobreexpresión de PTN en esta área cerebral comparada con la CPF de ratones PTN-Tg (Vicente-Rodriguez y col., 2014a). En comparación, observamos que LPS induce menos cambios en los parámetros morfológicos de la microglía en ratones *Ptn^{-/-}* y *Mk^{-/-}* comparado con ratones Wt. Por ejemplo, el aumento en el área de células microgliales inducido por LPS tiende a ser mayor en los ratones *knock-out* mientras que la circularidad tiende a ser menor, en el caso de la CPF. Estas tendencias podrían apuntar a un moderado incremento de la activación microglial inducida por LPS en ratones *Ptn^{-/-}* y *Mk^{-/-}*; sin embargo, la magnitud de estas diferencias en comparación con los animales Wt y la ausencia de diferencias en la mayoría de los parámetros, sugieren que la ausencia de niveles endógenos de cada una de estas citoquinas no tiene efectos demasiado relevantes en la activación microglial inducida por LPS. A los posibles mecanismos

compensatorios en ratones $Ptn^{-/-}$ y $Mk^{-/-}$ ya mencionados, deberíamos añadir que los niveles endógenos de PTN y MK en el cerebro adulto sano son bajos (Gonzalez-Castillo y col., 2014; Herradon y col., 2014). Teniendo en cuenta que la expresión de PTN y MK en el SNC sólo incrementa de forma muy significativa en patologías centrales o situaciones de daño del SNC (Ezquerro y col., 2008; Ma y col., 2014; Marchionini y col., 2007; Martin y col., 2011), parecen más relevantes de nuevo los datos obtenidos en ratones PTN-Tg tratados con LPS. En conjunto, los resultados sugieren que PTN y MK son citoquinas que regulan la activación microglial y demuestran que la sobreexpresión de PTN en el cerebro potencia la activación de la microglía tras el tratamiento con LPS.

Aunque se conoce que la activación de la microglía y la astrocitosis en respuesta al daño del SNC son procesos fundamentales en el desarrollo de la neuroinflamación, es importante la determinación de citoquinas en el cerebro para calibrar la importancia de esta. Por este motivo resultaba esencial estudiar si la sobreexpresión de PTN en el cerebro, además de potenciar las modificaciones morfológicas microgliales y afectar a la respuesta astrocítica inducidas por LPS, también influye sobre el contenido de citoquinas. Nuestros resultados demuestran que la sobreexpresión de PTN promueve una potenciación del incremento de los niveles de TNF- α , IL-6 y MCP-1 (del inglés *monocyte chemoattractant protein 1*) en la CPF (Fernandez-Calle y col., 2017) de ratones PTN-Tg tratados con LPS. Se ha postulado que la activación de los astrocitos a un fenotipo inflamatorio está mediada a través de la liberación de citoquinas proinflamatorias como TNF- α o IL-1 β por parte de la microglía, y que la microglía activada por estimulación de TLR4 parece necesaria para inducir este tipo de fenotipo astrocitario (Liddelow y col., 2017). Por tanto, resulta interesante el hecho de que la sobreexpresión de PTN por un lado incrementa los niveles de TNF- α en la CPF, mientras que por otro reduce (o prácticamente anula) la reactividad astrocítica frente a la administración sistémica de LPS (Fernandez-Calle y col., 2017). Esta posible contradicción en los efectos de la sobreexpresión cerebral de PTN en este contexto, urge a profundizar en los efectos de esta citoquina en la comunicación entre astrocitos y microglía.

Resulta importante señalar que no se observaron diferencias en la expresión de las citoquinas antiinflamatorias IL-4 e IL-10 en la CPF de animales Wt y PTN-Tg 16 horas tras el tratamiento con LPS. Este hecho, sin embargo, no debería llevarnos a descartar por completo la posibilidad de que la PTN pueda regular la producción de citoquinas antiinflamatorias por parte de la microglía. En estudios recientes sobre la función microglial en dolor crónico, por ejemplo, se ha observado que el pico de producción de IL-4 e IL-10 tiene lugar 24h tras la administración de LPS (Ha y col., 2019).

Por otra parte, durante el proceso inflamatorio, además de fomentarse la producción de citoquinas proinflamatorias, también se incrementa la liberación de radicales libres, especies reactivas de oxígeno y derivados del nitrógeno, lo que se ha demostrado que contribuye al daño neuronal y la neurotoxicidad *in vitro* (Chitnis y col., 2017). Con el fin de determinar si la PTN regula también estos procesos, estudiamos en un modelo *in vitro* de microglía de ratón los efectos de la PTN sobre la producción de nitritos inducida por LPS mediante el método de Griess

(Giustarini y col., 2008). Los datos demuestran que la PTN potencia la liberación de nitritos por parte de la microglía activada con LPS (Fernandez-Calle y col., 2017).

En conjunto, nuestros datos demuestran que la sobreexpresión de PTN en el cerebro potencia de forma muy significativa la activación microglial y la neuroinflamación producida por la administración aguda de LPS. Estos resultados concuerdan con estudios muy recientes en otros modelos de daño en el SNC, por ejemplo, de esclerosis múltiple, en los que la PTN incrementa la transformación de la microglía a un fenotipo activado, la liberación de citoquinas proinflamatorias y la inflamación (Miao y col., 2019).

Para conocer el mecanismo a través del cual la PTN ejerce su efecto proinflamatorio, nos centramos en el principal receptor de PTN y MK, RPTP β/ζ (Meng y col., 2000), sus sustratos y su posible relación con la vía p38-MAPK. Aunque como se indicó en el capítulo introductorio de esta memoria la PTN tiene otros receptores, en este trabajo nos hemos centrado en la vía de señalización a través de RPTP β/ζ , ya que este receptor se encuentra expresado en el SNC, donde se sabe que media muchos de los efectos centrales de la PTN (Herradon y col., 2019). La vía p38-MAPK contribuye a la neuroinflamación mediada por células gliales, incluidos astrocitos y microglía, y puede activarse en respuesta a distintos tipos de estrés oxidativo, osmótico y citoquinas proinflamatorias (Kim y col., 2015). Del mismo modo, se ha observado que la quinasa Fyn, sustrato de RPTP β/ζ (Pariser y col., 2005a), contribuye a la activación de esta vía de señalización (Panicker y col., 2015). Estudios previos señalan la participación de PTN en la vía de señalización de las MAPK, en la que está implicada también ERK1/2, y destaca su importancia como reguladores en la señalización proinflamatoria (Miao y col., 2012; Panicker y col., 2015). En base a todo lo anterior, y al hecho de que ya conocíamos que la PTN potencia la producción de nitritos inducida por LPS en células microgliales BV2 (Fernandez-Calle y col., 2017), decidimos estudiar la posible modulación de los niveles de fosforilación de las quinasas Fyn y ERK1/2 en células BV2 tratadas con LPS y/o PTN. Se conoce que la fosforilación en el residuo de tirosina (Tyr ó Y) 416, entre otros, conlleva la activación de Fyn (Kouadir y col., 2012; Larson y col., 2012; Um y col., 2012; Wake y col., 2011). Sin embargo, el tratamiento de las células BV2 con LPS no produjo cambios apreciables en la fosforilación de Fyn (Fernandez-Calle y col., 2018a), independientemente de la suplementación o no con PTN. Sin embargo, estos resultados sólo demuestran que la regulación de los efectos de LPS en células BV2 por parte de la PTN, no parece implicar la modulación de la activación de Fyn a través de la regulación de sus niveles de fosforilación en Tyr416. En este sentido, es importante señalar que hay otros residuos Tyr implicados en la activación de Fyn y que existen otras fosfatasa que controlan la actividad de las SFKs (del inglés *Src family kinases*), familia a la que pertenece Fyn; por ejemplo, se sabe que PTP-1B, SHP1 y 2 (del inglés *Src homology 2 domain-containing tyrosine phosphatases*), CD45 (cúmulo de diferenciación 45, del inglés *cluster of differentiation 45*), RPTP- α , RPTP- ϵ y RPTP- λ (Roskoski, 2005) regulan los niveles de fosforilación de Tyr527 en Fyn. Por otro lado, el aumento de la fosforilación de ERK1/2 inducido por LPS no se vio alterado por el tratamiento con

PTN, por lo que podemos deducir que ERK1/2 no parece estar implicado en el efecto de la PTN sobre la activación microglial inducida por LPS.

También contemplamos la posibilidad de que tuviera lugar una comunicación efectiva entre la vía de TLR4, probablemente la vía de señalización involucrada en neuroinflamación más estudiada, y la vía de PTN/RPTP β/ζ . Con el fin de estudiar la posible regulación de la cascada de señalización de TLR4 por parte de la PTN y su trascendencia en procesos inflamatorios, se llevó a cabo el tratamiento de ratones con TAK-242 antes de la administración sistémica de LPS (Fernandez-Calle y col., 2017). El inhibidor selectivo de TLR4, TAK-242, se une al dominio intracelular de TLR4 provocando interferencias de tipo proteína-proteína entre TLR4 y sus moléculas adaptadoras, tanto de la vía independiente como de la dependiente de MyD88 (Matsunaga y col., 2011). Estudios *in vitro* e *in vivo* han corroborado que TAK-242 bloquea la activación de TLR4 en diferentes modelos (Matsunaga y col., 2011; Nduhirabandi y col., 2016), incluidos modelos animales de endotoxemia (Li y col., 2006). A pesar de estos antecedentes, nuestros resultados muestran que el pretratamiento con TAK-242 en animales Wt y PTN-Tg tratados con LPS no tiene efectos apreciables sobre los parámetros morfológicos microgliales. Este resultado sugiere que una única dosis de TAK-242 de 3 mg/kg no es suficiente para modular las alteraciones morfológicas inducidas por LPS en la microglia, independientemente de los niveles endógenos de expresión de PTN. En este sentido, cabe señalar que existen estudios en modelos animales de esclerosis lateral amiotrófica (ELA) en los que un patrón distinto de administración de TAK-242 reduce la activación microglial (Fellner y col., 2017). Sin embargo, como cabía esperar, el tratamiento con TAK-242 causó una disminución significativa de la producción de citoquinas proinflamatorias inducida por LPS en la CPF y de forma independiente del genotipo. Teniendo en cuenta que la activación de la vía de TLR4 por LPS está muy bien documentada, estos resultados indican que TAK-242, a pesar de no ser capaz de prevenir la transformación morfológica microglial inducida por LPS, bloquea la producción de citoquinas proinflamatorias a través de su capacidad para inhibir la activación de TLR4 inducida por LPS. Más allá, nuestros resultados sugieren que la medida de activación microglial mediante parámetros morfológicos debe ser acompañada de la determinación de distintos mediadores proinflamatorios para estudiar en detalle los procesos neuroinflamatorios.

Por otro lado, no hay que obviar el hecho de que el LPS puede participar en otras vías de señalización inflamatorias además de la de vía TLR4-NF κ B. Se conoce, por ejemplo, que el LPS también puede llevar a cabo la activación no canónica de inflamasomas, que resulta independiente de TLR4, en la cual la Caspasa-11 (en humanos corresponde a las caspasas 4 y 5 (Shi y col., 2014)) detecta el LPS intracelular y media directamente la muerte celular y la producción de IL- α (Kayagaki y col., 2013). El LPS también puede interactuar con el receptor RAGE (del inglés *receptor for advanced glycation endproducts*) presente principalmente en neuronas dopaminérgicas y que constituye un receptor clave en el eje inflamatorio (Gasparotto y col., 2019). Sin embargo, teniendo en cuenta los datos presentados en esta tesis sobre la capacidad de PTN de modular los efectos neuroinflamatorios de LPS, nuestros resultados

sugieren que la PTN no potenciaría la neuroinflamación inducida por LPS principalmente a través de estas vías, sino que lo haría en gran medida a través de TLR4 ya que el antagonista de este receptor, TAK-242, bloquea la producción de distintas citoquinas proinflamatorias de forma independiente del genotipo.

2. Modulación farmacológica de RPTPβ/ζ como estrategia terapéutica para regular el consumo de alcohol y los efectos conductuales de esta droga.

Los resultados previamente discutidos destacan la implicación de la PTN y la MK en la respuesta neuroinmune que tiene lugar durante un proceso inflamatorio en el SNC. El alcoholismo es una enfermedad central que conlleva el consumo excesivo de alcohol y que provoca una fuerte activación de la respuesta neuroinmune y el desarrollo de neuroinflamación (Coleman y col., 2018a). En este sentido, se han observado marcadores astrocíticos y microgliales sobreexpresados en el cerebro *postmortem* de pacientes alcohólicos, junto con otros marcadores neuroinmunes, incluyendo TLR4 (He y col., 2008; Rubio-Araiz y col., 2017). También se conoce que la interacción del alcohol con TLR4 promueve que los astrocitos liberen vesículas extracelulares que contienen mediadores inflamatorios que amplifican la neuroinflamación (Ibanez y col., 2019). Es muy importante señalar que la exacerbación de la respuesta neuroinmune provocada por el alcohol es a su vez un mecanismo patogénico implicado en la adicción a esta sustancia y al aumento de su consumo (Coleman y col., 2018a; Guerri y col., 2019). Por otro lado, se sabe que el alcohol provoca una elevación de los niveles de PTN y MK en la CPF de pacientes alcohólicos y en ratones (Flatscher-Bader y col., 2008; Vicente-Rodriguez y col., 2014a). Dado que ha quedado demostrado en los primeros artículos de esta tesis, junto a otros del grupo, que estas citoquinas regulan la respuesta glial y la neuroinflamación producida por distintos estímulos como el LPS o la administración de anfetamina, nos pareció razonable hipotetizar que la modulación farmacológica de la vía de PTN/MK podría regular los efectos comportamentales producidos por el alcohol.

Nuestra hipótesis se ve además apoyada por evidencias previas de nuestro grupo y de otros que establecen una relación entre los niveles endógenos de PTN y MK y los efectos comportamentales del alcohol. La CPF es un área cerebral implicada en la pérdida del control sobre el consumo de alcohol y el aumento de posibilidades de recaída (Abernathy y col., 2010). Como ya hemos comentado, las proteínas PTN y MK son citoquinas que se sobreexpresan en la corteza cerebral de pacientes alcohólicos y en la CPF de ratones tras la administración de alcohol (Herradon y col., 2014), lo que sugiere la posibilidad de que estas proteínas regulen los efectos del alcohol. En esta línea, nuestro grupo demostró que los efectos reforzadores del alcohol aumentan significativamente en los ratones $Mk^{-/-}$ y $Ptn^{-/-}$, mientras que la sobreexpresión transgénica de PTN en el cerebro de ratón bloquea los efectos reforzadores de esta droga (Vicente-Rodriguez y col., 2014a; Vicente-Rodriguez y col., 2014b). Además, el grupo de la Dra. Lasek en la Universidad de Illinois ha demostrado recientemente que los ratones $Mk^{-/-}$ consumen más alcohol utilizando el modelo de *drinking in the dark* (DID) (Chen y col., 2017).

Según lo descrito anteriormente, PTN y MK son ligandos inhibidores endógenos del receptor RPTP β/ζ . Ambas proteínas, PTN y MK, inhiben la actividad fosfatasa de este receptor provocando un aumento en los niveles de fosforilación de sus sustratos, algunos de los cuales juegan un papel importante en el consumo de alcohol como ha demostrado el grupo de la Dra. Dorit Ron en el caso de la quinasa Fyn (Ron y col., 2018) y el grupo de la Dra. Amy Lasek en el caso de ALK (Dutton y col., 2017). Además, se conoce que algunos polimorfismos de un solo nucleótido (SNPs) en este receptor se encuentran asociados a una mayor susceptibilidad a patologías mentales como la esquizofrenia (Buxbaum y col., 2008). Es importante señalar que RPTP β/ζ se encuentra principalmente expresado en el SNC en áreas importantes en el circuito de recompensa y el consumo de alcohol, como la CPF o la amígdala (Cressant y col., 2017). Todo ello nos llevó a pensar que compuestos inhibidores de RPTP β/ζ ejercerían las mismas acciones que PTN y MK en el sistema nervioso, incluidos los efectos limitadores del consumo de alcohol en modelos animales. Para probar esta hipótesis, se diseñaron inhibidores con un perfil farmacocinético y farmacodinámico óptimo para actuar en cerebro tras su administración sistémica (Pastor y col., 2018). El 4-trifluorometilsulfonilbenzil 4-trifluorometilsulfonilfenil éter era el único inhibidor de RPTP β/ζ descrito con cierto grado de selectividad por esta fosfatasa (Huang y col., 2003). Por ello, se seleccionó este compuesto para llevar a cabo su síntesis, y la de análogos estructurales diseñados utilizando técnicas computacionales. Esto nos llevó a identificar el compuesto MY10 como líder de los inhibidores de RPTP β/ζ estudiados ($IC_{50} \sim 0.1\mu M$). Además, estudios farmacocinéticos llevados a cabo en colaboración con el Dr. Antonio Pineda (Centro de Investigación Príncipe Felipe, Hospital Universitario y Politécnico La Fe, Valencia), en idénticas condiciones a las utilizadas en la presente tesis (1h tras la administración oral del compuesto (60 mg/kg)), demostraron que el compuesto MY10 cruza la BHE y presenta un ratio cerebro:plasma 3:1 (Pastor y col., 2018). El segundo compuesto en interés fue MY33-3, que presentó una potencia similar a MY10, aunque menor selectividad, ya que también era capaz de inhibir la actividad fosfatasa de PTP-1B ($IC_{50} \sim 0.7\mu M$) (Pastor y col., 2018).

Nuestros resultados demuestran que el compuesto MY10 reduce de manera significativa el consumo de alcohol en ratones, mientras que el MY33-3 mostró la misma tendencia, pero de forma más modesta. Estos efectos de MY10 sobre el consumo de alcohol parecen ser específicos de esta droga puesto que el mismo experimento realizado con un reforzador natural, la sacarosa, no modificó el consumo o la preferencia de los animales por esta sustancia. No se puede obviar el hecho de que los ratones, en general, bebieron menos cantidad de alcohol en nuestro protocolo DID comparado con estudios previos (Blednov y col., 2017; Dutton y col., 2017) y de forma independiente del tratamiento. Esto puede achacarse a diferencias experimentales relevantes. Por ejemplo, en nuestro ensayo, los animales pueden escoger entre una botella con alcohol y otra con agua en lugar de tener acceso a una única botella con alcohol. También puede tener cierta influencia el pretratamiento con MY10 o vehículo mediante administración intragástrica, al suponer cierto estrés para los animales.

Para evaluar la posibilidad de que los efectos de MY10 sobre el consumo estén mediados por la modulación de los efectos reforzadores del alcohol, llevamos a cabo un protocolo de CPP con el compuesto MY10, puesto que fue el inhibidor de RPTP β/ζ con resultados más prometedores en el test DID (Fernandez-Calle y col., 2018b). Los datos obtenidos demuestran que MY10 es capaz de bloquear el CPP generado por el alcohol, lo que sugiere que la inhibición de RPTP β/ζ no sólo limita el consumo de alcohol, sino que también reduce los efectos reforzadores de esta droga. En este sentido, es interesante recordar que resultados previos de nuestro grupo demostraron que la sobreexpresión cerebral de PTN bloquea los efectos reforzadores del alcohol en ratones, por lo que los datos obtenidos en esta tesis confirman que la inhibición exógena del receptor que produce MY10 replica los efectos anteriores descritos en modelos transgénicos de animales con sobreexpresión del inhibidor endógeno PTN (Fernandez-Calle y col., 2018b; Vicente-Rodriguez y col., 2014a). Es importante señalar que estos efectos de MY10 sobre el condicionamiento inducido por el alcohol no deberían estar enmascarados por efectos reforzadores o aversivos *per se* de MY10, ya que en estudios de condicionamiento llevados a cabo únicamente con MY10 demostraron la carencia de efectos de este compuesto en este tipo de ensayos. Sin embargo, sí que debemos tener en cuenta que el CPP depende del aprendizaje de la asociación del alcohol a un determinado contexto y que el compuesto MY10 podría tener algún efecto sobre dicho proceso de aprendizaje, lo que podría contribuir en la modulación de los efectos reforzadores del alcohol. De hecho, se ha observado que los ratones *knock-out* de RPTP β/ζ presentan deficiencias en el aprendizaje dependiente de hipocampo, ya que RPTP β/ζ participa en la memoria modulando la actividad de la GTPasa Rho a través de la desfosforilación del residuo Tyr1105 de esta proteína (Niisato y col., 2005; Tamura y col., 2006). En este sentido, cabe destacar que como parte de esta tesis llevamos a cabo también una caracterización de los efectos comportamentales de MY10 en ratón (Fernandez-Calle y col., 2019), y en el ensayo de memoria y aprendizaje realizado, el test del laberinto en Y, MY10 no mostró efectos significativos. Por último, quisimos ir un paso más allá teniendo en cuenta los resultados del MY10 sobre el consumo y los efectos reforzadores del alcohol, y comprobar si este compuesto es capaz de rescatar del condicionamiento preferencial al sitio inducido por alcohol a los ratones Ptn^{-/-}, carentes del inhibidor endógeno de RPTP β/ζ , que resultan más vulnerables a los efectos reforzadores del alcohol (Vicente-Rodriguez y col., 2014a). Efectivamente, nuestros resultados demuestran que el compuesto MY10 también es capaz de bloquear los efectos reforzadores del alcohol en ratones Ptn^{-/-} de forma similar a como lo hizo en ratones Wt.

La inhibición de RPTP β/ζ con MY10 produjo una marcada potenciación del efecto sedante/hipnótico del alcohol en los ratones Wt durante el ensayo de LORR (del inglés *loss of righting reflex*). En el laberinto elevado en cruz, se apreció un potencial efecto ansiolítico de MY10 únicamente en los animales Ptn^{-/-} (Fernandez-Calle y col., 2019). Estos hechos podrían relacionarse con la modulación de la actividad de dos sustratos de RPTP β/ζ , ALK y TrkA, por parte de MY10 ya que los animales Ptn^{-/-}, al no tener PTN endógena, podrían ser más sensibles

a la inhibición de RPTP β/ζ con MY10. En este sentido, es importante señalar que los ratones *knock-out* de ALK sufren una mayor sedación inducida por el alcohol (Lasek y col., 2011) y que TrkA, aparte de en el sistema límbico, se expresa en poblaciones neuronales del núcleo interpeduncular (Holtzman y col., 1995), lo que sugiere un posible papel de TrkA en la modulación de los efectos sedantes del alcohol por MY10. Además, ALK podría tener un papel en los efectos de MY10 sobre el consumo de alcohol y las propiedades reforzadoras de esta droga ya que se ha observado que ciertos polimorfismos en ALK están asociados con la dependencia del alcohol (Kapoor y col., 2013) y que ALK regula las respuestas comportamentales al alcohol tanto en la amígdala (Schweitzer y col., 2016) como en el ATV (Dutton y col., 2017). Por todas estas razones, nos pareció interesante acometer ciertos estudios *in vitro* para observar los efectos de MY10 sobre las cascadas de señalización del alcohol, centrándonos en TrkA y ALK.

Se había demostrado previamente que el alcohol induce la fosforilación del residuo Tyr1278 de ALK (Guan y col., 2017; He y col., 2015). Por otra lado, se conoce que la exposición paterna al alcohol puede provocar la disrupción del eje NGF-TrkA en la descendencia (Ceccanti y col., 2016), lo cual apunta a TrkA, otro sustrato de RPTP β/ζ , como potencial mediador de los efectos del alcohol. Usando el modelo de células de neuroblastoma (SH-SY5Y) tratadas con etanol, decidimos estudiar la posible modulación de la fosforilación de TrkA y ALK inducida por alcohol a través de la inhibición de RPTP β/ζ con MY10 y MY33-3. Los resultados confirmaron que el alcohol aumenta la fosforilación de Tyr1278 en ALK y dejaron patente, por primera vez, que el etanol también induce la fosforilación de Tyr490 en TrkA (Fernandez-Calle y col., 2018b). Como cabía esperar, el tratamiento de las células SH-SY5Y únicamente con MY10 o MY33-3 provoca un aumento de los niveles de fosforilación de ALK y de TrkA. Sin embargo, la preincubación con los inhibidores MY10 y MY33-3 seguida de una exposición a alcohol bloquea la fosforilación de ALK y TrkA inducida por el alcohol (Fernandez-Calle y col., 2018b). Este efecto podría explicarse teniendo en cuenta que las células SH-SY5Y tienen una membrana celular muy enriquecida en ALK, y que esta proteína tiende a internalizarse para su degradación por el proteosoma o lisosoma cuando está excesivamente activada (Mazot y col., 2012). Por tanto, resulta posible que la activación de ALK a través del incremento de la fosforilación de su residuo Tyr1278 por MY10 o MY33-3, unida a un efecto similar inducido por el alcohol, provoque una excesiva activación de ALK y su consiguiente internalización. Aunque se deberían llevar a cabo más estudios para terminar de dilucidar el mecanismo completo de la implicación de RPTP β/ζ en las respuestas comportamentales al alcohol, estos resultados nos llevan a hipotetizar que el tratamiento con MY10 puede causar una disminución del consumo de alcohol en animales por la capacidad de MY10 de provocar la disminución de los niveles de ALK mediante su internalización. Esta hipótesis se ve fundamentada por el hecho de que tanto la disminución de la expresión de ALK en el ATV como el tratamiento con inhibidores de ALK provocan un descenso significativo del consumo de alcohol en ratones (Dutton y col., 2017).

Los resultados obtenidos con MY10 sobre los efectos comportamentales del alcohol sugieren que la inhibición farmacológica de RPTP β/ζ en general, y el uso de este compuesto en

particular, puede ser una nueva estrategia terapéutica en los desórdenes por consumo excesivo de alcohol. Es importante destacar como limitación de nuestros estudios la falta de más ensayos de selectividad de este compuesto. Como hemos comentado, se ha demostrado que MY10 no tiene efecto inhibitorio sobre la actividad de otra fosfatasa, PTP-1B. Sin embargo, investigaciones recientes de nuestro grupo han mostrado una inhibición residual de RPTPy por parte de MY10, por lo que no se puede desechar la posibilidad de que acciones de MY10 sobre otras fosfatasas, o incluso otras dianas, pueda contribuir a los efectos farmacológicos de este compuesto. En este sentido, es interesante señalar que no existen evidencias que apunten a un papel de otros receptores de membrana con actividad fosfatasa en la modulación del consumo de alcohol; sin embargo, recientemente, el grupo de Uhl y colaboradores han observado que la inhibición de otro subtipo de esta familia de fosfatasas, RPTPD, causa una disminución de los efectos reforzadores de la cocaína y disminuye su autoadministración en modelos animales (Uhl y col., 2019). Por tanto, se necesitan estudios adicionales para descartar posibles efectos de MY10 sobre otras fosfatasas, especialmente sobre RPTPD por su relevancia en el campo de las adicciones.

Dado el potencial de MY10 discutido en este capítulo, como ya hemos ido apuntando cuando resultaba relevante, decidimos hacer una caracterización de otros posibles efectos conductuales de MY10 en ratones Wt y Ptn^{-/-}. En general, MY10 presentó pocos efectos relevantes en los ratones Wt. Por ejemplo, los resultados obtenidos en el laberinto del campo abierto señalan que MY10 disminuye la distancia recorrida por los animales Wt, lo que podría influenciar las acciones de MY10 sobre los efectos conductuales del alcohol. Sin embargo, en el ensayo del Rotarod para observar el efecto del MY10 sobre la recuperación de la ataxia inducida por alcohol, no se observaron diferencias entre los animales tratados con MY10 y los tratados con su vehículo. Respecto a los efectos de MY10 en ratones Ptn^{-/-}, aparte del ya discutido bloqueo de los efectos reforzadores del alcohol, tan sólo cabe destacar cierta tendencia a incrementar el número de visitas al brazo abierto en el laberinto elevado en cruz, así como el tiempo de estancia en dicho brazo. Estos datos sugieren que MY10 podría causar efectos ansiolíticos, aunque únicamente en situaciones de carencia de PTN endógena, ya que estos efectos no se observan en animales Wt. No obstante, estos resultados, a nuestro juicio, son demasiado preliminares y únicamente apoyan la necesidad de hacer más ensayos comportamentales para evaluar en profundidad un posible efecto ansiolítico de MY10.

3. Modulación del eje de señalización de PTN//MK/RPTPβ/ζ como estrategia terapéutica. Perspectivas futuras.

Los artículos y resultados derivados de esta tesis, así como otros trabajos del grupo, demuestran que se pueden reproducir los efectos de la PTN (y/o MK) con inhibidores selectivos del receptor RPTPβ/ζ obtenidos a través del programa de diseño racional de fármacos discutido en esta memoria (Pastor y col., 2018). Aún más importante, el compuesto líder inhibitor de

RPTP β / ζ descubierto a través de dicho programa, MY10, disminuye significativamente el consumo de alcohol en ratones en un modelo de consumo por atracción y bloquea el condicionamiento preferencial al sitio inducido por el alcohol, probablemente a través de la capacidad de MY10 de activar ALK y, a través de este mecanismo, provocar la disminución de su expresión por internalización (Fernandez-Calle y col., 2019; Fernandez-Calle y col., 2018b). Estos resultados demuestran por primera vez el papel fundamental de RPTP β / ζ en la modulación de los efectos comportamentales del alcohol.

Por otra parte, se ha demostrado que el eje PTN/MK/RPTP β / ζ regula la neuroinflamación desencadenada por distintos estímulos como la administración de anfetamina (Vicente-Rodriguez y col., 2016b) o LPS (Fernandez-Calle y col., 2017). Tras haber demostrado ya que este eje regula el consumo de alcohol y sus efectos reforzadores, se podría plantear que esta vía de señalización también regula la respuesta neuroinmune desencadenada por el alcohol, la neuroinflamación y el daño neuronal, todos ellos efectos conocidos del alcohol. Resultaría interesante estudiar esta hipótesis ya que, de confirmarse, la inhibición farmacológica de RPTP β / ζ podría ser una nueva estrategia terapéutica no sólo para su uso potencial en la reducción del consumo de alcohol, sino también para la modulación de la neuroinflamación y la reducción del daño neuronal observados tras el consumo crónico y excesivo de alcohol.

En esta tesis, hemos hablado fundamentalmente de la potenciación farmacológica de la vía de PTN y MK a través del uso de inhibidores de RPTP β / ζ . Las evidencias demuestran que esta estrategia es efectiva en la prevención del consumo excesivo de alcohol y la reducción de las propiedades reforzadoras de esta droga. Los datos provenientes de los modelos animales genéticos de carencia o sobreexpresión de MK y PTN sugieren que esta estrategia farmacológica también podría causar efectos neuroprotectores ante el daño producido por las drogas de abuso, por ejemplo. Sin embargo, en el campo de la neuroinflamación, nuestros datos demuestran que el eje PTN/MK/RPTP β / ζ regula la neuroinflamación, pero el signo de esta modulación parece depender de la naturaleza del estímulo y, probablemente, de la duración de este ya que en esta memoria sólo hemos analizado el efecto neuroinflamatorio de la administración aguda de LPS. Además, aunque no sea el objeto de esta tesis, también se ha observado que la PTN y la MK modulan la inflamación mediante su capacidad para regular la respuesta inmune en el marco de las patologías con componente inflamatorio periférico como la artritis o las asociadas a resistencia a insulina, como la obesidad o el envejecimiento (Sevillano y col., 2019). Para hacer el contexto aún más complejo, estas patologías se asocian a estados de neuroinflamación crónica de baja intensidad, lo cual ha llevado a sugerir que este fenómeno puede estar detrás de la mayor prevalencia de patologías centrales, como las neurodegenerativas, en pacientes obesos, por ejemplo (Herradon y col., 2019). Tomando todas estas evidencias en conjunto, podríamos concluir que todavía no conocemos lo suficiente para afirmar cuando convendría potenciar la vía PTN/MK/RPTP β / ζ , o inhibirla, para lograr la modulación adecuada de la inflamación periférica y la neuroinflamación en las diferentes patologías en las que se encuentran. Afortunadamente, existen distintas estrategias con potencial de trasladarse a la

clínica en el medio plazo con el objetivo de potenciar o inhibir estas vías de señalización en diferentes contextos patológicos (Herradon y col., 2019). En la figura 6 se resumen las distintas estrategias existentes actualmente para la inhibición o potenciación de la vía de señalización de PTN y MK. Debido a la implicación de la PTN y la MK en angiogénesis, proliferación de células tumorales y metástasis, se ha señalado estas citoquinas como dianas para la terapia de distintos tipos de cáncer (Takei y col., 2001; Zha y col., 2017). En este caso, la opción más estudiada es el silenciamiento de la PTN y la MK mediante siRNA (del inglés *small interfering RNA*) para el tratamiento de tumores y metástasis (Erdogan y col., 2019; Zha y col., 2017). En este campo también se han sugerido pequeñas moléculas inhibitoras de MK, como el llamado iMDK (Figura 6A), que han mostrado eficacia significativa en modelos animales de distintos tipos de cáncer (Erdogan y col., 2017; Hao y col., 2013; Matsui y col., 2010). Por otro lado, debido a la implicación de la MK en procesos inflamatorios sistémicos, también se han diseñado aptámeros de ARN anti-Mk para el tratamiento de enfermedades autoinmunes como la encefalitis (Wang y col., 2008).

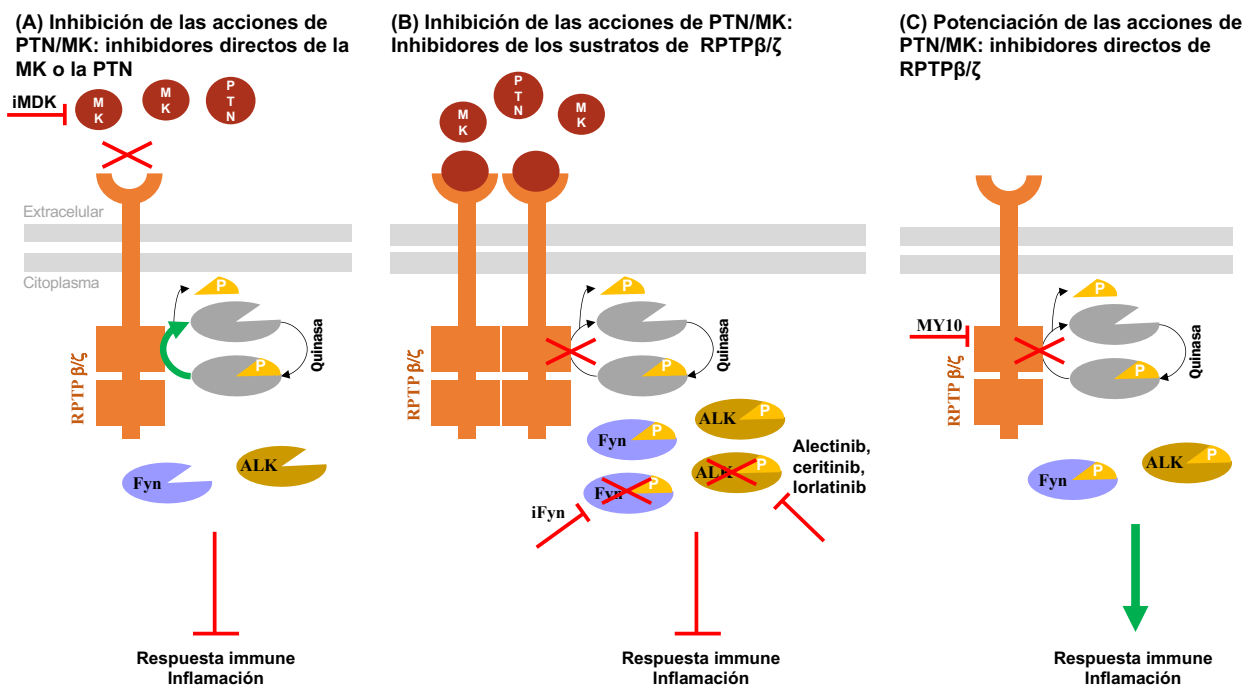
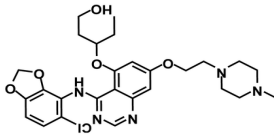
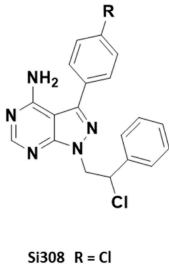
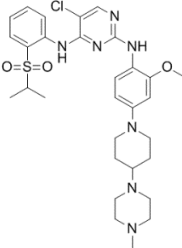
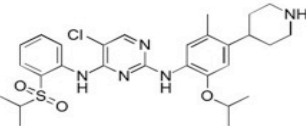
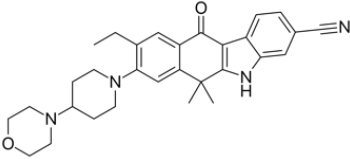
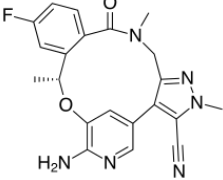
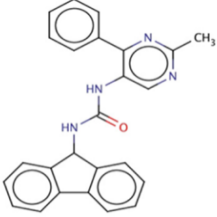


Figura 6. Estrategias de modulación de la vía de señalización de PTN/MK/RPTPβ/ζ. (A) Inhibidores directos de la PTN o de la MK. De acuerdo con las evidencias existentes, esto se traduciría en la disminución de la respuesta inmune e inflamación. (B) La inhibición de las acciones de la PTN o la MK mediante la inhibición directa de los sustratos de RPTPβ/ζ se traduciría en la disminución de la respuesta inmune e inflamación. (C) La potenciación de las acciones de la PTN y la MK mediante la inhibición directa de RPTPβ/ζ con MY10 podría dar lugar al aumento de la respuesta inmune e inflamación características de las acciones de PTN y MK.

Otra alternativa, con mayor potencial de traslación a la clínica actualmente, sería el bloqueo de estas vías de señalización a través de la inhibición directa de los sustratos de RPTP β/ζ . En la Tabla 1 se resumen los inhibidores de diferentes sustratos de RPTP β/ζ que podrían emplearse para minimizar las consecuencias de la interacción de la PTN o la MK con su receptor (Figura 6). En este sentido, cabe destacar que se han propuesto inhibidores de la quinasa ALK o de Fyn para tratar trastornos por abuso del alcohol y distintos tipos de cáncer, e inhibidores de TrkA para dolor crónico o sarcoma.

Por último, la estrategia de potenciación de esta vía consiste en el uso de inhibidores de RPTP β/ζ como MY10, objeto de esta tesis, y que se esquematiza en la figura 6C. Los datos preclínicos presentados en esta tesis sugieren el posible uso de esta estrategia para tratar enfermedades relacionadas con el consumo excesivo de alcohol y la dependencia de esta droga. Basados en las acciones conocidas de los inhibidores endógenos de RPTP β/ζ , PTN y MK, podríamos sugerir que la administración de inhibidores exógenos como MY10 podría redundar en un aumento de la respuesta inmune y los procesos inflamatorios subsecuentes (Figura 6C), lo cual podría resultar beneficioso en la reparación de tejidos a corto plazo, pero podría provocar efectos deletéreos a largo plazo si contribuye a la cronificación de la inflamación.

Nombre	Estructura	Mecanismo de acción	Indicación	Evidencias
Sacarinib (AZD0530)		Inhibidor de Fyn	Trastornos por abuso de alcohol, enfermedad de Alzheimer, cáncer.	Modelos animales (Morisot y col., 2018). Ensayos clínicos fase II (fracaso) (Hennequin y col., 2006).
Si308	 Si308 R = Cl	Inhibidor de Fyn	Linfoma.	Ensayos <i>in vitro</i> (Fallacara y col., 2019).
NVP-TAVE684 (TAE684)		Inhibidor de ALK	Neuroblastoma, trastornos por abuso de alcohol.	Ensayos <i>in vitro</i> (Najem y col., 2016). Modelos animales de consumo de alcohol (Mangieri y col., 2017).
Ceritinib (Zykadia®)		Inhibidor 2 ^a generación de ALK	Cáncer de pulmón tipo NSCLC.	Aprobado para su uso clínico y comercializado en 2014 (Raedler, 2015).
Alectinib (Alecensa®)		Inhibidor 2 ^a generación de ALK	Carcinomas de pulmón con el gen de fusión de ALK-EML4.	Aprobado para su uso clínico en 2015 (Gadgeel, 2018).
Lorlatinib (Lorbrena®)		Inhibidor 3 ^a generación de ALK	Cáncer de pulmón tipo NSCLC.	Aprobado para su uso clínico y comercializado en 2018 (Akamine y col., 2018).
Compuesto 1		Inhibidor de TrkA	Dolor crónico.	Ensayos <i>in vitro</i> (Su y col., 2017).

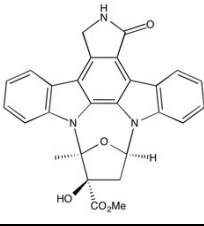
K252a		Inhibidor de TrkA	Sarcoma de Ewing.	Ensayos <i>in vitro</i> (Heinen y col., 2016).
-------	---	-------------------	-------------------	--

Tabla 1. Algunos de los inhibidores existentes de los sustratos de RPTP β/ζ y sus posibles indicaciones terapéuticas. ALK (*anaplastic lymphoma kinase*), EML4 (del inglés *chinoderm microtubule-associated protein-like 4*) NSCLC (del inglés *non-small-cell lung cancer*), TrkA (*Tropomyosin receptor kinase A*).

CONCLUSIONES/CONCLUSIONS

CONCLUSIONES

- 1) La pleiotrofina y la midkina endógenas modulan la respuesta astrocítica y la activación microglial inducida por LPS. Los datos indican que los niveles fisiológicos de ambas citoquinas son necesarios para la astrocitosis inducida por LPS, mientras que sus efectos reguladores sobre la activación microglial son más limitados y aparentemente independientes de la vía de señalización FYN-MAP quinasas.
- 2) La pleiotrofina es un potente modulador de la neuroinflamación y su sobreexpresión aumenta la activación microglial inducida por LPS. Los datos sugieren que la regulación de la vía de señalización de la PTN puede ser una nueva estrategia terapéutica en patologías centrales caracterizadas por el incremento de los niveles cerebrales de PTN.
- 3) El tratamiento con inhibidores de RPTP β/ζ , como MY33-3 y MY10, reduce significativamente el consumo de alcohol y los efectos reforzadores de esta droga en ratones. MY10 emerge como posible nueva estrategia terapéutica para tratar los desórdenes por consumo excesivo de alcohol.
- 4) El tratamiento con el inhibidor de RPTP β/ζ MY10 es capaz de reducir significativamente el condicionamiento preferencial al sitio inducido por el alcohol en ratones carentes de pleiotrofina, inhibidor endógeno de RPTP β/ζ , que son más sensibles a los efectos reforzadores de esta droga. En conjunto, los resultados sugieren que la inhibición farmacológica de RPTP β/ζ puede ser una nueva estrategia terapéutica en trastornos por consumo excesivo de alcohol, incluso en individuos más susceptibles a los efectos reforzadores de esta droga.
- 5) El tratamiento con el inhibidor de RPTP β/ζ MY10 causa efectos comportamentales muy limitados y de poca relevancia en ratones salvajes y en ratones *knock-out* de pleiotrofina.

CONCLUSIONS

- 1) Endogenous levels of pleiotrophin and midkine modulate the astrocytic response and microglial activation induced by LPS. The data indicate that physiological levels of both cytokines are required for LPS-induced astrocytosis, whereas their modulatory effects on microglial activation are more limited and, apparently, independent of the FYN-MAPK pathway.
- 2) Pleiotrophin is a potent modulator of neuroinflammation and its overexpression enhances LPS-induced microglial activation. The data suggest that modulation of the PTN signaling pathway may represent a novel therapeutic strategy for the treatment of CNS pathologies characterized by increased PTN brain levels.
- 3) The treatment with RPTP β/ζ inhibitors, such as MY10 and MY33-3, significantly reduces alcohol consumption and its rewarding effects in mice. MY10 emerges as a potential new therapeutic strategy for the treatment of alcohol use disorders.
- 4) The treatment with the RPTP β/ζ inhibitor MY10 significantly reduces alcohol-induced conditioned place preference in mice lacking pleiotrophin, the endogenous inhibitor of RPTP β/ζ , which are more vulnerable to the rewarding effects of alcohol. Taking together, the results suggest that pharmacological inhibition of RPTP β/ζ may be a novel therapeutic approach for the treatment of alcohol use disorders, even in more vulnerable individuals to the rewarding effects of alcohol.
- 5) The treatment with the RPTP β/ζ inhibitor MY10 induces very limited and slightly relevant behavioral effects in wild-type mice and in Pleiotrophin knockout mice.

REFERENCIAS

REFERENCIAS

- Abernathy, K., Chandler, L. J., Woodward, J. J., 2010. Alcohol and the prefrontal cortex. *Int Rev Neurobiol* 91, 289-320.
- Akamine, T., Toyokawa, G., Tagawa, T., Seto, T., 2018. Spotlight on lorlatinib and its potential in the treatment of NSCLC: the evidence to date. *Onco Targets Ther* 11, 5093-5101.
- Akira, S., Uematsu, S., Takeuchi, O., 2006. Pathogen recognition and innate immunity. *Cell* 124, 783-801.
- Allen, S. J., Watson, J. J., Shoemark, D. K., Barua, N. U., Patel, N. K., 2013. GDNF, NGF and BDNF as therapeutic options for neurodegeneration. *Pharmacol Ther* 138, 155-175.
- Amet, L. E., Lauri, S. E., Hienola, A., Croll, S. D., Lu, Y., Levorse, J. M., Prabhakaran, B., Taira, T., Rauvala, H., Vogt, T. F., 2001. Enhanced hippocampal long-term potentiation in mice lacking heparin-binding growth-associated molecule. *Mol Cell Neurosci* 17, 1014-1024.
- Amor, S., Woodroffe, M. N., 2014. Innate and adaptive immune responses in neurodegeneration and repair. *Immunology* 141, 287-291.
- Andersen, J. N., Mortensen, O. H., Peters, G. H., Drake, P. G., Iversen, L. F., Olsen, O. H., Jansen, P. G., Andersen, H. S., Tonks, N. K., Moller, N. P., 2001. Structural and evolutionary relationships among protein tyrosine phosphatase domains. *Mol Cell Biol* 21, 7117-7136.
- Antoine, M., Tag, C. G., Wirz, W., Borkham-Kamphorst, E., Sawitza, I., Gressner, A. M., Kiefer, P., 2005. Upregulation of pleiotrophin expression in rat hepatic stellate cells by PDGF and hypoxia: implications for its role in experimental biliary liver fibrogenesis. *Biochem Biophys Res Commun* 337, 1153-1164.
- Ares-Santos, S., Granado, N., Espadas, I., Martinez-Murillo, R., Moratalla, R., 2014. Methamphetamine causes degeneration of dopamine cell bodies and terminals of the nigrostriatal pathway evidenced by silver staining. *Neuropsychopharmacology* 39, 1066-1080.
- Bachiller, S., Jimenez-Ferrer, I., Paulus, A., Yang, Y., Swanberg, M., Deierborg, T., Boza-Serrano, A., 2018. Microglia in Neurological Diseases: A Road Map to Brain-Disease Dependent-Inflammatory Response. *Front Cell Neurosci* 12, 488.
- Barr, A. J., Ugochukwu, E., Lee, W. H., King, O. N., Filippakopoulos, P., Alfano, I., Savitsky, P., Burgess-Brown, N. A., Muller, S., Knapp, S., 2009. Large-scale structural analysis of the classical human protein tyrosine phosphatome. *Cell* 136, 352-363.
- Becker, H. C., 2012. Effects of alcohol dependence and withdrawal on stress responsiveness and alcohol consumption. *Alcohol Res* 34, 448-458.
- Beltran, P. J., Bixby, J. L., 2003. Receptor protein tyrosine phosphatases as mediators of cellular adhesion. *Front Biosci* 8, d87-99.
- Bilsland, J. G., Wheeldon, A., Mead, A., Znamenskiy, P., Almond, S., Waters, K. A., Thakur, M., Beaumont, V., Bonnert, T. P., Heavens, R., Whiting, P., McAllister, G., Munoz-Sanjuan, I., 2008. Behavioral and neurochemical alterations in mice deficient in anaplastic lymphoma kinase suggest therapeutic potential for psychiatric indications. *Neuropsychopharmacology* 33, 685-700.
- Blanco, A. M., Perez-Arago, A., Fernandez-Lizarbe, S., Guerri, C., 2008. Ethanol mimics ligand-mediated activation and endocytosis of IL-1RI/TLR4 receptors via lipid rafts caveolae in astroglial cells. *J Neurochem* 106, 625-639.
- Blednov, Y. A., Black, M., Chernis, J., Da Costa, A., Mayfield, J., Harris, R. A., 2017. Ethanol Consumption in Mice Lacking CD14, TLR2, TLR4, or MyD88. *Alcohol Clin Exp Res* 41, 516-530.
- Bodnar, R. J., 2016. Endogenous opiates and behavior: 2014. *Peptides* 75, 18-70.

- Bolton, J. M., Robinson, J., Sareen, J., 2009. Self-medication of mood disorders with alcohol and drugs in the National Epidemiologic Survey on Alcohol and Related Conditions. *J Affect Disord* 115, 367-375.
- Bortell, N., Basova, L., Semenova, S., Fox, H. S., Ravasi, T., Marcondes, M. C., 2017. Astrocyte-specific overexpressed gene signatures in response to methamphetamine exposure in vitro. *J Neuroinflammation* 14, 49.
- Bowyer, J. F., Ali, S., 2006. High doses of methamphetamine that cause disruption of the blood-brain barrier in limbic regions produce extensive neuronal degeneration in mouse hippocampus. *Synapse* 60, 521-532.
- Bradl, M., Hohlfeld, R., 2003. Molecular pathogenesis of neuroinflammation. *J Neurol Neurosurg Psychiatry* 74, 1364-1370.
- Burmeister, A. R., Marriott, I., 2018. The Interleukin-10 Family of Cytokines and Their Role in the CNS. *Front Cell Neurosci* 12, 458.
- Buxbaum, J. D., Georgieva, L., Young, J. J., Plescia, C., Kajiwara, Y., Jiang, Y., Moskvina, V., Norton, N., Peirce, T., Williams, H., Craddock, N. J., Carroll, L., Corfas, G., Davis, K. L., Owen, M. J., Harroch, S., Sakurai, T., O'Donovan, M. C., 2008. Molecular dissection of NRG1-ERBB4 signaling implicates PTPRZ1 as a potential schizophrenia susceptibility gene. *Mol Psychiatry* 13, 162-172.
- Cadet, J. L., Brannock, C., 1998. Free radicals and the pathobiology of brain dopamine systems. *Neurochem Int* 32, 117-131.
- Cadet, J. L., Krasnova, I. N., 2009. Molecular bases of methamphetamine-induced neurodegeneration. *Int Rev Neurobiol* 88, 101-119.
- Cadet, J. L., Krasnova, I. N., Jayanthi, S., Lyles, J., 2007. Neurotoxicity of substituted amphetamines: molecular and cellular mechanisms. *Neurotox Res* 11, 183-202.
- Camara, M. L., Corrigan, F., Jaehne, E. J., Jawahar, M. C., Anscomb, H., Koerner, H., Baune, B. T., 2013. TNF-alpha and its receptors modulate complex behaviours and neurotrophins in transgenic mice. *Psychoneuroendocrinology* 38, 3102-3114.
- Canoll, P. D., Petanceska, S., Schlessinger, J., Musacchio, J. M., 1996. Three forms of RPTP-beta are differentially expressed during gliogenesis in the developing rat brain and during glial cell differentiation in culture. *J Neurosci Res* 44, 199-215.
- Carson, M. J., Doose, J. M., Melchior, B., Schmid, C. D., Ploix, C. C., 2006. CNS immune privilege: hiding in plain sight. *Immunol Rev* 213, 48-65.
- Castro, D. C., Cole, S. L., Berridge, K. C., 2015. Lateral hypothalamus, nucleus accumbens, and ventral pallidum roles in eating and hunger: interactions between homeostatic and reward circuitry. *Front Syst Neurosci* 9, 90.
- Ceccanti, M., Coccurello, R., Carito, V., Ciafre, S., Ferraguti, G., Giacobuzzo, G., Mancinelli, R., Tirassa, P., Chaldakov, G. N., Pascale, E., Ceccanti, M., Codazzo, C., Fiore, M., 2016. Paternal alcohol exposure in mice alters brain NGF and BDNF and increases ethanol-elicited preference in male offspring. *Addict Biol* 21, 776-787.
- Chattopadhyaya, B., Baho, E., Huang, Z. J., Schachner, M., Di Cristo, G., 2013. Neural cell adhesion molecule-mediated Fyn activation promotes GABAergic synapse maturation in postnatal mouse cortex. *J Neurosci* 33, 5957-5968.
- Chen, H., He, D., Lasek, A. W., 2017. Midkine in the mouse ventral tegmental area limits ethanol intake and Ccl2 gene expression. *Genes Brain Behav* 16, 699-708.
- Chen, Y., Takita, J., Choi, Y. L., Kato, M., Ohira, M., Sanada, M., Wang, L., Soda, M., Kikuchi, A., Igarashi, T., Nakagawara, A., Hayashi, Y., Mano, H., Ogawa, S., 2008. Oncogenic mutations of ALK kinase in neuroblastoma. *Nature* 455, 971-974.
- Chen, Z., Trapp, B. D., 2016. Microglia and neuroprotection. *J Neurochem* 136 Suppl 1, 10-17.

- Chitnis, T., Weiner, H. L., 2017. CNS inflammation and neurodegeneration. *J Clin Invest* 127, 3577-3587.
- Chiu, C. C., Liao, Y. E., Yang, L. Y., Wang, J. Y., Tweedie, D., Karnati, H. K., Greig, N. H., Wang, J. Y., 2016. Neuroinflammation in animal models of traumatic brain injury. *J Neurosci Methods* 272, 38-49.
- Chow, J. P., Fujikawa, A., Shimizu, H., Suzuki, R., Noda, M., 2008. Metalloproteinase- and gamma-secretase-mediated cleavage of protein-tyrosine phosphatase receptor type Z. *J Biol Chem* 283, 30879-30889.
- Coelho-Santos, V., Goncalves, J., Fontes-Ribeiro, C., Silva, A. P., 2012. Prevention of methamphetamine-induced microglial cell death by TNF-alpha and IL-6 through activation of the JAK-STAT pathway. *J Neuroinflammation* 9, 103.
- Coleman, L. G., Jr., Crews, F. T., 2018a. Innate Immune Signaling and Alcohol Use Disorders. *Handb Exp Pharmacol* 248, 369-396.
- Coleman, L. G., Jr., Zou, J., Qin, L., Crews, F. T., 2018b. HMGB1/IL-1beta complexes regulate neuroimmune responses in alcoholism. *Brain Behav Immun* 72, 61-77.
- Cressant, A., Dubreuil, V., Kong, J., Kranz, T. M., Lazarini, F., Launay, J. M., Callebert, J., Sap, J., Malaspina, D., Granon, S., Harroch, S., 2017. Loss-of-function of PTPR gamma and zeta, observed in sporadic schizophrenia, causes brain region-specific deregulation of monoamine levels and altered behavior in mice. *Psychopharmacology (Berl)* 234, 575-587.
- Crews, F. T., Collins, M. A., Dlugos, C., Littleton, J., Wilkins, L., Neafsey, E. J., Pentney, R., Snell, L. D., Tabakoff, B., Zou, J., Noronha, A., 2004. Alcohol-induced neurodegeneration: when, where and why? *Alcohol Clin Exp Res* 28, 350-364.
- Crews, F. T., Lawrimore, C. J., Walter, T. J., Coleman, L. G., Jr., 2017. The role of neuroimmune signaling in alcoholism. *Neuropharmacology* 122, 56-73.
- Crews, F. T., Vetreno, R. P., 2016. Mechanisms of neuroimmune gene induction in alcoholism. *Psychopharmacology (Berl)* 233, 1543-1557.
- Davis, B. M., Salinas-Navarro, M., Cordeiro, M. F., Moons, L., De Groef, L., 2017. Characterizing microglia activation: a spatial statistics approach to maximize information extraction. *Sci Rep* 7, 1576.
- Deuel, T. F., Zhang, N., Yeh, H. J., Silos-Santiago, I., Wang, Z. Y., 2002. Pleiotrophin: a cytokine with diverse functions and a novel signaling pathway. *Arch Biochem Biophys* 397, 162-171.
- DiSabato, D. J., Quan, N., Godbout, J. P., 2016. Neuroinflammation: the devil is in the details. *J Neurochem* 139 Suppl 2, 136-153.
- Dobrosotskaya, I., Guy, R. K., James, G. L., 1997. MAGI-1, a membrane-associated guanylate kinase with a unique arrangement of protein-protein interaction domains. *J Biol Chem* 272, 31589-31597.
- Dubessy, A. L., Mazuir, E., Rappeneau, Q., Ou, S., Abi Ghanem, C., Piquand, K., Aigrot, M. S., Thetiot, M., Desmazieres, A., Chan, E., Fitzgibbon, M., Fleming, M., Krauss, R., Zalc, B., Ranscht, B., Lubetzki, C., Sol-Foulon, N., 2019. Role of a Contactin multi-molecular complex secreted by oligodendrocytes in nodal protein clustering in the CNS. *Glia*.
- Dutton, J. W., 3rd, Chen, H., You, C., Brodie, M. S., Lasek, A. W., 2017. Anaplastic lymphoma kinase regulates binge-like drinking and dopamine receptor sensitivity in the ventral tegmental area. *Addict Biol* 22, 665-678.
- Eckardt, M. J., File, S. E., Gessa, G. L., Grant, K. A., Guerri, C., Hoffman, P. L., Kalant, H., Koob, G. F., Li, T. K., Tabakoff, B., 1998. Effects of moderate alcohol consumption on the central nervous system. *Alcohol Clin Exp Res* 22, 998-1040.
- Eng, L. F., 1985. Glial fibrillary acidic protein (GFAP): the major protein of glial intermediate filaments in differentiated astrocytes. *J Neuroimmunol* 8, 203-214.

- Erdogan, S., Doganlar, Z. B., Doganlar, O., Turkekul, K., Serttas, R., 2017. Inhibition of Midkine Suppresses Prostate Cancer CD133(+) Stem Cell Growth and Migration. *Am J Med Sci* 354, 299-309.
- Erdogan, S., Turkekul, K., Dibirdik, I., Doganlar, Z. B., Doganlar, O., Bilir, A., 2019. Midkine silencing enhances the anti-prostate cancer stem cell activity of the flavone apigenin: cooperation on signaling pathways regulated by ERK, p38, PTEN, PARP, and NF-kappaB. *Invest New Drugs*.
- Ezquerro, L., Alguacil, L. F., Nguyen, T., Deuel, T. F., Silos-Santiago, I., Herradon, G., 2008. Different pattern of pleiotrophin and midkine expression in neuropathic pain: correlation between changes in pleiotrophin gene expression and rat strain differences in neuropathic pain. *Growth Factors* 26, 44-48.
- Fakhoury, M., 2015. Role of Immunity and Inflammation in the Pathophysiology of Neurodegenerative Diseases. *Neurodegener Dis* 15, 63-69.
- Fallacara, A. L., Passannanti, R., Mori, M., Iovenitti, G., Musumeci, F., Greco, C., Crespan, E., Kissova, M., Maga, G., Tarantelli, C., Spriano, F., Gaudio, E., Bertoni, F., Botta, M., Schenone, S., 2019. Identification of a new family of pyrazolo[3,4-d]pyrimidine derivatives as multitarget Fyn-Blk-Lyn inhibitors active on B- and T-lymphoma cell lines. *Eur J Med Chem* 181, 111545.
- Fellner, A., Barhum, Y., Angel, A., Perets, N., Steiner, I., Offen, D., Lev, N., 2017. Toll-Like Receptor-4 Inhibitor TAK-242 Attenuates Motor Dysfunction and Spinal Cord Pathology in an Amyotrophic Lateral Sclerosis Mouse Model. *Int J Mol Sci* 18.
- Feltenstein, M. W., See, R. E., 2008. The neurocircuitry of addiction: an overview. *Br J Pharmacol* 154, 261-274.
- Fernandez-Calle, R., Gramage, E., Zapico, J. M., de Pascual-Teresa, B., Ramos, A., Herradon, G., 2019. Inhibition of RPTPbeta/zeta blocks ethanol-induced conditioned place preference in pleiotrophin knockout mice. *Behav Brain Res* 369, 111933.
- Fernandez-Calle, R., Vicente-Rodriguez, M., Gramage, E., de la Torre-Ortiz, C., Perez-Garcia, C., Ramos, M. P., Herradon, G., 2018a. Endogenous pleiotrophin and midkine regulate LPS-induced glial responses. *Neurosci Lett* 662, 213-218.
- Fernandez-Calle, R., Vicente-Rodriguez, M., Gramage, E., Pita, J., Perez-Garcia, C., Ferrer-Alcon, M., Uribarri, M., Ramos, M. P., Herradon, G., 2017. Pleiotrophin regulates microglia-mediated neuroinflammation. *J Neuroinflammation* 14, 46.
- Fernandez-Calle, R., Vicente-Rodriguez, M., Pastor, M., Gramage, E., Di Geronimo, B., Zapico, J. M., Coderch, C., Perez-Garcia, C., Lasek, A. W., de Pascual-Teresa, B., Ramos, A., Herradon, G., 2018b. Pharmacological inhibition of Receptor Protein Tyrosine Phosphatase beta/zeta (PTPRZ1) modulates behavioral responses to ethanol. *Neuropharmacology* 137, 86-95.
- Fernandez-Lizarbe, S., Pascual, M., Guerri, C., 2009. Critical role of TLR4 response in the activation of microglia induced by ethanol. *J Immunol* 183, 4733-4744.
- Fernandez-Sola, J., Planavila Porta, A., 2016. New Treatment Strategies for Alcohol-Induced Heart Damage. *Int J Mol Sci* 17.
- Ferrer-Alcón M, U. M., Díaz A, Del Olmo N, Valdizán EM, Gramage E., Martín M, C. E., Pérez-García C, Mengod G, Maldonado R, Herradon G., Pazos A, P. J., 2012. A new non-classical transgenic animal model of Depression Program. Society for Neurosciences, New Orleans.
- Flatscher-Bader, T., Wilce, P. A., 2006. Chronic smoking and alcoholism change expression of selective genes in the human prefrontal cortex. *Alcohol Clin Exp Res* 30, 908-915.
- Flatscher-Bader, T., Wilce, P. A., 2008. Impact of alcohol abuse on protein expression of midkine and excitatory amino acid transporter 1 in the human prefrontal cortex. *Alcohol Clin Exp Res* 32, 1849-1858.
- Flores-Bastias, O., Karahanian, E., 2018. Neuroinflammation produced by heavy alcohol intake is due to loops of interactions between Toll-like 4 and TNF receptors, peroxisome proliferator-activated receptors and the central melanocortin system: A novel hypothesis and new therapeutic avenues. *Neuropharmacology* 128, 401-407.

- Franco, R., Fernandez-Suarez, D., 2015. Alternatively activated microglia and macrophages in the central nervous system. *Prog Neurobiol* 131, 65-86.
- Fukada, M., Fujikawa, A., Chow, J. P., Ikematsu, S., Sakuma, S., Noda, M., 2006. Protein tyrosine phosphatase receptor type Z is inactivated by ligand-induced oligomerization. *FEBS Lett* 580, 4051-4056.
- Fukada, M., Kawachi, H., Fujikawa, A., Noda, M., 2005. Yeast substrate-trapping system for isolating substrates of protein tyrosine phosphatases: Isolation of substrates for protein tyrosine phosphatase receptor type z. *Methods* 35, 54-63.
- Gadgeel, S. M., 2018. The use of alectinib in the first-line treatment of anaplastic lymphoma kinase-positive non-small-cell lung cancer. *Future Oncol* 14, 1875-1882.
- Garcia-Perez, D., Laorden, M. L., Milanes, M. V., 2017. Acute Morphine, Chronic Morphine, and Morphine Withdrawal Differently Affect Pleiotrophin, Midkine, and Receptor Protein Tyrosine Phosphatase beta/zeta Regulation in the Ventral Tegmental Area. *Mol Neurobiol* 54, 495-510.
- Garwood, J., Heck, N., Reichardt, F., Faissner, A., 2003. Phosphacan short isoform, a novel non-proteoglycan variant of phosphacan/receptor protein tyrosine phosphatase-beta, interacts with neuronal receptors and promotes neurite outgrowth. *J Biol Chem* 278, 24164-24173.
- Gasparotto, J., Ribeiro, C. T., da Rosa-Silva, H. T., Bortolin, R. C., Rabelo, T. K., Peixoto, D. O., Moreira, J. C. F., Gelain, D. P., 2019. Systemic Inflammation Changes the Site of RAGE Expression from Endothelial Cells to Neurons in Different Brain Areas. *Mol Neurobiol* 56, 3079-3089.
- George, R. E., Sanda, T., Hanna, M., Frohling, S., Luther, W., 2nd, Zhang, J., Ahn, Y., Zhou, W., London, W. B., McGrady, P., Xue, L., Zozulya, S., Gregor, V. E., Webb, T. R., Gray, N. S., Gilliland, D. G., Diller, L., Greulich, H., Morris, S. W., Meyerson, M., Look, A. T., 2008. Activating mutations in ALK provide a therapeutic target in neuroblastoma. *Nature* 455, 975-978.
- Ginhoux, F., Lim, S., Hoeffel, G., Low, D., Huber, T., 2013. Origin and differentiation of microglia. *Front Cell Neurosci* 7, 45.
- Ginhoux, F., Prinz, M., 2015. Origin of microglia: current concepts and past controversies. *Cold Spring Harb Perspect Biol* 7, a020537.
- Giustarini, D., Rossi, R., Milzani, A., Dalle-Donne, I., 2008. Nitrite and nitrate measurement by Griess reagent in human plasma: evaluation of interferences and standardization. *Methods Enzymol* 440, 361-380.
- Gombash, S. E., Lipton, J. W., Collier, T. J., Madhavan, L., Steece-Collier, K., Cole-Strauss, A., Terpstra, B. T., Spieles-Engemann, A. L., Daley, B. F., Wohlgenant, S. L., Thompson, V. B., Manfredsson, F. P., Mandel, R. J., Sortwell, C. E., 2012. Striatal pleiotrophin overexpression provides functional and morphological neuroprotection in the 6-hydroxydopamine model. *Mol Ther* 20, 544-554.
- Gonzalez-Castillo, C., Ortuno-Sahagun, D., Guzman-Brambila, C., Pallas, M., Rojas-Mayorquin, A. E., 2014. Pleiotrophin as a central nervous system neuromodulator, evidences from the hippocampus. *Front Cell Neurosci* 8, 443.
- Goodman, J., Packard, M. G., 2016. Memory Systems and the Addicted Brain. *Front Psychiatry* 7, 24.
- Gramage, E., Alguacil, L. F., Herradon, G., 2008. Pleiotrophin prevents cocaine-induced toxicity in vitro. *Eur J Pharmacol* 595, 35-38.
- Gramage, E., Herradon, G., 2011a. Connecting Parkinson's disease and drug addiction: common players reveal unexpected disease connections and novel therapeutic approaches. *Curr Pharm Des* 17, 449-461.
- Gramage, E., Martin, Y. B., Ramanah, P., Perez-Garcia, C., Herradon, G., 2011b. Midkine regulates amphetamine-induced astrocytosis in striatum but has no effects on amphetamine-induced striatal dopaminergic denervation and addictive effects: functional differences between pleiotrophin and midkine. *Neuroscience* 190, 307-317.

- Gramage, E., Perez-Garcia, C., Vicente-Rodriguez, M., Bollen, S., Rojo, L., Herradon, G., 2013. Regulation of extinction of cocaine-induced place preference by midkine is related to a differential phosphorylation of peroxiredoxin 6 in dorsal striatum. *Behav Brain Res* 253, 223-231.
- Gramage, E., Putelli, A., Polanco, M. J., Gonzalez-Martin, C., Ezquerra, L., Alguacil, L. F., Perez-Pinera, P., Deuel, T. F., Herradon, G., 2010a. The neurotrophic factor pleiotrophin modulates amphetamine-seeking behaviour and amphetamine-induced neurotoxic effects: evidence from pleiotrophin knockout mice. *Addict Biol* 15, 403-412.
- Gramage, E., Rossi, L., Granado, N., Moratalla, R., Herradon, G., 2010b. Genetic inactivation of pleiotrophin triggers amphetamine-induced cell loss in the substantia nigra and enhances amphetamine neurotoxicity in the striatum. *Neuroscience* 170, 308-316.
- Granado, N., O'Shea, E., Bove, J., Vila, M., Colado, M. I., Moratalla, R., 2008. Persistent MDMA-induced dopaminergic neurotoxicity in the striatum and substantia nigra of mice. *J Neurochem* 107, 1102-1112.
- Grant, J. E., Chamberlain, S. R., 2016. Expanding the definition of addiction: DSM-5 vs. ICD-11. *CNS Spectr* 21, 300-303.
- Grant, S. G., O'Dell, T. J., Karl, K. A., Stein, P. L., Soriano, P., Kandel, E. R., 1992. Impaired long-term potentiation, spatial learning, and hippocampal development in *fyn* mutant mice. *Science* 258, 1903-1910.
- Guan, J., Yamazaki, Y., Chand, D., van Dijk, J. R., Ruuth, K., Palmer, R. H., Hallberg, B., 2017. Novel Mechanisms of ALK Activation Revealed by Analysis of the Y1278S Neuroblastoma Mutation. *Cancers (Basel)* 9.
- Guerri, C., Pascual, M., 2019. Impact of neuroimmune activation induced by alcohol or drug abuse on adolescent brain development. *Int J Dev Neurosci* 77, 89-98.
- Guo, M. L., Liao, K., Periyasamy, P., Yang, L., Cai, Y., Callen, S. E., Buch, S., 2015. Cocaine-mediated microglial activation involves the ER stress-autophagy axis. *Autophagy* 11, 995-1009.
- Ha, J. W., You, M. J., Park, H. S., Kim, J. W., Kwon, M. S., 2019. Differential effect of LPS and paclitaxel on microglial functional phenotypes and circulating cytokines: the possible role of CX3CR1 and IL-4/10 in blocking persistent inflammation. *Arch Pharm Res* 42, 359-368.
- Haddad, G. E., Saunders, L., Carles, M., Crosby, S. D., del Monte, F., Macgillivray, T. E., Semigran, M. J., Dec, G. W., Hajjar, R. J., Doye, A. A., Glass, R., El, M., Gwathmey, J. K., 2008. Fingerprint profile of alcohol-associated heart failure in human hearts. *Alcohol Clin Exp Res* 32, 814-821.
- Hamasaki, M. Y., Machado, M. C. C., Pinheiro da Silva, F., 2018. Animal models of neuroinflammation secondary to acute insults originated outside the brain. *J Neurosci Res* 96, 371-378.
- Hamilton, P. J., Nestler, E. J., 2019. Epigenetics and addiction. *Curr Opin Neurobiol* 59, 128-136.
- Hanisch, U. K., Kettenmann, H., 2007. Microglia: active sensor and versatile effector cells in the normal and pathologic brain. *Nat Neurosci* 10, 1387-1394.
- Hao, H., Maeda, Y., Fukazawa, T., Yamatsuji, T., Takaoka, M., Bao, X. H., Matsuoka, J., Okui, T., Shimo, T., Takigawa, N., Tomono, Y., Nakajima, M., Fink-Baldauf, I. M., Nelson, S., Seibel, W., Papoian, R., Whitsett, J. A., Naomoto, Y., 2013. Inhibition of the growth factor MDK/midkine by a novel small molecule compound to treat non-small cell lung cancer. *PLoS One* 8, e71093.
- Harricharan, R., Abboussi, O., Daniels, W. M. U., 2017. Addiction: A dysregulation of satiety and inflammatory processes. *Prog Brain Res* 235, 65-91.
- Harroch, S., Furtado, G. C., Brueck, W., Rosenbluth, J., Lafaille, J., Chao, M., Buxbaum, J. D., Schlessinger, J., 2002. A critical role for the protein tyrosine phosphatase receptor type Z in functional recovery from demyelinating lesions. *Nat Genet* 32, 411-414.
- Hawkins, B. T., Davis, T. P., 2005. The blood-brain barrier/neurovascular unit in health and disease. *Pharmacol Rev* 57, 173-185.

- He, D., Chen, H., Muramatsu, H., Lasek, A. W., 2015. Ethanol activates midkine and anaplastic lymphoma kinase signaling in neuroblastoma cells and in the brain. *J Neurochem* 135, 508-521.
- He, J., Crews, F. T., 2008. Increased MCP-1 and microglia in various regions of the human alcoholic brain. *Exp Neurol* 210, 349-358.
- Heck, N., Klausmeyer, A., Faissner, A., Garwood, J., 2005. Cortical neurons express PSI, a novel isoform of phosphacan/RPTPbeta. *Cell Tissue Res* 321, 323-333.
- Hegarty, S. V., Lee, D. J., O'Keeffe, G. W., Sullivan, A. M., 2017. Effects of intracerebral neurotrophic factor application on motor symptoms in Parkinson's disease: A systematic review and meta-analysis. *Parkinsonism Relat Disord* 38, 19-25.
- Heinen, T. E., Dos Santos, R. P., da Rocha, A., Dos Santos, M. P., Lopez, P. L., Silva Filho, M. A., Souza, B. K., Rivero, L. F., Becker, R. G., Gregianin, L. J., Brunetto, A. L., Brunetto, A. T., de Farias, C. B., Roesler, R., 2016. Trk inhibition reduces cell proliferation and potentiates the effects of chemotherapeutic agents in Ewing sarcoma. *Oncotarget* 7, 34860-34880.
- Hennequin, L. F., Allen, J., Breed, J., Curwen, J., Fennell, M., Green, T. P., Lambert-van der Brempt, C., Morgentin, R., Norman, R. A., Olivier, A., Otterbein, L., Ple, P. A., Warin, N., Costello, G., 2006. N-(5-chloro-1,3-benzodioxol-4-yl)-7-[2-(4-methylpiperazin-1-yl)ethoxy]-5- (tetrahydro-2H-pyran-4-yloxy)quinazolin-4-amine, a novel, highly selective, orally available, dual-specific c-Src/Abl kinase inhibitor. *J Med Chem* 49, 6465-6488.
- Herradon, G., Ezquerra, L., Nguyen, T., Silos-Santiago, I., Deuel, T. F., 2005. Midkine regulates pleiotrophin organ-specific gene expression: evidence for transcriptional regulation and functional redundancy within the pleiotrophin/midkine developmental gene family. *Biochem Biophys Res Commun* 333, 714-721.
- Herradon, G., Ezquerra, L., Nguyen, T., Vogt, T. F., Bronson, R., Silos-Santiago, I., Deuel, T. F., 2004. Pleiotrophin is an important regulator of the renin-angiotensin system in mouse aorta. *Biochem Biophys Res Commun* 324, 1041-1047.
- Herradon, G., Perez-Garcia, C., 2014. Targeting midkine and pleiotrophin signalling pathways in addiction and neurodegenerative disorders: recent progress and perspectives. *Br J Pharmacol* 171, 837-848.
- Herradon, G., Ramos-Alvarez, M. P., Gramage, E., 2019. Connecting Metainflammation and Neuroinflammation Through the PTN-MK-RPTPbeta/zeta Axis: Relevance in Therapeutic Development. *Front Pharmacol* 10, 377.
- Hida, H., Masuda, T., Sato, T., Kim, T. S., Misumi, S., Nishino, H., 2007. Pleiotrophin promotes functional recovery after neural transplantation in rats. *Neuroreport* 18, 179-183.
- Holtzman, D. M., Kilbridge, J., Li, Y., Cunningham, E. T., Jr., Lenn, N. J., Clary, D. O., Reichardt, L. F., Mobley, W. C., 1995. TrkA expression in the CNS: evidence for the existence of several novel NGF-responsive CNS neurons. *J Neurosci* 15, 1567-1576.
- Hommer, D. W., 2003. Male and female sensitivity to alcohol-induced brain damage. *Alcohol Res Health* 27, 181-185.
- Horiba, M., Kadomatsu, K., Nakamura, E., Muramatsu, H., Ikematsu, S., Sakuma, S., Hayashi, K., Yuzawa, Y., Matsuo, S., Kuzuya, M., Kaname, T., Hirai, M., Saito, H., Muramatsu, T., 2000. Neointima formation in a restenosis model is suppressed in midkine-deficient mice. *J Clin Invest* 105, 489-495.
- Hovanessian, A. G., 2006. Midkine, a cytokine that inhibits HIV infection by binding to the cell surface expressed nucleolin. *Cell Res* 16, 174-181.
- Huang, P., Ramphal, J., Wei, J., Liang, C., Jallal, B., McMahon, G., Tang, C., 2003. Structure-based design and discovery of novel inhibitors of protein tyrosine phosphatases. *Bioorg Med Chem* 11, 1835-1849.
- Hunter, T., 1987. A thousand and one protein kinases. *Cell* 50, 823-829.

- Ibanez, F., Montesinos, J., Urena-Peralta, J. R., Guerri, C., Pascual, M., 2019. TLR4 participates in the transmission of ethanol-induced neuroinflammation via astrocyte-derived extracellular vesicles. *J Neuroinflammation* 16, 136.
- Ii, M., Matsunaga, N., Hazeki, K., Nakamura, K., Takashima, K., Seya, T., Hazeki, O., Kitazaki, T., Iizawa, Y., 2006. A novel cyclohexene derivative, ethyl (6R)-6-[N-(2-Chloro-4-fluorophenyl)sulfamoyl]cyclohex-1-ene-1-carboxylate (TAK-242), selectively inhibits toll-like receptor 4-mediated cytokine production through suppression of intracellular signaling. *Mol Pharmacol* 69, 1288-1295.
- Ito, H., Morishita, R., Iwamoto, I., Mizuno, M., Nagata, K., 2013. MAGI-1 acts as a scaffolding molecule for NGF receptor-mediated signaling pathway. *Biochim Biophys Acta* 1833, 2302-2310.
- Iwahara, T., Fujimoto, J., Wen, D., Cupples, R., Bucay, N., Arakawa, T., Mori, S., Ratzkin, B., Yamamoto, T., 1997. Molecular characterization of ALK, a receptor tyrosine kinase expressed specifically in the nervous system. *Oncogene* 14, 439-449.
- Iwasaki, A., Medzhitov, R., 2015. Control of adaptive immunity by the innate immune system. *Nat Immunol* 16, 343-353.
- Jack, C. S., Arbour, N., Manusow, J., Montgrain, V., Blain, M., McCrea, E., Shapiro, A., Antel, J. P., 2005. TLR signaling tailors innate immune responses in human microglia and astrocytes. *J Immunol* 175, 4320-4330.
- Jin, L., Jianghai, C., Juan, L., Hao, K., 2009. Pleiotrophin and peripheral nerve injury. *Neurosurg Rev* 32, 387-393.
- Jung, C. G., Hida, H., Nakahira, K., Ikenaka, K., Kim, H. J., Nishino, H., 2004. Pleiotrophin mRNA is highly expressed in neural stem (progenitor) cells of mouse ventral mesencephalon and the product promotes production of dopaminergic neurons from embryonic stem cell-derived nestin-positive cells. *FASEB J* 18, 1237-1239.
- Kalivas, P. W., Stewart, J., 1991. Dopamine transmission in the initiation and expression of drug- and stress-induced sensitization of motor activity. *Brain Res Brain Res Rev* 16, 223-244.
- Kang, S. S., Ren, Y., Liu, C. C., Kurti, A., Baker, K. E., Bu, G., Asmann, Y., Fryer, J. D., 2018. Lipocalin-2 protects the brain during inflammatory conditions. *Mol Psychiatry* 23, 344-350.
- Kapoor, M., Wang, J. C., Wetherill, L., Le, N., Bertelsen, S., Hinrichs, A. L., Budde, J., Agrawal, A., Bucholz, K., Dick, D., Harari, O., Hesselbrock, V., Kramer, J., Nurnberger, J. I., Jr., Rice, J., Saccone, N., Schuckit, M., Tischfield, J., Porjesz, B., Edenberg, H. J., Bierut, L., Foroud, T., Goate, A., 2013. A meta-analysis of two genome-wide association studies to identify novel loci for maximum number of alcoholic drinks. *Hum Genet* 132, 1141-1151.
- Kawachi, H., Fujikawa, A., Maeda, N., Noda, M., 2001. Identification of GIT1/Cat-1 as a substrate molecule of protein tyrosine phosphatase zeta /beta by the yeast substrate-trapping system. *Proc Natl Acad Sci U S A* 98, 6593-6598.
- Kawai, T., Akira, S., 2007. Signaling to NF-kappaB by Toll-like receptors. *Trends Mol Med* 13, 460-469.
- Kawai, T., Akira, S., 2008. Toll-like receptor and RIG-I-like receptor signaling. *Ann N Y Acad Sci* 1143, 1-20.
- Kayagaki, N., Wong, M. T., Stowe, I. B., Ramani, S. R., Gonzalez, L. C., Akashi-Takamura, S., Miyake, K., Zhang, J., Lee, W. P., Muszynski, A., Forsberg, L. S., Carlson, R. W., Dixit, V. M., 2013. Noncanonical inflammasome activation by intracellular LPS independent of TLR4. *Science* 341, 1246-1249.
- Keenan, J. P., Freeman, P. R., Harrell, R., 1997. The effects of family history, sobriety length, and drinking history in younger alcoholics on P300 auditory-evoked potentials. *Alcohol Alcohol* 32, 233-239.
- Kierdorf, K., Prinz, M., 2013. Factors regulating microglia activation. *Front Cell Neurosci* 7, 44.

- Kikuchi, S., Muramatsu, H., Muramatsu, T., Kim, S. U., 1993. Midkine, a novel neurotrophic factor, promotes survival of mesencephalic neurons in culture. *Neurosci Lett* 160, 9-12.
- Kim, E. K., Choi, E. J., 2015. Compromised MAPK signaling in human diseases: an update. *Arch Toxicol* 89, 867-882.
- Kimelberg, H. K., 2004. The problem of astrocyte identity. *Neurochem Int* 45, 191-202.
- Kiyatkin, E. A., Brown, P. L., Sharma, H. S., 2007. Brain edema and breakdown of the blood-brain barrier during methamphetamine intoxication: critical role of brain hyperthermia. *Eur J Neurosci* 26, 1242-1253.
- Komiya, Y., Habas, R., 2008. Wnt signal transduction pathways. *Organogenesis* 4, 68-75.
- Koob, G. F., 2014. Neurocircuitry of alcohol addiction: synthesis from animal models. *Handb Clin Neurol* 125, 33-54.
- Koob, G. F., Le Moal, M., 1997. Drug abuse: hedonic homeostatic dysregulation. *Science* 278, 52-58.
- Koob, G. F., Volkow, N. D., 2010. Neurocircuitry of addiction. *Neuropsychopharmacology* 35, 217-238.
- Kosugi, T., Yuzawa, Y., Sato, W., Arata-Kawai, H., Suzuki, N., Kato, N., Matsuo, S., Kadomatsu, K., 2007. Midkine is involved in tubulointerstitial inflammation associated with diabetic nephropathy. *Lab Invest* 87, 903-913.
- Kouadir, M., Yang, L., Tan, R., Shi, F., Lu, Y., Zhang, S., Yin, X., Zhou, X., Zhao, D., 2012. CD36 participates in PrP(106-126)-induced activation of microglia. *PLoS One* 7, e30756.
- Koutsoumpa, M., Polytarchou, C., Courty, J., Zhang, Y., Kieffer, N., Mikelis, C., Skandalis, S. S., Hellman, U., Iliopoulos, D., Papadimitriou, E., 2013. Interplay between alphavbeta3 integrin and nucleolin regulates human endothelial and glioma cell migration. *J Biol Chem* 288, 343-354.
- Krasnova, I. N., Ladenheim, B., Cadet, J. L., 2005. Amphetamine induces apoptosis of medium spiny striatal projection neurons via the mitochondria-dependent pathway. *FASEB J* 19, 851-853.
- Krzystek-Korpacka, M., Neubauer, K., Matusiewicz, M., 2010. Circulating midkine in Crohn's disease: clinical implications. *Inflamm Bowel Dis* 16, 208-215.
- Kuboyama, K., Fujikawa, A., Suzuki, R., Tanga, N., Noda, M., 2016. Role of Chondroitin Sulfate (CS) Modification in the Regulation of Protein-tyrosine Phosphatase Receptor Type Z (PTPRZ) Activity: PLEIOTROPHIN-PTPRZ-A SIGNALING IS INVOLVED IN OLIGODENDROCYTE DIFFERENTIATION. *J Biol Chem* 291, 18117-18128.
- Kumar, V., 2019. Toll-like receptors in the pathogenesis of neuroinflammation. *J Neuroimmunol* 332, 16-30.
- Kuo, A. H., Stoica, G. E., Riegel, A. T., Wellstein, A., 2007. Recruitment of insulin receptor substrate-1 and activation of NF-kappaB essential for midkine growth signaling through anaplastic lymphoma kinase. *Oncogene* 26, 859-869.
- Kushner, M. G., Abrams, K., Borchardt, C., 2000. The relationship between anxiety disorders and alcohol use disorders: a review of major perspectives and findings. *Clin Psychol Rev* 20, 149-171.
- Kutlu, M. G., Gould, T. J., 2016. Effects of drugs of abuse on hippocampal plasticity and hippocampus-dependent learning and memory: contributions to development and maintenance of addiction. *Learn Mem* 23, 515-533.
- Lacagnina, M. J., Watkins, L. R., Grace, P. M., 2018. Toll-like receptors and their role in persistent pain. *Pharmacol Ther* 184, 145-158.
- Lamprianou, S., Chatzopoulou, E., Thomas, J. L., Bouyain, S., Harroch, S., 2011. A complex between contactin-1 and the protein tyrosine phosphatase PTPRZ controls the development of oligodendrocyte precursor cells. *Proc Natl Acad Sci U S A* 108, 17498-17503.

- Lamprianou, S., Vacaresse, N., Suzuki, Y., Meziane, H., Buxbaum, J. D., Schlessinger, J., Harroch, S., 2006. Receptor protein tyrosine phosphatase gamma is a marker for pyramidal cells and sensory neurons in the nervous system and is not necessary for normal development. *Mol Cell Biol* 26, 5106-5119.
- Larson, M., Sherman, M. A., Amar, F., Nuvolone, M., Schneider, J. A., Bennett, D. A., Aguzzi, A., Lesne, S. E., 2012. The complex PrP(c)-Fyn couples human oligomeric Abeta with pathological tau changes in Alzheimer's disease. *J Neurosci* 32, 16857-16871a.
- Lasek, A. W., Lim, J., Kliethermes, C. L., Berger, K. H., Joslyn, G., Brush, G., Xue, L., Robertson, M., Moore, M. S., Vranizan, K., Morris, S. W., Schuckit, M. A., White, R. L., Heberlein, U., 2011. An evolutionary conserved role for anaplastic lymphoma kinase in behavioral responses to ethanol. *PLoS One* 6, e22636.
- Lawrimore, C. J., Coleman, L. G., Zou, J., Crews, F. T., 2019. Ethanol Induction of Innate Immune Signals Across BV2 Microglia and SH-SY5Y Neuroblastoma Involves Induction of IL-4 and IL-13. *Brain Sci* 9.
- Lehnardt, S., 2010. Innate immunity and neuroinflammation in the CNS: the role of microglia in Toll-like receptor-mediated neuronal injury. *Glia* 58, 253-263.
- Lehnardt, S., Henneke, P., Lien, E., Kasper, D. L., Volpe, J. J., Bechmann, I., Nitsch, R., Weber, J. R., Golenbock, D. T., Vartanian, T., 2006. A mechanism for neurodegeneration induced by group B streptococci through activation of the TLR2/MyD88 pathway in microglia. *J Immunol* 177, 583-592.
- Lemstra, M., Bennett, N. R., Neudorf, C., Kunst, A., Nannapaneni, U., Warren, L. M., Kershaw, T., Scott, C. R., 2008. A meta-analysis of marijuana and alcohol use by socio-economic status in adolescents aged 10-15 years. *Can J Public Health* 99, 172-177.
- Li, F., Tian, F., Wang, L., Williamson, I. K., Sharifi, B. G., Shah, P. K., 2010. Pleiotrophin (PTN) is expressed in vascularized human atherosclerotic plaques: IFN- γ /JAK/STAT1 signaling is critical for the expression of PTN in macrophages. *FASEB J* 24, 810-822.
- Li, Y. S., Hoffman, R. M., Le Beau, M. M., Espinosa, R., 3rd, Jenkins, N. A., Gilbert, D. J., Copeland, N. G., Deuel, T. F., 1992. Characterization of the human pleiotrophin gene. Promoter region and chromosomal localization. *J Biol Chem* 267, 26011-26016.
- Li, Y. S., Milner, P. G., Chauhan, A. K., Watson, M. A., Hoffman, R. M., Kodner, C. M., Milbrandt, J., Deuel, T. F., 1990. Cloning and expression of a developmentally regulated protein that induces mitogenic and neurite outgrowth activity. *Science* 250, 1690-1694.
- Liberto, C. M., Albrecht, P. J., Herx, L. M., Yong, V. W., Levison, S. W., 2004. Pro-regenerative properties of cytokine-activated astrocytes. *J Neurochem* 89, 1092-1100.
- Liddelow, S. A., Guttenplan, K. A., Clarke, L. E., Bennett, F. C., Bohlen, C. J., Schirmer, L., Bennett, M. L., Munch, A. E., Chung, W. S., Peterson, T. C., Wilton, D. K., Frouin, A., Napier, B. A., Panicker, N., Kumar, M., Buckwalter, M. S., Rowitch, D. H., Dawson, V. L., Dawson, T. M., Stevens, B., Barres, B. A., 2017. Neurotoxic reactive astrocytes are induced by activated microglia. *Nature* 541, 481-487.
- Lin, E., Li, L., Guan, Y., Soriano, R., Rivers, C. S., Mohan, S., Pandita, A., Tang, J., Modrusan, Z., 2009. Exon array profiling detects EML4-ALK fusion in breast, colorectal, and non-small cell lung cancers. *Mol Cancer Res* 7, 1466-1476.
- Liu, J., Lewohl, J. M., Dodd, P. R., Randall, P. K., Harris, R. A., Mayfield, R. D., 2004. Gene expression profiling of individual cases reveals consistent transcriptional changes in alcoholic human brain. *J Neurochem* 90, 1050-1058.
- Liu, J., Lewohl, J. M., Harris, R. A., Iyer, V. R., Dodd, P. R., Randall, P. K., Mayfield, R. D., 2006. Patterns of gene expression in the frontal cortex discriminate alcoholic from nonalcoholic individuals. *Neuropsychopharmacology* 31, 1574-1582.

- Liu, X., Mashour, G. A., Webster, H. F., Kurtz, A., 1998. Basic FGF and FGF receptor 1 are expressed in microglia during experimental autoimmune encephalomyelitis: temporally distinct expression of midkine and pleiotrophin. *Glia* 24, 390-397.
- Liu, X., Nemeth, D. P., Tarr, A. J., Belevych, N., Syed, Z. W., Wang, Y., Ismail, A. S., Reed, N. S., Sheridan, J. F., Yajnik, A. R., Disabato, D. J., Zhu, L., Quan, N., 2016. Euflammation attenuates peripheral inflammation-induced neuroinflammation and mitigates immune-to-brain signaling. *Brain Behav Immun* 54, 140-148.
- Lu, Y. C., Yeh, W. C., Ohashi, P. S., 2008. LPS/TLR4 signal transduction pathway. *Cytokine* 42, 145-151.
- Ma, J., Lang, B., Wang, X., Wang, L., Dong, Y., Hu, H., 2014. Co-expression of midkine and pleiotrophin predicts poor survival in human glioma. *J Clin Neurosci* 21, 1885-1890.
- Maeda, N., Ichihara-Tanaka, K., Kimura, T., Kadomatsu, K., Muramatsu, T., Noda, M., 1999. A receptor-like protein-tyrosine phosphatase PTPzeta/RPTPbeta binds a heparin-binding growth factor midkine. Involvement of arginine 78 of midkine in the high affinity binding to PTPzeta. *J Biol Chem* 274, 12474-12479.
- Maeda, N., Nishiwaki, T., Shintani, T., Hamanaka, H., Noda, M., 1996. 6B4 proteoglycan/phosphacan, an extracellular variant of receptor-like protein-tyrosine phosphatase zeta/RPTPbeta, binds pleiotrophin/heparin-binding growth-associated molecule (HB-GAM). *J Biol Chem* 271, 21446-21452.
- Mangieri, R. A., Maier, E. Y., Buske, T. R., Lasek, A. W., Morrisett, R. A., 2017. Anaplastic Lymphoma Kinase Is a Regulator of Alcohol Consumption and Excitatory Synaptic Plasticity in the Nucleus Accumbens Shell. *Front Pharmacol* 8, 533.
- Marchionini, D. M., Lehmann, E., Chu, Y., He, B., Sortwell, C. E., Becker, K. G., Freed, W. J., Kordower, J. H., Collier, T. J., 2007. Role of heparin binding growth factors in nigrostriatal dopamine system development and Parkinson's disease. *Brain Res* 1147, 77-88.
- Markiewicz, I., Lukomska, B., 2006. The role of astrocytes in the physiology and pathology of the central nervous system. *Acta Neurobiol Exp (Wars)* 66, 343-358.
- Martin, Y. B., Herradon, G., Ezquerra, L., 2011. Uncovering new pharmacological targets to treat neuropathic pain by understanding how the organism reacts to nerve injury. *Curr Pharm Des* 17, 434-448.
- Matias, I., Morgado, J., Gomes, F. C. A., 2019. Astrocyte Heterogeneity: Impact to Brain Aging and Disease. *Front Aging Neurosci* 11, 59.
- Matsubara, S., Take, M., Pedraza, C., Muramatsu, T., 1994. Mapping and characterization of a retinoic acid-responsive enhancer of midkine, a novel heparin-binding growth/differentiation factor with neurotrophic activity. *J Biochem* 115, 1088-1096.
- Matsui, T., Ichihara-Tanaka, K., Lan, C., Muramatsu, H., Kondou, T., Hirose, C., Sakuma, S., Muramatsu, T., 2010. Midkine inhibitors: application of a simple assay procedure to screening of inhibitory compounds. *Int Arch Med* 3, 12.
- Matsunaga, N., Tsuchimori, N., Matsumoto, T., Ii, M., 2011. TAK-242 (resatorvid), a small-molecule inhibitor of Toll-like receptor (TLR) 4 signaling, binds selectively to TLR4 and interferes with interactions between TLR4 and its adaptor molecules. *Mol Pharmacol* 79, 34-41.
- Mazot, P., Cazes, A., Dingli, F., Degoutin, J., Irinopoulou, T., Bouterin, M. C., Lombard, B., Loew, D., Hallberg, B., Palmer, R. H., Delattre, O., Janoueix-Lerosey, I., Vigny, M., 2012. Internalization and down-regulation of the ALK receptor in neuroblastoma cell lines upon monoclonal antibodies treatment. *PLoS One* 7, e33581.
- Meng, K., Rodriguez-Pena, A., Dimitrov, T., Chen, W., Yamin, M., Noda, M., Deuel, T. F., 2000. Pleiotrophin signals increased tyrosine phosphorylation of beta-catenin through inactivation of the intrinsic catalytic activity of the receptor-type protein tyrosine phosphatase beta/zeta. *Proc Natl Acad Sci U S A* 97, 2603-2608.

- Mews, P., Calipari, E. S., 2017. Cross-talk between the epigenome and neural circuits in drug addiction. *Prog Brain Res* 235, 19-63.
- Mi, R., Chen, W., Hoke, A., 2007. Pleiotrophin is a neurotrophic factor for spinal motor neurons. *Proc Natl Acad Sci U S A* 104, 4664-4669.
- Miao, J., Ding, M., Zhang, A., Xiao, Z., Qi, W., Luo, N., Di, W., Tao, Y., Fang, Y., 2012. Pleiotrophin promotes microglia proliferation and secretion of neurotrophic factors by activating extracellular signal-regulated kinase 1/2 pathway. *Neurosci Res* 74, 269-276.
- Miao, J., Wang, F., Wang, R., Zeng, J., Zheng, C., Zhuang, G., 2019. Pleiotrophin regulates functional heterogeneity of microglia cells in EAE animal models of multiple sclerosis by activating CCR-7/CD206 molecules and functional cytokines. *Am J Transl Res* 11, 2013-2027.
- Michael, B. D., Griffiths, M. J., Granerod, J., Brown, D., Keir, G., Wnek, M., Cox, D. J., Vidyasagar, R., Borrow, R., Parkes, L. M., Solomon, T., 2016. The Interleukin-1 Balance During Encephalitis Is Associated With Clinical Severity, Blood-Brain Barrier Permeability, Neuroimaging Changes, and Disease Outcome. *J Infect Dis* 213, 1651-1660.
- Mikelis, C., Koutsoumpa, M., Papadimitriou, E., 2007. Pleiotrophin as a possible new target for angiogenesis-related diseases and cancer. *Recent Pat Anticancer Drug Discov* 2, 175-186.
- Mikelis, C., Sfaelou, E., Koutsoumpa, M., Kieffer, N., Papadimitriou, E., 2009. Integrin alpha(v)beta(3) is a pleiotrophin receptor required for pleiotrophin-induced endothelial cell migration through receptor protein tyrosine phosphatase beta/zeta. *FASEB J* 23, 1459-1469.
- Milev, P., Meyer-Puttlitz, B., Margolis, R. K., Margolis, R. U., 1995. Complex-type asparagine-linked oligosaccharides on phosphacan and protein-tyrosine phosphatase-zeta/beta mediate their binding to neural cell adhesion molecules and tenascin. *J Biol Chem* 270, 24650-24653.
- Milner, P. G., Li, Y. S., Hoffman, R. M., Kodner, C. M., Siegel, N. R., Deuel, T. F., 1989. A novel 17 kD heparin-binding growth factor (HBGF-8) in bovine uterus: purification and N-terminal amino acid sequence. *Biochem Biophys Res Commun* 165, 1096-1103.
- Minnone, G., De Benedetti, F., Bracci-Laudiero, L., 2017. NGF and Its Receptors in the Regulation of Inflammatory Response. *Int J Mol Sci* 18.
- Mizumura, K., Murase, S., 2015. Role of nerve growth factor in pain. *Handb Exp Pharmacol* 227, 57-77.
- Mohammad Ahmadi Soleimani, S., Ekhtiari, H., Cadet, J. L., 2016. Drug-induced neurotoxicity in addiction medicine: From prevention to harm reduction. *Prog Brain Res* 223, 19-41.
- Monahan, A. J., Warren, M., Carvey, P. M., 2008. Neuroinflammation and peripheral immune infiltration in Parkinson's disease: an autoimmune hypothesis. *Cell Transplant* 17, 363-372.
- Monji, A., Yoshida, I., Tashiro, K., Hayashi, Y., Matsuda, K., Tashiro, N., 2000. Inhibition of A beta fibril formation and A beta-induced cytotoxicity by senile plaque-associated proteins. *Neurosci Lett* 278, 81-84.
- Moratalla, R., Khairnar, A., Simola, N., Granado, N., Garcia-Montes, J. R., Porceddu, P. F., Tizabi, Y., Costa, G., Morelli, M., 2017. Amphetamine-related drugs neurotoxicity in humans and in experimental animals: Main mechanisms. *Prog Neurobiol* 155, 149-170.
- Moretti, S., Franchi, S., Castelli, M., Amodeo, G., Somaini, L., Panerai, A., Sacerdote, P., 2015. Exposure of Adolescent Mice to Delta-9-Tetrahydrocannabinol Induces Long-Lasting Modulation of Pro- and Anti-Inflammatory Cytokines in Hypothalamus and Hippocampus Similar to that Observed for Peripheral Macrophages. *J Neuroimmune Pharmacol* 10, 371-379.
- Morganti, J. M., Riparip, L. K., Rosi, S., 2016. Call Off the Dog(ma): M1/M2 Polarization Is Concurrent following Traumatic Brain Injury. *PLoS One* 11, e0148001.
- Morisot, N., Berger, A. L., Phamluong, K., Cross, A., Ron, D., 2018. The Fyn kinase inhibitor, AZD0530, suppresses mouse alcohol self-administration and seeking. *Addict Biol*.

- Muramatsu, H., Muramatsu, T., 1991. Purification of recombinant midkine and examination of its biological activities: functional comparison of new heparin binding factors. *Biochem Biophys Res Commun* 177, 652-658.
- Muramatsu, T., 2010. Midkine, a heparin-binding cytokine with multiple roles in development, repair and diseases. *Proc Jpn Acad Ser B Phys Biol Sci* 86, 410-425.
- Muramatsu, T., 2011. Midkine: a promising molecule for drug development to treat diseases of the central nervous system. *Curr Pharm Des* 17, 410-423.
- Muramatsu, T., 2014. Structure and function of midkine as the basis of its pharmacological effects. *Br J Pharmacol* 171, 814-826.
- Muramatsu, T., Muramatsu, H., Kojima, T., 2006. Identification of proteoglycan-binding proteins. *Methods Enzymol* 416, 263-278.
- Najem, S., Langemann, D., Appl, B., Trochimiuk, M., Hundsdorfer, P., Reinshagen, K., Eschenburg, G., 2016. Smac mimetic LCL161 supports neuroblastoma chemotherapy in a drug class-dependent manner and synergistically interacts with ALK inhibitor TAE684 in cells with ALK mutation F1174L. *Oncotarget* 7, 72634-72653.
- Nakamura, E., Kadomatsu, K., Yuasa, S., Muramatsu, H., Mamiya, T., Nabeshima, T., Fan, Q. W., Ishiguro, K., Igakura, T., Matsubara, S., Kaname, T., Horiba, M., Saito, H., Muramatsu, T., 1998. Disruption of the midkine gene (Mdk) resulted in altered expression of a calcium binding protein in the hippocampus of infant mice and their abnormal behaviour. *Genes Cells* 3, 811-822.
- Nandi, S., Cioce, M., Yeung, Y. G., Nieves, E., Tesfa, L., Lin, H., Hsu, A. W., Halenbeck, R., Cheng, H. Y., Gokhan, S., Mehler, M. F., Stanley, E. R., 2013. Receptor-type protein-tyrosine phosphatase zeta is a functional receptor for interleukin-34. *J Biol Chem* 288, 21972-21986.
- Nduhirabandi, F., Lamont, K., Albertyn, Z., Opie, L. H., Lecour, S., 2016. Role of toll-like receptor 4 in melatonin-induced cardioprotection. *J Pineal Res* 60, 39-47.
- NIAAA, N. I. o. D. A. a. A., 2019. Alcohol facts and Statistics. National Institute on Drug Abuse and Alcoholism.
- Niisato, K., Fujikawa, A., Komai, S., Shintani, T., Watanabe, E., Sakaguchi, G., Katsuura, G., Manabe, T., Noda, M., 2005. Age-dependent enhancement of hippocampal long-term potentiation and impairment of spatial learning through the Rho-associated kinase pathway in protein tyrosine phosphatase receptor type Z-deficient mice. *J Neurosci* 25, 1081-1088.
- Nikolakopoulou, A. M., Montagne, A., Kisler, K., Dai, Z., Wang, Y., Huuskonen, M. T., Sagare, A. P., Lazic, D., Sweeney, M. D., Kong, P., Wang, M., Owens, N. C., Lawson, E. J., Xie, X., Zhao, Z., Zlokovic, B. V., 2019. Pericyte loss leads to circulatory failure and pleiotrophin depletion causing neuron loss. *Nat Neurosci* 22, 1089-1098.
- Nishiwaki, T., Maeda, N., Noda, M., 1998. Characterization and developmental regulation of proteoglycan-type protein tyrosine phosphatase zeta/RPTPbeta isoforms. *J Biochem* 123, 458-467.
- Nolen-Hoeksema, S., Hilt, L., 2006. Possible contributors to the gender differences in alcohol use and problems. *J Gen Psychol* 133, 357-374.
- Norden, D. M., Fenn, A. M., Dugan, A., Godbout, J. P., 2014. TGFbeta produced by IL-10 redirected astrocytes attenuates microglial activation. *Glia* 62, 881-895.
- Norden, D. M., Trojanowski, P. J., Villanueva, E., Navarro, E., Godbout, J. P., 2016. Sequential activation of microglia and astrocyte cytokine expression precedes increased Iba-1 or GFAP immunoreactivity following systemic immune challenge. *Glia* 64, 300-316.
- O.E.D.T., 2019. Informe Europeo sobre drogas 2019: Tendencias y novedades. Oficina de Publicaciones de la Unión Europea, Luxemburgo, p. 100.
- O'Callaghan, J. P., Kelly, K. A., VanGilder, R. L., Sofroniew, M. V., Miller, D. B., 2014. Early activation of STAT3 regulates reactive astrogliosis induced by diverse forms of neurotoxicity. *PLoS One* 9, e102003.

- Obad, A., Peeran, A., Little, J. I., Haddad, G. E., Tarzami, S. T., 2018. Alcohol-Mediated Organ Damages: Heart and Brain. *Front Pharmacol* 9, 81.
- Ohgake, S., Shimizu, E., Hashimoto, K., Okamura, N., Koike, K., Koizumi, H., Fujisaki, M., Kanahara, N., Matsuda, S., Sutoh, C., Matsuzawa, D., Muramatsu, H., Muramatsu, T., Iyo, M., 2009. Dopaminergic hypofunctions and prepulse inhibition deficits in mice lacking midkine. *Prog Neuropsychopharmacol Biol Psychiatry* 33, 541-546.
- Ohnishi, H., Murata, Y., Okazawa, H., Matozaki, T., 2011. Src family kinases: modulators of neurotransmitter receptor function and behavior. *Trends Neurosci* 34, 629-637.
- Ooboshi, H., 2011. Gene therapy as a novel pharmaceutical intervention for stroke. *Curr Pharm Des* 17, 424-433.
- Oscar-Berman, M., Bowirrat, A., 2005. Genetic influences in emotional dysfunction and alcoholism-related brain damage. *Neuropsychiatr Dis Treat* 1, 211-229.
- Ostman, A., Hellberg, C., Bohmer, F. D., 2006. Protein-tyrosine phosphatases and cancer. *Nat Rev Cancer* 6, 307-320.
- Owada, K., Sanjo, N., Kobayashi, T., Mizusawa, H., Muramatsu, H., Muramatsu, T., Michikawa, M., 1999. Midkine inhibits caspase-dependent apoptosis via the activation of mitogen-activated protein kinase and phosphatidylinositol 3-kinase in cultured neurons. *J Neurochem* 73, 2084-2092.
- Palmisano, M., Pandey, S. C., 2017. Epigenetic mechanisms of alcoholism and stress-related disorders. *Alcohol* 60, 7-18.
- Panicker, N., Saminathan, H., Jin, H., Neal, M., Harischandra, D. S., Gordon, R., Kanthasamy, K., Lawana, V., Sarkar, S., Luo, J., Anantharam, V., Kanthasamy, A. G., Kanthasamy, A., 2015. Fyn Kinase Regulates Microglial Neuroinflammatory Responses in Cell Culture and Animal Models of Parkinson's Disease. *J Neurosci* 35, 10058-10077.
- Panicker, N., Sarkar, S., Harischandra, D. S., Neal, M., Kam, T. I., Jin, H., Saminathan, H., Langley, M., Charli, A., Samidurai, M., Rokad, D., Ghaisas, S., Pletnikova, O., Dawson, V. L., Dawson, T. M., Anantharam, V., Kanthasamy, A. G., Kanthasamy, A., 2019. Fyn kinase regulates misfolded alpha-synuclein uptake and NLRP3 inflammasome activation in microglia. *J Exp Med* 216, 1411-1430.
- Papadimitriou, E., Mikelis, C., Lampropoulou, E., Koutsioumpa, M., Theochari, K., Tsirmoula, S., Theodoropoulou, C., Lamprou, M., Sfaelou, E., Vourtsis, D., Boudouris, P., 2009. Roles of pleiotrophin in tumor growth and angiogenesis. *Eur Cytokine Netw* 20, 180-190.
- Papadimitriou, E., Pantazaka, E., Castana, P., Tsalios, T., Polyzos, A., Beis, D., 2016. Pleiotrophin and its receptor protein tyrosine phosphatase beta/zeta as regulators of angiogenesis and cancer. *Biochim Biophys Acta* 1866, 252-265.
- Papageorgiou, M., Raza, A., Fraser, S., Nurgali, K., Apostolopoulos, V., 2019. Methamphetamine and its immune-modulating effects. *Maturitas* 121, 13-21.
- Pariser, H., Ezquerra, L., Herradon, G., Perez-Pinera, P., Deuel, T. F., 2005a. Fyn is a downstream target of the pleiotrophin/receptor protein tyrosine phosphatase beta/zeta-signaling pathway: regulation of tyrosine phosphorylation of Fyn by pleiotrophin. *Biochem Biophys Res Commun* 332, 664-669.
- Pariser, H., Herradon, G., Ezquerra, L., Perez-Pinera, P., Deuel, T. F., 2005b. Pleiotrophin regulates serine phosphorylation and the cellular distribution of beta-adducin through activation of protein kinase C. *Proc Natl Acad Sci U S A* 102, 12407-12412.
- Pariser, H., Perez-Pinera, P., Ezquerra, L., Herradon, G., Deuel, T. F., 2005c. Pleiotrophin stimulates tyrosine phosphorylation of beta-adducin through inactivation of the transmembrane receptor protein tyrosine phosphatase beta/zeta. *Biochem Biophys Res Commun* 335, 232-239.
- Pastor, I. J., Laso, F. J., Ines, S., Marcos, M., Gonzalez-Sarmiento, R., 2009. Genetic association between -93A/G polymorphism in the Fyn kinase gene and alcohol dependence in Spanish men. *Eur Psychiatry* 24, 191-194.

- Pastor, M., Fernandez-Calle, R., Di Geronimo, B., Vicente-Rodriguez, M., Zapico, J. M., Gramage, E., Coderch, C., Perez-Garcia, C., Lasek, A. W., Puchades-Carrasco, L., Pineda-Lucena, A., de Pascual-Teresa, B., Herradon, G., Ramos, A., 2018. Development of inhibitors of receptor protein tyrosine phosphatase beta/zeta (PTPRZ1) as candidates for CNS disorders. *Eur J Med Chem* 144, 318-329.
- Peckham, H., Giuffrida, L., Wood, R., Gonsalvez, D., Ferner, A., Kilpatrick, T. J., Murray, S. S., Xiao, J., 2016. Fyn is an intermediate kinase that BDNF utilizes to promote oligodendrocyte myelination. *Glia* 64, 255-269.
- Perez-Pinera, P., Zhang, W., Chang, Y., Vega, J. A., Deuel, T. F., 2007. Anaplastic lymphoma kinase is activated through the pleiotrophin/receptor protein-tyrosine phosphatase beta/zeta signaling pathway: an alternative mechanism of receptor tyrosine kinase activation. *J Biol Chem* 282, 28683-28690.
- Pryce, K. D., Powell, R., Agwa, D., Evely, K. M., Sheehan, G. D., Nip, A., Tomasello, D. L., Gururaj, S., Bhattacharjee, A., 2019. Magi-1 scaffolds NaV1.8 and Slack KNa channels in dorsal root ganglion neurons regulating excitability and pain. *FASEB J* 33, 7315-7330.
- Qu, J., Tao, X. Y., Teng, P., Zhang, Y., Guo, C. L., Hu, L., Qian, Y. N., Jiang, C. Y., Liu, W. T., 2017. Blocking ATP-sensitive potassium channel alleviates morphine tolerance by inhibiting HSP70-TLR4-NLRP3-mediated neuroinflammation. *J Neuroinflammation* 14, 228.
- Raedler, L. A., 2015. Zykadia (Ceritinib) Approved for Patients with Crizotinib-Resistant ALK - Positive Non-Small-Cell Lung Cancer. *Am Health Drug Benefits* 8, 163-166.
- Ramirez-Exposito, M. J., Martinez-Martos, J. M., 1998. [Structure and functions of the macroglia in the central nervous system. Response to degenerative disorders]. *Rev Neurol* 26, 600-611.
- Raulo, E., Chernousov, M. A., Carey, D. J., Nolo, R., Rauvala, H., 1994. Isolation of a neuronal cell surface receptor of heparin binding growth-associated molecule (HB-GAM). Identification as N-syndecan (syndecan-3). *J Biol Chem* 269, 12999-13004.
- Rauvala, H., 1989. An 18-kd heparin-binding protein of developing brain that is distinct from fibroblast growth factors. *Embo j* 8, 2933-2941.
- Rehm, J., Gmel, G. E., Sr., Gmel, G., Hasan, O. S. M., Imtiaz, S., Popova, S., Probst, C., Roerecke, M., Room, R., Samokhvalov, A. V., Shield, K. D., Shuper, P. A., 2017. The relationship between different dimensions of alcohol use and the burden of disease-an update. *Addiction* 112, 968-1001.
- Reiff, T., Huber, L., Kramer, M., Delattre, O., Janoueix-Lerosey, I., Rohrer, H., 2011. Midkine and Alk signaling in sympathetic neuron proliferation and neuroblastoma predisposition. *Development* 138, 4699-4708.
- Remick, D., 2013. Use of animal models for the study of human disease-a shock society debate. *Shock* 40, 345-346.
- Resh, M. D., 1998. Fyn, a Src family tyrosine kinase. *Int J Biochem Cell Biol* 30, 1159-1162.
- Ridet, J. L., Malhotra, S. K., Privat, A., Gage, F. H., 1997. Reactive astrocytes: cellular and molecular cues to biological function. *Trends Neurosci* 20, 570-577.
- Rodriguez, J. J., Yeh, C. Y., Terzieva, S., Olabarria, M., Kulijewicz-Nawrot, M., Verkhratsky, A., 2014. Complex and region-specific changes in astroglial markers in the aging brain. *Neurobiol Aging* 35, 15-23.
- Rohrbough, J., Broadie, K., 2010. Anterograde Jelly belly ligand to Alk receptor signaling at developing synapses is regulated by Mind the gap. *Development* 137, 3523-3533.
- Ron, D., Berger, A., 2018. Targeting the intracellular signaling "STOP" and "GO" pathways for the treatment of alcohol use disorders. *Psychopharmacology (Berl)* 235, 1727-1743.
- Roskoski, R., Jr., 2005. Src kinase regulation by phosphorylation and dephosphorylation. *Biochem Biophys Res Commun* 331, 1-14.

- Roskoski, R., Jr., 2013. Anaplastic lymphoma kinase (ALK): structure, oncogenic activation, and pharmacological inhibition. *Pharmacol Res* 68, 68-94.
- Rubio-Araiz, A., Porcu, F., Perez-Hernandez, M., Garcia-Gutierrez, M. S., Aracil-Fernandez, M. A., Gutierrez-Lopez, M. D., Guerri, C., Manzanares, J., O'Shea, E., Colado, M. I., 2017. Disruption of blood-brain barrier integrity in postmortem alcoholic brain: preclinical evidence of TLR4 involvement from a binge-like drinking model. *Addict Biol* 22, 1103-1116.
- Sakakima, H., Yoshida, Y., Yamazaki, Y., Matsuda, F., Ikutomo, M., Ijiri, K., Muramatsu, H., Muramatsu, T., Kadomatsu, K., 2009. Disruption of the midkine gene (Mdk) delays degeneration and regeneration in injured peripheral nerve. *J Neurosci Res* 87, 2908-2915.
- Salama, R. H., Muramatsu, H., Shimizu, E., Hashimoto, K., Ohgake, S., Watanabe, H., Komatsu, N., Okamura, N., Koike, K., Shinoda, N., Okada, S., Iyo, M., Muramatsu, T., 2005. Increased midkine levels in sera from patients with Alzheimer's disease. *Prog Neuropsychopharmacol Biol Psychiatry* 29, 611-616.
- Sato, W., Kadomatsu, K., Yuzawa, Y., Muramatsu, H., Hotta, N., Matsuo, S., Muramatsu, T., 2001. Midkine is involved in neutrophil infiltration into the tubulointerstitium in ischemic renal injury. *J Immunol* 167, 3463-3469.
- Satoh, J., Muramatsu, H., Moretto, G., Muramatsu, T., Chang, H. J., Kim, S. T., Cho, J. M., Kim, S. U., 1993. Midkine that promotes survival of fetal human neurons is produced by fetal human astrocytes in culture. *Brain Res Dev Brain Res* 75, 201-205.
- Schumann, G., Rujescu, D., Kissling, C., Soyka, M., Dahmen, N., Preuss, U. W., Wieman, S., Depner, M., Wellek, S., Lascorz, J., Bondy, B., Giegling, I., Anghelescu, I., Cowen, M. S., Poustka, A., Spanagel, R., Mann, K., Henn, F. A., Szegedi, A., 2003. Analysis of genetic variations of protein tyrosine kinase *fyn* and their association with alcohol dependence in two independent cohorts. *Biol Psychiatry* 54, 1422-1426.
- Schweitzer, P., Cates-Gatto, C., Varodayan, F. P., Nadav, T., Roberto, M., Lasek, A. W., Roberts, A. J., 2016. Dependence-induced ethanol drinking and GABA neurotransmission are altered in *Alk* deficient mice. *Neuropharmacology* 107, 1-8.
- Senis, Y. A., Barr, A. J., 2018. Targeting Receptor-Type Protein Tyrosine Phosphatases with Biotherapeutics: Is Outside-in Better than Inside-Out? *Molecules* 23.
- Sevillano, J., Sanchez-Alonso, M. G., Zapateria, B., Calderon, M., Alcalá, M., Limones, M., Pita, J., Gramage, E., Vicente-Rodriguez, M., Horrillo, D., Medina-Gomez, G., Obregon, M. J., Viana, M., Valladolid-Acebes, I., Herradon, G., Ramos-Alvarez, M. P., 2019. Pleiotrophin deletion alters glucose homeostasis, energy metabolism and brown fat thermogenic function in mice. *Diabetologia* 62, 123-135.
- Shabab, T., Khanabdali, R., Moghadamtousi, S. Z., Kadir, H. A., Mohan, G., 2017. Neuroinflammation pathways: a general review. *Int J Neurosci* 127, 624-633.
- Shanks, R. A., Anderson, J. R., Taylor, J. R., Lloyd, S. A., 2012. Amphetamine and methamphetamine have a direct and differential effect on BV2 microglia cells. *Bull Exp Biol Med* 154, 228-232.
- Sharma, H. S., Sjoquist, P. O., Ali, S. F., 2007. Drugs of abuse-induced hyperthermia, blood-brain barrier dysfunction and neurotoxicity: neuroprotective effects of a new antioxidant compound H-290/51. *Curr Pharm Des* 13, 1903-1923.
- Sharma, S., Carlson, S., Puttachary, S., Sarkar, S., Showman, L., Putra, M., Kanthasamy, A. G., Thippeswamy, T., 2018. Role of the *Fyn*-PKC δ signaling in SE-induced neuroinflammation and epileptogenesis in experimental models of temporal lobe epilepsy. *Neurobiol Dis* 110, 102-121.
- Shen, Y., Qin, H., Chen, J., Mou, L., He, Y., Yan, Y., Zhou, H., Lv, Y., Chen, Z., Wang, J., Zhou, Y. D., 2016. Postnatal activation of TLR4 in astrocytes promotes excitatory synaptogenesis in hippocampal neurons. *J Cell Biol* 215, 719-734.

- Shi, J., Zhao, Y., Wang, Y., Gao, W., Ding, J., Li, P., Hu, L., Shao, F., 2014. Inflammatory caspases are innate immune receptors for intracellular LPS. *Nature* 514, 187-192.
- Shintani, T., Maeda, N., Nishiwaki, T., Noda, M., 1997. Characterization of rat receptor-like protein tyrosine phosphatase gamma isoforms. *Biochem Biophys Res Commun* 230, 419-425.
- Shintani, T., Noda, M., 2008. Protein tyrosine phosphatase receptor type Z dephosphorylates TrkA receptors and attenuates NGF-dependent neurite outgrowth of PC12 cells. *J Biochem* 144, 259-266.
- Shintani, T., Watanabe, E., Maeda, N., Noda, M., 1998. Neurons as well as astrocytes express proteoglycan-type protein tyrosine phosphatase zeta/RPTPbeta: analysis of mice in which the PTPzeta/RPTPbeta gene was replaced with the LacZ gene. *Neurosci Lett* 247, 135-138.
- Sil, S., Niu, F., Tom, E., Liao, K., Periyasamy, P., Buch, S., 2019. Cocaine Mediated Neuroinflammation: Role of Dysregulated Autophagy in Pericytes. *Mol Neurobiol* 56, 3576-3590.
- Skaper, S. D., 2018. Neurotrophic Factors: An Overview. *Methods Mol Biol* 1727, 1-17.
- Sochocka, M., Diniz, B. S., Leszek, J., 2017. Inflammatory Response in the CNS: Friend or Foe? *Mol Neurobiol* 54, 8071-8089.
- Soda, M., Choi, Y. L., Enomoto, M., Takada, S., Yamashita, Y., Ishikawa, S., Fujiwara, S., Watanabe, H., Kurashina, K., Hatanaka, H., Bando, M., Ohno, S., Ishikawa, Y., Aburatani, H., Niki, T., Sohara, Y., Sugiyama, Y., Mano, H., 2007. Identification of the transforming EML4-ALK fusion gene in non-small-cell lung cancer. *Nature* 448, 561-566.
- Sorrelle, N., Dominguez, A. T. A., Brekken, R. A., 2017. From top to bottom: midkine and pleiotrophin as emerging players in immune regulation. *J Leukoc Biol* 102, 277-286.
- Stiegler, A. L., Boggon, T. J., 2017. p190RhoGAP proteins contain pseudoGTPase domains. *Nat Commun* 8, 506.
- Stoica, G. E., Kuo, A., Aigner, A., Sunitha, I., Souttou, B., Malerczyk, C., Caughey, D. J., Wen, D., Karavanov, A., Riegel, A. T., Wellstein, A., 2001. Identification of anaplastic lymphoma kinase as a receptor for the growth factor pleiotrophin. *J Biol Chem* 276, 16772-16779.
- Stoica, G. E., Kuo, A., Powers, C., Bowden, E. T., Sale, E. B., Riegel, A. T., Wellstein, A., 2002. Midkine binds to anaplastic lymphoma kinase (ALK) and acts as a growth factor for different cell types. *J Biol Chem* 277, 35990-35998.
- Strazielle, N., Gherzi-Egea, J. F., 2016. Potential Pathways for CNS Drug Delivery Across the Blood-Cerebrospinal Fluid Barrier. *Curr Pharm Des* 22, 5463-5476.
- Streit, W. J., Xue, Q. S., Braak, H., del Tredici, K., 2014. Presence of severe neuroinflammation does not intensify neurofibrillary degeneration in human brain. *Glia* 62, 96-105.
- Su, H. P., Rickert, K., Burlein, C., Narayan, K., Bukhtiyarova, M., Hurzy, D. M., Stump, C. A., Zhang, X., Reid, J., Krasowska-Zoladek, A., Tummala, S., Shipman, J. M., Kornienko, M., Lemaire, P. A., Krosky, D., Heller, A., Achab, A., Chamberlin, C., Saradjian, P., Sauvagnat, B., Yang, X., Ziebell, M. R., Nickbarg, E., Sanders, J. M., Bilodeau, M. T., Carroll, S. S., Lumb, K. J., Soisson, S. M., Henze, D. A., Cooke, A. J., 2017. Structural characterization of nonactive site, TrkA-selective kinase inhibitors. *Proc Natl Acad Sci U S A* 114, E297-E306.
- Suk, K., 2016. Lipocalin-2 as a therapeutic target for brain injury: An astrocentric perspective. *Prog Neurobiol* 144, 158-172.
- Sumi, N., Nishioku, T., Takata, F., Matsumoto, J., Watanabe, T., Shuto, H., Yamauchi, A., Dohgu, S., Kataoka, Y., 2010. Lipopolysaccharide-activated microglia induce dysfunction of the blood-brain barrier in rat microvascular endothelial cells co-cultured with microglia. *Cell Mol Neurobiol* 30, 247-253.
- Szepesi, Z., Manouchehrian, O., Bachiller, S., Deierborg, T., 2018. Bidirectional Microglia-Neuron Communication in Health and Disease. *Front Cell Neurosci* 12, 323.

- Takada, T., Toriyama, K., Muramatsu, H., Song, X. J., Torii, S., Muramatsu, T., 1997. Midkine, a retinoic acid-inducible heparin-binding cytokine in inflammatory responses: chemotactic activity to neutrophils and association with inflammatory synovitis. *J Biochem* 122, 453-458.
- Takei, Y., Kadomatsu, K., Matsuo, S., Itoh, H., Nakazawa, K., Kubota, S., Muramatsu, T., 2001. Antisense oligodeoxynucleotide targeted to Midkine, a heparin-binding growth factor, suppresses tumorigenicity of mouse rectal carcinoma cells. *Cancer Res* 61, 8486-8491.
- Takeuchi, O., Akira, S., 2001. Toll-like receptors; their physiological role and signal transduction system. *Int Immunopharmacol* 1, 625-635.
- Tamura, H., Fukada, M., Fujikawa, A., Noda, M., 2006. Protein tyrosine phosphatase receptor type Z is involved in hippocampus-dependent memory formation through dephosphorylation at Y1105 on p190 RhoGAP. *Neurosci Lett* 399, 33-38.
- Tang, C., Wang, M., Wang, P., Wang, L., Wu, Q., Guo, W., 2019. Neural Stem Cells Behave as a Functional Niche for the Maturation of Newborn Neurons through the Secretion of PTN. *Neuron* 101, 32-44 e36.
- Tang, S. L., Gao, Y. L., Chen, X. B., 2015. Wnt/beta-catenin up-regulates Midkine expression in glioma cells. *Int J Clin Exp Med* 8, 12644-12649.
- Tang, Y., Le, W., 2016. Differential Roles of M1 and M2 Microglia in Neurodegenerative Diseases. *Mol Neurobiol* 53, 1181-1194.
- Tanga, N., Kuboyama, K., Kishimoto, A., Kihara, M., Kiyonari, H., Watanabe, T., Fujikawa, A., Noda, M., 2019. Behavioral and neurological analyses of adult mice carrying null and distinct loss-of-receptor function mutations in protein tyrosine phosphatase receptor type Z (PTPRZ). *PLoS One* 14, e0217880.
- Travini, I. R., Chertoff, M., Cafferata, E. G., Courty, J., Murer, M. G., Pitossi, F. J., Gershanik, O. S., 2011. Pleiotrophin over-expression provides trophic support to dopaminergic neurons in parkinsonian rats. *Mol Neurodegener* 6, 40.
- Tarr, A. J., Liu, X., Reed, N. S., Quan, N., 2014. Kinetic characteristics of euflammation: the induction of controlled inflammation without overt sickness behavior. *Brain Behav Immun* 42, 96-108.
- Thurgur, H., Pinteaux, E., 2019. Microglia in the Neurovascular Unit: Blood-Brain Barrier-microglia Interactions After Central Nervous System Disorders. *Neuroscience* 405, 55-67.
- Tonks, N. K., 2006. Protein tyrosine phosphatases: from genes, to function, to disease. *Nat Rev Mol Cell Biol* 7, 833-846.
- Tyler, R. E., Kim, S. W., Guo, M., Jang, Y. J., Damadzic, R., Stodden, T., Vendruscolo, L. F., Koob, G. F., Wang, G. J., Wiers, C. E., Volkow, N. D., 2019. Detecting neuroinflammation in the brain following chronic alcohol exposure in rats: A comparison between in vivo and in vitro TSPO radioligand binding. *Eur J Neurosci*.
- Tzschentke, T. M., 2007. Measuring reward with the conditioned place preference (CPP) paradigm: update of the last decade. *Addict Biol* 12, 227-462.
- Uhl, G. R., Martinez, M. J., 2019. PTPRD: neurobiology, genetics, and initial pharmacology of a pleiotropic contributor to brain phenotypes. *Ann N Y Acad Sci* 1451, 112-129.
- Um, J. W., Nygaard, H. B., Heiss, J. K., Kostylev, M. A., Stagi, M., Vortmeyer, A., Wisniewski, T., Gunther, E. C., Strittmatter, S. M., 2012. Alzheimer amyloid-beta oligomer bound to postsynaptic prion protein activates Fyn to impair neurons. *Nat Neurosci* 15, 1227-1235.
- UNODC, U. N. O. o. D. a. C., 2019. World Drug Report. United Nations Office on Drugs and Crime, Viena, p. 80.
- Valenta, T., Hausmann, G., Basler, K., 2012. The many faces and functions of beta-catenin. *Embo j* 31, 2714-2736.

- Vernersson, E., Khoo, N. K., Henriksson, M. L., Roos, G., Palmer, R. H., Hallberg, B., 2006. Characterization of the expression of the ALK receptor tyrosine kinase in mice. *Gene Expr Patterns* 6, 448-461.
- Vicente-Rodriguez, M., Fernandez-Calle, R., Gramage, E., Perez-Garcia, C., Ramos, M. P., Herradon, G., 2016a. Midkine Is a Novel Regulator of Amphetamine-Induced Striatal Gliosis and Cognitive Impairment: Evidence for a Stimulus-Dependent Regulation of Neuroinflammation by Midkine. *Mediators Inflamm* 2016, 9894504.
- Vicente-Rodriguez, M., Herradon, G., Ferrer-Alcon, M., Uribarri, M., Perez-Garcia, C., 2015. Chronic Cocaine Use Causes Changes in the Striatal Proteome Depending on the Endogenous Expression of Pleiotrophin. *Chem Res Toxicol* 28, 1443-1454.
- Vicente-Rodriguez, M., Perez-Garcia, C., Ferrer-Alcon, M., Uribarri, M., Sanchez-Alonso, M. G., Ramos, M. P., Herradon, G., 2014a. Pleiotrophin differentially regulates the rewarding and sedative effects of ethanol. *J Neurochem* 131, 688-695.
- Vicente-Rodriguez, M., Perez-Garcia, C., Haro, M., Ramos, M. P., Herradon, G., 2014b. Genetic inactivation of midkine modulates behavioural responses to ethanol possibly by enhancing GABA(A) receptor sensitivity to GABA(A) acting drugs. *Behav Brain Res* 274, 258-263.
- Vicente-Rodriguez, M., Rojo Gonzalez, L., Gramage, E., Fernandez-Calle, R., Chen, Y., Perez-Garcia, C., Ferrer-Alcon, M., Uribarri, M., Bailey, A., Herradon, G., 2016b. Pleiotrophin overexpression regulates amphetamine-induced reward and striatal dopaminergic denervation without changing the expression of dopamine D1 and D2 receptors: Implications for neuroinflammation. *Eur Neuropsychopharmacol* 26, 1794-1805.
- Wake, H., Lee, P. R., Fields, R. D., 2011. Control of local protein synthesis and initial events in myelination by action potentials. *Science* 333, 1647-1651.
- Walker, B. M., Valdez, G. R., McLaughlin, J. P., Bakalkin, G., 2012. Targeting dynorphin/kappa opioid receptor systems to treat alcohol abuse and dependence. *Alcohol* 46, 359-370.
- Walters, R. K., Polimanti, R., Johnson, E. C., McClintick, J. N., Adams, M. J., Adkins, A. E., Aliev, F., Bacanu, S. A., Batzler, A., Bertelsen, S., Biernacka, J. M., Bigdeli, T. B., Chen, L. S., Clarke, T. K., Chou, Y. L., Degenhardt, F., Docherty, A. R., Edwards, A. C., Fontanillas, P., Foo, J. C., Fox, L., Frank, J., Giegling, I., Gordon, S., Hack, L. M., Hartmann, A. M., Hartz, S. M., Heilmann-Heimbach, S., Herms, S., Hodgkinson, C., Hoffmann, P., Jan Hottenga, J., Kennedy, M. A., Alanne-Kinnunen, M., Konte, B., Lahti, J., Lahti-Pulkkinen, M., Lai, D., Ligthart, L., Loukola, A., Maher, B. S., Mbarek, H., McIntosh, A. M., McQueen, M. B., Meyers, J. L., Milaneschi, Y., Palviainen, T., Pearson, J. F., Peterson, R. E., Ripatti, S., Ryu, E., Saccone, N. L., Salvatore, J. E., Sanchez-Roige, S., Schwandt, M., Sherva, R., Streit, F., Strohmaier, J., Thomas, N., Wang, J. C., Webb, B. T., Wedow, R., Wetherill, L., Wills, A. G., Boardman, J. D., Chen, D., Choi, D. S., Copeland, W. E., Culverhouse, R. C., Dahmen, N., Degenhardt, L., Domingue, B. W., Elson, S. L., Frye, M. A., Gabel, W., Hayward, C., Ising, M., Keyes, M., Kiefer, F., Kramer, J., Kuperman, S., Lucae, S., Lynskey, M. T., Maier, W., Mann, K., Mannisto, S., Muller-Myhsok, B., Murray, A. D., Nurnberger, J. I., Palotie, A., Preuss, U., Raikkonen, K., Reynolds, M. D., Ridinger, M., Scherbaum, N., Schuckit, M. A., Soyka, M., Treutlein, J., Witt, S., Wodarz, N., Zill, P., Adkins, D. E., Boden, J. M., Boomsma, D. I., Bierut, L. J., Brown, S. A., Bucholz, K. K., Cichon, S., Costello, E. J., de Wit, H., Diazgranados, N., Dick, D. M., Eriksson, J. G., Farrer, L. A., Foroud, T. M., Gillespie, N. A., Goate, A. M., Goldman, D., Grucza, R. A., Hancock, D. B., Harris, K. M., Heath, A. C., Hesselbrock, V., Hewitt, J. K., Hopfer, C. J., Horwood, J., Iacono, W., Johnson, E. O., Kaprio, J. A., Karpyak, V. M., Kendler, K. S., Kranzler, H. R., Krauter, K., Lichtenstein, P., Lind, P. A., McGue, M., MacKillop, J., Madden, P. A. F., Maes, H. H., Magnusson, P., Martin, N. G., Medland, S. E., Montgomery, G. W., Nelson, E. C., Nothen, M. M., Palmer, A. A., Pedersen, N. L., Penninx, B., Porjesz, B., Rice, J. P., Rietschel, M., Riley, B. P., Rose, R., Rujescu, D., Shen, P. H., Silberg, J., Stallings, M. C., Tarter, R. E., Vanyukov, M. M., Vrieze, S., Wall, T. L., Whitfield, J. B., Zhao, H., Neale, B. M., Gelernter, J., Edenberg, H. J., Agrawal, A., 2018. Transancestral GWAS of alcohol dependence reveals common genetic underpinnings with psychiatric disorders. *Nat Neurosci* 21, 1656-1669.

- Wang, J., Takeuchi, H., Sonobe, Y., Jin, S., Mizuno, T., Miyakawa, S., Fujiwara, M., Nakamura, Y., Kato, T., Muramatsu, H., Muramatsu, T., Suzumura, A., 2008. Inhibition of midkine alleviates experimental autoimmune encephalomyelitis through the expansion of regulatory T cell population. *Proc Natl Acad Sci U S A* 105, 3915-3920.
- Wang, K. S., Liu, X., Zhang, Q., Pan, Y., Aragam, N., Zeng, M., 2011. A meta-analysis of two genome-wide association studies identifies 3 new loci for alcohol dependence. *J Psychiatr Res* 45, 1419-1425.
- Weckbach, L. T., Muramatsu, T., Walzog, B., 2011. Midkine in inflammation. *ScientificWorldJournal* 11, 2491-2505.
- Wellstein, A., 2012. ALK receptor activation, ligands and therapeutic targeting in glioblastoma and in other cancers. *Front Oncol* 2, 192.
- WHO, W. H. O., 2017. alcohol fact sheet, 2.
- WHO, W. H. O., 2018. Global status report on alcohol and health 2018, Geneva.
- Wilkinson, D. A., Carlen, P. L., 1980. Neuropsychological and neurological assessment of alcoholism; discrimination between groups of alcoholics. *J Stud Alcohol* 41, 129-139.
- Xing, C., Li, W., Deng, W., Ning, M., Lo, E. H., 2018. A potential gliovascular mechanism for microglial activation: differential phenotypic switching of microglia by endothelium versus astrocytes. *J Neuroinflammation* 15, 143.
- Xu, C., Zhu, S., Wu, M., Han, W., Yu, Y., 2014. Functional receptors and intracellular signal pathways of midkine (MK) and pleiotrophin (PTN). *Biol Pharm Bull* 37, 511-520.
- Xu, E., Liu, J., Liu, H., Wang, X., Xiong, H., 2017a. Role of microglia in methamphetamine-induced neurotoxicity. *Int J Physiol Pathophysiol Pharmacol* 9, 84-100.
- Xu, E., Liu, J., Wang, X., Xiong, H., 2017b. Inflammasome in drug abuse. *Int J Physiol Pathophysiol Pharmacol* 9, 165-177.
- Xu, Y., Fisher, G. J., 2012. Receptor type protein tyrosine phosphatases (RPTPs) - roles in signal transduction and human disease. *J Cell Commun Signal* 6, 125-138.
- Yaka, R., Tang, K. C., Camarini, R., Janak, P. H., Ron, D., 2003. Fyn kinase and NR2B-containing NMDA receptors regulate acute ethanol sensitivity but not ethanol intake or conditioned reward. *Alcohol Clin Exp Res* 27, 1736-1742.
- Yao, J., Ma, Q., Wang, L., Zhang, M., 2009. Pleiotrophin expression in human pancreatic cancer and its correlation with clinicopathological features, perineural invasion, and prognosis. *Dig Dis Sci* 54, 895-901.
- Yao, S., Cheng, M., Zhang, Q., Wasik, M., Kelsh, R., Winkler, C., 2013. Anaplastic lymphoma kinase is required for neurogenesis in the developing central nervous system of zebrafish. *PLoS One* 8, e63757.
- Yeh, H. J., He, Y. Y., Xu, J., Hsu, C. Y., Deuel, T. F., 1998. Upregulation of pleiotrophin gene expression in developing microvasculature, macrophages, and astrocytes after acute ischemic brain injury. *J Neurosci* 18, 3699-3707.
- Yoshida, Y., Ikematsu, S., Moritoyo, T., Goto, M., Tsutsui, J., Sakuma, S., Osame, M., Muramatsu, T., 2001. Intraventricular administration of the neurotrophic factor midkine ameliorates hippocampal delayed neuronal death following transient forebrain ischemia in gerbils. *Brain Res* 894, 46-55.
- Yu, G. S., Hu, J., Nakagawa, H., 1998. Inhibition of beta-amyloid cytotoxicity by midkine. *Neurosci Lett* 254, 125-128.
- Zamanian, J. L., Xu, L., Foo, L. C., Nouri, N., Zhou, L., Giffard, R. G., Barres, B. A., 2012. Genomic analysis of reactive astrogliosis. *J Neurosci* 32, 6391-6410.

- Zamberletti, E., Gabaglio, M., Prini, P., Rubino, T., Parolaro, D., 2015. Cortical neuroinflammation contributes to long-term cognitive dysfunctions following adolescent delta-9-tetrahydrocannabinol treatment in female rats. *Eur Neuropsychopharmacol* 25, 2404-2415.
- Zanier, E. R., Fumagalli, S., Perego, C., Pischiutta, F., De Simoni, M. G., 2015. Shape descriptors of the "never resting" microglia in three different acute brain injury models in mice. *Intensive Care Med Exp* 3, 39.
- Zeigler, D. W., Wang, C. C., Yoast, R. A., Dickinson, B. D., McCaffree, M. A., Robinowitz, C. B., Sterling, M. L., Council on Scientific Affairs, A. M. A., 2005. The neurocognitive effects of alcohol on adolescents and college students. *Prev Med* 40, 23-32.
- Zeng, L., Kang, R., Zhu, S., Wang, X., Cao, L., Wang, H., Billiar, T. R., Jiang, J., Tang, D., 2017. ALK is a therapeutic target for lethal sepsis. *Sci Transl Med* 9.
- Zha, L., He, L., Xie, W., Cheng, J., Li, T., Mohsen, M. O., Lei, F., Storni, F., Bachmann, M., Chen, H., Zhang, Y., 2017. Therapeutic silence of pleiotrophin by targeted delivery of siRNA and its effect on the inhibition of tumor growth and metastasis. *PLoS One* 12, e0177964.
- Zhang, B., Wei, W., Qiu, J., 2018. ALK is required for NLRP3 inflammasome activation in macrophages. *Biochem Biophys Res Commun* 501, 246-252.
- Zhang, S., Wu, M., Peng, C., Zhao, G., Gu, R., 2017. GFAP expression in injured astrocytes in rats. *Exp Ther Med* 14, 1905-1908.
- Zhang, Y., Zhou, Y., Chen, S., Hu, Y., Zhu, Z., Wang, Y., Du, N., Song, T., Yang, Y., Guo, A., Wang, Y., 2019. Macrophage migration inhibitory factor facilitates prostaglandin E2 production of astrocytes to tune inflammatory milieu following spinal cord injury. *J Neuroinflammation* 16, 85.
- Zhu, R., Bu, Q., Fu, D., Shao, X., Jiang, L., Guo, W., Chen, B., Liu, B., Hu, Z., Tian, J., Zhao, Y., Cen, X., 2018. Toll-like receptor 3 modulates the behavioral effects of cocaine in mice. *J Neuroinflammation* 15, 93.
- Zou, P., Muramatsu, H., Miyata, T., Muramatsu, T., 2006. Midkine, a heparin-binding growth factor, is expressed in neural precursor cells and promotes their growth. *J Neurochem* 99, 1470-1479.

ANEXOS

ANEXO 1. Pleiotrophin overexpression regulates amphetamine-induced reward and striatal dopaminergic denervation without changing the expression of dopamine D1 and D2 receptors: Implications for neuroinflammation.

Marta Vicente-Rodríguez, Loreto Rojo Gonzalez, Esther Gramage, Rosalía Fernández-Calle, Carmen Pérez-García, Marcel Ferrer-Alcón, María Uribarri, Alexis Bailey y Gonzalo Herradón.

European Neuropsychopharmacology, 2016. ISSN: 1873-7862

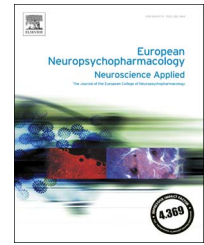
Volumen: 26

Número de páginas: 1794-1805

DOI: 10.1016/j.euroneuro.2016.09.002



ELSEVIER

www.elsevier.com/locate/euroneuro


Pleiotrophin overexpression regulates amphetamine-induced reward and striatal dopaminergic denervation without changing the expression of dopamine D1 and D2 receptors: Implications for neuroinflammation

Marta Vicente-Rodríguez^a, Loreto Rojo Gonzalez^c,
 Esther Gramage^a, Rosalía Fernández-Calle^a, Ying Chen^b,
 Carmen Pérez-García^a, Marcel Ferrer-Alcón^e, María Uribarri^e,
 Alexis Bailey^{c,d}, Gonzalo Herradón^{a,*}

^aPharmacology lab, Department of Pharmaceutical and Health Sciences, Facultad de Farmacia, Universidad CEU San Pablo, Madrid, Spain

^bInstitute of Psychiatry, Psychology and Neuroscience, Division of Academic Psychiatry London, Kings College London, London, UK

^cDepartment of Biochemistry & Physiology, Faculty of Health & Medical Sciences, University of Surrey, Guildford, UK

^dInstitute of Medical and Biomedical Education, St George's University of London, London SW17 0RE, UK

^eBRAINco Biopharma, S.L., Bizkaia Technology Park, Spain

Received 5 February 2016; received in revised form 2 June 2016; accepted 1 September 2016

KEYWORDS

Pleiotrophin;
 Midkine;
 Astrogliosis;
 Inflammation;
 Methamphetamine;
 Reward

Abstract

It was previously shown that mice with genetic deletion of the neurotrophic factor pleiotrophin (PTN^{-/-}) show enhanced amphetamine neurotoxicity and impair extinction of amphetamine conditioned place preference (CPP), suggesting a modulatory role of PTN in amphetamine neurotoxicity and reward. We have now studied the effects of amphetamine (10 mg/kg, 4 times, every 2 h) in the striatum of mice with transgenic PTN overexpression (PTN-Tg) in the brain and in wild type (WT) mice. Amphetamine caused an enhanced loss of striatal dopaminergic terminals, together with a highly significant aggravation of amphetamine-induced increase in the number of GFAP-positive astrocytes, in the striatum of PTN-Tg mice

*Correspondence to: Lab. Pharmacology, Faculty of Pharmacy, Universidad CEU San Pablo, Urb. Montepríncipe, 28668 Boadilla del Monte, Madrid, Spain. Fax: +34 91 3510475.

E-mail address: herradon@ceu.es (G. Herradón).

<http://dx.doi.org/10.1016/j.euroneuro.2016.09.002>

0924-977X/© 2016 Elsevier B.V. and ECNP. All rights reserved.

compared to WT mice. Given the known contribution of D1 and D2 dopamine receptors to the neurotoxic effects of amphetamine, we also performed quantitative receptor autoradiography of both receptors in the brains of PTN-Tg and WT mice. D1 and D2 receptors binding in the striatum and other regions of interest was not altered by genotype or treatment. Finally, we found that amphetamine CPP was significantly reduced in PTN-Tg mice. The data demonstrate that PTN overexpression in the brain blocks the conditioning effects of amphetamine and enhances the characteristic striatal dopaminergic denervation caused by this drug. These results indicate for the first time deleterious effects of PTN in vivo by mechanisms that are probably independent of changes in the expression of D1 and D2 dopamine receptors. The data also suggest that PTN-induced neuroinflammation could be involved in the enhanced neurotoxic effects of amphetamine in the striatum of PTN-Tg mice.

© 2016 Elsevier B.V. and ECNP. All rights reserved.

1. Introduction

According to the European Monitoring Centre for Drugs and Drug Addiction, it is estimated that more than 2% of young people (15-34) used amphetamines in 2010 in different European countries including Czech Republic (3.2%), Denmark (3.1%), and the United Kingdom (2.3%). Ever in lifetime use of amphetamines among young people in those countries varies considerably, with levels of 30-70%. Despite widespread use of amphetamine-type stimulants, the long-term medical consequences of these drugs abuse and dependence have not been addressed until recently. During the past two decades, pre-clinical studies have demonstrated that this type of psychostimulants damages dopaminergic neurons, causing striatal dopaminergic denervation and dopaminergic cell death in the substantia nigra among other effects (Moratalla et al., 2015). However, clinical correlation was not studied until Callaghan et al. (2012) probed a ~77% increased risk of Parkinson's disease (PD) in amphetamine-type drug abusers (Callaghan et al., 2012). Similarly, a recent report indicates a 3-fold increased risk of PD in these drugs users (Curtin et al., 2015). Existence of genetic factors underlying individual vulnerability to the rewarding effects of amphetamine and dopaminergic neurotoxicity after consumption of this type of psychostimulants is known. Uncovering those genetic factors is not only clinically relevant but will also help to develop new therapeutic strategies for substance use disorders.

Pleiotrophin (PTN) is a neurotrophic factor known to play a role in amphetamine-induced neurotoxicity (Alguacil and Herradon, 2015). A single amphetamine administration causes a significant upregulation of PTN mRNA levels in the rat brain (Le Greves, 2005) suggesting that PTN takes part in a modulatory mechanism against the effects of amphetamine in the brain. Accordingly, extinction of amphetamine-induced conditioned place preference (CPP) is impaired in PTN genetically deficient (PTN^{-/-}) mice (Gramage et al., 2010a). Furthermore, a periadolescent amphetamine treatment was found to produce transient cognitive deficits only in PTN^{-/-} mice, not in wild type (WT) mice (Gramage et al., 2013a). Interestingly, amphetamine-induced neurotoxic effects in the nigrostriatal pathway are enhanced in PTN^{-/-} mice compared to WT mice (Gramage et al., 2010b; Soto-Montenegro et al., 2015). Also, it has to be noted that amphetamine-induced increase of GFAP-

positive astrocytes, a hallmark of the neuroinflammation induced by this type of psychostimulants, was slightly increased in the striatum of PTN^{-/-} mice (Gramage et al., 2010a). Overall, the data clearly suggest a modulatory role of PTN on amphetamine effects (Herradon and Perez-Garcia, 2014). However, the knockout mouse models, although invaluable as screening tools in research, have intrinsic limitations including ubiquitous absence of the targeted gene and possible developmentally-related mechanisms of compensation. To overcome these limitations, we have now studied the rewarding and neurotoxic effects of amphetamine in mice with transgenic neuronal PTN overexpression in the brain (PTN-Tg mice). In addition, it is interesting to note that overstimulation of dopamine D1 (D1R) and D2 receptors (D2R) significantly contributes to the neurotoxic effects of amphetamine (Moratalla et al., 2015). Furthermore, dopamine is a crucial transmitter in the neuroimmune network (Kustrimovic et al., 2014) and D2R is identified as an important component controlling innate immunity and inflammatory response in central nervous system (Shao et al., 2013). To test the possibility that differences in these receptors could underlie the different genotypic susceptibility to the neurotoxic and neuroinflammatory effects of amphetamine, we carried out quantitative receptor autoradiography of D1, D2 receptors in the brains of PTN-Tg and WT mice.

2. Experimental procedures

2.1. Animals

PTN-Tg mice on a C57BL/6J background were generated by pronuclear injection as recently described (Ferrer-Alcón et al., 2012; Vicente-Rodríguez et al., 2014a). The acceptor vector used was pTSC-a2 and contained the regulatory regions responsible for tissue specific expression of Thy-1 gene, which drives neuron-specific expression of transgenes (Aigner et al., 1995; Caroni, 1997). PTN specific overexpression in different brain areas, including a 20% increase of PTN protein levels in striatum, was established by quantitative Real Time-Polymerase Chain Reaction (qRT-PCR), in situ hybridization, and by Western blot (Ferrer-Alcón et al., 2012; Vicente-Rodríguez et al., 2015, 2014b). Relevant to the behavioral study presented here, there were no differences in motor activity and exploration between both genotypes at baseline (Ferrer-Alcón et al., 2012).

We used male PTN-Tg and WT animals of 9-10 weeks (20-25 g). Mice were housed under controlled environmental conditions (22 ± 1 °C and a 12-h light/12-h dark cycle) with free access to food and water.

All the animals used in this study were maintained in accordance with European Union Laboratory Animal Care Rules (86/609/ECC directive) and the protocols were approved by the Animal Research Committee of USP-CEU.

2.2. Amphetamine treatment

PTN-Tg and WT mice received 4 injections (i.p.) of amphetamine (10 mg/kg) or saline (control, 10 ml/kg), allowing between injections a 2 h interval. This regimen of administrations of amphetamine was previously used to dissect differences between WT and PTN-/- mice (Gramage et al., 2010a, 2010b) and is known to cause significant damage to striatal dopaminergic terminals (Krasnova et al., 2001) and astrogliosis (Krasnova et al., 2005), a neuroinflammatory hallmark in the striatum that has been suggested to underlie the cognitive deficits, depression, and parkinsonism reported in amphetamine-type drugs addicts (Krasnova et al., 2016). Four days after the animals received the first administration of amphetamine or saline (control), mice were euthanized differently for immunohistochemistry and autoradiography studies.

2.3. Immunohistochemistry studies

Mice were transcardially perfused with 4% p-formaldehyde and brains were removed and conserved in p-formaldehyde for 24 h and transferred to a 30% sucrose solution containing 0.02% sodium azide for storage at 4 °C. The brains were cut at a thickness of 30 μ m using a vibratome (Leica, Wetzlar, Germany). Immunostaining was performed in one slice per 180 μ m from bregma 1.54 mm to bregma 0.10 mm. Striatal free-floating sections were processed as previously described (Gramage et al., 2010a,b). In order to study astrogliosis or dopaminergic terminals, sections were incubated overnight at 4 °C with anti-GFAP antibodies (1:1000) ($n=4$ /group) or anti-TH antibodies (1:1000) ($n=6-7$ /group), respectively. Both antibodies were purchased from Millipore (Madrid, Spain). The sections were then rinsed in PBS three times for 10 min and incubated for 30 min with the biotinylated secondary antibodies in PBS at room temperature. The avidin-biotin reaction was performed using a Vectastain Elite ABC peroxidase kit following the protocol suggested by the manufacturer. The immunoreactivity was visualized using 0.06% diaminobenzidine and 0.03% H₂O₂ diluted in PBS. The sections were mounted on gelatin/chrome alum-coated slides, air-dried overnight, dehydrated through graded ethanols, cleared in xylene, and coverslipped with DPX medium. Photomicrographs were captured with a digital camera coupled to an optical microscope (DMLS, Leica, Solms, Germany).

Image analysis was performed in the three most central slices of each animal. GFAP-positive astrocytes were counted in 325×435 μ m standardized areas and TH-immunostaining density was analyzed in 230×140 μ m areas, both located in the medial striatum (Gramage et al., 2010a,b).

The counting of GFAP-positive cells was accomplished with the help of the software Scion Image 4.02 (Scion Corporation, Frederick, MD, USA). As previously performed (Gramage et al., 2010b), cell counts were made in standardized areas obtaining the mean from three sections per animal. Striatal TH-positive fiber staining was assessed by optical density (OD) measurements using Image-Pro Plus software (Version 3.0.1; Media Cybernetics, Silver Spring, MD). For each animal, the nonspecific background correction in each section was done by subtracting the OD value of the corpus callosum from the striatal OD value obtained from the same section.

2.4. D1, D2 dopamine receptor and DAT autoradiography

Different cohorts of mice ($n=5-6$ /group) were sacrificed 4 days after the last injection of saline or amphetamine. The brains were immediately removed, quickly frozen in isopentane (-35 °C) and stored at -80 °C until sectioning. Quantitative autoradiography was performed as detailed previously for D1, D2 dopamine receptor binding and DAT binding (Bailey et al., 2008) using general procedures of Kitchen et al. (1997). Adjacent 20- μ m brain coronal sections were cut at an interval of 300 μ m for the determination of total and non-specific binding (NSB) of [³H]SCH-23390 (containing 1 μ M mianserin), [³H]raclopride and [³H]mazindol (containing 0.3 μ M desipramine) to D1R, D2R and DAT, respectively. Ligand concentrations were 3-4 x K_d, with all ligands used at a concentration of 4 nM. This sub-saturation concentration of radioligand was deliberately chosen in order to maximize the detection of binding differences if present. For instance, following this rationale we previously showed a clear downregulation of striatal [³H]raclopride (4 nM) receptors in rats treated with chronic escalating dose “binge” cocaine administration paradigm but not following chronic steady dose “binge” cocaine administration (Bailey et al., 2008). NSB was defined in the presence of cis-flupentixol (10 μ M), sulphiride (10 μ M) or unlabeled mazindol (10 μ M) for [³H]SCH-23390, [³H]raclopride and [³H]mazindol binding, respectively. Following incubation binding for a period of 90 min or 60 min at room temperature or 45 min at 4 °C for D1R, D2R and DAT, respectively, and washing in ice-cold buffer (6 \times 1 min for D1R and D2R binding and 2 \times 1 min for DAT binding), the slides were apposed to MR film (Eastman Kodak Co., Rochester, NY, USA) in X-ray cassettes together with a set of tritium standards ([³H]Microscale™, Amersham, UK) for 6 weeks. Sections were processed together in a paired protocol. Films were developed using 50% Kodak D19 developer. Quantitative analysis of brain receptors was performed as detailed previously (Kitchen et al., 1997; Lena et al., 2004). Using a MCID image analyser (Image Research, Canada), brain structures were identified using the mouse brain atlas of Franklin and Paxinos (1997). Brain images were analyzed using left and right hemispheres to allow duplication of results. The cortical and olfactory tubercle structures were analyzed by sampling five to eight times with a box size 15 \times 15 mm² in a box tool. All other regions were analyzed by freehand drawing tools.

2.5. Conditioned place preference (CPP)

A biased apparatus was used as previously described (Vicente-Rodriguez et al., 2014a). One compartment had black floor and walls, and the other had black floor and white walls. The phases of CPP included preconditioning (day 1), conditioning (days 2-4) and testing (day 5). During preconditioning, mice were free to explore the two compartments for a 30-min period; their behavior was monitored by a videotracking system (San Diego, California, USA) to calculate the time spent in each compartment. Mice were counterbalanced such that half the animals started in one chamber and half started in the other. The compartment with white walls was the non-preferred compartment in a similar manner by both genotypes (30-40% stay of total time in the preconditioning phase). This ‘biased’ apparatus and subject assignment, in which mice are paired with the drug in the non-preferred compartment, was previously used to study genotypic differences in amphetamine- and cocaine-induced CPP (Gramage et al., 2013b, 2010b). The conditioning phase consisted of double conditioning sessions (Gramage et al., 2013b). The first one involved a morning session starting at 8 a.m.. All animals received a single injection of saline i.p. (10 ml/kg) and were confined to the initially preferred compartment for 30 min. In the evening session, starting at 3 p.m., the animals were injected (i.p.) with 3.0 mg/kg amphetamine ($n=10-15$ /group), or 10 ml/kg saline ($n=5-7$ /group) as a conditioning control, and confined to the initially non-preferred compartment for 30 min.

The procedure used in days 3 and 4 was the same but the order of the treatments (morning/evening) was changed to avoid the influence of circadian variability. In the testing phase, mice received a drug-free, 30-min preference test. The time-spent in the non-preferred (drug-paired) compartment was calculated in all cases. The increase in the time-spent in the drug-paired compartment in day 5 compared to day 1 (preference score) was considered as indicative of the degree of conditioning induced by amphetamine.

2.6. Statistics

All data were expressed as the mean \pm SEM and analyzed using Prism software (GraphPad, La Jolla, CA, USA). Data obtained from image analysis of striatal immunostaining and autoradiography were analyzed using two-way ANOVA. Relevant differences were analyzed pair-wise by post-hoc comparisons with Bonferroni's post-hoc tests, considering genotype (PTN-Tg, WT) and treatment (saline,

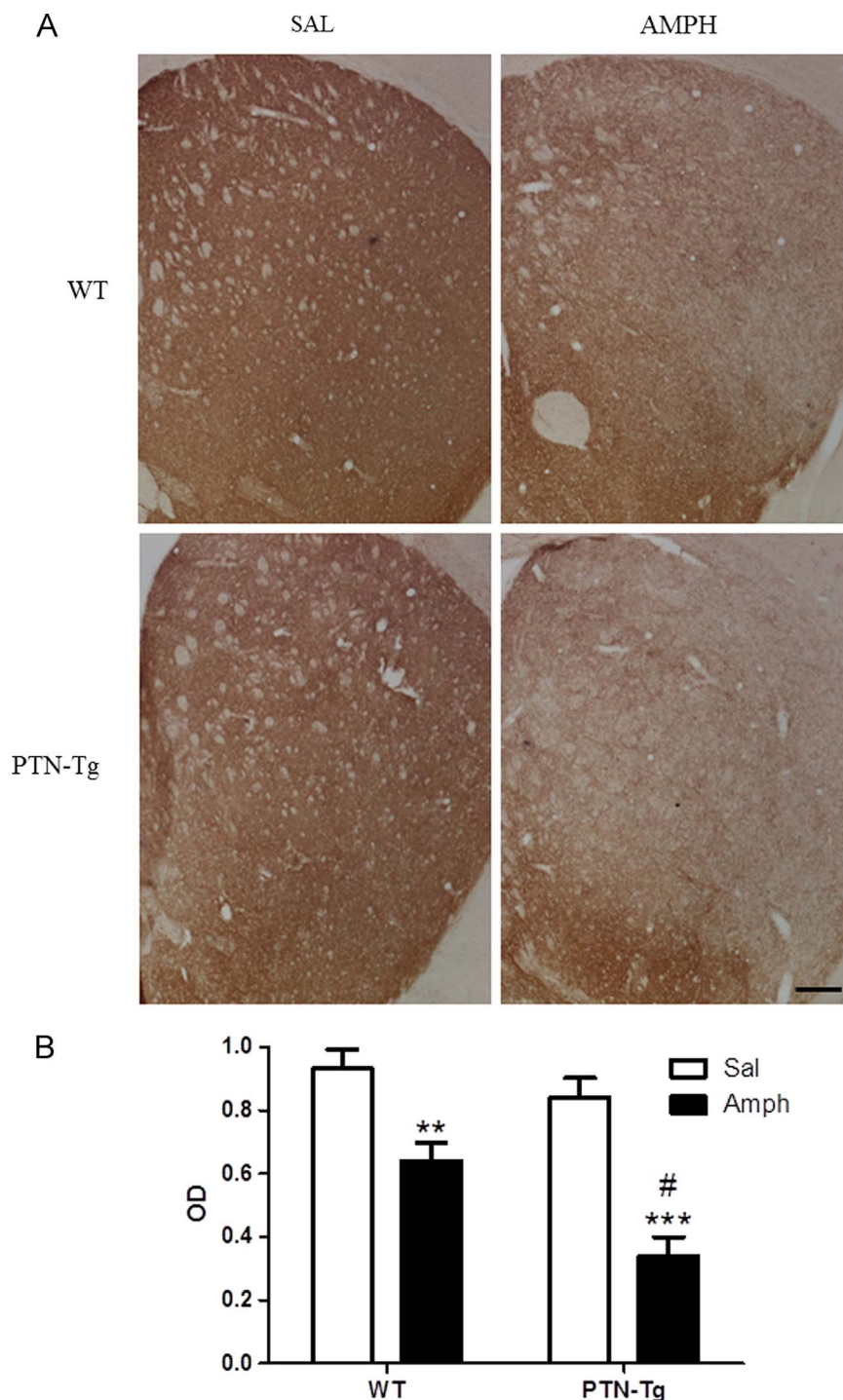


Figure 1 TH expression in striatum of PTN-Tg and WT mice after amphetamine administration. TH-immunostained striatal sections of mice treated with saline (Sal) or amphetamine (Amph) ($n=6-7$ /group). (A) Photomicrographs illustrate that PTN overexpression increases amphetamine-induced TH loss. (B) Graph represents the optical density (OD) measures of TH-ir in the striatum. ** $p < 0.01$ vs. Sal. *** $p < 0.001$ vs. Sal. # $p < 0.05$ vs. WT-Amph. Scale bar 300 μ m.

amphetamine) as between-subjects factors. Amphetamine preference scores from CPP were confirmed to follow a normal distribution with Kolmogorov-Smirnov, D'Agostino and Pearson Omnibus and Shapiro-Wilk normality tests, so they were analyzed using a Student's t-test. $P < 0.05$ was considered as statistically significant.

3. Results

3.1. Enhanced amphetamine-induced loss of dopaminergic terminals in the striatum of PTN-Tg mice

Since one of the most relevant consequences of amphetamine administration is the loss of dopaminergic terminals in the striatum (Bowyer et al., 1998), we analyzed TH expression by immunohistochemistry and DAT expression by autoradiography in the Caudate Putamen (CPu) of PTN-Tg and WT mice treated with either amphetamine or saline (control). Two-way ANOVA revealed a significant effect of the genotype ($F(1,21)=9.148$; $P=0.0064$), of the treatment ($F(1,21)=44.66$; $P < 0.0001$) and a significant interaction between genotype

and treatment ($F(1,21)=5.749$; $P < 0.0259$) on striatal TH expression. Amphetamine caused a $\sim 40\%$ depletion of TH contents in the CPu of WT mice compared with saline-treated WT mice (Figure 1). We detected a significantly greater decrease of TH levels in the CPu of amphetamine-treated PTN-Tg mice compared to WT mice (Figure 1). However, we did not find significant differences in the levels of TH in the striatum of saline-treated PTN-Tg and WT mice (Figure 1).

In order to discard the possibility that genotypic differences in amphetamine-induced TH loss could be related to differences in this enzyme's transcription and non-necessarily to an enhanced loss of dopaminergic terminals, we tested DAT expression by autoradiography in the CPu (Figure 2). As expected, amphetamine showed a significant impact in striatal DAT contents ($F(1,20)=28.54$; $P < 0.0001$). Amphetamine tended to produce a greater decrease of DAT levels in the CPu of PTN-Tg mice (Figure 2(B)). Considering the medial CPu, DAT levels were significantly reduced by amphetamine treatment only in PTN-Tg mice (Figure 2(C)), whereas reduction of DAT levels was not statistically different in the lateral CPu of both genotypes (Figure 2(B)).

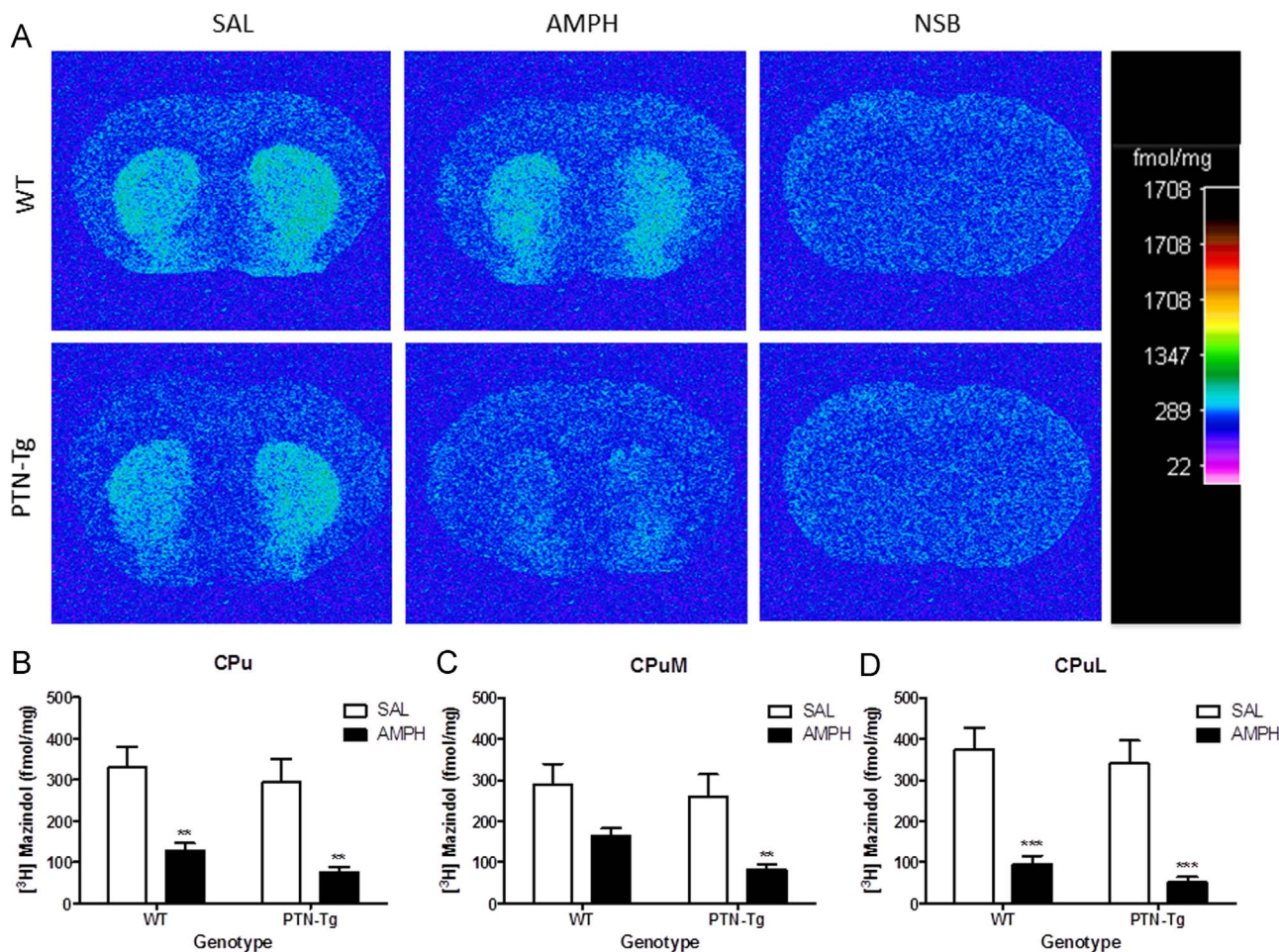


Figure 2 $[^3\text{H}]$ mazindol binding in WT and PTN-Tg mice treated with amphetamine. (A) Representative autoradiograms of $[^3\text{H}]$ mazindol binding to DAT in the brain sections of WT and PTN-Tg mice treated with saline (Sal) or amphetamine (Amph) ($n=6$ /group). Representative autoradiograms of non-specific binding (NSB) was determined in the presence of $10 \mu\text{M}$ mazindol. The color bar represents pseudo-color interpretation of black and white film images in fmol/mg tissue. (B) Quantitative autoradiography of $[^3\text{H}]$ mazindol binding in the brain of amphetamine- and saline-treated WT and PTN-Tg mice in CPu, (C) in CPuM and (D) in CPuL. ** $p < 0.01$ vs. Sal. *** $p < 0.001$ vs. Sal. Abbreviations: CPu, Caudate putamen; CPuL, Lateral part of CPu; CPuM, Medial part of CPu.

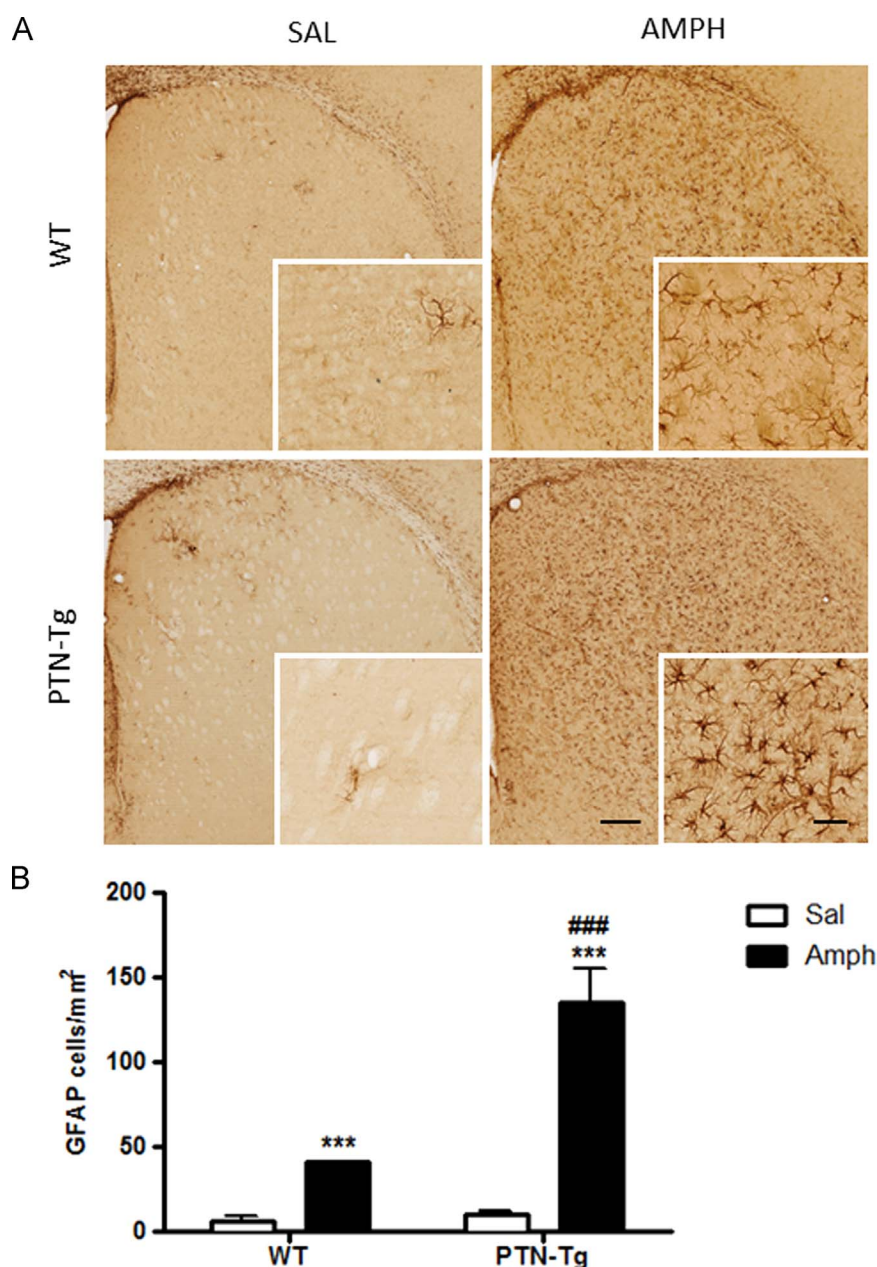


Figure 3 Amphetamine induces astrocytosis in the striatum of WT and PTN-Tg mice. (A) Photomicrographs are from GFAP-immunostained striatal sections of saline (Sal)- or amphetamine (Amph)-treated animals ($n=4$ /group). Higher magnification images in the lower right corner of every representative picture show that some of the astrocytes were hypertrophic and densely stained in WT mice treated with amphetamine whereas this effect was generalized in PTN-Tg mice treated with amphetamine. (B) The graph represents quantification of data obtained from the counts of GFAP-positive cells in standardized areas of the striatum. *** $P < 0.001$ vs. Sal. ### $P < 0.001$ vs. WT-Amph. Scale bar 5x=200 μ m, 40x=50 μ m.

3.2. Enhanced amphetamine-induced increase of GFAP-positive astrocytes in the striatum of PTN-Tg mice

In these experiments, very few GFAP-positive astrocytes were observed in the striata of saline-treated mice (Figure 3(A)). These cells were characterized by small cell bodies as well as very fine and short processes. In contrast, after amphetamine administrations, GFAP-positive astrocytes developed large cell bodies as well as long and extensive

processes (Figure 3(A)). In the case of amphetamine-treated PTN-Tg mice, astrocytes developed larger densely stained cell bodies as well as longer processes compared with WT mice (Figure 3(A)). In addition, two-way ANOVA revealed a significant effect of the genotype ($F(1,12)=24.08$; $P=0.0004$), of the treatment ($F(1,12)=62.93$; $P < 0.0001$) and a significant interaction between genotype and treatment ($F(1,12)=20.48$; $P < 0.001$) on the number of GFAP+ cells/mm² in the striatum. The number of GFAP+ cells in amphetamine-treated mice increased in both genotypes

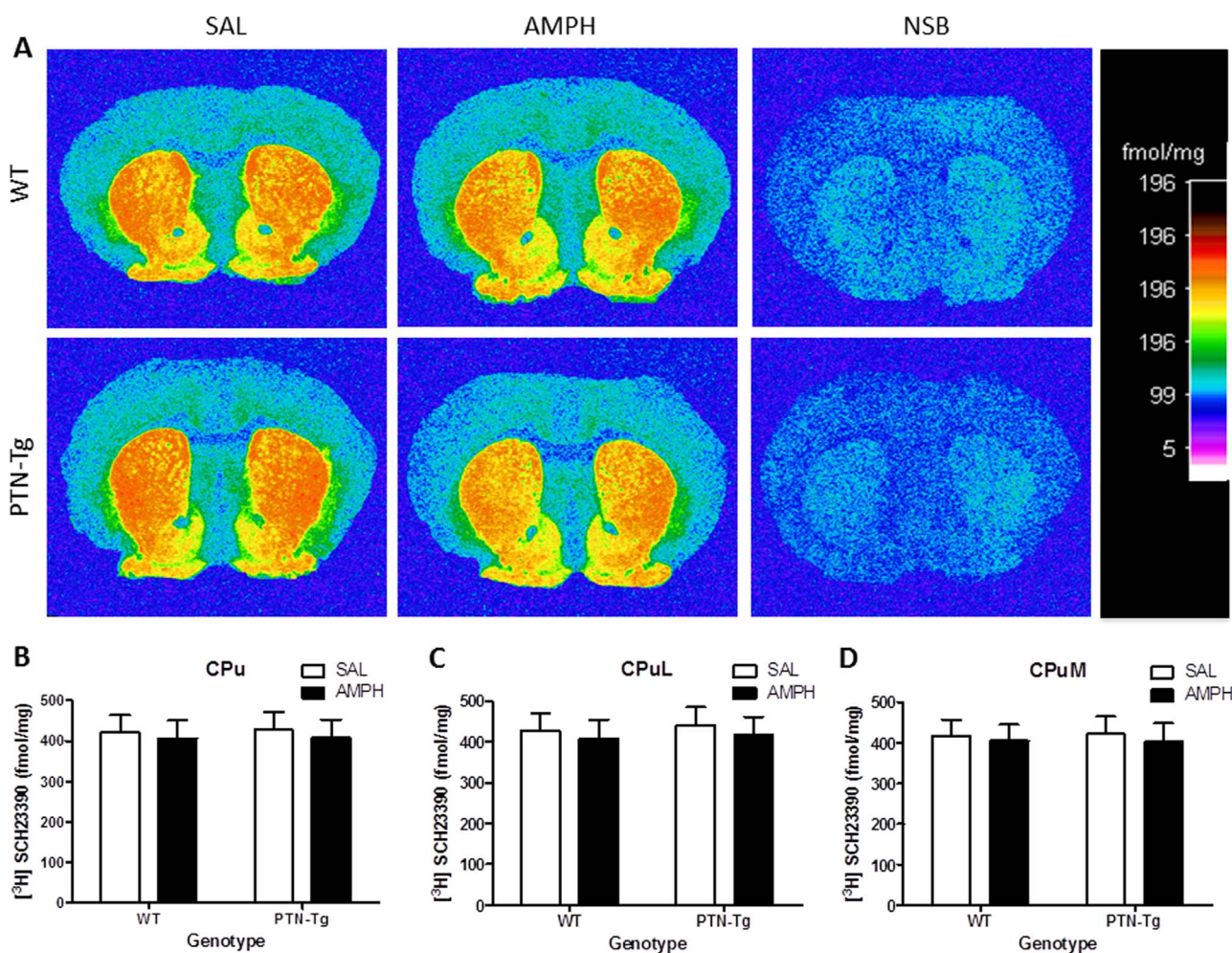


Figure 4 [³H] SCH23390 binding in WT and PTN-Tg mice treated with amphetamine. (A) Representative autoradiograms of [³H] SCH23390 binding to D1 in the brain sections of WT and PTN-Tg mice treated with saline (Sal) or amphetamine (Amph) ($n=6$ /group). Representative autoradiograms of non-specific binding (NSB) was determined in adjacent sections in the presence of 10 μ M cis-flupentixol. The color bar represents pseudo-color interpretation of black and white film images in fmol/mg tissue. (B) Quantitative autoradiography of [³H] SCH23390 binding in the brain of amphetamine- and saline-treated WT and PTN-Tg mice in CPu, (C) in CPuL and (D) in CPuM. Abbreviations: CPu, Caudate putamen; CPuL, Lateral part of CPu; CPuM, Medial part of CPu.

when compared to the saline-treated groups (Figure 3(B)). However, a highly significant increase in the number of GFAP-positive astrocytes in the striata of PTN-Tg mice compared to WT mice was found (Figure 3(B)).

3.3. D1, D2 binding in the brains of WT and PTN-Tg mice

No significant differences in D1, D2 receptors binding were observed in the CPu of PTN-Tg and WT mice (Figures 4 and 5). When medial and lateral CPu were analyzed separately, D1R and D2R binding was found to be similar in both genotypes (Figures 4 and 5). In addition, no significant genotype or treatment effect was detected in D1 binding (Table 1) and in D2 binding (Table 2) in any of the regions analyzed.

3.4. Decreased amphetamine-induced conditioned place preference in PTN-Tg mice

To test the possibility that PTN could modulate amphetamine rewarding effects, we performed conditioning studies. We used a medium dose of amphetamine (3.0 mg/kg, i.p.) known to induce CPP in this mouse strain (Gramage et al., 2010a; Tzschentke, 2007). Thus, as expected, amphetamine caused a robust CPP in WT mice (Figure 6). However, amphetamine place preference score was decreased by 65% in PTN-Tg mice (Figure 6, [$t_{(22)}=2.29$, $P=0.031$]). As shown before with the same genotypes (Vicente-Rodriguez et al., 2014a), saline conditioning did not show significant changes on place preference compared to preconditioning values of both genotypes (data not shown). The data confirm an important role of PTN in the regulation of the rewarding effects of amphetamine.

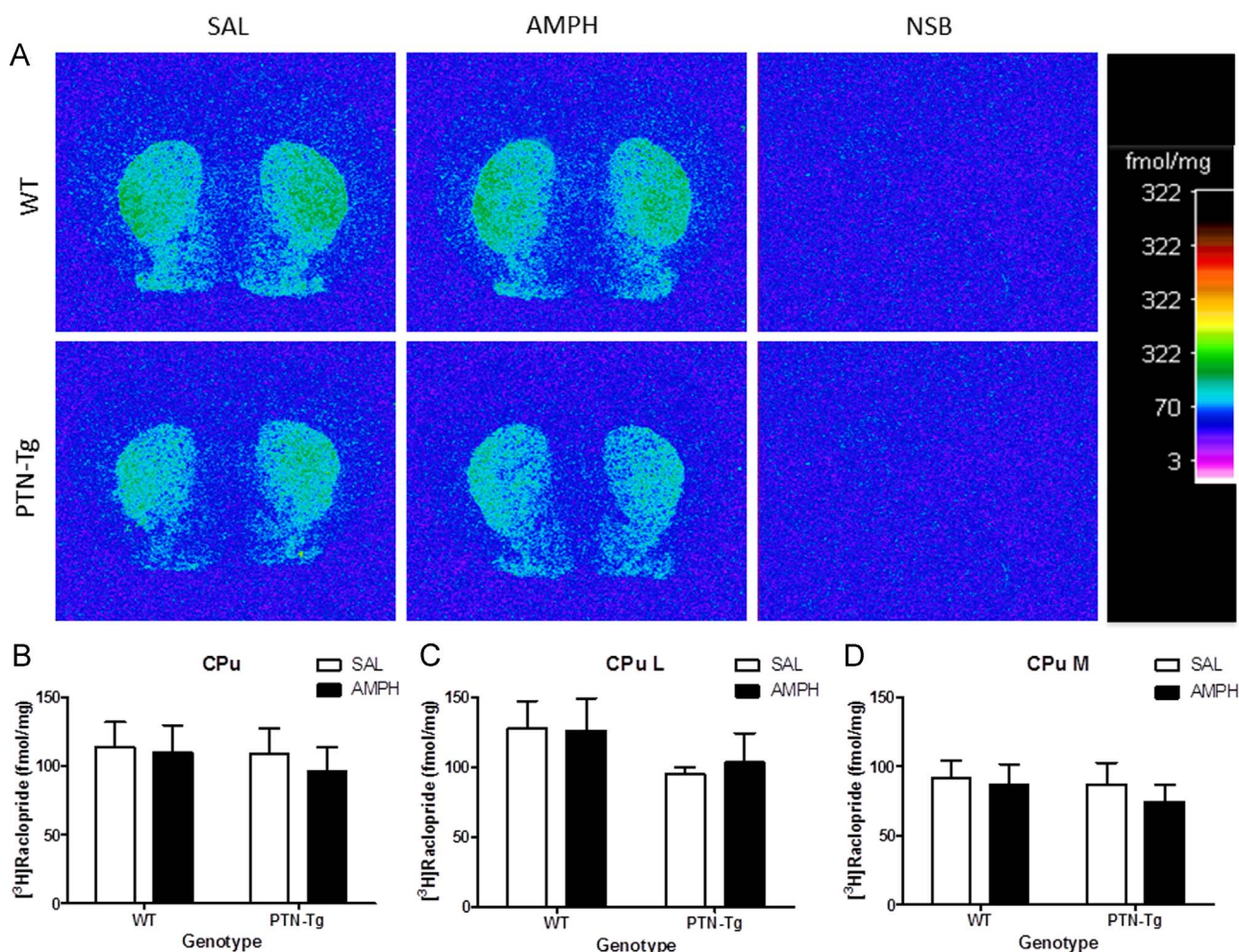


Figure 5 [³H]raclopride binding in WT and PTN-Tg mice treated with amphetamine. (A) Representative autoradiograms of [³H]raclopride binding to D2 in the brain sections of WT and PTN-Tg mice treated with saline (Sal) or amphetamine (Amph) (*n*=6/group). Representative autoradiograms of non-specific binding (NSB) was determined in adjacent sections in the presence of 10 μM sulpiride. The color bar represents pseudo-color interpretation of black and white film images in fmol/mg tissue. (B) Quantitative autoradiography of [³H]raclopride binding in the brain of amphetamine- and saline-treated WT and PTN-Tg mice in CPu, (C) in CPuL and (D) in CPuM. Abbreviations: CPu, Caudate putamen; CPuL, Lateral part of CPu; CPuM, Medial part of CPu.

4. Discussion

In previous studies, it was shown that PTN^{-/-} mice exhibit exacerbated amphetamine-induced dopaminergic damage in the nigrostriatal pathway (Gramage et al., 2010a, 2010b). Thus, we hypothesized a possible neuroprotective role of PTN in response to the neurotoxic effects of amphetamine. However, one has to be cautious in making conclusions from knockout mice assays as data collected in these mice are subjected to the inherent limitations of a constitutive knockout animal model. To evaluate the potential neuroprotective role of PTN against amphetamine-induced neurotoxicity, we have now studied the effects of this drug in the striatum of mice with transgenic overexpression of PTN in the brain. In support of this rationale, studies with parkinsonian toxins had previously shown that overexpression of PTN exerts neuroprotection in mouse models of PD (Gombash et al., 2012, 2014). Unexpectedly, we found that amphetamine-induced loss of striatal TH and DAT contents is increased in PTN-Tg mice, suggesting that dopaminergic denervation caused by

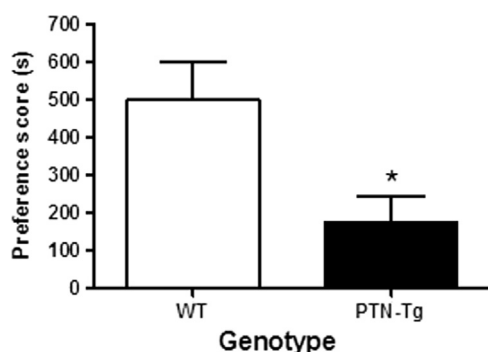
amphetamine is facilitated by PTN overexpression. This apparent discrepancy in the data collected from amphetamine-treated PTN^{-/-} and PTN-Tg mice may reflect the possibility of compensatory mechanisms triggered by the elimination of PTN during development in the PTN knockout mice. These compensatory mechanisms are not clear but could be related to the signaling pathways regulated by PTN. PTN binds Receptor Protein Tyrosine Phosphatase (RPTP) β/ζ (also known as PTPRZ1) and inactivate its intrinsic tyrosine phosphatase activity (Gramage and Herradon, 2011). As a result, PTN causes increases in the phosphorylation levels of substrates of RPTPβ/ζ known to be important for neuronal function (e.g. Fyn kinase and β-catenin) which, in turn, trigger other signaling pathways involved in different functions including mitogenic, differentiation, survival and inflammation (Herradon and Perez-Garcia, 2014). Thus, it seems reasonable to hypothesize that some substrates of RPTPβ/ζ, or downstream factors in their signaling pathways, could be involved in compensatory developmental mechanisms in PTN^{-/-} mice.

Table 1 Quantitative autoradiography of [³H]SCH23390 binding to D1 in brain sections of WT and PTN-Tg treated with amphetamine (Amph) or saline (Sal) (n=6/group).

Region	[³ H]SCH23390-specific binding (fmol/mg tissue)			
	Sal		Amph	
	WT	PTN-Tg	WT	PTN-Tg
Nucleus accumbens core	360.8±40.3	369.2±39.2	367.5±43.7	362.8±44
Nucleus accumbens shell	332±44.1	346.8±42.7	349.1±37.4	339.7±40
Olfactory tubercle	290±26.4	285.9±24.2	288.4±31	299.4±34.8
Clastrum	112.2±19.3	99.8±15	101.7±15.3	95.4±14.6
Cingulate cortex	26.9±2.9	25.2±2	24.8±6.7	29±4.4
Motor cortex	17.5±2.5	19.4±2.5	20±3.9	20.8±3.1
Amygdala	46.2±6.9	49.6±7.5	52.7±6.7	47.2±7.2
Thalamus	18.4±2.9	24.3±5.1	26.9±5.6	26.1±6.9
Hypothalamus	14.6±3.5	21.5±4.2	18.6±3.3	21±3.6
Hippocampus	26.2±4	26.3±6.6	38.5±6.4	28.1±6.1
Substantia nigra	184±18.3	191.8±10.8	204.1±13.6	181±10.2
Ventral tegmental area	21.3±3.4	13.6±2.9	18.6±5.2	25.8±8.2

Table 2 Quantitative autoradiography of [³H]raclopride binding to D2 in brain sections of WT and PTN-Tg treated with amphetamine (Amph) or saline (Sal) (n=6/group).

Region	[³ H]raclopride-specific binding (fmol/mg tissue)			
	Sal		Amph	
	WT	PTN-Tg	WT	PTN-Tg
Nucleus accumbens core	67.5±11.8	54.2±2.1	67.63±11.8	60.6±11.1
Nucleus accumbens shell	71.5±12.5	70±11.4	64.8±11.4	69.3±12.6
Olfactory tubercle	86.8±16.5	76.6±14.6	81.1±15.6	82±21.2

**Figure 6** Amphetamine-induced conditioned place preference in PTN-Tg and WT mice. Preference score after amphetamine (3.0 mg/kg) conditioning, showing a significantly decreased amphetamine CPP in PTN-Tg mice. **P*<0.05 vs. WT.

The neuroprotective effects of PTN against cocaine- and amphetamine-induced toxicity have been proven in vitro. PTN (3 μM) limits amphetamine- and cocaine-induced decrease in PC12 and NG108-15 cell viability (Gramage et al., 2008, 2010a, 2010b). However, our results show that the net effect produced by PTN seems to differ in vivo, suggesting overall deleterious effects triggered by activation of PTN downstream pathways that could counteract its trophic actions

on neurons. For instance, PTN induces the proliferation of immune cells and the expression of inflammatory cytokines including TNF-α, IL-1β and IL-6 (Achour et al., 2001, 2008), suggesting a proinflammatory role of PTN. Previously, we showed a modest increase (~20%) of amphetamine-induced GFAP-positive astrocytes in PTN^{-/-} mice (Gramage et al., 2010a). We now show a 13-fold upregulation of GFAP+ cells in the striatum of amphetamine-treated PTN-Tg mice. Since merely a few astrocytes were sparsely detected throughout the striatum of control mice and it is known that GFAP labeling of striatal astrocytes can be sparse compared with other astrocyte markers in naïve animals (Kalman and Hajos, 1989; Krasnova et al., 2005; Tong et al., 2014), our data should not be interpreted as changes to astrocyte density without further confirmation. Most likely, our data reflect a highly significant amphetamine-induced upregulation of GFAP protein concentrations in astrocytes. Although a limitation of the present study is that microglial response has not been assessed, it has to be noted that overexpression of GFAP is an indicator of reactive astrogliosis and neuroinflammation, important events in a wide variety of CNS disorders and pathologies (Sofroniew and Vinters, 2010). Thus, the robust increase of GFAP-positive astrocytes in amphetamine-treated PTN-Tg mice suggests an enhanced neuroinflammation induced by amphetamine in the presence

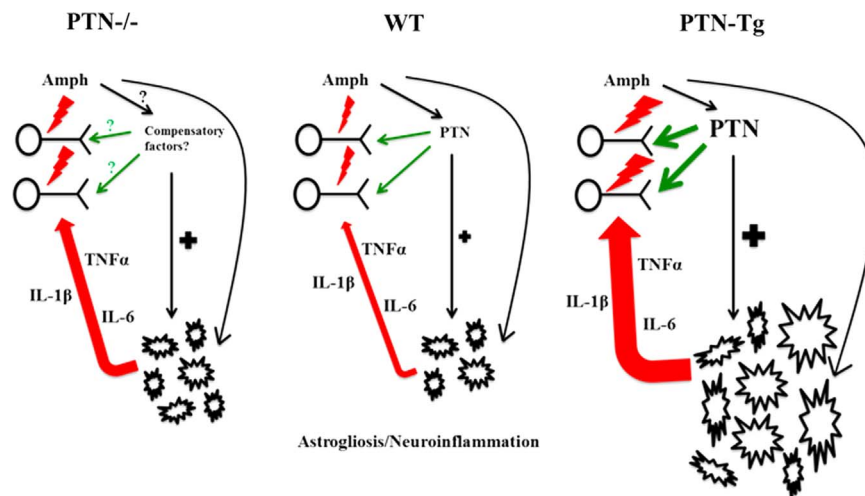


Figure 7 Schematic model of the effects of amphetamine in genetically engineered PTN mouse models. In normal WT mice, amphetamine (Amph) induces striatal denervation and an increase in the expression levels of PTN. PTN exerts neurotrophic actions on striatal dopaminergic terminals but also contribute to astroglia and cytokine release causing deleterious effects in the striatum. PTN^{-/-} mice show an increased striatal denervation and a modest increase of astroglia, possibly caused by compensatory mechanisms triggered by factors downstream of PTN signaling pathways. PTN-Tg mice show an exacerbated striatal dopaminergic denervation after amphetamine treatment, together with a highly significant (4-fold) increase of astroglia which will overtake the possibly augmented neurotrophic effects caused by overexpression of PTN and will aggravate striatal dopaminergic injury.

of higher levels of PTN. Indeed these findings clearly indicate that PTN is involved in the neuroinflammatory promoting effect of amphetamine. A proposed model for this is illustrated in Figure 7. It is important to note that different drugs of abuse, including amphetamine and its derivatives, induce neuroinflammation (Coelho-Santos et al., 2012) and that exacerbated neuroinflammatory responses, including astrogliosis, have been linked to neurodegenerative processes and CNS injury in different models (Qin et al., 2007; Sanchez-Guajardo et al., 2013). Our current findings, together with the fact that amphetamine administration increases the levels of expression of PTN in the brain (Le Greves, 2005), suggest the possibility that PTN may be one of the mediators facilitating amphetamine-induced neuroinflammation and, as a result, neurotoxicity (Figure 7).

The major cause of amphetamines neurotoxicity in the striatum is the dysregulation of dopamine and dopamine receptors (Ares-Santos et al., 2013). It has been shown that D1R antagonists protect against amphetamines-induced decreases in DAT binding in the striatum (Angulo et al., 2004) and inhibit the striatal denervation caused by these drugs (Xu et al., 2005). In a similar manner, inactivation of D2R prevents methamphetamine-induced reductions of striatal TH and DAT levels (Ares-Santos et al., 2013). Interestingly, the use of antagonists or genetic inactivation of D1R and D2R has been shown to reduce the enhanced striatal astrogliosis induced by amphetamines (Ares-Santos et al., 2013; Xu et al., 2005), suggesting that both receptors are also involved in the neuroinflammation caused by this type of drugs. However, our data demonstrate that D1R and D2R binding is not altered by amphetamine treatment and is similar in all the brain regions analyzed, including striatum, of PTN-Tg and WT mice. The data clearly suggest that amphetamine-induced enhanced fiber loss and astrogliosis in the striatum of PTN-Tg mice is independent of D1R- and D2R-related mechanisms at least at the receptor expression level.

Finally, we also tested the rewarding effects of amphetamine in PTN-Tg and WT mice. We previously found that amphetamine induces place preference in both PTN knockout and WT mice in a similar manner (Gramage et al., 2010a). However, extinction of amphetamine-induced CPP was delayed in PTN^{-/-} mice suggesting a possible role of PTN in amphetamine reward. In the present work, our results uncover that overexpression of PTN significantly blocks amphetamine-induced conditioned place preference, suggesting an important role of PTN in the limitation of the rewarding effects of amphetamine. Interestingly, it was recently shown that alcohol-induced CPP was completely absent in PTN-Tg mice (Vicente-Rodríguez et al., 2014a). Overall, the data suggest a hyporeactive rewarding system of PTN-Tg mice in response to different drugs of abuse that is not related to deficits in D1, D2 receptors expression levels.

In summary, the present study clarifies the role of PTN in amphetamine-induced neurotoxicity and reward. We demonstrate for the first time that brain overexpression of PTN blocks amphetamine-induced CPP. We also demonstrate that the net effect of brain overexpression of PTN is the enhancement of amphetamine-induced neurotoxic effects in the striatum despite previous evidences in PTN^{-/-} mice pointing to an overall neuroprotective role of PTN in this context. In addition, the data demonstrate that increased amphetamine neurotoxicity in the striatum caused by overexpression of PTN is not related to changes in D1R and D2R expression. The data suggest that enhanced neuroinflammation triggered by PTN overexpression could be involved in the greater striatal dopaminergic denervation caused by amphetamine in PTN-Tg mice.

Role of funding source

Funding for this study was provided by Grants SAF2014-56671-R from Ministerio de Economía y Competitividad of Spain and

USP-BS-APP03/2014 from Universidad CEU San Pablo and Banco de Santander; the Ministerio de Economía y Competitividad of Spain and USP-BS had no further role in study design; in the collection, analysis and interpretation of data; in the writing of the report; and in the decision to submit the paper for publication.

Contributors

GH and AB designed the research. MV-R, LRG, EG and RF-C performed the research. GH, AB, YC and CP-G analyzed the data. MF-A, MU provided PTN-TG mice, phenotypic and genotypic characterization. GH and AB wrote the paper.

Conflict of Interest

None to declare.

Acknowledgments

This work has been supported by Grants SAF2014-56671-R from Ministerio de Economía y Competitividad of Spain and USP-BS-APP03/2014 from Universidad CEU San Pablo and Banco de Santander to GH. M V-R and R F-C are supported by fellowships from Fundación Universitaria San Pablo CEU. M V-R was supported by a travel grant CEU-Banco de Santander in Biochemistry & Physiology Department, University of Surrey, Guildford (UK).

References

- Achour, A., Laaroubi, D., Caruelle, D., Barritault, D., Courty, J., 2001. The angiogenic factor heparin affinity regulatory peptide (HARP) induces proliferation of human peripheral blood mononuclear cells. *Cell Mol. Biol. (Noisy-Le-Grand)* 47 (Online Pub, OL73-77).
- Achour, A., M'Bika, J.P., Baudouin, F., Caruelle, D., Courty, J., 2008. Pleiotrophin induces expression of inflammatory cytokines in peripheral blood mononuclear cells. *Biochimie* 90, 1791-1795.
- Aigner, L., Arber, S., Kapfhammer, J.P., Laux, T., Schneider, C., Botteri, F., Brenner, H.R., Caroni, P., 1995. Overexpression of the neural growth-associated protein GAP-43 induces nerve sprouting in the adult nervous system of transgenic mice. *Cell* 83, 269-278.
- Alguacil, L.F., Herradon, G., 2015. Midkine and pleiotrophin in the treatment of neurodegenerative diseases and drug addiction. *Recent Pat. CNS Drug Discov.* 10, 28-33.
- Angulo, J.A., Angulo, N., Yu, J., 2004. Antagonists of the neurokinin-1 or dopamine D1 receptors confer protection from methamphetamine on dopamine terminals of the mouse striatum. *Ann. N Y Acad. Sci.* 1025, 171-180.
- Ares-Santos, S., Granado, N., Moratalla, R., 2013. The role of dopamine receptors in the neurotoxicity of methamphetamine. *J. Intern. Med.* 273, 437-453.
- Bailey, A., Metaxas, A., Yoo, J.H., McGee, T., Kitchen, I., 2008. Decrease of D2 receptor binding but increase in D2-stimulated G-protein activation, dopamine transporter binding and behavioural sensitization in brains of mice treated with a chronic escalating dose 'binge' cocaine administration paradigm. *Eur. J. Neurosci.* 28, 759-770.
- Bowyer, J.F., Frame, L.T., Clausing, P., Nagamoto-Combs, K., Osterhout, C.A., Sterling, C.R., Tank, A.W., 1998. Long-term effects of amphetamine neurotoxicity on tyrosine hydroxylase mRNA and protein in aged rats. *J. Pharmacol. Exp. Ther.* 286, 1074-1085.
- Callaghan, R.C., Cunningham, J.K., Sykes, J., Kish, S.J., 2012. Increased risk of Parkinson's disease in individuals hospitalized with conditions related to the use of methamphetamine or other amphetamine-type drugs. *Drug Alcohol Depend.* 120, 35-40.
- Caroni, P., 1997. Overexpression of growth-associated proteins in the neurons of adult transgenic mice. *J. Neurosci. Methods* 71, 3-9.
- Coelho-Santos, V., Goncalves, J., Fontes-Ribeiro, C., Silva, A.P., 2012. Prevention of methamphetamine-induced microglial cell death by TNF-alpha and IL-6 through activation of the JAK-STAT pathway. *J. Neuroinflamm.* 9, 103.
- Curtin, K., Fleckenstein, A.E., Robison, R.J., Crookston, M.J., Smith, K.R., Hanson, G.R., 2015. Methamphetamine/amphetamine abuse and risk of Parkinson's disease in Utah: a population-based assessment. *Drug Alcohol Depend.* 146, 30-38.
- Ferrer-Alcón, M., Uribarri, M., Díaz, A., Del Olmo, N., Valdizán, E.M., Gramage, E., Martín, M., Castro, E., Pérez-García, C., Mengod, G., Maldonado, R., Herradon, G., Pazos, A., Palacios, J.M., 2012. A New Non-classical Transgenic Animal Model of Depression Program No. 776.04/FF9 Neuroscience Meeting Planner. Society for Neuroscience, New Orleans, LA, 2012 (Online).
- Franklin, K.B.J., Paxinos, G., 1997. *The Mouse Brain in Stereotaxic Coordinates*. Academic, San Diego.
- Gombash, S.E., Manfredsson, F.P., Mandel, R.J., Collier, T.J., Fischer, D.L., Kemp, C.J., Kuhn, N.M., Wohlgenant, S.L., Fleming, S.M., Sortwell, C.E., 2014. Neuroprotective potential of pleiotrophin overexpression in the striatonigral pathway compared with overexpression in both the striatonigral and nigrostriatal pathways. *Gene Ther.* 21, 682-693.
- Gombash, S.E., Lipton, J.W., Collier, T.J., Madhavan, L., Steece-Collier, K., Cole-Strauss, A., Terpstra, B.T., Spieles-Engemann, A.L., Daley, B.F., Wohlgenant, S.L., Thompson, V.B., Manfredsson, F.P., Mandel, R.J., Sortwell, C.E., 2012. Striatal pleiotrophin overexpression provides functional and morphological neuroprotection in the 6-hydroxydopamine model. *Mol. Ther.* 20, 544-554.
- Gramage, E., Herradon, G., 2011. Connecting Parkinson's disease and drug addiction: common players reveal unexpected disease connections and novel therapeutic approaches. *Curr. Pharm. Des.* 17, 449-461.
- Gramage, E., Alguacil, L.F., Herradon, G., 2008. Pleiotrophin prevents cocaine-induced toxicity in vitro. *Eur. J. Pharmacol.* 595, 35-38.
- Gramage, E., Rossi, L., Granado, N., Moratalla, R., Herradon, G., 2010b. Genetic inactivation of pleiotrophin triggers amphetamine-induced cell loss in the substantia nigra and enhances amphetamine neurotoxicity in the striatum. *Neuroscience* 170, 308-316.
- Gramage, E., Del Olmo, N., Fole, A., Martín, Y.B., Herradon, G., 2013a. Periadolescent amphetamine treatment causes transient cognitive disruptions and long-term changes in hippocampal LTP depending on the endogenous expression of pleiotrophin. *Addict. Biol.* 18, 19-29.
- Gramage, E., Perez-Garcia, C., Vicente-Rodriguez, M., Bollen, S., Rojo, L., Herradon, G., 2013b. Regulation of extinction of cocaine-induced place preference by midkine is related to a differential phosphorylation of peroxiredoxin 6 in dorsal striatum. *Behav. Brain Res.* 253, 223-231.
- Gramage, E., Putelli, A., Polanco, M.J., Gonzalez-Martin, C., Ezquerro, L., Alguacil, L.F., Perez-Pinera, P., Deuel, T.F., Herradon, G., 2010a. The neurotrophic factor pleiotrophin modulates amphetamine-seeking behaviour and amphetamine-induced neurotoxic effects: evidence from pleiotrophin knockout mice. *Addict. Biol.* 15, 403-412.
- Herradon, G., Perez-Garcia, C., 2014. Targeting midkine and pleiotrophin signaling pathways in addiction and neurodegenerative disorders: recent progress and perspectives. *Br. J. Pharmacol.* 171, 837-848.
- Kalman, M., Hajos, F., 1989. Distribution of glial fibrillary acidic protein (GFAP)-immunoreactive astrocytes in the rat brain. *Exp. Brain Res.* 78, 147-163.
- Kitchen, I., Slowe, S.J., Matthes, H.W., Kieffer, B., 1997. Quantitative autoradiographic mapping of mu-, delta- and kappa-

- opioid receptors in knockout mice lacking the mu-opioid receptor gene. *Brain Res.* 778, 73-88.
- Krasnova, I.N., Ladenheim, B., Cadet, J.L., 2005. Amphetamine induces apoptosis of medium spiny striatal projection neurons via the mitochondria-dependent pathway. *FASEB J.* 19, 851-853.
- Krasnova, I.N., Justinova, Z., Cadet, J.L., 2016. Methamphetamine addiction: involvement of CREB and neuroinflammatory signaling pathways. *Psychopharmacology* 233, 1945-1962.
- Krasnova, I.N., Ladenheim, B., Jayanthi, S., Oyler, J., Moran, T.H., Huestis, M.A., Cadet, J.L., 2001. Amphetamine-induced toxicity in dopamine terminals in CD-1 and C57BL/6J mice: complex roles for oxygen-based species and temperature regulation. *Neuroscience* 107, 265-274.
- Kustrimovic, N., Rasini, E., Legnaro, M., Marino, F., Cosentino, M., 2014. Expression of dopaminergic receptors on human CD4+ T lymphocytes: flow cytometric analysis of naive and memory subsets and relevance for the neuroimmunology of neurodegenerative disease. *J. Neuroimmune Pharmacol.* 9, 302-312.
- Le Greves, P., 2005. Pleiotrophin gene transcription in the rat nucleus accumbens is stimulated by an acute dose of amphetamine. *Brain Res. Bull.* 65, 529-532.
- Lena, I., Matthes, H., Kieffer, B., Kitchen, I., 2004. Quantitative autoradiography of dopamine receptors in the brains of micro-opioid receptor knockout mice. *Neurosci. Lett.* 356, 220-224.
- Moratalla, R., Khairnar, A., Simola, N., Granado, N., Garcia-Montes, J.R., Porceddu, P.F., Tizabi, Y., Costa, G., Morelli, M., 2015. Amphetamine-related drugs neurotoxicity in humans and in experimental animals: main mechanisms. *Prog. Neurobiol.*
- Qin, L., Wu, X., Block, M.L., Liu, Y., Breese, G.R., Hong, J.S., Knapp, D.J., Crews, F.T., 2007. Systemic LPS causes chronic neuroinflammation and progressive neurodegeneration. *Glia* 55, 453-462.
- Sanchez-Guajardo, V., Barnum, C.J., Tansey, M.G., Romero-Ramos, M., 2013. Neuroimmunological processes in Parkinson's disease and their relation to alpha-synuclein: microglia as the referee between neuronal processes and peripheral immunity. *ASN Neuro* 5, 113-139.
- Shao, W., Zhang, S.Z., Tang, M., Zhang, X.H., Zhou, Z., Yin, Y.Q., Zhou, Q.B., Huang, Y.Y., Liu, Y.J., Wawrousek, E., Chen, T., Li, S. B., Xu, M., Zhou, J.N., Hu, G., Zhou, J.W., 2013. Suppression of neuroinflammation by astrocytic dopamine D2 receptors via alphaB-crystallin. *Nature* 494, 90-94.
- Sofroniew, M.V., Vinters, H.V., 2010. Astrocytes: biology and pathology. *Acta Neuropathol.* 119, 7-35.
- Soto-Montenegro, M.L., Vicente-Rodríguez, M., Perez-García, C., Gramage, E., Desco, M., Herradon, G., 2015. Functional neuroimaging of amphetamine-induced striatal neurotoxicity in the pleiotrophin knockout mouse model. *Neurosci. Lett.* 591, 132-137.
- Tong, X., Ao, Y., Faas, G.C., Nwaobi, S.E., Xu, J., Hausteine, M.D., Anderson, M.A., Mody, I., Olsen, M.L., Sofroniew, M.V., Khakh, B.S., 2014. Astrocyte Kir4.1 ion channel deficits contribute to neuronal dysfunction in Huntington's disease model mice. *Nat. Neurosci.* 17, 694-703.
- Tzschentke, T.M., 2007. Measuring reward with the conditioned place preference (CPP) paradigm: update of the last decade. *Addict. Biol.* 12, 227-462.
- Vicente-Rodríguez, M., Perez-García, C., Haro, M., Ramos, M.P., Herradon, G., 2014b. Genetic inactivation of midkine modulates behavioural responses to ethanol possibly by enhancing GABA (A) receptor sensitivity to GABA(A) acting drugs. *Behav. Brain Res.* 274, 258-263.
- Vicente-Rodríguez, M., Herradon, G., Ferrer-Alcon, M., Uribarri, M., Perez-García, C., 2015. Chronic cocaine use causes changes in the striatal proteome depending on the endogenous expression of pleiotrophin. *Chem. Res. Toxicol.* 28, 1443-1454.
- Vicente-Rodríguez, M., Perez-García, C., Ferrer-Alcon, M., Uribarri, M., Sanchez-Alonso, M.G., Ramos, M.P., Herradon, G., 2014a. Pleiotrophin differentially regulates the rewarding and sedative effects of ethanol. *J. Neurochem.* 131, 688-695.
- Xu, Z.C., Ling, G., Sahr, R.N., Neal-Beliveau, B.S., 2005. Asymmetrical changes of dopamine receptors in the striatum after unilateral dopamine depletion. *Brain Res.* 1038, 163-170.

ANEXO 2. Midkine Is a Novel Regulator of Amphetamine-Induced Striatal Gliosis and Cognitive Impairment: Evidence for a Stimulus-Dependent Regulation of Neuroinflammation by Midkine.

Marta Vicente-Rodríguez, Rosalía Fernández-Calle, Esther Gramage, Carmen Pérez-García, María P. Ramos y Gonzalo Herradón.

Mediators of inflammation, 2016. ISSN: 1466-1861

Volumen: 2016

Página de inicio: 9894504

DOI: 10.1155/2016/9894504

Research Article

Midkine Is a Novel Regulator of Amphetamine-Induced Striatal Gliosis and Cognitive Impairment: Evidence for a Stimulus-Dependent Regulation of Neuroinflammation by Midkine

Marta Vicente-Rodríguez,¹ Rosalía Fernández-Calle,¹ Esther Gramage,¹
 Carmen Pérez-García,¹ María P. Ramos,² and Gonzalo Herradón¹

¹Pharmacology Lab, Department of Pharmaceutical and Health Sciences, Facultad de Farmacia, Universidad CEU San Pablo, Madrid, Spain

²Biochemistry and Molecular Biology Lab, Department of Chemistry and Biochemistry, Facultad de Farmacia, Universidad CEU San Pablo, Madrid, Spain

Correspondence should be addressed to Gonzalo Herradón; herradon@ceu.es

Received 25 August 2016; Accepted 7 November 2016

Academic Editor: Vera L. Petricevich

Copyright © 2016 Marta Vicente-Rodríguez et al. This is an open access article distributed under the Creative Commons Attribution License, which permits unrestricted use, distribution, and reproduction in any medium, provided the original work is properly cited.

Midkine (MK) is a cytokine that modulates amphetamine-induced striatal astrogliosis, suggesting a possible role of MK in neuroinflammation induced by amphetamine. To test this hypothesis, we studied astrogliosis and microglial response induced by amphetamine (10 mg/kg i.p. four times, every 2 h) in different brain areas of MK^{-/-} mice and wild type (WT) mice. We found that amphetamine-induced microgliosis and astrocytosis are enhanced in the striatum of MK^{-/-} mice in a region-specific manner. Surprisingly, LPS-induced astrogliosis in the striatum was blocked in MK^{-/-} mice. Since striatal neuroinflammation induced by amphetamine-type stimulants correlates with the cognitive deficits induced by these drugs, we also tested the long-term effects of periadolescent amphetamine treatment (3 mg/kg i.p. daily for 10 days) in a memory task in MK^{-/-} and WT mice. Significant deficits in the Y-maze test were only observed in amphetamine-pretreated MK^{-/-} mice. The data demonstrate for the first time that MK is a novel modulator of neuroinflammation depending on the inflammatory stimulus and the brain area considered. The data indicate that MK limits amphetamine-induced striatal neuroinflammation. In addition, our data demonstrate that periadolescent amphetamine treatment in mice results in transient disruption of learning and memory processes in absence of endogenous MK.

1. Introduction

Drugs of abuse, such as alcohol and amphetamine and its derivatives, induce neuroinflammation [1]. Proliferation of inflammatory cells such as microglia and astrocytes [2] is a signature of neuroinflammation and a hallmark of pathogenesis associated with different events including neurodegeneration [3–5]. Evidence suggests the possibility that neuroinflammatory processes in drug addiction disorders could lead to neurodegeneration in specific brain areas targeted by drugs of abuse. Accordingly, striatal neuroinflammation induced by methamphetamine seems to underlie cognitive

deficits, depression, and parkinsonism reported in methamphetamine addicts [6]. In addition, independent studies have demonstrated a highly significant increase in the prevalence of Parkinson's disease (PD) among addicts to amphetamine-type stimulants [7, 8]. Thus, identification and characterization of new genetic factors involved in drug addiction disorders and inflammation are relevant for validation of new biomarkers and for the development of new drugs that could modulate neuroinflammation processes underlying addiction disorders [9].

Midkine (MK) is a cytokine with important functions in peripheral inflammatory processes in different pathological

conditions [10, 11]. MK facilitates the migration of macrophages and neutrophils [12–14] and prevents differentiation of regulatory T-cells by inhibiting the development of tolerogenic dendritic cells [15, 16]. In the central nervous system (CNS), the role of MK in inflammation is poorly understood. It has been shown that this cytokine is not involved in the development of astrogliosis or activation of microglia in a spinal cord injury model [17]. However, MK is found highly upregulated in pathologies characterized by inflammation such as cerebral infarction and neurodegenerative diseases [18, 19] and in different brain areas after administration of drugs of abuse [20]. This evidence supports the hypothesis that MK could play an important role in neuroinflammation. To test this hypothesis, we have now confirmed that amphetamine-induced striatal astrogliosis is enhanced in MK knockout (MK^{-/-}) mice [21], and we have tested for the first time striatal microglial response induced by amphetamine in MK^{-/-} and wild type (WT) mice. To test the possibility of a region-specific regulation of astrogliosis by MK, we have also tested the effects of amphetamine in the hippocampus, an area that draws increasing attention as a responsive brain region in psychostimulants actions [22]. We have also investigated if MK regulates glial response depending on the inflammatory stimulus by comparing the effects of lipopolysaccharide (LPS) injection in MK^{-/-} and WT mice. In addition, since early onset of drug abuse causes a wide range of adverse outcomes in adulthood including cognitive deficits [23], which correlates with the capacity of these drugs to induce striatal neuroinflammation [6], we also tested the long-term effects of periadolescent amphetamine treatment in a memory task in MK^{-/-} mice.

2. Materials and Methods

2.1. Animals. MK^{-/-} mice were kindly provided by Dr. Thomas F. D'uel (The Scripps Research Institute, La Jolla, CA). MK^{-/-} mice were generated as previously described [24]; 8–10-week-old male MK^{-/-} and WT mice on a C57BL/6J background were used for immunohistochemistry studies; 4-week-old male MK^{-/-} and WT mice were used for periadolescent amphetamine treatment prior to behavioral assessment.

The animals used in this study were maintained in accordance with both the ARRIVE guidelines and the European Union Laboratory Animal Care Rules (Directive 2010/63/EU for animal experiments) and the protocols were approved by the Animal Research Committee of USP-CEU.

2.2. Histological Studies: Gliosis

2.2.1. Treatments. MK^{-/-} and WT mice received 4 injections (i.p.) of amphetamine (10 mg/kg) or saline (control, 10 mL/kg), allowing between injections a 2-hour interval. This regimen of administration of amphetamine was previously used to observe differences in the striatal astrogliosis induced by this drug in WT and MK^{-/-} mice [21]. Four days after the animals received the first administration of amphetamine or saline (control), mice were euthanized for immunohistochemistry studies as described below.

In the study with LPS, MK^{-/-} and WT mice received a single i.p. injection of LPS (Sigma, Madrid, Spain) (0.5 mg/kg) or saline (control, 10 mL/kg) and were sacrificed 8 h after the treatment. In order to better dissect possible genotypic differences we used a low dose of LPS that was shown to be useful to test neuroinflammation in mice [25].

2.2.2. Immunohistochemistry Analysis. An equal or greater $n = 4$ /group was used in all studies. Mice were transcardially perfused with 4% *p*-formaldehyde, and brains were removed and conserved in *p*-formaldehyde for 24 h and transferred to a 30% sucrose solution containing 0.02% sodium azide for storage at 4°C. 30 μ m striatal and hippocampal free-floating sections were processed as previously described [21, 26, 27]. Immunohistochemistry studies were performed in one slice per 180 μ m (striatum from bregma 1.54 mm to 0.10 mm; hippocampus from bregma -1.06 mm to -2.54 mm).

In order to study astrogliosis, sections were incubated overnight at 4°C with anti-GFAP antibody (Millipore, Madrid, Spain; 1:1000) and then for 30 minutes with the appropriate biotinylated secondary antibody (Vector Laboratories, Burlingame, CA, USA; 1:5000) in PBS at room temperature; the avidin-biotin reaction was performed using Vectastain Elite ABC peroxidase kit (Vector Laboratories) following the protocol suggested by the manufacturer; immunolabeling was visualized by using 3,3'-diaminobenzidine (DAB). Sections were mounted on gelatin-coated slides, air-dried overnight, dehydrated through graded ethanol, cleared in xylene, and mounted with DPX medium. To study striatal microgliosis, sections were incubated overnight at 4°C with anti-Iba1 antibody (Wako, Osaka, Japan; 1:1000), followed by 30 minutes of incubation with Alexa-Fluor-488 secondary antibody (Invitrogen, Waltham, MA USA; 1:500). Photomicrographs were captured with a digital camera coupled to an optical microscope (DM5500B, Leica, Solms, Germany). Analysis was performed using ImageJ (NIH), in the three most central slices of each area. GFAP+ astrocytes were counted in 325 \times 435 μ m standardized areas in the medial striatum as previously described [21, 26] and in the lacunosum moleculare (LMol) located in CA1 area, in the hippocampus. Iba1+ cells were counted in 1100 μ m \times 1400 μ m standardized areas in the striatum.

2.3. Behavioral Studies: Y-Maze. Four independent experiments were performed to reach an appropriate number of subjects per experimental group in Y-maze assays. Treatments began during periadolescence (4-week-old mice). Male MK^{-/-} and WT mice were randomly allocated and injected with either amphetamine (3 mg/kg, i.p.) dissolved in saline or saline (10 mL/kg, i.p.), once daily for 10 consecutive days. Six days after the last administration of amphetamine (or saline), behavioral testing started following previously published protocols [28] and leaving appropriate “washing” periods of time between different Y-maze assays.

In order to study recognition processes in response to novelty and working memory in mice, we used the Y-maze test as previously described [29]. Memory was measured with a 60 min intertrial interval (ITI) between acquisition and retrieval. During the first trial (acquisition), the animal is

placed in the centre of the maze and allowed to visit for 5 min two arms (“start” and “other” arms) of a Y-maze with three arms each 34 cm long, 8 cm wide, and 14.5 cm high, the third being blocked with a door. During the second trial (retrieval, 5 min), the door is opened, and the animal is free to access all three arms (“start”; “other”; and “novel” arms). During the test, the number of entries into each arm (when a mouse places all four paws into an arm) was recorded. Discrimination of novelty versus familiarity was studied by calculating the preference for the “novel” arm as a discrimination ratio ($\text{Novel}/[\text{Novel} + \text{Other}]$) for number of arm entries. Scores greater than 0.5 show preference for the “novel” arm indicating the establishment of spatial memory.

Mice (WT: saline, $n = 15$; amphetamine, $n = 15$, and MK $^{-/-}$: saline, $n = 9$; amphetamine, $n = 9$) were tested in the Y-maze at 6 weeks of age (6 days after last amphetamine administration) and 7 and 9 weeks of age. All the experiments were conducted during the light phase.

2.4. Statistical Analysis. Data were analyzed using two-way ANOVA considering genotype and treatment as variants. Relevant differences were analyzed by post hoc comparisons with Bonferroni’s post hoc tests. All statistical analyses were performed using GraphPad Prism 6 program (San Diego, CA, USA).

3. Results

3.1. Amphetamine-Induced Gliosis in the Striatum Is Enhanced in MK $^{-/-}$ Mice. In order to confirm the previously reported enhanced astrocytosis induced by amphetamine in MK $^{-/-}$ mice [21], immunohistochemical analysis of GFAP-positive cells in the striata of MK $^{-/-}$ and WT mice was performed. Compared to saline-treated animals from both genotypes, amphetamine induced reactive astrocytes characterized by large densely stained bodies with longer and extensive processes (Figure 1(a), black arrows). As expected, amphetamine efficiently increased the number of GFAP+ cells in both genotypes (Figure 1(b)). The number of GFAP+ astrocytes in the striata of amphetamine-treated MK $^{-/-}$ mice was significantly higher than that in WT mice (Figure 1(b)). The data confirm that MK regulates amphetamine-induced striatal astrocytic response.

Augmented microglial response is a hallmark of amphetamine derivative-induced neurotoxicity [30] and a signature of neuroinflammation. Immunohistochemistry for Iba1 revealed a significant increase in the number of Iba1+ cells in the striata of WT mice 4 days after amphetamine treatment (Figure 2). Compared to saline-treated mice, we found a more pronounced increase in Iba1-ir following amphetamine administration to MK $^{-/-}$ mice (Figure 2). The data demonstrate for the first time that MK modulates the microglial response induced by amphetamine.

3.2. Genetic Inactivation of Midkine Prevents Amphetamine-Induced Astroglial Gliosis in Hippocampus. The data obtained in the striatum of WT and MK $^{-/-}$ mice suggest that MK regulates the glial response induced by amphetamine. The data are particularly robust in the case of the astrocytic response

which is highly increased after amphetamine treatment in MK $^{-/-}$ mice. To test the possibility that MK regulates astrocytosis depending on the brain area considered, we also assessed the effects of amphetamine in the hippocampus of MK $^{-/-}$ and WT mice (Figure 3(a)). Amphetamine induced different effects in WT and MK $^{-/-}$ mice (Figure 3). In contrast to the astrocytic response in the striatum, a significant decrease of GFAP+ astrocytes in amphetamine-treated MK $^{-/-}$ mice compared to WT mice (Figure 3(b)) was observed. The data demonstrate a regional-specific regulation of amphetamine-induced astrocytosis by MK.

3.3. Genetic Inactivation of Midkine Differentially Regulates LPS-Induced Striatal Gliosis. MK is not only found upregulated in the brain after administration of different drugs of abuse. The cerebral levels of expression of MK are increased in different diseases that share neuroinflammation as a common pathogenic mechanism, including ischemia and neurodegenerative diseases [20]. To test the possibility that MK regulates the glial response depending on the inflammatory stimulus used, we assessed the effects of LPS in MK $^{-/-}$ and WT mice. As expected, a low dose of LPS (0.5 mg/kg) induced a moderate ~2-fold increase in the number of GFAP+ cells in the striatum of WT mice, an effect that was completely absent in MK $^{-/-}$ mice (Figure 4). In the case of microglia, LPS induced a robust response in both genotypes (Figure 5). However, compared to their corresponding saline-paired control groups, the increases in the number of Iba1+ cells in the striatum after LPS administration tended to be similar in WT and MK $^{-/-}$ mice (Figure 5(b)). The data demonstrate that MK modulates the astrocytic, but not microglial, response induced by LPS in the striatum.

3.4. Effect of Amphetamine on Y-Maze Behavior. The data presented here demonstrate for the first time an important role of MK in the modulation of the neuroinflammatory processes induced by amphetamine in the striatum. These processes have been related to the cognitive deficits caused by amphetamines abuse in humans [6]. Thus, we next tested the possibility that endogenous MK modulates the cognitive effects caused by a 10-day amphetamine treatment during adolescence, a stage especially vulnerable to the cognitive deficits induced by these drugs [23, 31]. Six days after the last amphetamine (or saline) administration, we assessed for the first time the behavior of six-week-old mice from both genotypes on the Y-maze (Figure 6). To test the possible long-term effects of amphetamine treatment during adolescence on the behavioral performance of WT and MK $^{-/-}$ mice on a memory task, we tested them again one week (7-week-old mice) and three weeks later (9-week-old mice). First, it was found that control (saline-treated) WT and MK $^{-/-}$ mice efficiently established spatial memory in a similar manner (Figures 6(a)–6(c)). Amphetamine treatment during adolescence tended to impair the recognition memory in the Y-maze in 6-week-old MK $^{-/-}$ mice (Figure 6(a)). This amphetamine-induced impairment of the recognition memory was exacerbated in 7-week-old MK $^{-/-}$ compared to WT mice (Figure 6(b)). However, this effect of amphetamine in recognition memory of 6- and 7-week-old MK $^{-/-}$ mice

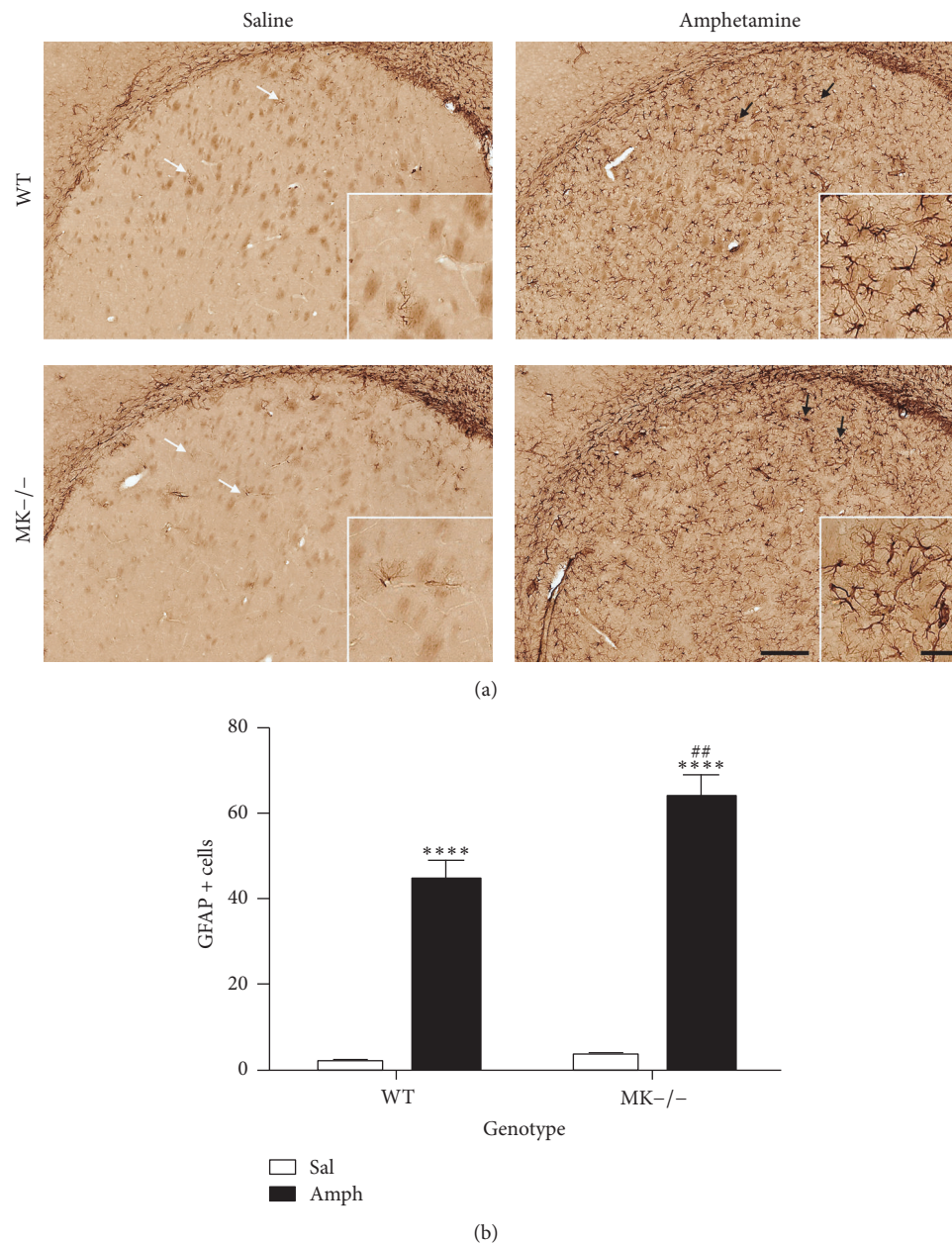


FIGURE 1: Amphetamine induces astrocytosis in the striatum of WT and MK^{-/-} mice. (a) Photomicrographs are from GFAP-immunostained striatal sections of saline- (Sal-) or amphetamine- (Amph-) treated animals. Amphetamine induced reactive astrocytes characterized by larger densely stained bodies with longer and extensive processes (black arrows) compared to saline-treated mice (white arrows). (b) The graph represents quantification of data (mean ± SEM) obtained from the counts of GFAP-positive cells in standardized areas of the striatum. Significant effects of the genotype ($F_{(1,16)} = 8.051$, $P = 0.01$), the treatment ($F_{(1,16)} = 200.3$, $P < 0.0001$), and genotype by treatment variant interaction ($F_{(1,16)} = 5.896$, $P = 0.03$) were found. **** $P < 0.0001$ versus Sal. ### $P < 0.01$ versus WT. Scale bar = 200 μm . Magnified inset = 50 μm .

was found to be transient since it was abolished in 9-week-old mice (Figure 6(c)). The data indicate that the cognitive impairment caused by periadolescent amphetamine treatment is modulated by endogenous MK.

4. Discussion

According to the European Monitoring Centre for Drugs and Drug Addiction, ever in lifetime use of amphetamines

among young people in Europe varies considerably, with levels of 30–70%. Despite widespread use of amphetamine-type stimulants, the medical consequences of these drugs abuse and the mechanisms underlying them are only partially understood. These drugs cause neuroinflammation [1], a pathogenic mechanism contributing to amphetamine-induced dopaminergic injury in the nigrostriatal pathway [32]. Accordingly, significant increases in the prevalence of PD in amphetamine-type drug abusers have been

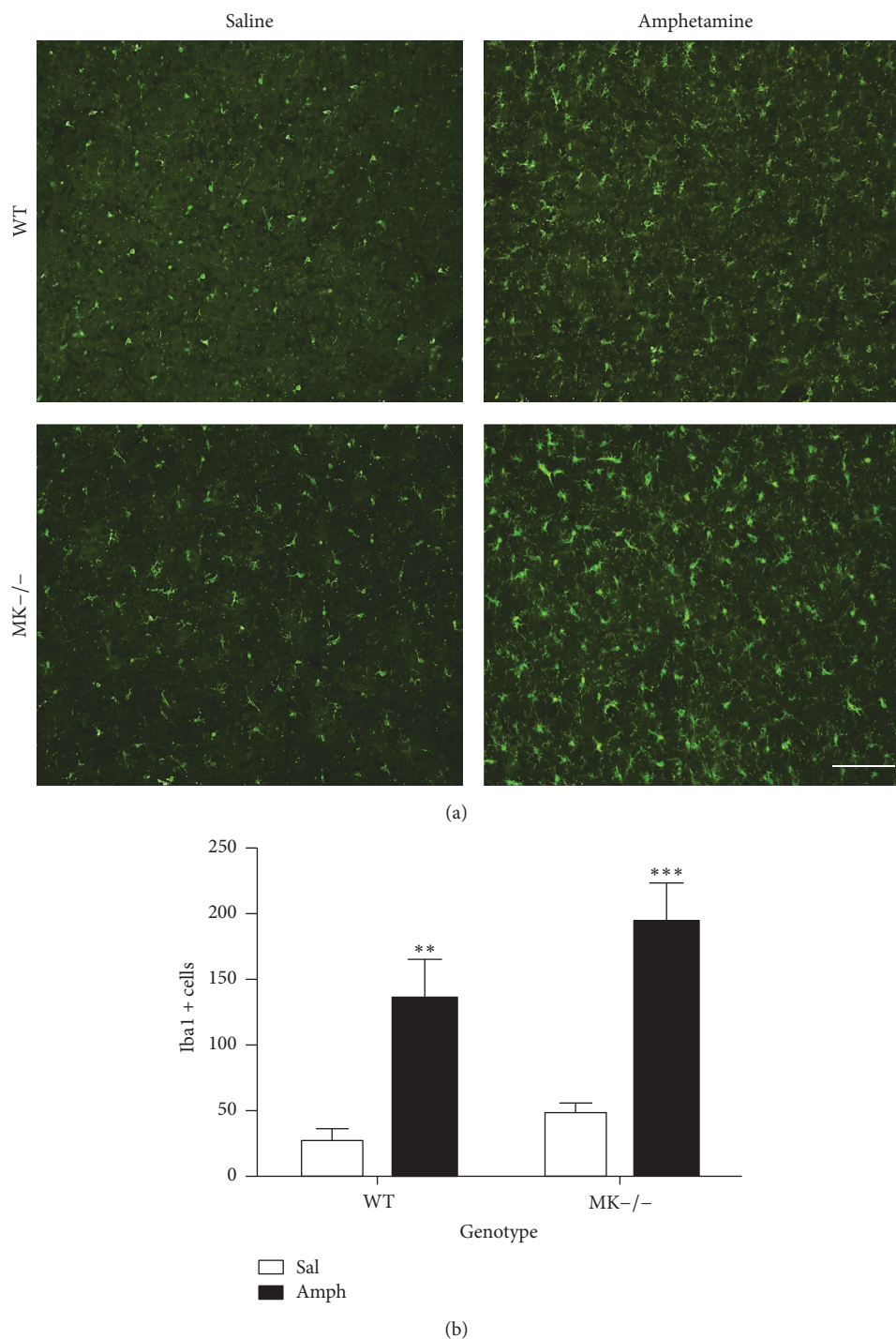


FIGURE 2: Amphetamine induces microglial in the striatum of WT and MK^{-/-} mice. (a) Photomicrographs are from Iba-1-immunostained striatal sections of saline- (Sal-) or amphetamine- (Amph-) treated animals. (b) The graph represents quantification of data (mean ± SEM) obtained from the counts of Iba-1-positive cells in standardized areas of the striatum. Significant effects of the genotype ($F_{(1,10)} = 4.597$, $P = 0.05$) and treatment ($F_{(1,10)} = 46.12$, $P < 0.0001$) were found. ** $P < 0.01$ and *** $P < 0.001$ versus Sal. Scale bar = 200 μm .

reported [7, 8]. In the present work, we have confirmed that amphetamine-induced astrogliosis in the striatum, a hallmark of amphetamine-type drugs-induced neuroinflammation, is potentiated by genetic inactivation of MK [21]. More importantly, we demonstrate for the first time that

amphetamine-induced striatal microglial response is also enhanced in MK^{-/-} mice. The data indicate that MK is a genetic factor that regulates the neuroinflammatory effects induced by this type of psychostimulants. In this context, it is also important to note that MK expression and signaling are

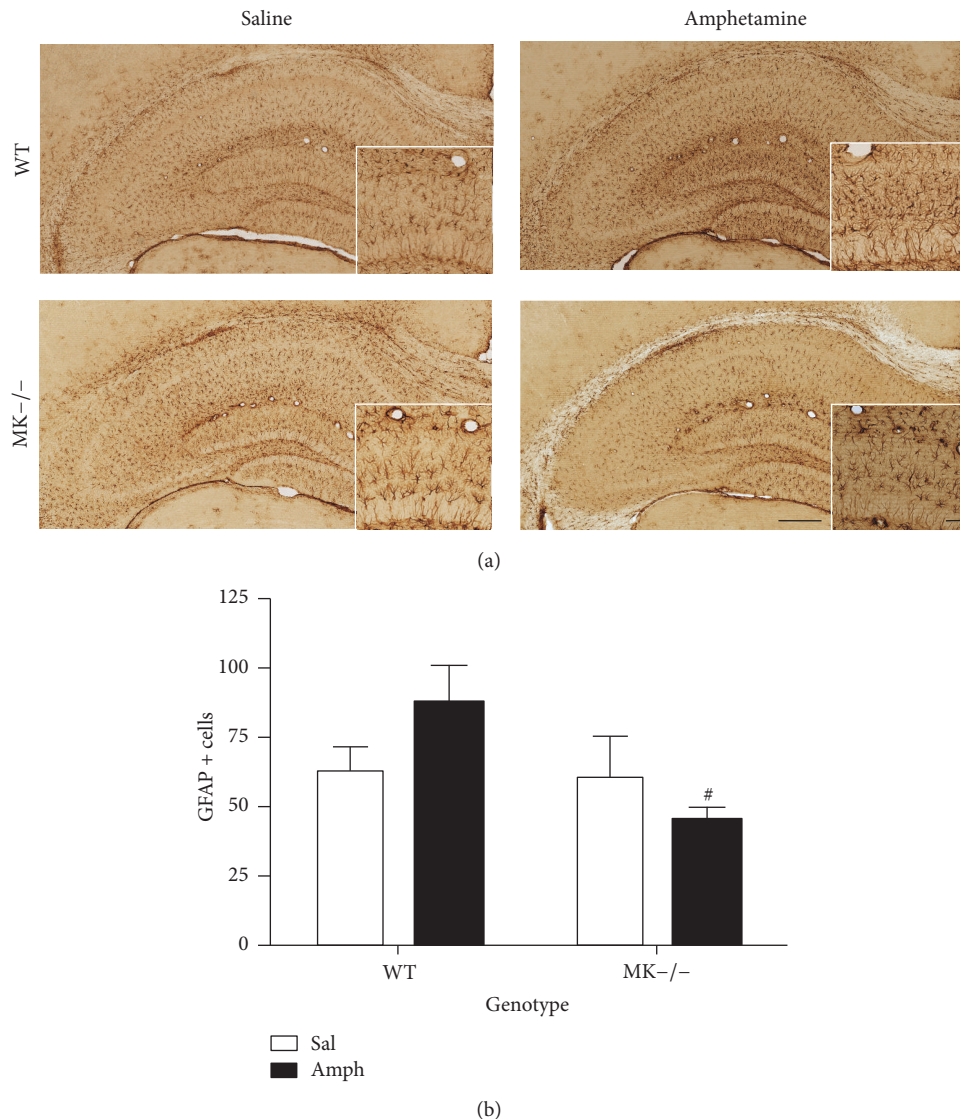


FIGURE 3: Amphetamine-induced astrocytosis in the hippocampus of WT and MK^{-/-} mice. (a) Photomicrographs are from GFAP-immunostained hippocampal sections of saline- (Sal-) or amphetamine- (Amph-) treated animals. (b) The graph represents quantification of data (mean \pm SEM) obtained from the counts of GFAP-positive cells in standardized areas of the CA1 region of hippocampus. A significant effect of the genotype ($F_{(1,12)} = 4.88, P = 0.04$) was found. [#] $P < 0.05$ versus WT. Scale bar = 200 μ m. Magnified inset = 50 μ m.

activated in the brain after administration of different drugs of abuse [33–35]. Taking together, our data suggest that the previously shown neuroprotective effects of MK against drug-induced neurotoxicity [20, 36] could be related to its ability to prevent neuroinflammation.

The counteractive effect of MK against amphetamine astrogliosis seems to be region-specific since it is observed in the striatum, the main area affected by the neurotoxic effects of amphetamine, but not in the hippocampus. One possible explanation for these differences could be related to the different pattern of expression of MK after injury in both areas. While increased expression of MK is found in GFAP+ astrocytes in the injured mouse hippocampus [37], MK expression in the neurodegenerative nigrostriatal pathway is mainly found in neurons [20]. Thus, it is reasonable to hypothesize that constitutive genetic deletion of MK could

cause different effects in response to injury depending on the area considered.

Midkine expression levels in the brain are also upregulated in different pathologies characterized by overt neuroinflammation [3, 10, 20, 38]. Midkine is known to exert neuroprotective effects in some of these pathologies including Alzheimer's disease [18] and brain ischemia [39]. Thus, it is reasonable to hypothesize that the ability of MK to limit neuroinflammation could contribute to its neuroprotective actions in different pathological contexts. However, our data indicate that microglial response after LPS administration is not significantly regulated by MK. In contrast, LPS-induced striatal astrogliosis was blocked by genetic inactivation of MK. The data demonstrate a differential regulation of astrogliosis by MK depending on the inflammatory stimulus. The data presented here provide novel insights in the

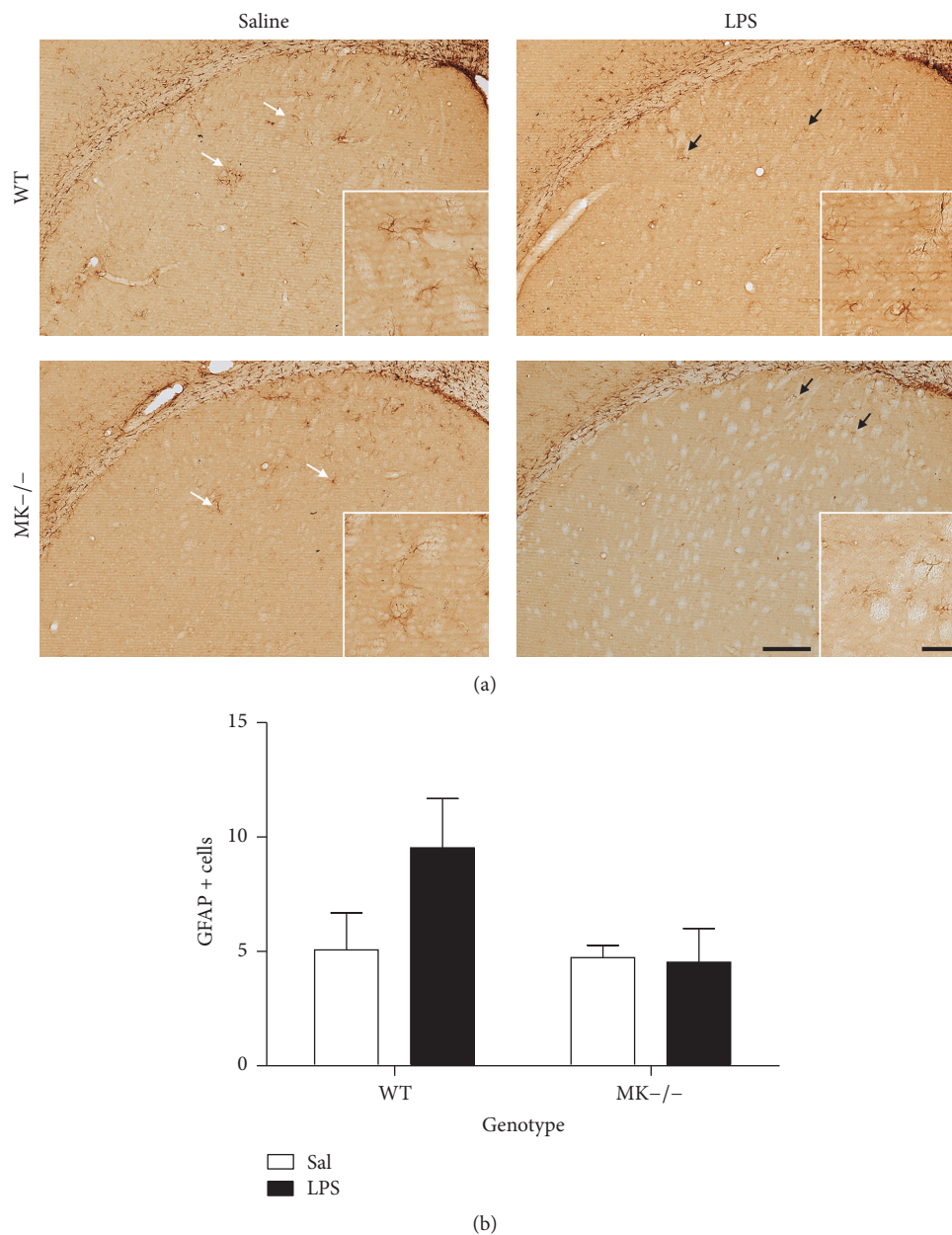


FIGURE 4: LPS-induced astrocytosis in the striatum of WT and MK^{-/-} mice. (a) Photomicrographs are from GFAP-immunostained striatal sections of saline- (Sal-) treated or 0.5 mg/kg lipopolysaccharide- (LPS-) treated animals. (b) The graph represents quantification of data (mean \pm SEM) obtained from the counts of GFAP-positive cells in standardized areas of the striatum. Scale bar = 200 μ m. Magnified inset = 50 μ m.

mechanisms and roles played by MK in CNS disorders in which astrogliosis is known to play pivotal roles. For instance, MK is expressed in senile plaques of Alzheimer's disease patients [40]. Astrogliosis facilitates A β plaque deposition in Alzheimer's disease [41] suggesting the interesting possibility that MK decreases A β plaque deposition [18] through its ability to prevent astrogliosis.

The mechanism of action of MK supports our findings. One receptor for MK is Receptor Protein Tyrosine Phosphatase β/ζ (RPTP β/ζ) (a.k.a. PTPRZ1) [42]. MK binds to RPTP β/ζ and inactivates its phosphatase activity. Inhibition

of the phosphatase activity of RPTP β/ζ by MK binding regulates the tyrosine phosphorylation levels of substrates of RPTP β/ζ which are known regulators of neuroinflammatory processes such as TrkA [43]. Signaling pathways downstream of MK/RPTP β/ζ which are also known to participate in gliosis include MAPK pathways [10]. Further studies are needed to test the possible involvement of these signaling pathways in the modulatory actions of MK in neuroinflammation.

Overall, the data presented here are relevant because the roles of MK in promoting inflammation had been described in detail in peripheral organs such as kidney and liver [10]

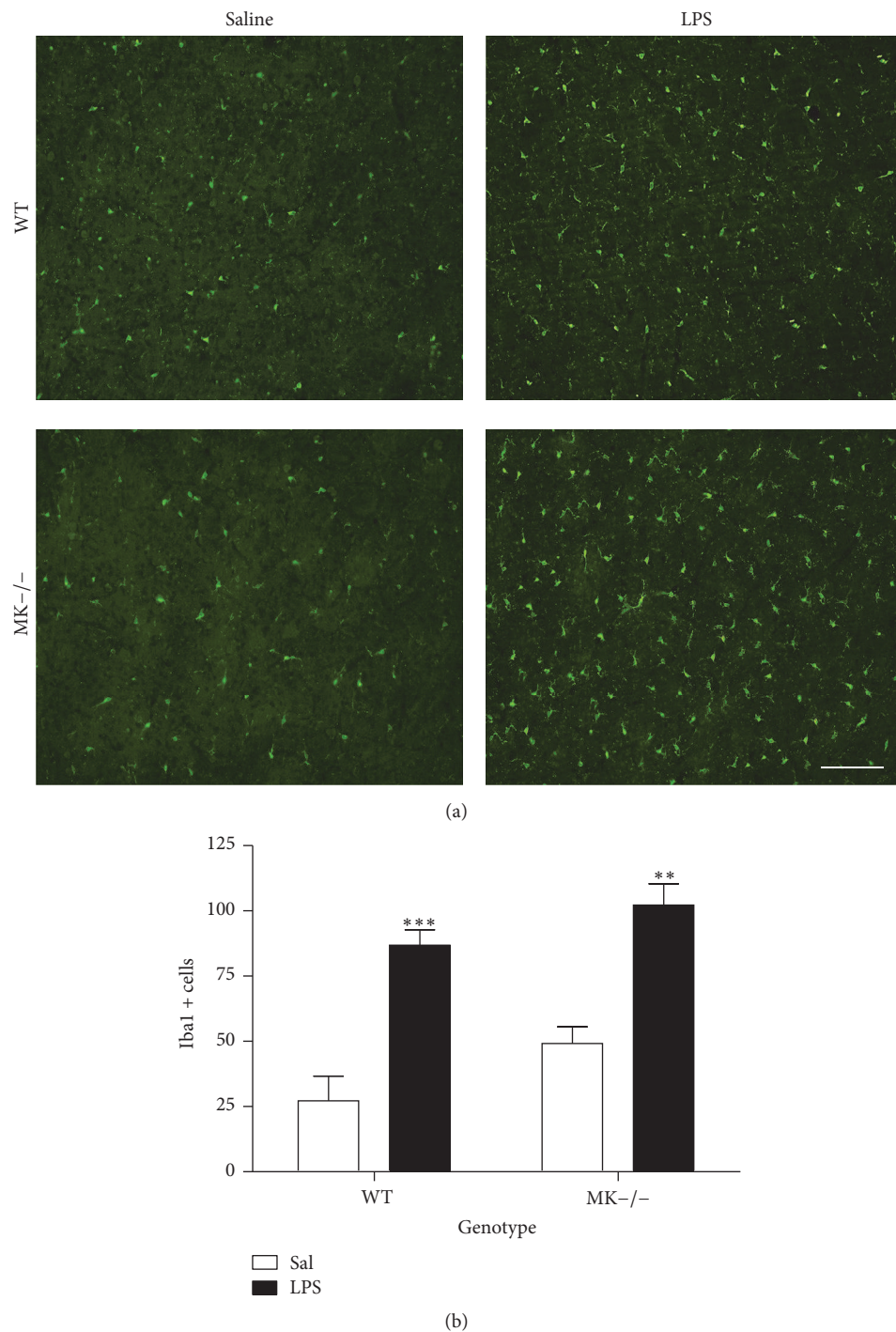


FIGURE 5: LPS-induced microgliosis in the striatum of WT and MK^{-/-} mice. (a) Photomicrographs are from Iba-1-immunostained striatal sections of saline- (Sal-) treated or 0.5 mg/kg lipopolysaccharide- (LPS-) treated animals. (b) The graph represents quantification of data (mean \pm SEM) obtained from the counts of Iba-1-positive cells in standardized areas of the striatum. Significant effects of the genotype ($F_{(1,12)} = 5.17, P = 0.04$) and treatment ($F_{(1,12)} = 47.41, P < 0.0001$) were found. ** $P < 0.01$ and *** $P < 0.001$ versus Sal. Scale bar = 200 μm .

but little was known about a possible role of MK in central inflammation. We now demonstrate for the first time that MK is a novel modulator of amphetamine-induced neuroinflammation in a brain area-dependent manner. We also show that MK differentially regulates astroglial processes depending on the noxious stimulus that triggers neuroinflammatory processes.

Our data support the need of further studies to dissect the specific modulatory roles of MK on neuroinflammation in the different brain pathologies in which MK has been shown to be upregulated.

In addition to its involvement in neurotoxicity and neurodegeneration, neuroinflammation significantly contributes

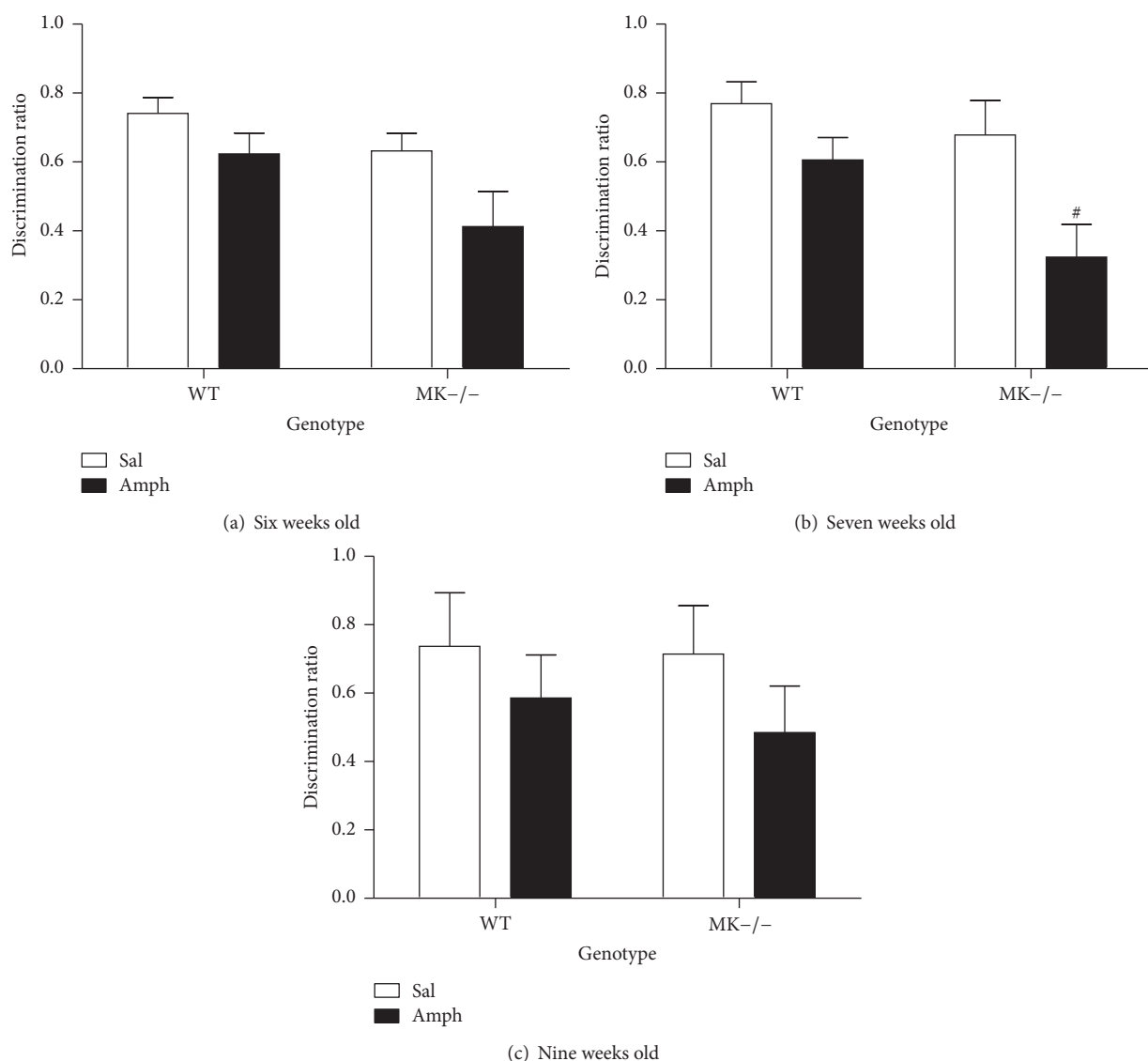


FIGURE 6: Behavioral performance in the Y-maze of WT and MK^{-/-} mice treated with amphetamine during adolescence. (a) Figure shows mean \pm SEM of discrimination ratio for 6-week-old WT and MK^{-/-} mice pretreated with amphetamine during adolescence. Significant effects of the genotype ($F_{(1,44)} = 5.04$, $P = 0.03$) and the treatment ($F_{(1,44)} = 6.03$, $P = 0.02$) were found. (b) Figure shows mean \pm SEM of discrimination ratio for 7-week-old WT and MK^{-/-} mice pretreated with amphetamine. Significant effects of the genotype ($F_{(1,44)} = 5.1$, $P = 0.03$) and treatment ($F_{(1,44)} = 10.46$, $P = 0.002$) were found. (c) Figure shows mean \pm SEM of discrimination ratio for 9-week-old WT and MK^{-/-} mice pretreated with amphetamine. # $P < 0.05$ versus WT.

to behavioral alterations possibly by affecting synaptic function [44]. Accordingly, new experimental therapeutics provide correlation between reduction of neuroinflammation and improved cognitive impairment in Alzheimer's disease [45]. Interestingly, behavioral changes associated with amphetamine treatment during adolescence are cognitive deficits [31]. Our data demonstrate that periadolescent amphetamine treatment has modest consequences in WT mice in the Y-maze test but causes a transient disruption of the working memory in the Y-maze in MK^{-/-} mice. The data suggest that genetic inactivation of MK confers greater vulnerability to the transient cognitive impairment associated with a periadolescent amphetamine treatment. It is tempting to connect these behavioral data with the reduced

amphetamine-induced astrocytosis in the MK^{-/-} mouse hippocampus, a relevant area for recognition memory. However, in the case of this type of drugs, it has been recently shown that neuroinflammatory processes induced by methamphetamine in the striatum underlie cognitive deficits in this drug's addicts [6]. Our data support the correlation between cognitive deficits and enhanced amphetamine-induced striatal neuroinflammation in MK^{-/-} mice.

5. Conclusions

The data demonstrate for the first time that MK is a novel regulator of neuroinflammation in a stimulus and brain region-dependent manner. The data presented here indicate

that MK limits amphetamine-induced striatal neuroinflammation. The data also demonstrate that periadolescent amphetamine treatment in mice results in transient disruption of learning and memory processes in MK^{-/-} mice, effect that could be related to the absence of the counteractive actions of MK in striatal neuroinflammation.

Competing Interests

The authors do not have any conflict of interests to declare.

Acknowledgments

This work has been supported by Grants SAF2014-56671-R from Ministerio de Economía y Competitividad of Spain and USP-BS-APP03/2014 from Universidad CEU San Pablo and Banco de Santander. Marta Vicente-Rodríguez and Rosalía Fernández-Calle are supported by fellowships from Fundación Universitaria San Pablo CEU.

References

- [1] V. Coelho-Santos, J. Gonçalves, C. Fontes-Ribeiro, and A. P. Silva, "Prevention of methamphetamine-induced microglial cell death by TNF- α and IL-6 through activation of the JAK-STAT pathway," *Journal of Neuroinflammation*, vol. 9, article 103, 2012.
- [2] L. S. Feder and D. L. Laskin, "Regulation of hepatic endothelial cell and macrophage proliferation and nitric oxide production by GM-CSF, M-CSF, and IL-1 β following acute endotoxemia," *Journal of Leukocyte Biology*, vol. 55, pp. 507–513, 1994.
- [3] L. C. Freeman and J. P.-Y. Ting, "The pathogenic role of the inflammasome in neurodegenerative diseases," *Journal of Neurochemistry*, vol. 136, supplement 1, pp. 29–38, 2016.
- [4] V. Sanchez-Guajardo, C. J. Barnum, M. G. Tansey, and M. Romero-Ramos, "Neuroimmunological processes in Parkinson's disease and their relation to α -synuclein: microglia as the referee between neuronal processes and peripheral immunity," *ASN Neuro*, vol. 5, no. 2, pp. 113–139, 2013.
- [5] L. Qin, X. Wu, M. L. Block et al., "Systemic LPS causes chronic neuroinflammation and progressive neurodegeneration," *Glia*, vol. 55, no. 5, pp. 453–462, 2007.
- [6] I. N. Krasnova, Z. Justinova, and J. L. Cadet, "Methamphetamine addiction: involvement of CREB and neuroinflammatory signaling pathways," *Psychopharmacology*, vol. 233, no. 10, pp. 1945–1962, 2016.
- [7] R. C. Callaghan, J. K. Cunningham, J. Sykes, and S. J. Kish, "Increased risk of Parkinson's disease in individuals hospitalized with conditions related to the use of methamphetamine or other amphetamine-type drugs," *Drug and Alcohol Dependence*, vol. 120, no. 1–3, pp. 35–40, 2012.
- [8] K. Curtin, A. E. Fleckenstein, R. J. Robison, M. J. Crookston, K. R. Smith, and G. R. Hanson, "Methamphetamine/amphetamine abuse and risk of Parkinson's disease in Utah: a population-based assessment," *Drug and Alcohol Dependence*, vol. 146, no. 1, pp. 30–38, 2015.
- [9] A. J. Nimmo and R. Vink, "Recent patents in CNS drug discovery: the management of inflammation in the central nervous system," *Recent Patents on CNS Drug Discovery*, vol. 4, no. 2, pp. 86–95, 2009.
- [10] T. Muramatsu, "Structure and function of midkine as the basis of its pharmacological effects," *British Journal of Pharmacology*, vol. 171, no. 4, pp. 814–826, 2014.
- [11] L. T. Weckbach, A. Gola, M. Winkelmann et al., "The cytokine midkine supports neutrophil trafficking during acute inflammation by promoting adhesion via β_2 integrins (CD11/CD18)," *Blood*, vol. 123, no. 12, pp. 1887–1896, 2014.
- [12] M. Horiba, K. Kadomatsu, E. Nakamura et al., "Neointima formation in a restenosis model is suppressed in midkine-deficient mice," *Journal of Clinical Investigation*, vol. 105, no. 4, pp. 489–495, 2000.
- [13] W. Sato, K. Kadomatsu, Y. Yuzawa et al., "Midkine is involved in neutrophil infiltration into the tubulointerstitium in ischemic renal injury," *The Journal of Immunology*, vol. 167, no. 6, pp. 3463–3469, 2001.
- [14] T. Takada, K. Toriyama, H. Muramatsu, X. J. Song, S. Torii, and T. Muramatsu, "Midkine, a retinoic acid-inducible heparin-binding cytokine in inflammatory responses: chemotactic activity to neutrophils and association with inflammatory synovitis," *Journal of Biochemistry*, vol. 122, no. 2, pp. 453–458, 1997.
- [15] Y. Sonobe, H. Li, S. Jin et al., "Midkine inhibits inducible regulatory T cell differentiation by suppressing the development of tolerogenic dendritic cells," *The Journal of Immunology*, vol. 188, no. 6, pp. 2602–2611, 2012.
- [16] J. Wang, H. Takeuchi, Y. Sonobe et al., "Inhibition of midkine alleviates experimental autoimmune encephalomyelitis through the expansion of regulatory T cell population," *Proceedings of the National Academy of Sciences of the United States of America*, vol. 105, no. 10, pp. 3915–3920, 2008.
- [17] A. Muramoto, S. Imagama, T. Natori et al., "Midkine overcomes neurite outgrowth inhibition of chondroitin sulfate proteoglycan without glial activation and promotes functional recovery after spinal cord injury," *Neuroscience Letters*, vol. 550, pp. 150–155, 2013.
- [18] T. Muramatsu, "Midkine: a promising molecule for drug development to treat diseases of the central nervous system," *Current Pharmaceutical Design*, vol. 17, no. 5, pp. 410–423, 2011.
- [19] E. Gramage and G. Herradón, "Connecting Parkinson's disease and drug addiction: common players reveal unexpected disease connections and novel therapeutic approaches," *Current Pharmaceutical Design*, vol. 17, no. 5, pp. 449–461, 2011.
- [20] G. Herradón and C. Pérez-García, "Targeting midkine and pleiotrophin signalling pathways in addiction and neurodegenerative disorders: Recent progress and perspectives," *British Journal of Pharmacology*, vol. 171, no. 4, pp. 837–848, 2014.
- [21] E. Gramage, Y. B. Martín, P. Ramanah, C. Pérez-García, and G. Herradón, "Midkine regulates amphetamine-induced astrogliosis in striatum but has no effects on amphetamine-induced striatal dopaminergic denervation and addictive effects: functional differences between pleiotrophin and midkine," *Neuroscience*, vol. 190, pp. 307–317, 2011.
- [22] L.-M. Mao, B. Xue, D.-Z. Jin, and J. Q. Wang, "Dynamic increases in AMPA receptor phosphorylation in the rat hippocampus in response to amphetamine," *Journal of Neurochemistry*, vol. 133, no. 6, pp. 795–805, 2015.
- [23] D. I. Lubman, M. Yücel, and W. D. Hall, "Substance use and the adolescent brain: a toxic combination?" *Journal of Psychopharmacology*, vol. 21, no. 8, pp. 792–794, 2007.
- [24] E. Nakamura, K. Kadomatsu, S. Yuasa et al., "Disruption of the midkine gene (Mdk) resulted in altered expression of a calcium binding protein in the hippocampus of infant mice and their

- abnormal behaviour," *Genes to Cells*, vol. 3, no. 12, pp. 811–822, 1998.
- [25] A. Jacob, L. K. Hensley, B. D. Safratowich, R. J. Quigg, and J. J. Alexander, "The role of the complement cascade in endotoxin-induced septic encephalopathy," *Laboratory Investigation*, vol. 87, no. 12, pp. 1186–1194, 2007.
- [26] E. Gramage, A. Putelli, M. J. Polanco et al., "The neurotrophic factor pleiotrophin modulates amphetamine-seeking behaviour and amphetamine-induced neurotoxic effects: evidence from pleiotrophin knockout mice," *Addiction Biology*, vol. 15, no. 4, pp. 403–412, 2010.
- [27] E. Gramage, L. Rossi, N. Granado, R. Moratalla, and G. Herradón, "Genetic inactivation of pleiotrophin triggers amphetamine-induced cell loss in the substantia nigra and enhances amphetamine neurotoxicity in the striatum," *Neuroscience*, vol. 170, no. 1, pp. 308–316, 2010.
- [28] E. Gramage, N. Del Olmo, A. Fole, Y. B. Martín, and G. Herradón, "Periadolescent amphetamine treatment causes transient cognitive disruptions and long-term changes in hippocampal LTP depending on the endogenous expression of pleiotrophin," *Addiction biology*, vol. 18, no. 1, pp. 19–29, 2013.
- [29] N. del Olmo, E. Gramage, L. F. Alguacil, P. Pérez-Pinera, T. F. Deuel, and G. Herradón, "Pleiotrophin inhibits hippocampal long-term potentiation: a role of pleiotrophin in learning and memory," *Growth Factors*, vol. 27, no. 3, pp. 189–194, 2009.
- [30] N. T. Boyle and T. J. Connor, "Methylenedioxymethamphetamine ('Ecstasy')-induced immunosuppression: a cause for concern?" *British Journal of Pharmacology*, vol. 161, no. 1, pp. 17–32, 2010.
- [31] T. Featherby, M. Van Den Buuse, D. I. Lubman, and A. J. Lawrence, "Persistent downregulation of hippocampal CREB mRNA parallels a Y-maze deficit in adolescent rats following semi-chronic amphetamine administration," *British Journal of Pharmacology*, vol. 154, no. 2, pp. 417–428, 2008.
- [32] R. Moratalla, A. Khairnar, N. Simola et al., "Amphetamine-related drugs neurotoxicity in humans and in experimental animals: main mechanisms," *Progress in Neurobiology*, vol. S0301-0082, no. 15, pp. 00100–00108, 2015.
- [33] L. Ezquerra, C. Pérez-García, E. Garrido et al., "Morphine and yohimbine regulate midkine gene expression in the rat hippocampus," *European Journal of Pharmacology*, vol. 557, no. 2-3, pp. 147–150, 2007.
- [34] T. Flatscher-Bader and P. A. Wilce, "Impact of alcohol abuse on protein expression of midkine and excitatory amino acid transporter 1 in the human prefrontal cortex," *Alcoholism: Clinical and Experimental Research*, vol. 32, no. 10, pp. 1849–1858, 2008.
- [35] Y. He, L. Xu, B. Li et al., "Macrophage-inducible C-type lectin/spleen tyrosine kinase signaling pathway contributes to neuroinflammation after subarachnoid hemorrhage in rats," *Stroke*, vol. 46, no. 8, pp. 2277–2286, 2015.
- [36] G. Herradon, L. Ezquerra, E. Gramage, and L. F. Alguacil, "Targeting the pleiotrophin/receptor protein tyrosine phosphatase β/ζ signaling pathway to limit neurotoxicity induced by drug abuse," *Mini-Reviews in Medicinal Chemistry*, vol. 9, no. 4, pp. 440–447, 2009.
- [37] Y. B. Kim, J. K. Ryu, H. J. Lee et al., "Midkine, heparin-binding growth factor, blocks kainic acid-induced seizure and neuronal cell death in mouse hippocampus," *BMC Neuroscience*, vol. 11, article 42, 2010.
- [38] T. Kielian, "Multifaceted roles of neuroinflammation: the need to consider both sides of the coin," *Journal of Neurochemistry*, vol. 136, supplement 1, pp. 5–9, 2016.
- [39] S. Otsuka, H. Sakakima, M. Sumizono, S. Takada, T. Terashi, and Y. Yoshida, "The neuroprotective effects of preconditioning exercise on brain damage and neurotrophic factors after focal brain ischemia in rats," *Behavioural Brain Research*, vol. 303, pp. 9–18, 2016.
- [40] O. Yasuhara, H. Muramatsu, S. U. Kim, T. Muramatsu, H. Maruta, and P. L. McGeer, "Midkine, a novel neurotrophic factor, is present in senile plaques of Alzheimer disease," *Biochemical and Biophysical Research Communications*, vol. 192, no. 1, pp. 246–251, 1993.
- [41] E. Rodriguez-Vieitez, R. Ni, B. Gulyás et al., "Astrocytosis precedes amyloid plaque deposition in Alzheimer APPswe transgenic mouse brain: a correlative positron emission tomography and in vitro imaging study," *European Journal of Nuclear Medicine and Molecular Imaging*, vol. 42, no. 7, pp. 1119–1132, 2015.
- [42] N. Sakaguchi, H. Muramatsu, K. Ichihara-Tanaka et al., "Receptor-type protein tyrosine phosphatase ζ as a component of the signaling receptor complex for midkine-dependent survival of embryonic neurons," *Neuroscience Research*, vol. 45, no. 2, pp. 219–224, 2003.
- [43] T. Shintani and M. Noda, "Protein tyrosine phosphatase receptor type Z dephosphorylates TrkA receptors and attenuates NGF-dependent neurite outgrowth of PC12 cells," *The Journal of Biochemistry*, vol. 144, no. 2, pp. 259–266, 2008.
- [44] J. Di, L. S. Cohen, C. P. Corbo, G. R. Phillips, A. El Idrissi, and A. D. Alonso, "Abnormal tau induces cognitive impairment through two different mechanisms: synaptic dysfunction and neuronal loss," *Scientific Reports*, vol. 6, Article ID 20833, 2016.
- [45] V. Echeverria, A. Yarkov, and G. Aliev, "Positive modulators of the $\alpha 7$ nicotinic receptor against neuroinflammation and cognitive impairment in Alzheimer's disease," *Progress in Neurobiology*, vol. 144, pp. 142–157, 2016.

ANEXO 3. Development of inhibitors of receptor protein tyrosine phosphatase β/ζ (PTPRZ1) as candidates for CNS disorders.

Myriam Pastor*, Rosalía Fernández-Calle*, Bruno Di Geronimo*, Marta Vicente-Rodríguez, José María Zapico, Claire Coderch, Carmen Pérez-García, Amy W. Lasek, Loreto Puchades-Carrasco, Antonio Pineda-Lucena, Beatriz de Pascual-Teresa, Gonzalo Herradón y Ana Ramos.

European Journal of Medicinal Chemistry, 2018. ISSN: 1768-3254

Volumen: 144

Número de páginas: 318-329

DOI: 10.1016/j.ejmech.2017.11.080

*Rosalía Fernández Calle comparte en este artículo primera autoría junto con Myriam Pastor y Bruno Di Geronimo.



Contents lists available at ScienceDirect

European Journal of Medicinal Chemistry

journal homepage: <http://www.elsevier.com/locate/ejmech>

Research paper

Development of inhibitors of receptor protein tyrosine phosphatase β/ζ (PTPRZ1) as candidates for CNS disorders

Miryam Pastor ^{a,1}, Rosalía Fernández-Calle ^{b,1}, Bruno Di Geronimo ^{a,1},
 Marta Vicente-Rodríguez ^b, José María Zapico ^a, Esther Gramage ^b, Claire Coderch ^a,
 Carmen Pérez-García ^b, Amy W. Lasek ^d, Leonor Puchades-Carrasco ^c,
 Antonio Pineda-Lucena ^c, Beatriz de Pascual-Teresa ^{a,***}, Gonzalo Herradón ^{b,**},
 Ana Ramos ^{a,*}

^a Departamento de Química y Bioquímica, Facultad de Farmacia, Universidad San Pablo-CEU, CEU Universities, Urbanización Montepríncipe, 28925, Alcorcón, Madrid, Spain

^b Departamento de Ciencias Farmacéuticas y de la Salud, Facultad de Farmacia, Universidad San Pablo-CEU, CEU Universities, Urbanización Montepríncipe, 28925, Alcorcón, Madrid, Spain

^c Unidad Mixta en Metabolómica Clínica Instituto de Investigación Sanitaria La Fe – Centro de Investigación Príncipe Felipe, Hospital Universitario y Politécnico La Fe, Avenida Fernando Abril Martorell, 106, Torre A, 6-17, 46026 Valencia, Spain

^d Department of Psychiatry, University of Illinois at Chicago, 1601 West Taylor Street, Chicago, IL 60612, USA

ARTICLE INFO

Article history:

Received 18 September 2017

Received in revised form

10 November 2017

Accepted 27 November 2017

Available online 28 November 2017

Keywords:

PTPRZ1

CNS disorders

Drug addiction

Molecular dynamics

Synthesis

ABSTRACT

A new series of blood-brain barrier permeable molecules designed to mimic the activity of Pleiotrophin in the CNS has been designed and synthesized. These compounds exert their action by interacting with the intracellular domain PD1 of the Protein Tyrosine-Phosphatase Receptor Z1 (PTPRZ1), and inhibiting its tyrosine phosphatase activity. The most potent compounds **10a** and **12b** ($IC_{50} = 0,1 \mu M$) significantly increase the phosphorylation of key tyrosine residues of PTPRZ1 substrates involved in neuronal survival and differentiation, and display protective effects against amphetamine-induced toxicity. Docking and molecular dynamics experiments have been used to analyze the binding mode and to explain the observed selectivity against PTP1B. An *In vivo* experiment has demonstrated that **10a** can cross the BBB, thus promoting the possibility of moving forward these candidates for the development of drugs for the treatment of CNS disorders, such as drug addiction and neurodegenerative diseases.

© 2017 Elsevier Masson SAS. All rights reserved.

1. Introduction

Pleiotrophin (PTN) and Midkine (MK) are neurotrophic factors that share over 50% identity in amino acid sequence [1]. Both PTN and MK play important roles in development and repair of the

central nervous system (CNS) [2]. The PTN and MK genes are widely expressed at different times in different cell types during development [3]. However, their expression levels are highly restricted to a few cell types in adults [4]. Both PTN and MK are upregulated at sites of injury, inflammation and repair in different cells of the CNS [5]. It is important to note that both PTN and MK regulate neuro-inflammation depending on the inflammatory stimulus and the brain area considered [6]. In addition, MK and PTN are expressed in senile plaques of patients with Alzheimer's disease [7] and PTN upregulation has been also observed in the substantia nigra of Parkinson's Disease (PD) patient [8]. Both cytokines are also upregulated in different brain areas after administration of different drugs of abuse [9], suggesting PTN and MK signaling may be critical in different steps of wound repair in neurotoxic and neurodegenerative processes. Accordingly, in studies carried out in PTN knockout (PTN^{-/-}) mice, it was shown that PTN prevents

Abbreviations: EDCl, 1-Ethyl-3-(3-dimethylaminopropyl)carbodiimide; HOBT, hydroxybenzotriazole; MCPBA, meta-chloroperbenzoic acid; MK, Midkine; PAMPA-BBB, membrane permeability assay for the blood-brain barrier; PTN, Pleiotrophin; PTPRZ1, Protein Tyrosine-Phosphatase Receptor Z1; SDDB, strategic drug delivery to brain; TPSA, topological polar surface area.

* Corresponding author.

** Corresponding author.

*** Corresponding author.

E-mail addresses: bpaster@ceu.es (B. de Pascual-Teresa), herradon@ceu.es (G. Herradón), aramgon@ceu.es (A. Ramos).

¹ M. P., R. F-C, and B. di G. contributed equally.

<https://doi.org/10.1016/j.ejmech.2017.11.080>

0223-5234/© 2017 Elsevier Masson SAS. All rights reserved.

amphetamine-induced dopaminergic injury in the nigrostriatal pathway [10]. In concordance with these data, striatal over-expression of PTN in different mouse models of dopaminergic injury exerts neuroprotective effects [11].

These cytokines also modulate addictive behaviors. MK and PTN contribute to the extinction of cocaine- and amphetamine-seeking behaviors, respectively [10c,12] PTN limits morphine withdrawal syndrome [13] and both, PTN and MK, are potent regulators of behavioral effects induced by ethanol [14]. Particularly, it has been demonstrated that PTN transgenic overexpression in the brain blocks the rewarding effects of alcohol [14a,14b]. Overall, the data suggest that PTN and MK could be used for the treatment of neurodegenerative diseases, for prevention of drugs of abuse-induced neurotoxicity and for the treatment of a wide variety of drug addiction disorders. Like other proteins, PTN and MK exert suboptimal drug-like properties/inability to cross the blood-brain barrier (BBB). Although strategic drug delivery to the brain has been successfully used with other proteins [15], the risks in many occasions outweigh the benefits. If possible, pharmacological modulation of the signaling pathways triggered by PTN and MK may be preferred [9].

Both PTN and MK bind to the Protein Tyrosine-Phosphatase Receptor Z1 (PTPRZ1; a.k.a. (R)PTP β or RPTP β/ζ), induce its oligomerization and inactivate its phosphatase activity [16]. This leads to an increase in tyrosine phosphorylation of substrates critical for the effects of these cytokines such as β -catenin16b, Fyn kinase [17] and Anaplastic Lymphoma Kinase (ALK) [18]. We hypothesize that PTN and MK actions on neurodegenerative diseases and drug addiction disorders described above can be reproduced with rationally designed small molecule inhibitors of PTPRZ1 [5a,9].

PTPRZ1 inhibitors have been recently tested in tumor models [19]. However, these molecules were unable to cross the cell membrane and required intracellular delivery by liposome carriers precluding use for the treatment of CNS diseases. In the present work, we propose to modulate the phosphatase activity of PTPRZ1 through the design and synthesis of small molecules that can cross the BBB and mimic the actions of PTN and MK.

Many known phosphatase inhibitors contain multi-charged phosphate-mimicking components, and show poor cellular uptake. Huang et al. [20] described, for the first time, one compound carrying an uncharged phosphate mimic (compound **1**, Table 1) with a moderate activity against PTPRZ1 ($IC_{50} = 3.5 \mu M$), and a certain degree of selectivity against other related phosphatases.

Table 1
Values of calculated TPSA, logP/logD and results of the Phospho-Tyr and PTPRZ1 inhibition test at 1.0 μM .

Comp.	TPSA	LogP/LogD	Phospho-Tyr	PTPRZ1 inhibition at 1.0 μM
1	94.27	5.35	X	–
4a	79.70	7.26	✓	X
4b	79.70	7.37	✓	X
4c	79.70	6.99	✓	✓
4d	79.70	6.88	✓	✓
5a	114.14	4.88	X	–
5b	114.14	5.00	✓	✓
5c	114.14	4.62	✓	X
10a	59.83	7.73	✓	✓
10b	51.75	6.54	X	–
10c	47.42	4.34	✓	X
12a	62.63	7.55	✓	X
12b	62.63	7.50/6.64	✓	✓
12c	41.91	5.43/4.41	X	–
12d	37.33	5.48	✓	✓
12e	37.33	5.99	X	–
13	79.14	11.72/11.56	✓	X

Considering **1** as a hit compound, we have followed a classical medicinal hit to lead optimization for the discovery of new PTPRZ1 inhibitors with a potential increased activity and selectivity and, more importantly, capable of crossing the BBB.

2. Results and discussion

2.1. Design rationale

The structure of compound **1** and all the analogs synthesized in this work is depicted in Schemes 1–3.

We have analyzed the effect of the substitution in the aromatic rings present in **1**, and the nature and length of the connecting linker. In compounds **5a-c**, the ether linkage was substituted by amides of different length (Scheme 1). Topological Polar Surface Area (TPSA) for these sulfoxides and the possibility of establishing ten hydrogen bond acceptors (see Table 1) predict a low bioavailability for a successful CNS drug [21]. To analyze whether the sulfoxide group is necessary for activity, and with the aim of improving pharmacokinetic properties, sulfides **4a-d**, and **10a-b** (Scheme 2) were also biologically tested. Calculated logP values for these sulfides are higher than the optimal 5 value. For this reason, sulfide **10c**, where an aromatic ring was substituted by a pyridine, and sulfides **12a-e** (Scheme 3) carrying an amino linker, were also selected for synthesis and biological evaluation.

2.2. Chemistry

The synthesis of compounds **4** and **5** is depicted in Scheme 1. Sulfides **4a** and **4d** were synthesized by reaction of 4-((trifluoromethyl)thio) benzoyl chloride (**2a**) and the corresponding amine **3**. For the synthesis of amides **4b** and **4c**, a (EDCI) catalyzed coupling between 2-(4-((trifluoromethyl)thio)phenyl)acetic acid (**2b**) and the corresponding amine **3** was followed. Oxidation of **4a-c** with *m*-chloroperbenzoic acid provided sulfones **5a-c**.

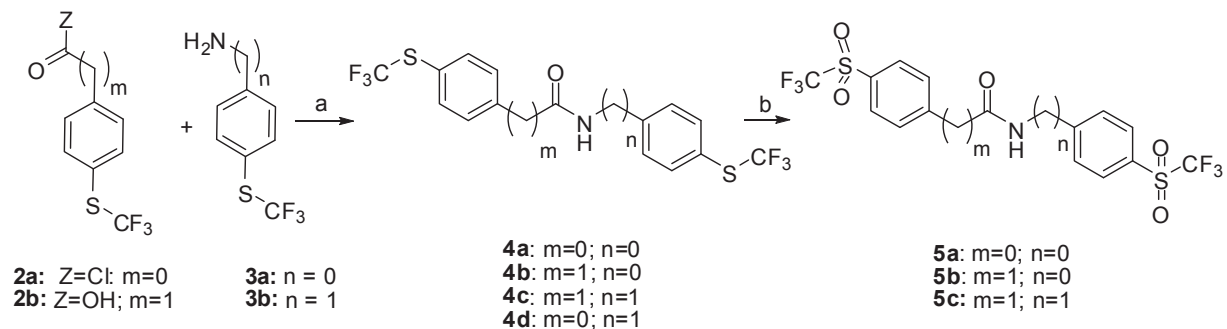
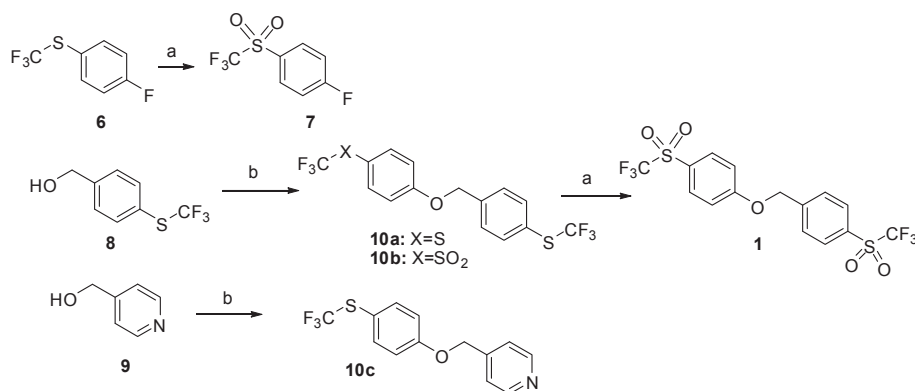
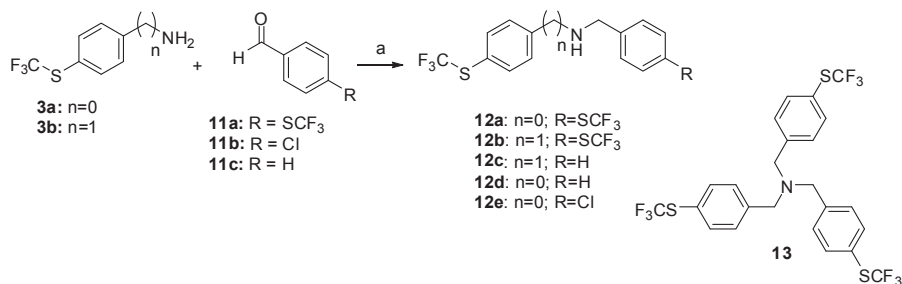
Compounds **10** were synthesized by arylation of benzylic alcohols **8** and **9** with (4-fluorophenyl)(trifluoromethyl)sulfane (**6**) or 1-fluoro-4-(trifluoromethylsulfonyl)benzene (**7**), using sodium hydride as base (Scheme 2). Sulfones **7** and **1** were obtained by oxidation of **6** and **10a** with *m*-chloroperbenzoic acid.

Amines **12a-e** were obtained by reductive amination of aldehydes **11** with amines **3** using sodium triacetoxyborohydride as reductive agent (Scheme 3).

Reductive amination of **11a** with **3b** gave, together with the expected compound **12b**, a tertiary amine **13**, which was also included for biological evaluation.

2.3. Biological evaluation

As a preliminary screening, we tested the total levels of phosphorylation of tyrosine residues in HeLa cells treated with different concentrations (0.1, 1.0 and 10.0 μM) of all 17 compounds (Phospho-Tyr in Table 1). The compounds that induced at least a 10% increase of Phospho-Tyr levels at any of the used concentrations were selected for further evaluation of inhibition of the phosphatase activity of PTPRZ1 (Fig. 1S, see supplementary material). The selected compounds were **4a-d**, **5b-c**, **10a**, **12a-b**, **12d**, and **13**. A limitation of this approach is that HeLa cells constitutively express other tyrosine phosphatases that may compensate for the inhibition of PTPRZ1 induced by these compounds. Thus, it is possible that some of the inhibitors of PTPRZ1 that we designed and synthesized were discarded as false negatives. This may be the case of compound **1**, the PTP1B inhibitor synthesized by Huang et al.²⁰ that also exerted some inhibition on PTPRZ1 ($IC_{50} = 3.5 \mu M$) and other phosphatases. However, we chose this strict selection criterion to

**Scheme 1.** Synthetic route to **4** and **5**^a.^a Reagents and conditions: (a) for **4a** and **4d**: K₂CO₃, THF; for **4c** and **4b**: HOBt, EDCI, DMF; (b) MCPBA, DCM, 80 °C, sealed tube.**Scheme 2.** Synthetic route to **1** and **10**.^a Reagents and conditions: (a) MCPBA, DCM, 80 °C, sealed tube; (b) NaH, DMF and compound **6** for **10a** and **10c** respectively, or compound **7** for **10b**.**Scheme 3.** Synthetic route to **12a-e**^a.^a Reagents and conditions: (a) NaBH(OAc)₃, CH₃CO₂H or CF₃CO₂H, DCM.

select the most potent inhibitors for the next phase.

Next, we performed an enzymatic assay of PTPRZ1 using the selected 11 compounds mentioned above. After optimizing the assay conditions, we performed a screening test to assess the capacity of a single concentration (1.0 μM) of each of these compounds to induce at least a 10% inhibition of the phosphatase activity of PTPRZ1. Six compounds, **4c-d**, **5b**, **10a**, **12b** and **12d**, met this criterion and underwent concentration-response studies to calculate the half-maximal inhibitory concentration (IC₅₀). Among the remaining compounds, we found that **10a**, **12b** and **4c** exhibited the most potent inhibition, with a range of IC₅₀ values between 0.1 and 0.8 μM (Table 2). In contrast with the results of Huang et al. [20], it should be noted that compound **1** failed to inhibit PTPRZ1 phosphatase activity in our assays. These apparent discrepancies may reflect significant methodological differences. First, while we have used a commercial PTPRZ1 protein, plasmids containing the

Table 2IC₅₀ Values (in μM) of PTPRZ1 and PTP1B inhibition.

Phosphatase	4c	4d	5b	10a	12b	12d
PTPRZ1	0.8	>100	>10	0.1	0.1	5.0
PTP1B	ND ^a	–	–	ND ^a	0.7	1.0

^a ND = Non Detected.

PTPRZ1 active domain fragment were used in the previous report to subclone the fragment for expression in insect cells [20]. Second, we have used a different method of detection of inorganic phosphate in the PTPRZ1 enzymatic assay, the phosphate sensor reagent that binds inorganic phosphate in a rapid, tight (K_d ~ 0.1 μM) and more sensitive manner.

We also assessed the inhibitor selectivity of all six compounds for PTP1B. We selected PTP1B as the most prominent PTP currently

investigated as a pharmacological target [22]. As shown in Table 2, **10a** and **12b** strongly and selectively inhibit PTPRZ1. Compound **4c**, although less potent, displays a remarkable selectivity against PTP1B. To further study the selectivity of the most potent compounds, we decided to test their effects on the phosphorylation levels of specific substrates of PTPRZ1 in an *in vitro* biological assay. As relevant substrates of PTPRZ1, we chose TrkA [23] and anaplastic lymphoma kinase (ALK) [18] because they are known to be involved in the neuroprotective effects of PTN, the endogenous inhibitor of PTPRZ1 [9]. We used neuroblastoma SH-SY5Y cells, which are known to express PTPRZ1 [24]. We stimulated SH-SY5Y cells with different concentrations of **10a** and **12b** (1.0, 5.0 and 10.0 μM) for 20 min, and evaluated using western blots the phosphorylation of those specific tyrosine residues in TrkA (Tyr⁴⁹⁰) and ALK (Tyr¹²⁷⁸), which are involved in the activation of both proteins. It has to be noted that previous evidence suggests that PTPRZ1 preferentially dephosphorylates Y674 and/or Y675 [23]. However, we chose to study Y490 because phosphorylation of this residue results in a cascade of molecular events and survival effects *in vitro* that resembles the ones found in PTN-stimulated cells [10c]. We chose to study ALK (Tyr¹²⁷⁸) because treatment of SH-SY5Y cells with midkine (MK), the only other member of the PTN family of cytokines that also binds PTPRZ1 and inhibits its phosphatase activity [25], causes a significant increase in the phosphorylation of ALK (Tyr¹²⁷⁸) in SH-SY5Y cells [26]. We chose these concentrations of the inhibitors as relevant for the subsequent functional studies described below. Western blots probed with anti-phospho-TrkA antibodies demonstrated that steady state levels of tyrosine phosphorylation of TrkA increased 2–3-fold after treatment with both **10a** and **12b** (Fig. 1). Western blots probed with anti-phospho-ALK antibodies demonstrated that both compounds caused a 2-fold increase in the phosphorylation of one isoform of ALK (the 140 kDa protein [27]) (Fig. 1).

The data clearly demonstrate that two of the inhibitors, **10a** and **12b**, significantly increase the phosphorylation of key tyrosine residues of the PTPRZ1 substrates TrkA and ALK, in agreement with

their IC₅₀ values (Table 2). It is interesting to note that TrkA is the high affinity nerve growth factor (NGF) receptor. NGF activates the kinase activity of TrkA by increasing the phosphorylation of Y⁴⁹⁰ in TrkA, which is critical for NGF-induced survival and neuroprotective effects [28]. Increased phosphorylation of Y¹²⁷⁸ in ALK is also involved in neuronal survival and differentiation [9]. The data suggest that the ability of PTPRZ1 inhibitors to increase the phosphorylation of the same residues in TrkA and ALK, by inhibiting the phosphatase activity of PTPRZ1 on its substrates, will induce similar neuroprotective effects. Accordingly, the endogenous inhibitor of the phosphatase activity of PTPRZ1, PTN, has been shown to prevent amphetamine-induced neuronal injury *in vitro* and *in vivo* [10b,10c]. To test the possibility that PTPRZ1 inhibitors could protect cell cultures from amphetamine-induced toxicity, we used catecholaminergic PC12 cells, which express readable levels of PTPRZ1 [29]. PC12 cells were incubated for 24 h with amphetamine (1 mM) and/or **10a** or **12b** (1.0 μM). Interestingly, **10a** significantly prevented amphetamine-induced loss of PC12 cell viability (Fig. 2a) and the same trend was observed with **12b** ($p = 0.06$). These data demonstrate that PTPRZ1 inhibitors mimic the protective effects of PTN against amphetamine-induced toxicity in PC12 cells [10c].

2.4. *In vivo* permeability study

To test the ability of the designed compounds to cross the BBB, compound **10a** was selected to carry out an *in vivo* experiment. Samples were obtained from mice sacrificed 1h post-gavage with 60 mg/kg of **10a** and analyzed by GC-MS. Extracted ion chromatograms (EIC) showed the presence of a peak at the same retention time as a standard **10a** solution, in both plasma and brain samples, while this peak was not present in samples from untreated mice. A preliminary quantification of the permeability has been carried out, showing that the estimated concentration of **10a** in brain samples is of 500–1000 ng/mL, while the concentration in plasma is 100–300 ng/mL. Moreover, we have recently shown that treatment with **10a** completely blocked alcohol-induced reward in

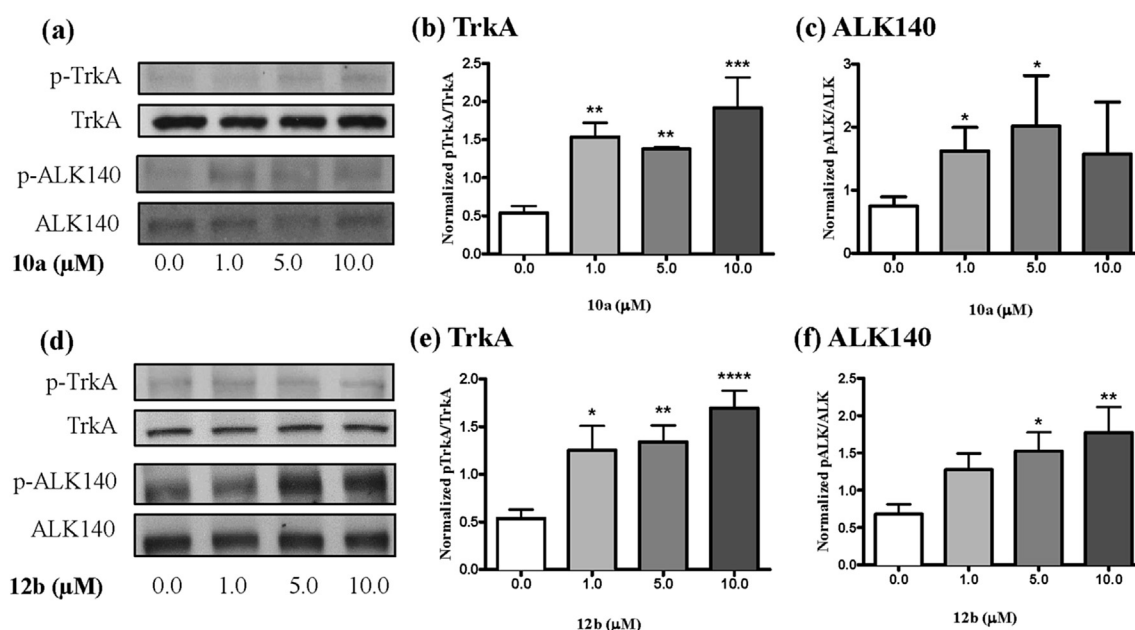


Fig. 1. (a) Representative western blots showing **10a**-induced increases in phosphorylated TrkA (pTrkA) and the 140 kDa ALK isoform (pALK). Total TrkA and ALK western blots are shown below each phosphorylated protein blot for comparison. (b–c) Quantification of western blots using ImageJ. (d) Representative western blots showing **12b**-induced increases in pTrkA and pALK. Total TrkA and ALK western blots are shown below each phosphorylated protein blot for comparison. (e–f) Quantification of western blots using ImageJ. Data are presented as mean \pm S.E.M. * $p < 0.05$, ** $p < 0.01$, *** $p < 0.001$, **** $p < 0.0001$ compared to vehicle controls (0.0 μM).

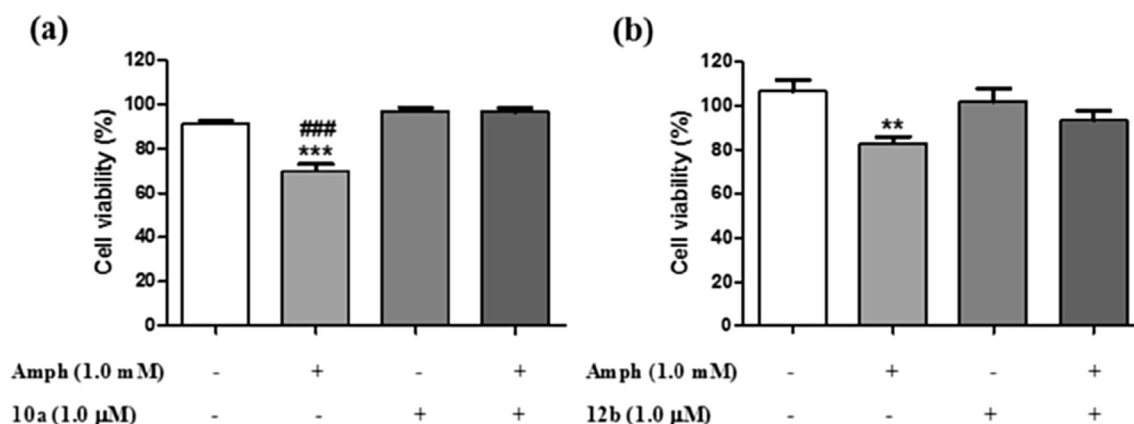


Fig. 2. Effects of **10a** and **12b** on amphetamine-induced toxicity in PC12 cells. PC12 cells cultured with media supplemented with amphetamine (Amph; 1 mM) and/or **10a** (1.0 μM) and/or **12b** (1.0 μM) for 24 h. Cellular viability was assessed by the MTT test. Results are expressed as mean \pm S.E.M. ** $p < 0.01$, *** $p < 0.001$ vs. vehicle-treated (control) cells. ### $p < 0.001$ vs. Amph+**10a**-treated cells.

mice [30] and modulation of the rewarding effects of drugs of abuse such alcohol, requires direct actions in the brain.

2.5. Computational studies

Despite its biological interest, PTPRZ1 has not been thoroughly studied to date as a druggable target. The first crystal structure obtained for PTPRZ1 was deposited as 5AWX [19]. However, inhibitors failed to crystallize along with the protein. To consider several conformations of the target macromolecule, together with the available apo form (5AWX), a computational study was carried out. Since no crystal structure was available for holo conformations of PTPRZ1, homology models were built using Receptor-type Tyrosine-Protein Phosphatase Gamma (PTPRG) [19] as a template, based on the 73.61% of sequence homology between both phosphatases [31]. PTPRZ1 belongs to the receptor-associated Class I PTP subfamily, which contains a highly conserved phosphatase domain (PD1) and a cysteine in the active site [32]. The general structure of the PD1 is constituted by an active site motif C(X)5R [33] and several surrounding loops implicated in the catalytic cycle and substrate recognition process. The WPD-loop plays an acid-base role, carried out by the Trp-Pro-Asp motif and therefore is implicated in the recycling of the active site. The pTyr-loop [34] is implicated in the recognition of the phosphotyrosine substrate; and the Q-loop, has a relevant role in the activation of a key water molecule during the catalytic cycle. The templates used for the homology modeling can be classified according to the different conformations of the WPD-loop as follows: i) closed conformation: when the phosphatase domain is bound to a substrate-like ligand [35] or a competitive inhibitor (PDB code 3QCC) [35,36]; ii) a “superopen” conformation: when the phosphatase is bound to an inhibitor that alters the overall conformation of the WPD-loop (PDB code 3QCH) [35] by acting as a wedge between the WPD-loop and the rest of the protein; and iii) open conformation: when the protein is in the apo form (PDB code 5AWX) [33,37]. Models for PTPRZ1 were generated with the SWISS-MODEL web server [38] as described elsewhere [31]. They were subsequently used for docking experiments carried out as described in the experimental section, using compounds **4c**, **4d**, **5b**, **10a**, **12b** and **12d**, as ligands. The highest docking scores for all compounds inside the different conformations of PTPRZ1 were obtained for the “superopen” conformation. The general binding mode predicted for these compounds implies the enclosing of the trifluoromethylthiobenzyl moiety within the hydrophobic pocket that is accessible by the

displacement of the WPD-loop. Among the amino acids that line the hydrophobic pocket, the main van der Waals interactions are established between the trifluoromethylthiobenzyl moiety and the aromatic side chains of Trp¹⁹⁸⁹ and Phe¹⁹⁸⁴, and the aliphatic and cycloaliphatic side chains of Arg¹⁹³⁹ and Pro¹⁹⁰⁵, respectively. The rest of the molecule, in all cases, interacts with the surroundings of the WPD-loop and the active site, with no direct interaction with the catalytic site (Table S1 and Fig. S2, see Supplementary material).

To assess the stability of the proposed binding modes, 10 ns molecular dynamics (MD) simulations were carried out for all complexes. Binding energies were analyzed making use of the fast and versatile MM-ISMSA program [39]. Results confirm the complexes stability in the “superopen” conformation for all compounds bound to PTPRZ1 as can be seen by the stable RMSD values (Table S2 and Fig. S3, see Supplementary material).

Given their high selectivity and drug-like properties, the binding modes for **4c**, **10a** and **12b** were intensively inspected, and the most populated conformations explored during 97% (**4c**), 78% (**10a**) and 77% (**12b**) of the simulation time, respectively, were selected for the per-residue energy decompositions (Fig. 3). Results show that the previously described van der Waals interactions established with the hydrophobic pocket in the initial docking binding models are maintained during most of the simulation time for the three complexes and that those having a higher energetic contribution are the π - π stacking and T-shaped interactions established between the trifluoromethylthiobenzyl moiety of the ligands and the aromatic side chains of Phe¹⁹⁸⁴ and Trp¹⁸⁸⁹. Furthermore, compound **4c** interacts strongly with the side chains of Pro¹⁹⁰⁰, Val¹⁹⁰⁴ and the aliphatic part of the side chain of Glu¹⁹⁸⁰ of the WPD-loop. In addition, the amide moiety of **4c** establishes alternating hydrogen bonding interactions to either the side chain NH of Gln¹⁹⁸¹ or the backbone carbonyls of Pro¹⁹⁰⁵ and Glu¹⁹⁸⁰. In the complex of **10a** with PTPRZ1, the hydrophobic interactions persist, whereas electrostatic interactions are weaker, since the previously described hydrogen bonds cannot be established. This binding mode is shared by all the other studied compounds in their most populated conformers except for **12b**-PTPRZ1 complex, because of its protonated state. Compound **12b** can establish strong interactions between the positively charged amine moiety and the side chains of Glu¹⁹⁸⁰ and Asp¹⁹⁸⁷ and with the backbone carbonyl of Glu¹⁹⁰⁶, all three located at the entrance of the hydrophobic pocket. Furthermore, compound **12b**, due to its high flexibility, folds to establish an intramolecular π - π interaction between the two trifluoromethylthiobenzyl moieties. In this folded conformation, compound **12b** establishes van

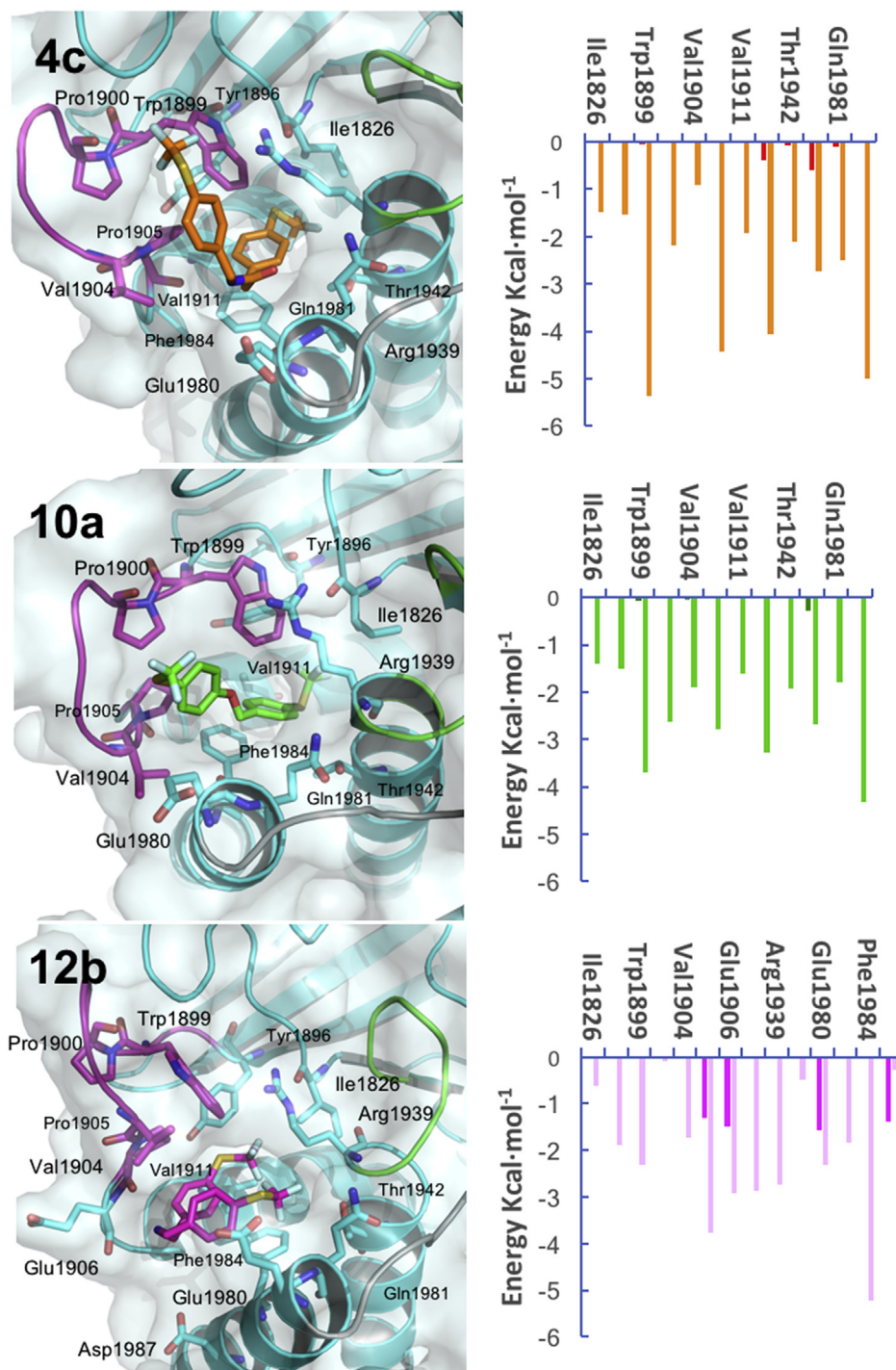


Fig. 3. Proposed binding modes of **4c**, **10a** and **12b** inside PTPRZ1. (Left) PyMOL stick and cartoon representation of the proposed binding modes for **4c**, **10a** and **12b** inside PTPRZ1. Structures shown correspond to the most populated conformations along the MD simulations in the PTPRZ1 superopen conformation. **4c**, **10a** and **12b** are represented in orange, green and light pink sticks, respectively. Residues involved in interactions are shown as sticks. The protein is colored cyan and the active site, WPD-loop and Q-loop are highlighted in green, magenta and grey, respectively. (Right) Per-residue energy decomposition of each complex with PTPRZ1. Orange, green and pale magenta bars represent the van der Waals contributions and deep green, red and magenta bars represent electrostatic binding energies for **4c**, **10a** and **12b**. (For interpretation of the references to color in this figure legend, the reader is referred to the Web version of this article.)

der Waals interactions between the trifluoromethylthiobenzyl moieties and the hydrophobic residues that line the hydrophobic pocket, some of which are located in the WPD-loop (Fig. S4, see Supplementary material).

With the aim of rationalizing the high selectivity displayed by **4c**, **10a** and **12b**, the same computational approach was carried out

for PTP1B. The PTP1B structures were obtained from the PDB in the closed and open conformation (PDB codes 1PTY and 3A5J, respectively) and a homology model for the “superopen” conformation was built using as template PDB structure 3QCH. Docking calculations were carried out as described previously and, in this case, the highest docking scores were obtained for all compounds bound to

the closed conformation of PTP1B (Table S1, see Supplementary material) where they share an overall similar binding mode (Fig. S5, see Supplementary material). Corresponding 10 ns MD simulations were carried out and the binding modes were further analyzed. Lower affinity towards PTP1B were found, as demonstrated by the unstable binding modes calculated through MM-ISMSA and the shifting RMSD values, that are comparatively higher than the ones obtained for the PTPRZ1 complexes (Table S2 and Fig. S3, see supplementary material). It is noteworthy that the only stable binding modes in PTP1B, which have the most similar RMSD fluctuations if compared to those of PTPRZ1 complexes, are shown by compounds **4d** and **5b** along with **4c**. The other compounds fluctuate during the MD simulation and slowly unbind from the original binding mode, resulting in completely different conformations that can be extracted from the MD simulations (Fig. S6, see Supplementary material). The per-residue energy decompositions of the complexes between PTP1B and **4c**, **10a** and **12b** were also carried out. The **4c**-PTP1B complex showed worse energy interactions compared to those found for PTPRZ1. The main interactions established by compound **4c** are with Tyr⁴⁶, Asp⁴⁸ and Val⁴⁹ from the described P-loop, Phe¹⁸² from the WPD-loop, Ser²¹⁶ and Ala²¹⁷ from the active site, and Gln²⁶² from the Q-loop (Fig. S7, see Supplementary material). Meanwhile, compound **10a** in complex with PTP1B, presented no stable binding mode during the simulations, which resulted in an unbounding from the active site, clearly observed by the rising RMSD values after 1.4 ns of the MD simulation and the reduced per-residue interactions of the binding. The complex of **12b** and PTP1B rendered no stable binding within the active site during the simulation. Nevertheless, after ~2.5 ns **12b** moves away from the active site and establishes a strong hydrogen bonding interaction between the protonated amine and the side chain of the Gln²⁶² present in the Q-loop, which is maintained throughout the rest of the simulation (Figs. S4 and S7, Supplementary material).

These results clearly account for the lower affinity towards PTP1B displayed by compounds **4c**, **10a** and **12b**, and most importantly, they are in complete agreement with the remarkable PTPRZ1/PTP1B selectivity profile described above.

3. Conclusion

PTN has a protective role in the CNS through its interaction with PTPRZ1. The interaction of PTN with PTPRZ1 inactivates its intrinsic tyrosine phosphatase activity, increasing the phosphorylation level of substrates which are crucial to prevent neurodegenerative and drug addiction disorders.

In this work, we have designed and synthesized a series of small molecules capable of mimicking the activity of PTN, by interacting with the active site of the intracellular domain PD1 of PTPRZ1.

The most active compounds **10a** and **12b** (IC₅₀ = 0.1 μM) are selective against PTP1B, and significantly increase the phosphorylation of key tyrosine residues of TrkA and ALK, two PTPRZ1 substrates involved in neuronal survival and differentiation. Moreover, both compounds mimic the PTN protective effects against amphetamine-induced toxicity in PC12 cells.

Docking and MD experiments have allowed to propose the binding mode of all these compounds inside PTPRZ1 and assess the stability of the corresponding complexes along the simulation time. More importantly, these methods have allowed to explain the remarkable PTPRZ1/PTP1B selectivity displayed by **4c** and **10a**.

We have demonstrated that **10a** can cross the BBB and, therefore, we propose this compound as a promising candidate for the development of new drugs for the treatment of CNS disorders, such as addictive and neurodegenerative diseases.

4. Experimental section

4.1. Chemistry

4.1.1. Materials

All reagents and solvents were obtained from different commercial sources (Sigma-Aldrich, Fluka, Acros Organics, Alfa Aesar or Scharlab) and used without further purification. Tetrahydrofuran and dichloromethane were dried by the solvent purification system Technical Bulletin AL-258.

4.1.2. General methods

Reaction progress was monitored using analytical thin-layer chromatography (TLC) on Merck silica gel 60 F-254 plate. Visualization was achieved by UV light (254 nm). Flash chromatography was performed with Scharlau silica gel 60 (0.04–0.06 mm) packing. ¹H and ¹³C spectra were recorded on a Bruker Advance III 400 MHz instrument. Signals are quoted as s (singlet), d (doublet), t (triplet), q (quartet) or m (multiplet). Chemical shifts (δ) are expressed in parts per million relative to solvent resonance as the internal standard. Coupling constants (*J*) are in hertz (Hz). Elemental analyses were performed by the Microanalytical Service Laboratory of the Universidad Complutense (Madrid) on a LECO CHNS-932 apparatus. Analyses indicated by the symbols of the elements or functions were within ±0.4% of the theoretical values. Melting points were determined on a Stuart Scientific (BIBBY) melting point apparatus. Mass spectrometry was performed by the CEMBio Analytical Service Laboratory of the Universidad CEU San Pablo on a MS/IT Esquire 3000 Bruker Daltonics apparatus. All final products were analyzed for purity by reverse-phase high-performance liquid chromatography (HPLC) on Agilent Technologies 1260 Infinity II apparatus. HPLC methods used for each compound shown in Supplementary material.

4.1.3. 1-((Trifluoromethyl)sulfonyl)-4-((4-((trifluoromethyl)sulfonyl)benzyl)oxy)benzene (**1**)

To a solution of **10a** (153 mg, 0.39 mmol) in dry DCM (10 mL) was added MCPBA (688 mg, 3.98 mmol). The reaction mixture was stirred at 80 °C for 48 h in a sealed tube. The crude was washed with NaOH 1M, brine and dried (MgSO₄). The drying agent was filtered off and the solvent was evaporated. The crude was purified by column chromatography on silica gel using hexane-EtOAc as eluent (8: 2 v/v) to afford 120 mg (67%) of **1** as a white solid. Mp. 139–141 °C. ¹H NMR (400 MHz, CDCl₃): δ 8.11 (d, *J* = 8.2 Hz, 2H, ArH), 8.02 (d, *J* = 8.9 Hz, 2H, ArH), 7.76 (d, *J* = 8.2 Hz, 2H, ArH), 7.21 (d, *J* = 8.9 Hz, 2H, ArH), 5.33 (s, 2H, -CH₂). ¹³C NMR (100 MHz, CDCl₃): δ 164.6, 144.9, 133.5, 131.4, 131.4 (“q”, *J* = 2.0 Hz), 128.3, 123.4 (q, *J* = 2.0 Hz), 112.0 (q, *J*_{CF} = 325.8 Hz), 112.0 (q, *J*_{CF} = 325.8 Hz), 116.1, 69.3. HPLC Purity >98%, t_R = 4.436, Method 1. Anal. C₁₅H₁₀F₆O₅S₂ (C, H, F, O, S).

4.1.4. 4-((Trifluoromethyl)thio)-N-(4-((trifluoromethyl)thio)phenyl)benzamide (**4a**)

To a solution of K₂CO₃ (174 mg, 1.26 mmol) in 4 mL of dry THF at 0 °C were subsequently added **11a** (100 mg, 0.42 mmol) and aniline **3a** (128 mg, 0.66 mmol). The resulting mixture was stirred at RT under argon till completion was seen by TLC (20 h). The solvent of the reaction was evaporated and the residue was suspended in H₂O. The aqueous layer was extracted with EtOAc, and the combined organic layers were washed with 1M HCl and brine, dried (MgSO₄), filtered and evaporated to give **4a** as a white solid (31 mg, 19%). Mp. 162–164 °C (hexane/EtOAc). ¹H NMR (400 MHz, CDCl₃): δ 7.91 (d, *J* = 8.4 Hz, 2H, ArH), 7.87 (s, 1H, -NH), 7.80 (d, *J* = 8.4 Hz, 2H, ArH), 7.73 (d, *J* = 8.8 Hz, 2H, ArH), 7.68 (d, *J* = 8.8 Hz, 2H, ArH). ¹³C NMR (100 MHz, CDCl₃): δ 164.8, 140.2, 137.8, 136.7, 136.4, 129.6(q,

$J_{CF} = 308.3$ Hz), 129.4 (q, $J_{CF} = 308.3$ Hz), 129.3 (q, $J = 2.0$ Hz), 128.2, 120.8, 119.9 (q, $J = 2.0$ Hz). HPLC Purity >98%, $t_R = 4.734$, Method 5. LC/MS (ESI) m/z 398.0 $[M+H]^+$. Anal. $C_{15}H_9F_6NOS_2$ (C, H, F, N, O, S).

4.1.5. *N*-2-Bis(4-((trifluoromethyl)thio)phenyl)acetamide (**4b**)

To a solution of acid **2b** (200 mg, 0.64 mmol) in 2.5 mL of DMF were added HOBt (104 mg, 0.77 mmol), EDCI (139 mg, 0.90 mmol) and the corresponding aniline **3a** (247 mg, 1.28 mmol). The resulting mixture was stirred at RT till completion was seen by TLC (72 h). The mixture was then diluted with EtOAc and washed with $NaHCO_3$ saturated solution, NH_4Cl and brine. The organic layer was dried ($MgSO_4$), filtered and evaporated to give **4b** as a white solid (208 mg, 78%). Mp. 163–165 °C (hexane/EtOAc). 1H NMR (400 MHz, $CDCl_3$): δ 7.69 (d, $J = 7.9$ Hz, 2H, ArH), 7.59 (d, $J = 8.5$ Hz, 2H, ArH), 7.54 (d, $J = 8.5$ Hz, 2H, ArH), 7.41 (d, $J = 7.9$ Hz, 2H, ArH), 7.18 (s, 1H, -NH), 3.78 (s, 2H, $-CH_2$). ^{13}C NMR (100 MHz, $CDCl_3$): δ 168.3, 140.1, 137.6, 137.1, 130.7, 129.6 (q, $J_{CF} = 308$ Hz), 129.6 (q, $J_{CF} = 308$ Hz), 124.1 (q, $J = 2.0$ Hz), 120.4, 119.5 (q, $J = 2.0$ Hz), 44.5. HPLC Purity >98%, $t_R = 3.690$, Method 5. LC/MS (ESI) m/z 412.00 $[M+H]^+$. Anal. $C_{16}H_{11}F_6NOS_2$ (C, H, F, N, O, S).

4.1.6. *N*-(4-((Trifluoromethyl)thio)benzyl)-2-(4-((trifluoromethyl)thio)phenyl)acetamide (**4c**)

To a solution of **2b** (200 mg, 0.64 mmol) in 2.5 mL of DMF were added HOBt (104 mg, 0.77 mmol), EDCI (139 mg, 0.90 mmol) and amine **3b** (199 mg, 0.96 mmol). The resulting mixture was stirred at RT till completion was seen by TLC (72 h). The mixture was then diluted with EtOAc and washed with $NaHCO_3$ saturated solution, NH_4Cl and brine. The organic layer was dried ($MgSO_4$), filtered and evaporated to give **4c** as a white solid (105 mg, 39%). Mp. 124–126 °C (hexane/EtOAc). 1H NMR (400 MHz, $CDCl_3$): δ 7.65 (d, $J = 8.1$ Hz, 2H, ArH), 7.59 (d, $J = 8.1$ Hz, 2H, ArH), 7.35 (d, $J = 8.2$ Hz, 2H, ArH), 7.25 (d, $J = 8.1$ Hz, 2H, ArH), 5.75 (s, 1H, -NH), 4.47 (d, $J = 6.0$ Hz, 2H, $-CH_2-NH-$), 3.65 (s, 2H, $-CH_2CO$). ^{13}C NMR (100 MHz, $CDCl_3$) δ 170.1, 141.3, 137.9, 137.0, 136.8, 130.6, 129.6 (q, $J_{CF} = 308.2$ Hz), 129.6 (q, $J_{CF} = 308.2$ Hz), 128.6, 123.7 (q, $J = 2.1$ Hz), 123.6 (d, $J = 2.1$ Hz), 43.2, 43.1. HPLC Purity >97%, $t_R = 3.073$, Method 6. LC/MS (ESI) m/z 425.9 $[M+H]^+$. Anal. $C_{17}H_{13}F_6NOS_2$ (C, H, F, N, O, S).

4.1.7. 4-((Trifluoromethyl)thio)-*N*-(4-((trifluoromethyl)thio)benzyl)benzamide (**4d**)

To a solution of K_2CO_3 (87 mg, 0.63 mmol) in 2 mL of dry THF at 0 °C were subsequently added chloride **2a** (50 mg, 0.21 mmol) and amine **3b** (68 mg, 0.33 mmol). The resulting mixture was stirred at RT under argon till completion was seen by TLC (20 h). The solvent of the reaction was evaporated and the residue was suspended in H_2O . The aqueous layer was extracted with EtOAc, and the combined organic layers were washed with 1M HCl and brine, dried ($MgSO_4$), filtered and evaporated. To give **4d** as a white solid (119.5 mg, 34%). Mp. 117–119 °C (hexane/EtOAc). 1H NMR (400 MHz, $CDCl_3$): δ 7.84 (d, $J = 8.3$ Hz, 2H, ArH), 7.74 (d, $J = 8.3$ Hz, 2H, ArH), 7.65 (d, $J = 8.1$ Hz, 2H, ArH), 7.41 (d, $J = 8.1$ Hz, 2H, ArH), 6.48 (s, 1H, -NH), 4.70 (d, $J = 5.9$ Hz, 2H, $-CH_2$). ^{13}C NMR (100 MHz, $CDCl_3$) δ 166.5, 141.2, 136.9, 136.3, 129.7 (q, $J_{CF} = 308.3$ Hz), 129.4 (q, $J_{CF} = 308.3$ Hz), 128.9, 128.7 (q, $J = 2.0$ Hz), 128.1, 123.8 (q, $J = 2.0$ Hz), 43.7. HPLC Purity >98%, $t_R = 4.534$, Method 5. LC/MS (ESI) m/z 412.00 $[M+H]^+$. Anal. $C_{16}H_{11}F_6NOS_2$ (C, H, F, N, O, S).

4.1.8. 4-((Trifluoromethyl)sulfonyl)-*N*-(4-((trifluoromethyl)thio)phenyl)benzamide (**5a**)

To a solution of **4a** (65 mg, 0.16 mmol) in dry DCM (10 mL) was added MCPBA (276 mg, 1.6 mmol). The resulting mixture was stirred at 100 °C in a sealed tube until the reaction was completed (TLC) (72 h). The reaction mixture was washed with NaOH 2M, NaCl sat.

and H_2O . The organic layer was then dried ($MgSO_4$), filtered and evaporated to give **5a** as a white solid (40.6 mg, 55%). Mp. 194–196 °C (hexane/EtOAc). 1H NMR (400 MHz, $CDCl_3$): δ 8.23 (d, $J = 8.4$ Hz, 2H, ArH), 8.17 (d, $J = 8.4$ Hz, 2H, ArH), 8.08 (d, $J = 8.8$ Hz, 2H, ArH), 8.00 (d, $J = 8.8$ Hz, 2H, ArH). ^{13}C NMR (100 MHz, DMSO) δ 165.0, 147.0, 142.3, 132.4, 132.2, 131.2, 130.2, 123.0, 120.9, 119.5 (“q”, $J = 324.11$), 119.4 (“q”, $J = 326.40$). HPLC Purity >97%, $t_R = 4.277$, Method 5. LC/MS (ESI) m/z 461.9 $[M+H]^+$. Anal. $C_{15}H_9F_6NO_5S_2$ (C, H, F, N, O, S).

4.1.9. *N*,2-bis(4-((trifluoromethyl)sulfonyl)phenyl)acetamide (**5b**)

To a solution of **4b** (102 mg, 0.248 mmol) in dry DCM (10 mL) was added MCPBA (428 mg, 2.48 mmol). The resulting mixture was stirred at 100 °C in a sealed tube until the reaction was completed (TLC) (24 h). The reaction mixture was washed with NaOH 2M, NaCl sat. and H_2O . The organic layer was then dried ($MgSO_4$), filtered and evaporated to give **5b** as a white solid (80 mg, 68%). Mp. 171–173 °C (hexane/EtOAc). 1H NMR (400 MHz, $CDCl_3$): δ 8.07 (d, $J = 8.3$ Hz, 2H, ArH), 8.00 (d, $J = 8.9$ Hz, 2H, ArH), 7.83 (d, $J = 8.9$ Hz, 2H, ArH), 7.67 (d, $J = 8.3$ Hz, 2H, ArH), 7.57 (bs, 1H, -NH), 3.97 (s, 2H, $-CH_2$); ^{13}C NMR (100 MHz, $CDCl_3$) δ 167.6, 144.9, 143.0, 132.6, 131.5, 131.1, 130.8, 125.9, 119.9 (q, $J_{CF} = 325.7$ Hz), 119.8 (q, $J_{CF} = 325.7$ Hz), 44.4. HPLC Purity >97%, $t_R = 5.674$, Method 3. LC/MS (ESI) m/z 475.9 $[M+H]^+$. Anal. $C_{16}H_{11}F_6NO_5S_2$ (C, H, F, N, O, S).

4.1.10. *N*-(4-((trifluoromethyl)sulfonyl)benzyl)-2-(4-((trifluoromethyl)sulfonyl)phenyl)acetamide (**5c**)

To a solution of **4c** (42 mg, 0.1 mmol) in dry DCM (10 mL) was added MCPBA (260 mg, 1.5 mmol). The resulting mixture was stirred at 100 °C in a sealed tube until the reaction was completed (TLC) (48 h). The reaction mixture was washed with NaOH 2M, NaCl sat. and H_2O . The organic layer was then dried ($MgSO_4$), filtered and evaporated to give **5c** as a white solid (33 mg, 67%). Mp. 164–170 °C (hexane/EtOAc). 1H NMR (400 MHz, $CDCl_3$): δ 8.03 (d, $J = 8.0$ Hz, 2H, ArH), 7.99 (d, $J = 8.0$ Hz, 2H, ArH), 7.63 (d, $J = 7.9$ Hz, 2H, ArH), 7.54 (d, $J = 7.9$ Hz, 2H, ArH), 6.03 (bs, 1H, -NH), 4.60 (d, $J = 6.1$ Hz, 2H, $-CH_2NH$), 3.77 (s, 2H, $-CH_2CO$). ^{13}C NMR (100 MHz, $CDCl_3$) δ 169.1, 147.7, 140.03, 131.4, 131.0, 130.5, 130.47, 128.95, 119.9 (q, $J_{CF} = 323.7$ Hz), 43.5, 43.3. HPLC Purity 95%, $t_R = 4.549$, Method 3. LC/MS (ESI) m/z 489.9 $[M+H]^+$. Anal. $C_{17}H_{13}F_6NO_5S_2$ (C, H, F, N, O, S).

4.1.11. 1-Fluoro-4-((trifluoromethyl)sulfonyl)benzene (**7**)

To a solution of **6** (100 mg, 0.51 mmol) in dry DCM (10 mL) MCPBA (440 mg, 2.55 mmol) was added and the mixture was heated at 80 °C in a sealed tube for 6 h. The reaction crude was diluted with DCM (10 mL) and the organic layer was washed with NaOH 1 M, brine and dried ($MgSO_4$). The drying agent was filtered off and the solvent was removed at vacuum to give **7** as a light-orange oil. The compound was used in the next reaction without further purification.

4.1.12. (Trifluoromethyl)(4-((4-((trifluoromethyl)thio)benzyl)oxy)phenyl)sulfane (**10a**)

To a solution of **8** (303 mg, 1.46 mmol) in 5 mL of dry DMF, was added NaH (60%) (42 mg, 1.75 mmol) at 0 °C under an argon atmosphere. After stirring for 15 min, compound **6** (0.22 mL, 1.53 mmol) was added and the mixture was stirred at RT. The reaction was monitored with TLC until completion (24 h). The solvent was evaporated, the residue was solved in EtOAc, washed with brine and H_2O , dried ($MgSO_4$), filtered and evaporated. The crude was purified by column chromatography on silica gel using hexane-EtOAc as eluent (9.75: 0.25 v/v) to afford **10a** as a white solid (350 mg, 62%). Mp. 114–116 °C. 1H NMR (400 MHz, $CDCl_3$): δ 7.69 (d, $J = 8.2$ Hz, 2H, ArH), 7.59 (d, $J = 8.8$ Hz, 2H, ArH), 7.48 (d, $J = 8.2$ Hz, 2H, ArH), 6.99 (d, $J = 8.8$ Hz, 2H, ArH), 5.12 (s, 2H, $-CH_2$). ^{13}C NMR

(100 MHz, CDCl₃): δ 160.8, 139.5, 138.5, 136.8, 129.8 (q, J_{CF} = 308 Hz), 129.7 (q, J_{CF} = 308 Hz), 128.3, 124.4 (q, J = 2.1 Hz), 115.9, 115.8 (q, J = 2.1 Hz), 69.4. HPLC Purity >98%, t_R = 5.215, Method 1. Anal. C₁₅H₁₀F₆O₂ (C, H, F, O, S).

4.1.13. (Trifluoromethyl)(4-((trifluoromethyl)sulfonyl)phenoxy)methyl)phenyl)sulfane (**10b**)

To a solution of **8** (106 mg, 0.51 mmol) in 5 mL of dry DMF, was added NaH (60%) (15 mg, 0.61 mmol) at 0 °C under an argon atmosphere. After stirring for 15 min, fluorine derivative **7** (116 mg, 0.51 mmol) was added, the mixture was stirred at RT and the reaction was monitored with TLC until completion (2 h). The reaction mixture was poured into a mixture of HCl (1M)/H₂O (1:1) and then extracted with DCM. The organic layer was dried (MgSO₄), filtered and evaporated. The crude was purified by column chromatography on silica gel using hexane-DCM as eluent (9:1 v/v) to afford **10b** as a white solid (121 mg, 31%). Mp. 110–112 °C. ¹H NMR (400 MHz, CDCl₃): δ 7.98 (d, J = 8.9 Hz, 2H, ArH), 7.72 (d, J = 8.1 Hz, 2H, ArH), 7.49 (d, J = 8.1 Hz, 2H, ArH), 7.18 (d, J = 8.9 Hz, 2H, ArH), 5.22 (s, 2H, -CH₂). ¹³C NMR (100 MHz, CDCl₃): δ 164.8, 138.2, 136.7, 133.4, 129.5 (q, J_{CF} = 308 Hz), 128.3, 124.7 (q, J = 2.0 Hz), 122.7 (q, J = 2.0 Hz), 119.9 (q, J_{CF} = 308 Hz), 115.9, 69.8. HPLC Purity >97%, t_R = 7.296, Method 2. Anal. C₁₅H₁₀F₆O₃S₂ (C, H, F, O, S).

4.1.14. 4-((4-((Trifluoromethyl)thio)phenoxy)methyl)pyridine (**10c**)

To a solution of **9** (111 mg, 1.02 mmol) in 5 mL of dry DMF, was added NaH (60%) (29 mg, 1.23 mmol) at 0 °C under an argon atmosphere. After stirring for 15 min, derivative **6** (0.15 mL, 1.02 mmol) was added, the mixture was stirred at RT until the reaction was completed (TLC) (72 h). The reaction mixture was poured into a mixture of H₂O/ice and the solution was taken to pH = 7 with NaHCO₃ saturated solution. The precipitate was then filtered and washed with H₂O. The crude was purified by column chromatography on silica gel using hexane-EtOAc as eluent (2: 8 v/v) to afford **10c** as a white solid (66 mg, 23%). Mp. 97–99 °C. ¹H NMR (400 MHz, CDCl₃): δ 8.63 (d, J = 4.6 Hz, 2H, ArH), 7.59 (d, J = 8.7 Hz, 2H, ArH), 7.34 (d, J = 5.2 Hz, 2H, ArH), 6.98 (d, J = 8.7 Hz, 2H, ArH), 5.11 (s, 2H, -CH₂). ¹³C NMR (100 MHz, CDCl₃): δ 160.4, 150.2, 145.3, 138.4, 129.6 (q, J_{CF} = 308.2 Hz), 121.4, 115.9 (q, J = 2.0 Hz), 115.7, 68.3. HPLC Purity >98%, t_R = 4.674, Method 3. LC/MS (ESI) m/z 286.0 [M+H]⁺. Anal. C₁₃H₁₀F₃NOS (C, H, F, N, O, S).

4.1.15. 4-((Trifluoromethyl)thio)-N-(4-((trifluoromethyl)thio)benzyl)aniline (**12a**)

To a solution of aldehyde **11a** (200 mg, 1.04 mmol) and aniline **3a** (214 mg, 1.04 mmol) in dry DCM (10 mL) were added, under argon, NaBH(OAc)₃ (438 mg, 2.07 mmol) and CH₃COOH (59 μ L). The resulting solution was stirred at RT until the reaction was completed (TLC) (6 h). The reaction mixture was neutralized with NaOH 1M aqueous solution, and the organic phase was washed with brine and H₂O, dried (MgSO₄), filter and evaporated. Column chromatography on silica gel using as eluent hexane-EtOAc (9.5: 0.5 v/v) gave **12a** as a white solid (207 mg, 52%). Mp. 87–89 °C. ¹H NMR (400 MHz, CDCl₃): δ 7.65 (d, J = 8.1 Hz, 2H, ArH), 7.43 (d, J = 8.8 Hz, 2H, ArH), 7.41 (d, J = 8.1 Hz, 2H, ArH), 6.61 (d, J = 8.8 Hz, 2H, ArH), 4.42 (s, 2H, -CH₂). ¹³C NMR (100 MHz, CDCl₃): δ 149.9, 141.9, 138.5, 137.0, 130.0 (q, J_{CF} = 308.1 Hz), 129.8 (q, J_{CF} = 308.1 Hz), 128.5, 123.7 (q, J = 1.8 Hz), 113.6, 111.0 (q, J = 1.8 Hz), 47.6. HPLC Purity >98%, t_R = 5.010, Method 4. Anal. C₁₅H₁₁F₆NS₂ (C, H, F, N, S).

4.1.16. Bis(4-((trifluoromethyl)thio)benzyl)amine hydrochloride (**12b**) & tris(4-((trifluoromethyl)thio)benzyl)amine (**13**)

To a solution of aldehyde **11a** (237 mg, 1.15 mmol) and amine **3b** (0.18 mL, 1.15 mmol) in dry DCM (10 mL) were added, under argon, NaBH(OAc)₃ (1459 mg, 6.88 mmol) and CH₃COOH (66 μ L). The

resulting solution was stirred at RT until the reaction was completed (TLC) (72 h). The reaction mixture was neutralized with NaOH 1M aqueous solution, and the organic phase was washed with brine and H₂O, dried (MgSO₄), filter and evaporated. Column chromatography on silica gel using hexane-EtOAc (gradient from 9.25:0.75 to pure EtOAc) as eluent, gave amines **13** (40 mg, 6%) and **12b** (80 mg, 17%).

For **13**: ¹H NMR (400 MHz, CDCl₃) δ 7.62 (d, J = 7.9 Hz, 6H, ArH), 7.45 (d, J = 7.9 Hz, 6H, ArH), 3.61 (s, 6H, 3x -CH₂). Bubbling HCl(g) through an ethereal solution of the compound and isolation by filtration gave the corresponding hydrochloride (84%). Mp. 115–117 °C. HPLC Purity >94%, t_R = 6.346, Method 5. LC/MS (ESI) m/z 588 [M+H]⁺. Anal. C₂₄H₁₉ClF₉NS₃ (C, H, Cl, F, N, S).

For **12b**: ¹H NMR (400 MHz, CDCl₃): δ 7.59 (d, J = 7.9 Hz, 4H, ArH), 7.42 (d, J = 7.9 Hz, 4H, ArH); 3.60 (s, 4H, 2 x -CH₂). ¹³C NMR (100 MHz, CDCl₃): δ 142.1, 135.5, 128.6 (q, J_{CF} = 309.0 Hz), 128.1, 121.8 (q, J_{CF} = 2.0 Hz), 51.5.

Bubbling HCl(g) through an ethereal solution of the compound and isolation by filtration gave the corresponding hydrochloride (87%). Mp. 197–199 °C. HPLC Purity >98%, t_R = 5.108, Method 5. LC/MS (ESI) m/z 398.00 [M+H]⁺. Anal. C₁₆H₁₄ClF₆NS₂ (C, H, Cl, F, N, S).

4.1.17. N-benzyl-1-(4-((trifluoromethyl)thio)phenyl)methanamine (**12c**)

To a solution of aldehyde **11c** (0.048 mL, 0.483 mmol) and amine **3b** (0.08 mL, 0.48 mmol) in dry DCM (5 mL) were added, under argon, NaBH(OAc)₃ (204 mg, 0.97 mmol) and CF₃COOH (96 μ L). The resulting solution was stirred at RT until the reaction was completed (TLC) (48 h). The reaction mixture was neutralized with NaOH 1M aqueous solution, and the organic phase was washed with brine and H₂O, dried (MgSO₄), filtered and evaporated. Column chromatography on silica gel using as eluent hexane-DCM (gradient from 4:6 v/v to 1:1 v/v) gave **12c** (50 mg, 34%). ¹H NMR (400 MHz, CDCl₃): δ 7.62 (d, J = 8.1 Hz, 2H), 7.42 (d, J = 8.1 Hz, 2H), 7.35–7.27 (m, 5H), 3.85 (s, 2H), 3.82 (s, 2H). ¹³C NMR (100 MHz, CDCl₃): δ 143.5, 139.9, 136.6, 129.8 (q, J_{CF} = 307.0 Hz), 129.3, 128.6, 128.3, 127.3, 122.8 (q, J = 2.0 Hz), 53.3, 52.5. Bubbling HCl(g) through an ethereal solution of the compound and isolation by filtration gave the corresponding hydrochloride (53%). Mp. 244–246 °C. HPLC Purity >97%, t_R = 3.020, Method 4. LC/MS (ESI) m/z 298.00 [M+H]⁺. Anal. C₁₅H₁₅ClF₃NS (C, H, Cl, F, N, S).

4.1.18. N-benzyl-4-((trifluoromethyl)thio)aniline (**12d**)

To a solution of aldehyde **11c** (329 mg, 3.11 mmol) and aniline **3a** (0.15 mL, 1.04 mmol) in dry DCM (10 mL) were added, under argon, NaBH(OAc)₃ (1974 mg, 9.32 mmol) and CH₃COOH (59 μ L). The resulting solution was stirred at RT until the reaction was completed (TLC) (72 h). The reaction mixture was neutralized with NaOH 1M aqueous solution, and the organic phase was washed with brine and H₂O, dried (MgSO₄), filtered and evaporated. Column chromatography on silica gel using as eluent hexane-EtOAc (9.7:0.4 v/v) gave the **12d** (83 mg, 73%). ¹H NMR (400 MHz, CDCl₃): δ 7.45 (d, J = 8.6 Hz, 2H, ArH), 7.39–7.33 (m, 5H, ArH), 6.63 (d, J = 8.6 Hz, 2H, ArH), 4.37 (s, 2H, -CH₂). ¹³C NMR (100 MHz, CDCl₃): δ 150.3, 138.5, 138.3, 129.9 (q, J_{CF} = 308.0 Hz), 128.9, 127.7, 127.6, 113.3, 110.1 (q, J = 2.0 Hz), 48.0. Bubbling HCl(g) through an ethereal solution of the compound and isolation by filtration gave the corresponding hydrochloride (27%). Mp. 146–148 °C. HPLC Purity >98%, t_R = 4.601, Method 5. LC/MS (ESI) m/z 284.00 [M+H]⁺. Anal. C₁₄H₁₃ClF₃NS requires (C, H, Cl, F, N, S).

4.1.19. N-(4-chlorobenzyl)-4-((trifluoromethyl)thio)aniline (**12e**)

To a solution of aldehyde **11b** (437 mg, 3.11 mmol) and aniline **3a** (0.15 mL, 1.04 mmol) in dry DCM (10 mL) were added, under argon, NaBH(OAc)₃ (1091 mg, 5.18 mmol) and then CH₃COOH (1.05 mL).

The resulting solution was stirred at RT until the reaction was completed (TLC) (48 h). The reaction mixture was neutralized with NaOH 1M aqueous solution, and the organic phase was washed with brine and H₂O, dried (MgSO₄), filtered and evaporated. Column chromatography on silica gel using as eluent hexane-DCM (9.8:0.2 v/v) gave **12e** (160 mg, 49%). ¹H NMR (400 MHz, CDCl₃): δ 7.44 (d, *J* = 8.6 Hz, 2H, ArH), 7.34 (d, *J* = 8.5 Hz, 2H, ArH), 7.29 (d, *J* = 8.5 Hz, 2H, ArH), 6.60 (d, *J* = 8.7 Hz, 2H, ArH) 4.39 (“t”, *J* = 5.4 Hz, -NH), 4.39 (d, *J* = 5.42 Hz, 2H, -CH₂). ¹³C NMR (100 MHz, CDCl₃): δ 150.0, 138.4, 137.1, 133.4, 129.8 (q, *J*_{CF} = 308 Hz), 128.7, 128.4, 110.4 (q, *J* = 2 Hz), 47.3. Bubbling HCl(g) through an ethereal solution of the compound and isolation by filtration gave the corresponding hydrochloride (68%). Mp. 170–172 °C. HPLC Purity >98%, *t*_R = 4.787, Method 5. LC/MS (ESI) *m/z* 318.00 [M+H]⁺. Anal. C₁₄H₁₂Cl₂F₃NS (C, H, Cl, F, N, S).

4.2. Molecular modelling

The crystal structure of PTPRZ1 in the open conformation was obtained from the Protein Data Bank deposited under the accession code 5AWX. Homology models for the closed and “superopen” conformations of PTPRZ1 were built using the SWISS-MODEL web server [40] and using the phosphatase domain (PD1) of PTPRG in the PDB structures 3QCC and 3QCH, respectively, as templates. The crystal structures of the open (PDB code 3A5J) and closed (PDB code 1PTY) conformations of PTP1B were used, and the homology model of the “superopen” conformation of PTP1B was also built using the PDB structure 3QCH as template.

Using the Protein Preparation Wizard module of the Schrödinger Suite (<http://www.Schrodinger.com>), missing chains and residues were added to the crystal structures and the receptor geometries were optimized. The protonation states of charged amino acids were calculated with the PROPKA module of the Schrödinger Suite, and the catalytic cysteine is protonated in all PTPRZ1 and PTP1B structures. The described ligands were built with the LigPrep module of Maestro, generating all possible states at pH 7 ± 2. Receptor grid was calculated using the catalytic cysteine as the center of the 13 Å-size box that enclosed the catalytic site and the induced pocket from the superopen conformation, ensuring all possible ligand poses. Docking calculations were performed using extra precision (XP) mode of the GLIDE module and a van der Waals radii scale factor of 1.0/0.8. The best ligand poses were considered for further analysis of the ligand-receptor interactions using molecular dynamics (MD) simulations.

For the selected compounds, geometry optimization and charge distributions were calculated quantum mechanically (RHF/3-21G**//RHF/6-31G**) with Gaussian 03 [41]. MD simulations for each complex in the lowest energy docking pose for PTPRZ1 and PTP1B were carried out with the general AMBER14 (<http://ambermd.org/>) force field and the GAFF force field for the parametrization of the small molecules [42]. Systems were introduced in a truncated octahedron box of approximately 10 000 TIP3P water molecules with 13 Å cut-off distance and adding from 2 or 15 chlorine ions depending on the system. Smooth particle mesh Ewald (PME) [43] method with a spacing grid of 1 Å was used for electrostatic interactions and SHAKE algorithm applied to all hydrogen bonds with 2.0 fs integration step [44]. An initial energy minimization of the water molecules and counter-ions was carried out on each system. The systems were further heated from 100K to 300K in 25 ps, and solvent molecules progressively allowed to move freely. To explore the complex between ligand and macromolecule 10 ns MD simulations where carried out without any restraints, generating snapshots each 20 ps for further analysis. The trajectories were collected and the cpptraj module [45] of AMBER14 was used to calculate the root mean square deviation (RMSD) of the atomic positions of the

ligands and the most populated conformers. The MM-ISMSA program was used to calculate the total binding energies for each complex [39] giving the complex per-residue energy decomposition.

4.3. Biological assays

4.3.1. ELISA

HeLa cells were cultured in RPMI-1640 medium (Sigma, Spain) supplemented with 10% fetal bovine serum (FBS; Sigma-Aldrich, Madrid, Spain), 0.005% Penicillin-Streptomycin and 0.005% Glutamine. Trypsin/EDTA (Sigma-Aldrich, Madrid, Spain) was used to release cells for subculturing. When cells reached 90% confluence they were seeded in 96 well-plates at 2 × 10⁴ cells per well in triplicates. After 24 h of serum starvation, HeLa cells were treated for 10 min with 50 ng/mL epidermal growth factor (EGF; Sigma-Aldrich, Madrid, Spain) as a positive control to induce tyrosine phosphorylation. Cells were treated for 10 min with three different concentrations of each compound (10.0, 1.0 and 0.1 μM) and control 0.25% DMSO. A tyrosine phosphorylation ELISA Kit (Raybiotech, Norcross, GA, USA) was used following the manufacturer's instructions.

4.3.2. In vitro dephosphorylation assays

Human recombinant PTPRZ1 and PTP1B proteins were purchased from Sigma (Madrid, Spain). The inhibitory activities of the studied compounds were determined using the phosphate sensor reagent (ThermoFisher, Waltham, MA, USA) [46], using p-NPP (Sigma-Aldrich, Madrid, Spain) as substrate. PTPRZ1 and PTP1B were used at a concentration of 0.1 μM. Increasing concentrations of the different compounds were used (0.001–100 μM) to calculate the IC₅₀. In each experiment, the hydrolysis of the p-NPP residue was determined as an increase in fluorescence at 450 nm (excitation at 430 nm) using a Hitachi F4500 Fluorescence Spectrometer.

4.3.3. Western-blots

The human neuroblastoma cell line SH-SY5Y was purchased from American Type Culture Collection (ATCC, Manassas, VA, USA) and was incubated at 37 °C in 5% CO₂. SH-SY5Y cells were cultured in a 1:1 mixture of Eagle's minimum essential medium (EMEM) and F12 medium containing 10% FBS. Just before treatments, medium was changed to 1:1 mixture of EMEM and F12 medium without serum. Cells were treated with **10a** and **12b** (1.0, 5.0 and 10.0 μM) and DMSO vehicle for 20 min. Cells were lysed in 20 mM Tris-HCl, pH 7.5, 150 mM NaCl, 1 mM EDTA, 1 mM EGTA, 1% Triton X-100, 2.5 mM sodium pyrophosphate, 1 mM β-glycerophosphate, leupeptin, 1 μg/mL aprotinin, and EDTA-free Complete Protease Inhibitor Cocktail tablets (Roche Diagnostics, Indianapolis, IN, USA). Lysate protein concentration was determined using the BCA Protein Assay Kit (Pierce, Rockford, IL, USA) and equal amounts of protein (20 μg) were subjected to sodium dodecyl sulfate–polyacrylamide gel electrophoresis and transferred to polyvinylidene difluoride membranes. Membranes incubated with anti-phospho-TrkA (Y⁴⁹⁰) and anti-phospho-ALK (Y¹²⁷⁸) antibodies and reprobed with anti-TrkA (Upstate, Charlottesville, VA) and anti-ALK (Life Technologies, Carlsbad, CA) antibodies to confirm the identities of the proteins. Secondary antibodies were horseradish peroxidase-conjugated goat anti-mouse or anti-rabbit IgG. The membranes were developed with enhanced chemiluminescence detection reagents (Pierce, Rockford, IL, USA). Films were scanned using a Chemidoc System (Bio-Rad, Madrid, Spain) and densitometry was performed with ImageJ software.

4.3.4. Cell viability

Rat pheochromocytoma PC12 cells (ATCC, Manassas, VA, USA)

were cultured with RPMI-1640 Medium supplemented with 10% FBS in 96-well plates (10^4 cells/well). To test the effects of **10a** and **12b** on amphetamine-induced toxicity in cell cultures, PC12 cells were incubated for 20 h with amphetamine (1.0 mM) and **10a** or **12b** (1.0 μ M). Cellular viability was studied with the MTT assay (Sigma-Aldrich, Madrid, Spain). Briefly, cells were washed with PBS and incubated in fresh medium including 20 μ L of 5 mg/mL MTT. MTT solution was removed after 4 h of incubation, DMSO added into each well and the plate was shaken for 10 min at RT. Absorbance was determined at 570 nm in a Versamax microplate reader (Bionova, Madrid, Spain).

4.3.5. Statistics

Data from Western blots and cell viability assays are presented as mean \pm standard error of the mean (S.E.M.). Data were analyzed using one-way ANOVA followed by post-hoc comparisons with Tukey's post-hoc tests. $P < 0.05$ was considered as statistically significant. All statistical analyses were performed using Graph-Pad Prism program (San Diego, CA, USA).

4.3.6. In vivo compound detection

Compound detection in plasma and brain tissue was performed using GC-MS analysis (Agilent 7890A gas chromatograph coupled to an Agilent 7200 accurate mass high resolution GC/Q-ToF). Separation was performed using an Agilent DB-5ms + DG capillary column (30 m \times 0.25 mm i.d., 0.25 μ m film thickness + 10 m Duraguard) using Helium as carrier gas. Mass analysis was operated on EI conditions, recording data in full-scan mode at 70 eV in a mass range of m/z 50 to 600. Ion source, quadrupole and transfer line temperatures were 250 $^{\circ}$ C, 150 $^{\circ}$ C and 290 $^{\circ}$ C respectively. The oven temperature program was: from 60 $^{\circ}$ C (1 min) to 325 $^{\circ}$ C (hold 10 min) at 20 $^{\circ}$ C/min.

Reliability of the method was based on the detection of a standard solution of **10a** at a concentration of 2 mg/mL in ethanol. Then, a working standard solution was prepared by dilution of this stock solution at 5 μ g/mL in heptane. Subsequent working solutions of the analyte were prepared by serial half dilution with heptane.

Biological samples were processed depending on their nature: i) frozen mouse brain tissues (50–100 mg) were placed in tubes containing CK14 ceramic beads from Precellys. ethyl acetate was added to each sample as extraction solvent and homogenization performed in a Precellys 24 Dual system equipped with a Cryolys cooler. Supernatants were evaporated to dryness in a speedvac concentrator and reconstituted in heptane before injection; ii) 100 μ L of mouse plasma samples were subjected to standard protein precipitation. For this, three volumes of cold methanol were added and then samples maintained at -2 $^{\circ}$ C for 20 min. After centrifugation, supernatants were dried in a speedvac concentrator and the residue was reconstituted in heptane for further analysis.

Detection of **10a** was performed on extracted ion chromatograms (EIC) at m/z 191.0137, corresponding to the fragment $C_8H_6F_3S$. The **10a** peak presented a limit of quantification (LOQ) in standards of 70 ng/mL, approximately.

Author contributions

The manuscript was written through contributions of all authors. All authors have given approval to the final version of the manuscript.

Acknowledgements

Funding: This work was supported by grant PNSD001I2015 from National Plan on Drug abuse, Ministerio de Sanidad, Servicios Sociales e Igualdad of Spain, MINECO (CTQ2014-52604-R and

SAF2014-53977-R) and the United States National Institute on Alcohol Abuse and Alcoholism (NIAAA, INIA consortium grant AA020912 to A.W.L.). B. di G, R. F-C and M. V-R thank Fundación Universitaria San Pablo CEU for FPI fellowships. B. di G. also thanks the Spanish MINECO for a FPU fellowship.

Appendix A. Supplementary data

Supplementary data related to this article can be found at <https://doi.org/10.1016/j.ejmech.2017.11.080>.

References

- [1] K. Kadomatsu, T. Muramatsu, Midkine and pleiotrophin in neural development and cancer, *Cancer Lett.* 204 (2004) 127–143.
- [2] K. Kadomatsu, S. Kishida, S. Tsubota, The heparin-binding growth factor midkine: the biological activities and candidate receptors, *J. Biochem.* 153 (2013) 511–521.
- [3] T.F. Deuel, N. Zhang, H.J. Yeh, I. Silos-Santiago, Z.Y. Wang, Pleiotrophin: a cytokine with diverse functions and a novel signaling pathway, *Arch. Biochem. Biophys.* 397 (2002) 162–171.
- [4] (a) Y.S. Li, P.G. Milner, A.K. Chauhan, M.A. Watson, R.M. Hoffman, C.M. Kodner, J. Milbrandt, T.F. Deuel, Cloning and expression of a developmentally regulated protein that induces mitogenic and neurite outgrowth activity, *Science* 250 (1990) 1690–1694; (b) H.J. Yeh, Y.Y. He, J. Xu, C.Y. Hsu, T.F. Deuel, Upregulation of pleiotrophin gene expression in developing microvasculature, macrophages, and astrocytes after acute ischemic brain injury, *J. Neurosci.* 18 (1998) 3699–3707; (c) K. Kadomatsu, M. Tomomura, T. Muramatsu, cDNA cloning and sequencing of a new gene intensely expressed in early differentiation stages of embryonal carcinoma cells and in mid-gestation period of mouse embryogenesis, *Biochem. Biophys. Res. Commun.* 151 (1988) 1312–1318.
- [5] (a) L.F. Alguacil, G. Herradon, Midkine and pleiotrophin in the treatment of neurodegenerative diseases and drug addiction, *Recent Pat. CNS Drug Discov.* 10 (2015) 28–33; (b) Y.B. Martin, G. Herradon, L. Ezquerro, Uncovering new pharmacological targets to treat neuropathic pain by understanding how the organism reacts to nerve injury, *Curr. Pharm. Res.* 17 (2011) 434–448; (c) T. Muramatsu, Midkine: a promising molecule for drug development to treat diseases of the central nervous system, *Curr. Pharm. Res.* 17 (2011) 410–423.
- [6] (a) M. Vicente-Rodriguez, L. Rojo Gonzalez, E. Gramage, R. Fernandez-Calle, Y. Chen, C. Perez-Garcia, M. Ferrer-Alcon, M. Uribarri, A. Bailey, G. Herradon, Pleiotrophin overexpression regulates amphetamine-induced reward and striatal dopaminergic denervation without changing the expression of dopamine D1 and D2 receptors: implications for neuroinflammation, *Eur. Neuropsychopharm.* 29 (2016) 1794–1805; (b) M. Vicente-Rodriguez, R. Fernandez-Calle, E. Gramage, C. Perez-Garcia, M.P. Ramos, G. Herradon, Midkine is a novel regulator of amphetamine-induced striatal gliosis and cognitive impairment: evidence for a stimulus-dependent regulation of neuroinflammation by midkine, *Mediat. Inflamm.* 2016 (2016) 9894504; (c) R. Fernandez-Calle, M. Vicente-Rodriguez, E. Gramage, J. Pita, C. Perez-Garcia, M. Ferrer-Alcon, M. Uribarri, M.P. Ramos, G. Herradon, Pleiotrophin regulates microglia-mediated neuroinflammation, *J. Neuroinflammation* 14 (2017) 46.
- [7] (a) T. Wisniewski, M. Lalowski, M. Baumann, H. Rauvala, E. Raulo, R. Nolo, B. Frangione, HB-GAM is a cytokine present in Alzheimer's and Down's syndrome lesions, *NeuroReport* 7 (1996) 667–671; (b) O. Yasuhara, H. Muramatsu, S.U. Kim, T. Muramatsu, H. Maruta, P.L. McGeer, Midkine, a novel neurotrophic factor, is present in senile plaques of Alzheimer disease, *Biochem. Biophys. Res. Commun.* 192 (1993) 246–251.
- [8] D.M. Marchionini, E. Lehrmann, Y. Chu, B. He, C.E. Sortwell, K.G. Becker, W.J. Freed, J.H. Kordower, T.J. Collier, Role of heparin binding growth factors in nigrostriatal dopamine system development and Parkinson's disease, *Brain Res.* 1147 (2007) 77–88.
- [9] G. Herradon, C. Perez-Garcia, Targeting midkine and pleiotrophin signalling pathways in addiction and neurodegenerative disorders: recent progress and perspectives, *Br. J. Pharmacol.* 171 (2014) 837–848.
- [10] (a) M.L. Soto-Montenegro, M. Vicente-Rodriguez, C. Perez-Garcia, E. Gramage, M. Desco, G. Herradon, Functional neuroimaging of amphetamine-induced striatal neurotoxicity in the pleiotrophin knockout mouse model, *Neurosci. Lett.* 591 (2015) 132–137; (b) E. Gramage, L. Rossi, N. Granado, R. Moratalla, G. Herradon, Genetic inactivation of pleiotrophin triggers amphetamine-induced cell loss in the substantia nigra and enhances amphetamine neurotoxicity in the striatum, *Neuroscience* 170 (2010) 308–316; (c) E. Gramage, A. Putelli, M.J. Polanco, C. Gonzalez-Martin, L. Ezquerro, L.F. Alguacil, P. Perez-Pinera, T.F. Deuel, G. Herradon, The neurotrophic factor pleiotrophin modulates amphetamine-seeking behaviour and amphetamine-induced neurotoxic effects: evidence from pleiotrophin knockout mice,

- Addict. Biol. 15 (2010) 403–412.
- [11] (a) S.E. Gombash, F.P. Manfredsson, R.J. Mandel, T.J. Collier, D.L. Fischer, C.J. Kemp, N.M. Kuhn, S.L. Wohlgenant, S.M. Fleming, C.E. Sortwell, Neuroprotective potential of pleiotrophin overexpression in the striatonigral pathway compared with overexpression in both the striatonigral and nigrostriatal pathways, *Gene Ther.* 21 (7) (2014) 682–693; (b) S.E. Gombash, J.W. Lipton, T.J. Collier, L. Madhavan, K. Steece-Collier, A. Cole-Strauss, B.T. Terpstra, A.L. Spieles-Engemann, B.F. Daley, S.L. Wohlgenant, V.B. Thompson, F.P. Manfredsson, R.J. Mandel, C.E. Sortwell, Striatal pleiotrophin overexpression provides functional and morphological neuroprotection in the 6-hydroxydopamine model, *Mol. Ther.* 20 (2012) 544–554.
- [12] E. Gramage, C. Perez-Garcia, M. Vicente-Rodriguez, S. Bollen, L. Rojo, G. Herradon, Regulation of extinction of cocaine-induced place preference by midkine is related to a differential phosphorylation of peroxiredoxin 6 in dorsal striatum, *Behav. Brain Res.* 253 (2013) 223–231.
- [13] E. Gramage, M. Vicente-Rodriguez, G. Herradon, Pleiotrophin modulates morphine withdrawal but has no effects on morphine-conditioned place preference, *Neurosci. Lett.* 604 (2015) 75–79.
- [14] (a) M. Vicente-Rodriguez, C. Perez-Garcia, M. Haro, M.P. Ramos, G. Herradon, Genetic inactivation of midkine modulates behavioural responses to ethanol possibly by enhancing GABA(A) receptor sensitivity to GABA(A) acting drugs, *Behav. Brain Res.* 274 (2014) 258–263; (b) M. Vicente-Rodriguez, C. Perez-Garcia, M. Ferrer-Alcon, M. Uribarri, M.G. Sanchez-Alonso, M.P. Ramos, G. Herradon, Pleiotrophin differentially regulates the rewarding and sedative effects of ethanol, *J. Neurochem.* 131 (2014) 688–695; (c) H. Chen, D. He, A.W. Lasek, Midkine in the mouse ventral tegmental area limits ethanol intake and Ccl2 gene expression, *Genes Brain Behav.* (2017, Apr 11), <https://doi.org/10.1111/gbb.12384>.
- [15] W.A. Banks, A. Gertler, G. Solomon, L. Niv-Spector, M. Shpilman, X. Yi, E. Batrakova, S. Vinogradov, A.V. Kabanov, Principles of strategic drug delivery to the brain (SDDb): development of anorectic and orexigenic analogs of leptin, *Physiol. Behav.* 105 (2011) 145–149.
- [16] (a) N. Maeda, T. Nishiwaki, T. Shintani, H. Hamanaka, M. Noda, 6B4 proteoglycan/phosphacan, an extracellular variant of receptor-like protein-tyrosine phosphatase zeta/RPTPbeta, binds pleiotrophin/heparin-binding growth-associated molecule (HB-GAM), *J. Biol. Chem.* 271 (1996) 21446–21452; (b) K. Meng, A. Rodriguez-Pena, T. Dimitrov, W. Chen, M. Yamin, M. Noda, T.F. Deuel, Pleiotrophin signals increased tyrosine phosphorylation of beta catenin through inactivation of the intrinsic catalytic activity of the receptor-type protein tyrosine phosphatase beta/zeta, *Proc. Natl. Acad. Sci. U. S. A.* 97 (2000) 2603–2608.
- [17] H. Pariser, L. Ezquerra, G. Herradon, P. Perez-Pinera, T.F. Deuel, Fyn is a downstream target of the pleiotrophin/receptor protein tyrosine phosphatase beta/zeta-signaling pathway: regulation of tyrosine phosphorylation of Fyn by pleiotrophin, *Biochem. Biophys. Res. Commun.* 332 (2005) 664–669.
- [18] P. Perez-Pinera, W. Zhang, Y. Chang, J.A. Vega, T.F. Deuel, Anaplastic lymphoma kinase is activated through the pleiotrophin/receptor protein-tyrosine phosphatase beta/zeta signaling pathway: an alternative mechanism of receptor tyrosine kinase activation, *J. Biol. Chem.* 282 (2007) 28683–28690.
- [19] A. Fujikawa, A. Nagahira, H. Sugawara, K. Ishii, S. Imajo, M. Matsumoto, K. Kuboyama, R. Suzuki, N. Tanga, M. Noda, S. Uchiyama, T. Tomoo, A. Ogata, M. Masumura, Small-molecule inhibition of PTPRZ reduces tumor growth in a rat model of glioblastoma, *Sci. Rep.* 6 (2016) 20473.
- [20] P. Huang, J. Rampal, J. Wei, C. Liang, B. Jallal, G. McMahon, C. Tang, Structure-based design and discovery of novel inhibitors of protein tyrosine phosphatases, *Bioorg. Med. Chem.* 11 (2003) 1835–1849.
- [21] H. Pajouhesh, G.R. Lenz, Medicinal chemical properties of successful central nervous system drugs, *NeuroRx* 2 (2005) 541–553.
- [22] M. Verma, S.J. Gupta, A. Chaudhary, V.K. Garg, Protein tyrosine phosphatase 1B inhibitors as antidiabetic agents - a brief review, *Bioorg. Chem.* 70 (2017) 267–283.
- [23] T. Shintani, M. Noda, Protein tyrosine phosphatase receptor type Z dephosphorylates TrkA receptors and attenuates NGF-dependent neurite outgrowth of PC12 cells, *J. Biochem.* 144 (2008) 259–266.
- [24] K.L. Abbott, R.T. Matthews, M. Pierce, Receptor tyrosine phosphatase beta (RTPbeta) activity and signaling are attenuated by glycosylation and subsequent cell surface galectin-1 binding, *J. Biol. Chem.* 283 (2008) 33026–33035.
- [25] N. Maeda, K. Ichihara-Tanaka, T. Kimura, K. Kadomatsu, T. Muramatsu, M. Noda, A receptor-like protein-tyrosine phosphatase PTPzeta/RTPbeta binds a heparin-binding growth factor midkine. Involvement of arginine 78 of midkine in the high affinity binding to PTPzeta, *J. Biol. Chem.* 274 (1999) 12474–12479.
- [26] D. He, H. Chen, H. Muramatsu, A.W. Lasek, Ethanol activates midkine and anaplastic lymphoma kinase signaling in neuroblastoma cells and in the brain, *J. Neurochem.* 135 (2015) 508–521.
- [27] C. Moog-Lutz, J. Degoutin, J.Y. Gouzi, Y. Frobert, N. Brunet-de Carvalho, J. Bureau, C. Creminon, M. Vigny, Activation and inhibition of anaplastic lymphoma kinase receptor tyrosine kinase by monoclonal antibodies and absence of agonist activity of pleiotrophin, *J. Biol. Chem.* 280 (2005) 26039–26048.
- [28] S.A. Mok, R.B. Campenot, A nerve growth factor-induced retrograde survival signal mediated by mechanisms downstream of TrkA, *Neuropharmacology* 52 (2007) 270–278.
- [29] E. Gramage, L.F. Alguacil, G. Herradon, Pleiotrophin prevents cocaine-induced toxicity in vitro, *Eur. J. Pharmacol.* 595 (2008) 35–38.
- [30] M. Vicente-Rodriguez, R. Fernandez-Calle, E. Gramage, C. Perez-Garcia, J.M. Zapico, C. Coderch, M. Pastor, B. Di Geronimo, B. De Pascual-Teresa, A. Ramos, A.W. Lasek, G. Herradon, Preclinical development and evaluation of inhibitors of Receptor Protein Tyrosine Phosphatase beta/zeta for the treatment of alcohol use disorder, *Alcohol. Clin. Exp. Res.* 41 (Suppl 1) (2017) 110A.
- [31] Di Geronimo, B.; Coderch, C.; Herradón, G.; Ramos, A.; de Pascual-Teresa, B. Exploring the Protein Tyrosine Phosphatase Receptor Z1 (PTPRZ1) in the search for new selective inhibitors for the prevention of alcohol abuse. Presented at 6th EUCHEMS Chemistry Congress, Seville, Spain, September 11-15, 2016; Abstract 999.
- [32] L. Tautz, D.A. Critton, S. Grotegut, Protein tyrosine phosphatases: structure, function, and implication in human disease, *Methods Mol. Biol.* 1053 (2013) 179–221.
- [33] A.J. Barr, E. Ugochukwu, W.H. Lee, O.N. King, P. Filippakopoulos, I. Alfano, P. Savitsky, N.A. Burgess-Brown, S. Muller, S. Knapp, Large-scale structural analysis of the classical human protein tyrosine phosphatome, *Cell* 136 (2009) 352–363.
- [34] T.A. Brandao, A.C. Hengge, S.J. Johnson, Insights into the reaction of protein-tyrosine phosphatase 1B: crystal structures for transition state analogs of both catalytic sites, *J. Biol. Chem.* 285 (2010) 15874–15883.
- [35] S. Sheriff, B.R. Beno, W. Zhai, W.A. Kostich, P.A. McDonnell, K. Kish, V. Goldfarb, M. Gao, S.E. Kiefer, J. Yanchunas, Y. Huang, S. Shi, S. Zhu, C. Dzierba, J. Bronson, J.E. Macor, K.K. Appiah, R.S. Westphal, J. O'Connell, S.W. Gerritz, Small molecule receptor protein tyrosine phosphatase gamma (RPTPgamma) ligands that inhibit phosphatase activity via perturbation of the tryptophan-proline-aspartate (WPD) loop, *J. Med. Chem.* 54 (2011) 6548–6562.
- [36] S.C. Almo, J.B. Bonanno, J.M. Sauder, S. Emtage, T.P. Dilenzo, V. Malashkevich, S.R. Wasserman, S. Swaminathan, S. Eswaramoorthy, R. Agarwal, D. Kumaran, M. Madegowda, S. Ragumani, Y. Patskovsky, J. Alvarado, U.A. Ramagopal, J. Faber-Barata, M.R. Chance, A. Sali, A. Fiser, Z.Y. Zhang, D.S. Lawrence, S.K. Burley, Structural genomics of protein phosphatases, *J. Struct. Funct. Genomics* 8 (2007) 121–140.
- [37] C. Wiesmann, K.J. Barr, J. Kung, J. Zhu, D.A. Erlanson, W. Shen, B.J. Fahr, M. Zhong, L. Taylor, M. Randal, R.S. McDowell, S.K. Hansen, Allosteric inhibition of protein tyrosine phosphatase 1B, *Nat. Struct. Mol. Biol.* 11 (2004) 730–737.
- [38] L. Bordoli, F. Kiefer, K. Arnold, P. Benkert, J. Battey, T. Schwede, Protein structure homology modeling using SWISS-MODEL workspace, *Nat. Protoc.* 4 (2009) 1–13.
- [39] J. Klett, A. Nunez-Salgado, H.G. Dos Santos, A. Cortes-Cabrera, A. Perona, R. Gil-Redondo, D. Abia, F. Gago, A. Morrales, MM-ISMSA: an ultrafast and accurate scoring function for protein-protein docking, *J. Chem. Theory Comput.* 8 (2012) 3395–3408.
- [40] N. Guex, M.C. Peitsch, T. Schwede, Automated comparative protein structure modeling with SWISS-MODEL and Swiss-PdbViewer: a historical perspective, *Electrophoresis* 30 (Suppl 1) (2009) S162–S173.
- [41] M.J. Frisch, G.W. Trucks, H.B. Schlegel, G.E. Scuseria, M.A. Robb, J.R. Cheeseman, J.A. Montgomery Jr., T. Vreven, K.N. Kudin, J.C. Burant, J.M. Millam, S.S. Iyengar, J. Tomasi, V. Barone, B. Mennucci, M. Cossi, G. Scalmani, N. Rega, G.A. Petersson, H. Nakatsuji, M. Hada, M. Ehara, K. Toyota, R. Fukuda, J. Hasegawa, M. Ishida, T. Nakajima, Y. Honda, O. Kitao, H. Nakai, M. Klene, X. Li, J.E. Knox, H.P. Hratchian, J.B. Cross, V. Bakken, C. Adamo, J. Jaramillo, R. Gomperts, R.E. Stratmann, O. Yazyev, A.J. Austin, R. Cammi, C. Pomelli, J.W. Ochterski, P.Y. Ayala, K. Morokuma, G.A. Voth, P. Salvador, J.J. Dannenberg, V.G. Zakrzewski, S. Dapprich, A.D. Daniels, M.C. Strain, O. Farkas, D.K. Malick, A.D. Rabuck, K. Raghavachari, J.B. Foresman, J.V. Ortiz, Q. Cui, A.G. Baboul, S. Clifford, J. Cioslowski, B.B. Stefanov, G. Liu, A. Liashenko, P. Piskorz, I. Komaromi, R.L. Martin, D.J. Fox, T. Keith, M.A. Al-Laham, C.Y. Peng, A. Nanayakkara, M. Challacombe, P.M.W. Gill, B. Johnson, W. Chen, M.W. Wong, C. Gonzalez, J.A. Pople, Gaussian 03, Revision C.02, Gaussian, Inc., Wallingford CT, 2004.
- [42] J. Wang, R.M. Wolf, J.W. Caldwell, P.A. Kollman, D.A. Case, Development and testing of a general amber force field, *J. Comput. Chem.* 25 (2004) 1157–1174.
- [43] T. Darden, D. York, L. Pedersen, Particle mesh Ewald: an N-log(N) method for Ewald sums in large systems, *J. Chem. Phys.* 98 (1993) 10089.
- [44] M.A. Lill, Efficient incorporation of protein flexibility and dynamics into molecular docking simulations, *Biochemistry* 50 (2011) 6157–6169.
- [45] D.R. Roe, T.E. Cheatham 3rd, PTRAJ and CPPTRAJ: software for processing and analysis of molecular dynamics trajectory data, *J. Chem. Theory Comput.* 9 (2013) 3084–3095.
- [46] K.K. Balavenkatraman, N. Aceto, A. Britschgi, U. Mueller, K.K. Bence, B.G. Neel, M. Bentires-Alj, Epithelial protein-tyrosine phosphatase 1B contributes to the induction of mammary tumors by HER2/Neu but is not essential for tumor maintenance, *Mol. Cancer Res.* 9 (2011) 1377–1384.